CHARACTERISATION OF THE EXPRESSION AND DEGRADATION OF THE PRO-INFLAMMATORY CYTOKINE INTERLEUKIN 1

A thesis submitted to the University of Manchester for the degree of Doctor of Philosophy in the Faculty of Life Sciences.

2011

Maryam S. Zahedi-Nejad

List of contents

Word Count: 45,720 words

List of Tables and Figures

Chapter 1 Introduction

Chapter 2: Materials and methods

Chapter 3: Cloning, expression and purification of pro-IL-1β N-terminus fragments in bacterial cells

Chapter 5: Stabilty of IL-1

Chapter 6: Effect of proteasome inhibition on the release of IL-1

Chapter 7: Discussion

Characterisation of the expression and degradation of the pro-inflammatory cytokine interleukin-1

M.S. Zahedi Nejad
PhD Thesis, The University of Manchester, 2011

Abstract

Inflammation plays a crucial role in protecting the host from infection and tissue injury. However, uncontrolled inflammation contributes to the pathogenesis of major auto-inflammatory diseases. Interleukin-1 (IL-1), a pleiotropic pro-inflammatory cytokine, is a pivotal mediator of many of these diseases. The best characterised IL-1 family members, IL-1α and IL-1β, are produced as precursor forms of 31 kDa in size. Both precursors are cleaved and secreted, activating transmembrane IL-1 receptors on IL-1-responsive cells. Many studies that focused on IL-1α have shown that the precursor and processed mature Ct peptide, as well as its N terminus (Nt) form, can elicit a signal. However, with IL-1β, only the processed mature Ct form is known to elicit an inflammatory response and no immunological activity has been attributed to Nt fragments of pro-IL-1β. Therefore, the first objective of this study was to produce recombinant human Nt-IL-1β fragments in bacterial and mammalian expression system to investigate their possible immunomodulatory functions. Recombinant His-tagged N-terminus fragments (10 and 14 kDa) of pro-IL-1β were cloned into the bacterial expression vector pET-22(+) and expressed in *E. coli* BL21(DE3) followed by purification using three consecutive columns (IMAC, SEC and AEC). Purification analysis of eluted proteins from columns indicated that the recombinant proteins were always co-purified with some other bacterial proteins. The Nt fragments of pro-IL-1β were cloned into the mammalian expression plasmid, pcDNA3.1(+). Expression of these proteins was monitored by transfection of two mammalian cell lines: Human Embryonic Kidney (HEK) 293 cells and monkey kidney cells (COS-7). No protein expression was observed with either construct.These limitations urged us to investigate the expression and degradation of endogenous IL-1 *in vitro.*

Previous studies have shown that the transcription of cytokine genes in response to lipopolysaccharide (LPS) is usually rapid and begins to decline within a few hours after stimulation. The proteasome is the major cellular proteolytic apparatus and controls the turn-over of cellular proteins. We investigated the intracellular stability of IL-1α and IL-1β in LPS-stimulated mouse J774 macrophages and primary mouse bone marrow derived macrophages (BMDMs). Exposure of LPS-stimulated J774 and BMDMs to three different classes of proteasome inhibitors (peptide alhedyde (ALLN), peptide boronate (MG262) and non-peptide inhibitor (β-lactone)) prevented the degradation of intracellular IL-1α and IL-1β in a concentration and time dependent manner. Furthermore, the release of IL-1 into the culture media was not affected by any of these inhibitors in LPS-stimulated J774 cells. However, in LPS-stimulated BMDMs, β-lactone increased the release of both IL-1α and IL-1β and ALLN only increased IL-1α release into culture supernatant compared to control. MG262 had no effect on the release of either.

These data suggest that the proteasome plays an important role in controlling the amount of IL-1α and IL-1β by restricting the intracellular levels of these cytokines in activated monocytes and macrophages. Therefore, this study provides evidence in support of the hypothesis that the proteasome is involved in the degradation of IL-1α and IL-1β and may offer a potential therapeutic target in inflammatory diseases.

Declaration

I, the undersigned, declare that no portion of the work referred to in this thesis has been submitted in support of an application for another degree or qualification of this or any other university or other institute of learning.

M.S.Zahedi Nejad

iv. Further information on the conditions under which disclosure, publication and exploitation of this thesis, the Copyright and any Intellectual Property Rights and/or Reproductions described in it may take place is available from the Vice-President and the Dean of the Faculty of Life Sciences.

Abbreviations

AD	Alzheimer disease
ALLN	Acetyl-Leu-Leu-norleucinal
ATP	Adenosine tri-phosphate
AEC	Anion-exchange chromatography
AP	Alkaline phosphatase
BCA	Bicinchoninic acid
B-CLL	B cell chronic lymphocytic leukaemia
BSA	Bovine serum albumin
^{o}C	Degree celsius
CAPS	Cryopyrin-associated periodic syndrome
cDNA	copy deoxy-ribonucleic Acid
CHX	Cyclohexamide
Ct	Carboxy-terminus
CMV	Cytomegalo virus
DAMPs	Danger mssociated Molecular patterns
DMEM	Dulbecco's modified eagle medium
DMSO	Dimethylsulfoxide
DNA	Deoxy-ribonucleic acid
E. coli	*Escherichia coli*
EDTA	Ethylene diaminetetra acetic acid
ELISA	Enzyme-linked immunosorbent assay
ER	Endoplasmic reticulum
x *g*	gravity x force
h	Hour
HIV	Human immunodeficiency virus

IL-1	Interleukin-1
IL-1F	Interlleukin-1 family
IL-1RI	IL-1 receptor type I
IL-RII	IL-1 receptor type II
IPTG	Isopropyl-β-thiogalactopyranoside
IMAC	Immobilised metal affinity chromatography
KDa	Kilo-dalton
KO	Knock out
LB medium	Luria Bertani medium
LDH	Lactate dehydrogenase
LPS	Lipopolysaccharide
MHC	Major histocompatibility complex
Min	Minute
MCS	Multiple cloning site
MS	Multiple sclerosis
NF-κB	Nuclear factor-κB
NOD	NOD like receptor
NLR-3	Nod-Like receptor pyrin domain-3
NLS	Nuclear localisation sequence
Nt	N-terminus
OD	Optical density
Ub	Ubiquitin
UPP	Ubiquitin-proteasome pathway
PPR	Pattern recognition receptors
P/S	Penicillin/streptomycin antibiotic solution
PBS	Phosphate buffered saline

PBST	Phosphate buffered saline with 0.1% tween
PCR	Polymerase chain reaction
pro-IL-1	pro-Interleukin-1
rpm	revolutions per minute
RT	Reverse transcription
RT	Room temperature
RA	Rheumatoid arthritis
SEC	Size exclusion chromatography
s.d.	standard deviation
sec	Second
SDS-PAGE	Sodium dodecyl sulfate-polyacrylamide gel electrophoresis
SOC	Super optimal catobolite repression medium
SP	Signal peptide
TCM buffer	TrisHCl 20 mM, $CaCl_2$ 20 mM, $MgCl_2$ 20 mM, pH 7.5
TLR	Toll like receptor
TMB	Tetramethylbenzidine
TAE buffer	Tris-acetate-EDTA buffer
TEMED	N,N,N',N'-Tetramethylethylenediamine
TTBS	Tween-tris-buffered saline
V	Volt
v/v	volume/volume
WT	Wild type
w/v	weight/volume
MG262	Z-Leu-Leu-Leu-boronate
β-gal	β-galactosidase

Acknowledgments

I would like to thank my supervisors Dr. David Brough and Dr. Pablo Pelegrin for their great help, support, advice and patience during my PhD. I could not imagine having had better supportive and understanding supervisors.

I also acknowledge Prof. Annmarrie Surpenant my first official supervisor, Prof. Alan Dixon, my advisor, who always advised me in several meetings. Special thanks also to Dr Nadia Luheshi and Dr Gloria Lopez-castejon who advised me on series of experiments. I cannot forget to express appreciation to other members of the Brough laboratory for their help and support, and for making working in the lab so enjoyable.

Finally, I would not be able to achieve my PhD, without the support, encouragment and tireless patience of all members of my family, specially my husband Dr Behnam Bastani and my two heros' Narges and Ehsan. I also have to thank my parents for their love and encouragement throughout my life.

CHAPTER 1

Introduction

1.1 Summary

Inflammation is a response of the innate immune system which protects organisms by clearing infections and healing injured tissue. Soluble secreted proteins called cytokines coordinate inflammatory responses. The interleukin-1 (IL-1) family of cytokines is composed of key pro-inflammatory mediators which are constitutively expressed at low levels in healthy tissue. Aberrant expression and degradation of the IL-1 family is involved in the pathogenesis of many inflammatory diseases (Reviewed in Dinarello, 2010), making the IL-1 system an attractive target for therapeutic intervention. The IL-1 family consists of eleven members (Dinarello, 1996; Smith et al., 2000; Dunn et al., 2001; Schmitz et al., 2005). The best characterised pro-inflammatory members of the IL-1 family are IL-1alpha (α) and lL-1beta (β). Both lL-1α and lL-1β are expressed as precursor proteins of 31 kDa called pro-IL-1 proteins that have to be processed for the release of the 17 kDa carboxyl terminus (Ct) to display biological activity. For IL-1α, both the immature precursor (pro-IL-1α) and processed mature form can initiate an inflammatory response (Maier et al., 1994; Hu et al., 2003). Several studies have also focused on the amino terminus (Nt) of pro-IL-1α and shown that it has effects on migration, growth and proliferation of the cells (Heguy et al., 1991; McMahon et al., 1997; Palmer et al., 2005). However, with IL-1β, only the processed mature form can initiate an inflammatory response and it is thought that the only function of its Nt is to inhibit the activity of the Ct. These considerations led us to this study which has two main aims:

- To express and purify pro-IL-1β Nt fragments in order to study their immunological functions.
- To study the expression and degradation of endogeneous IL-1α and IL-1β.

1.2 IL-1 family (IL-1F)

With the exception of IL-18, the genes coding for the IL-1F are clustered on the same region of human chromosome 2 (position 2q13) (Dunn et al., 2001) suggesting each new IL-1 family member arose from a common ancestral gene. All IL-1F members share a common secondary structure formed by 12 β-sheets connected by loop regions arranged in a β-trefoil secondary structure (Murzin et al., 1992; Nicola, 1994; Dunn et al., 2001).

1.3 IL-1α and IL-1β

The most studied members of the IL-1F are the IL-1 receptor type I (IL-1RI) agonists, IL-1α (IL-1F1), IL-1β (IL-1F2) and the receptor antagonist: IL-1Ra (IL-1F3). IL-1α and IL-1β share only 30% homology at the amino acid level (Auron et al., 1984; Thompson et al., 1997). They are produced by many cell types such as neutrophils, natural killer cells, B-lymphocytes, T-lymphocytes and cells of the central nervous system (CNS) (Oppenheim et al., 1986). However, the most prominent source of IL-1α and IL-1β are blood monocytes and tissue resident macrophages (Lepe-Zuniga and Gery, 1984; Arend et al., 1989; Dinarello, 1998). These cytokines exert different effects on their target cells and induce systemic symptoms such as fever, hypotension and production of other pro-inflammatory cytokines (Dinarello, 1998; Ferrari et al., 2006). Mature IL-1α and IL-1β can bind both of the high affinity IL-1 receptors; IL-1RI (Sims et al., 1988; Sims et al., 1993) and IL-1 receptor type II (IL-1RII) (McMahan et al., 1991). Whilst binding of IL-1α and IL-1β to IL-1RI in association with an accessory protein initiates an inflammatory signal (Greenfeder et al., 1995), binding to IL-1RII suppresses inflammation due to lack of signalling function. IL-1RII acts as a molecular trap for inhibiting IL-1 activity (Colotta et al., 1993; Greenfeder et al., 1995).

1.3.1 IL-1 expression

The IL-1α and IL-1β genes are transcriptionally silent in un-stimulated inflammatory cells (Warner et al., 1987). However, transcription of both IL-1α and IL-1β genes can be initiated by activation of the innate immune system. The innate immune response is initiated by identifying conserved motifs of non-self molecules (Matsushima et al., 1986) such as flagellin and lipoteichoic acid from gram positive bacteria or peptidoglycan and lipopolysaccharide (LPS) from gram negative bacteria (Dinarello, 1996). Collectively, these molecules are called pathogen associated molecular patterns (PAMPs). PAMPs are recognised by specific cytosolic or membrane bound receptors on inflammatory cells called pattern recognition receptors (PRR's) such as those of the toll-like receptor family (TLRs) (Kishimoto et al., 1994; Maier et al., 1994; Ihle, 1995; Martinon et al., 2005; Palmer et al., 2005). Upon TLR stimulation nuclear factor-κB (NF-κB) and/or mitogen activated protein kinase (MAPK) pathways are activated and there is a subsequent increase in gene transcription and translation of the precursors pro-IL-1α and pro-IL-1β (Dinarello, 1996; Watkins et al., 1999).

1.3.2 Mechanism of IL-1 processing

IL-1α and IL-1β are translated in the cytosol and, unlike other secreted proteins, lack a hydrophobic signal sequence to direct them to the classical secretion pathway *via* the endoplasmic reticulum (ER) and Golgi apparatus (March et al., 1985; Rubartelli et al., 1990; Stevenson et al., 1992; Rubartelli and Sitia, 1997). A second stimulus is required for the processing of pro-IL-1α and pro-IL-1β and subsequent release of the 17 kDa mature IL-1α and IL-1β (Perregaux and Gabel, 1998; Martinon et al., 2005). This second stimulus provides an additional checkpoint by which cells may regulate production of this important cytokine. In the absence of a second stimulus, cells release only small amount of mature

cytokine and most of the newly synthesised product remains unprocessed in the cytosol or is degraded within the cell (Ferrari et al., 2006). Mechanisms involved in these processes are poorly understood (Nickel, 2003; Prudovsky et al., 2003).

The cysteine protease caspase-1 catalyses the cleavage of pro-IL-1β to its mature active form, which is closely followed by its release (Thornberry et al., 1992). There are two caspase-1 cleavage sites in pro-IL-1β (Wewers et al., 1999). The cleavage of the first site (between Asp27 and Gly28) removes a 3.5 kDa fragment and the second cleavage (between Asp116 and Ala 117) produces a 10 kDa N-terminus (Nt-b) fragment and mature IL-1β. Single cleavage (between Asp116 and Ala117) produces a 14 kDa Nt fragment and 17 kDa IL-1β (Swaan et al., 2001) (Figure 3.1).

Caspase-1 is synthesised as an inactive precursor of 45 kDa, requiring proteolytic cleavage to two subunits of 10 and 20 kDa (p10 and p20), thereby forming the active heterotetrameric enzyme formed by two p10 and two p20 subunits (Wilson et al., 1994). Activation of caspase-1 is controlled by intracellular pattern recognition receptors called NOD like receptors (NLRs) (Figure 1.1). NLRs are stimulated by PAMPs and by danger associated molecular patterns (DAMPs) such as extracellular ATP (Adenosine tri-phosphate) (Perregaux and Gabel, 1998), monosodium urate crystals (Shi et al., 2003; Mariathasan and Monack, 2007), cytosolic DNA and bacterial flagellin (Muruve et al., 2008). NLR activation results in the assembly of an intracellular multi-protein complex known as the inflammasome (Mariathasan and Monack, 2007; Muruve et al., 2008) which induces proteolytic cleavage of pro-caspase-1 into its active form (Martinon et al., 2002; Martinon and Tschopp, 2004) (Figure 1.1).

Pro-IL-1α is processed by the calcium dependent protease calpain (Kobayashi et al., 1990; Carruth et al., 1991; Watanabe et al., 1994; Kavita et al.,

1995). Unlike pro-IL-1β, both pro-IL-1α (amino acids 1 to 271) and the Ct fragment of IL-1α (amino acids 113 to 271) are biologically active (Mosley et al., 1987; Fuhlbrigge et al., 1988). IL-1 production and processing is summarised in figure 1.1.

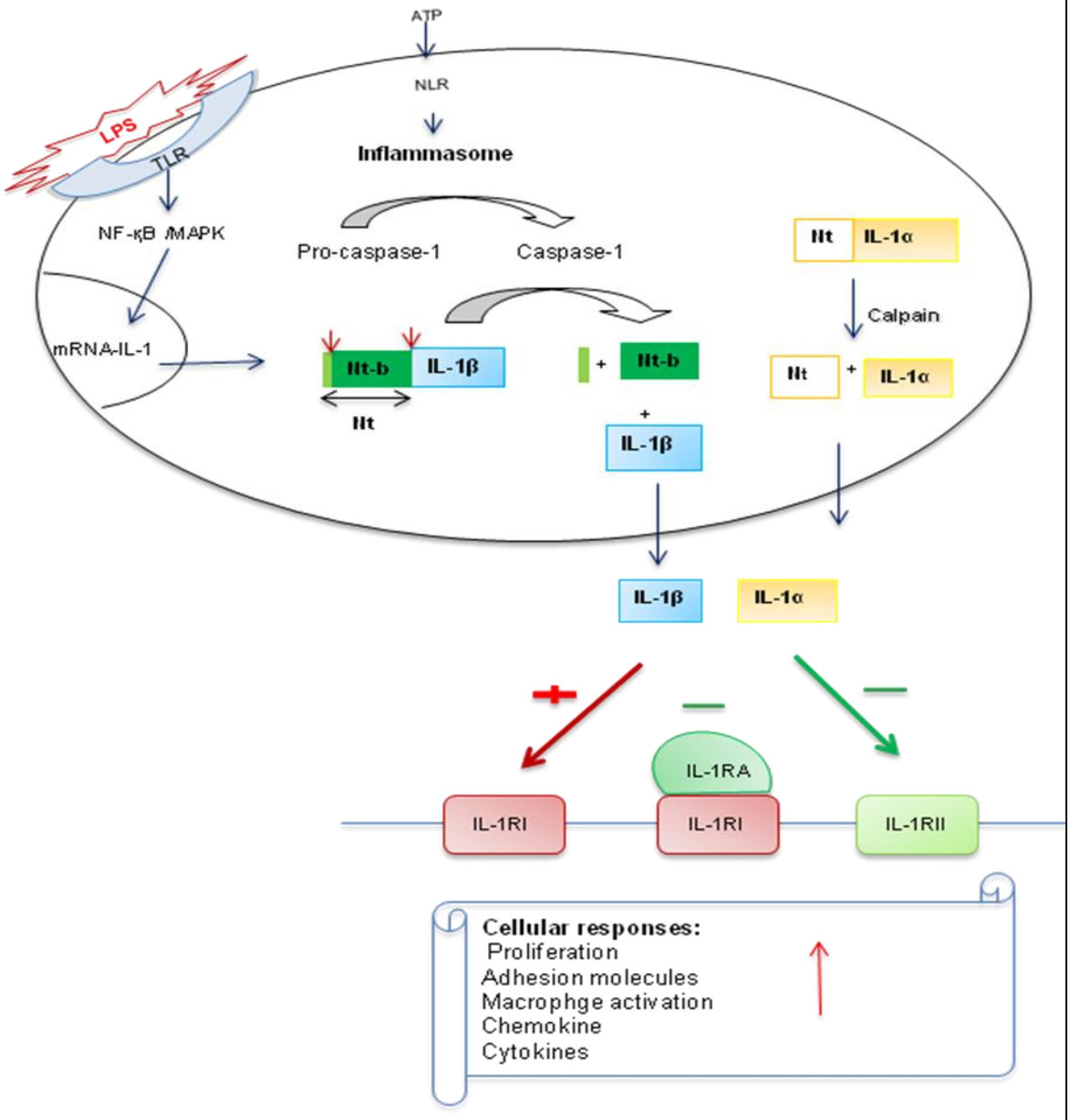

Figure 1.1 Production and processing of IL-1. Schematic representation showing activation of TLR by PAMPs (LPS) which activates transcription factor NF-κB and subsequently the transcription of pro-IL-1. Stimulation of a second type of receptor NLRs, by DAMPS (ATP), leads to assembly of the inflammasome and the activation of pro-caspase-1. There are two caspase-1 ceavage sites producing 3.5 and 10 kDa (Nt-b) and IL-1β mature form. Pro-IL-1α is processed by calpain resulting in the release of IL-1α. The binding of IL-1 to IL-1RI leads to different cellular responses. IL-1Ra competitively inhibits IL-1 signaling by binding to the IL-1RI. The IL-1 type II receptor is a decoy receptor, which inhibits IL-1 signalling by binding to it without causing a pro-inflammatory response.

1.3.3 Release of IL-1

The mechanism by which IL-1β is released from the cells is the subject of some controversy and active research (Reviewed in Lopez-Castejon and Brough, 2011). One proposed mechanism involves release of IL-1β by exocytosis of vesicles containing IL-1β (Rubartelli et al., 1990; Andrei et al., 1999; Bianco et al., 2005). Another mechanism is the shedding of extracellular micro-vesicles containing IL-1β from the cell surface (MacKenzie et al., 2001; Pizzirani et al., 2007). These mechanisms of release have been studied in ATP-activated human monocytes.

The release of mature IL-1α in macrophages and monocytes has been studied far less than that of IL-1β. Direct passage of IL-1α across the plasma membrane is suggested by the β-barrel secondary structure of IL-1α (Kobayashi et al., 1990a; Srisailam et al., 2002; Prudovsky et al., 2003). This hypothesis is based on the fact that IL-1α shares all features of Ca^{2+}-dependent phospholipid-binding proteins which are able to pass across the plasma membrane (Matsushima et al., 1986).

In vitro studies have shown that ATP, calcium ionophores and potassium ionophores such as nigericin can induce the release of IL-1α (Perregaux and Gabel, 1994; Watanabe and Kobayashi, 1994; Mandinova et al., 2003). Mature IL-1β also affects the release of IL-1α (Horai et al., 1998). ATP stimulated microglia from IL-1β knock out (KO) mice, release significantly lower levels of IL-1α compared with Wild Type (WT) cells (Horai et al., 1998).

1.3.4 Pro-pieces of IL-1 as immune regulatory molecules

Although the majority of extracellular activities attributed to IL-1 proteins are mediated through IL-1RI binding of their processed Ct peptide, different studies have shown that the precursor of IL-1α is also involved in various biochemical

changes independent of classical signalling through IL-1RI (Heguy et al., 1991; Maier et al., 1994; McMahon et al., 1997; Hu et al., 2003; Palmer et al., 2005).

This is due to the presence of a conserved cluster of basic amino acids (KVLKKRR) at its N-terminal that constitute a nuclear localisation signal (NLS) (Wessendorf et al., 1993). Wessendorf and colleagues showed that the NLS of IL-1α trafficks β-galactosidase (β-gal)-NLS fusion protein to the nucleus (Wessendorf et al., 1993). This discovery highlighted the potential of IL-1α as a *bona fide* nuclear protein.

Transfection of human umbilical vein endothelial cells with the copy Deoxy-Ribonucleic Acid (cDNA) encoding pro-IL-1α enhances cell-cell contacts and diminishes migratory potential in contrast to mutant pro-IL-1α K82N or mature IL-1α (McMahon et al., 1997). Over-expression of pro-IL-1α in an endothelial cell line (tumour endothelia cells (tEC)) or a human osteosarcoma cell line (SaOS-2) reduced cell proliferation (Maier et al., 1994; Palmer et al., 2005). Also, over-expression of pro-IL-1α in bone marrow causes transformation of IL-1α producing cells into a malignant phenotype (Stevenson et al., 1997).

In human embryonic kidney cell line 293T (HEK293T), over-expression of Nt of pro-IL-1α causes apoptosis by interacting with elements of the RNA processing apparatus and the alternate splicing of apoptosis regulatory proteins (Pollock et al., 2003). Using the yeast two-hybrid system, it was shown that Nt of pro-IL-1α associates with Heat Shock 1-Associated protein X-1 (HAX-1), a target of non-receptor protein tyrosine kinases within haematopoietic cells (Yin et al., 2001). Pro-IL-1α Nt binding to the nuclear protein necdin, a nuclear suppressor growth factor, reverses the activity of necdin on fibroblast growth by increasing proliferation and collagen production (Hu et al., 2003). In another study by Werman and colleagues in two other cell lines (Werman et al., 2004), COS-7

(Aftican green monkey kidney fibroblast cell line) and RAW264.7 (mouse macrophages), over-expression of pro-IL-1α and its Nt, but not the Ct mature form were sufficient to activate the transcriptional machinery in the GAL4 system by 90 and 50 fold, respectively. Under conditions of IL-1 receptor blockade, over-expression of pro-IL-1α and its Nt were also enough to activate NF-κB (Werman et al., 2004). Stable transfectants over-expressing pro-IL-1α induced the release of cytokines IL-8 and IL-6 but also exhibit a significantly lower threshold of activation to subpicomolar concentrations of tumour necrosis factor-α or interferon-γ (Werman et al., 2004).

In contrast to pro-IL-1α, pro-IL-1β is still viewed as a cytosolic and extracellular cytokine, despite its nuclear localisation in lipid A-stimulated mesangial cells (Stevenson et al., 1992) and microglia cells (Luheshi et al., 2009). This nuclear import is entirely passive and independent of any NLS (Luheshi et al., 2009). However, mutations on the putative NLS of IL-1β (Lys210Ala, Lys211Ala and Pro208Ala) retained the ability to bind to the IL-1RI but showed greater biological potency by the induction of IL-2 secretion (Grenfell et al., 1991).

These observations suggest that the putative NLS of pro-IL-1β and its Nt sequence may play an unforeseen role in the generation of biological responses during inflammation. The Nt sequence of pro-IL-1β is also still regarded only as something that sequesters pro-IL-1β. Whether these pro-pieces have any intracellular function is unclear. These questions persuaded us to construct clones of Nt of pro-IL-1β to express these proteins in bacteria and mammalian cell lines (chapters 3 and 4 of present thesis) in order to study their immunological function.

1.4 Diseases to which IL-1 contributes

IL-1 is regarded as the prototypic ‘’multifunctional’’ cytokine and is released in response to local or systemic injury or disease and affects nearly every cell

type. IL-1α and IL-1β orchestrate host defence responses often in concert with small mediator molecules or other cytokines. Because of its high potency and extensive functions, its tight regulation is very important. Overactive or improper gene expression, synthesis, processing, release or degradation of these pro-inflammatory cytokines is implicated in the pathogenesis of many acute and chronic peripheral diseases as determined by *in situ* hybridisation, steady state mRNA levels, antibody staining of tissues, circulating levels, or *ex vivo* production from cultured cells. Increased IL-1 production has been reported in numerous diseases (Reviewed in Dinarello, 2010).

IL-1 is an ‘’endogenous pyrogen’’ and it is able to elicit fever after peripheral administration (Duff, 1985). Over-expression of IL-1 and insufficient balance of endogenous IL-1Ra are crucial in development of rheumatoid arthritis (RA) (Kay and Calabrese, 2004) and also in chronic obstructive pulmonary disease characterised by chronic airway inflammation (Levine et al., 1995; Keatings, 1996). Abnormal expression of IL-1 is also associated with cardiovascular disease and pathological changes in the blood vessels and heart (Olofsson et al., 2009). One of the most highlighted IL-1 related heart diseases is coronary atherosclerosis. Coronary atherosclerosis is a condition in which the wall of an artery thickens as a result of the smooth muscle cell proliferation and also increasing vascular permeability (Willerson and Ridker, 2004). Preclinical studies have shown that IL-1 or IL-1RI KO mice demonstrate less atherosclerosis (Kirii et al., 2003; Chamberlain et al., 2006).

Diets consisting of high glucose and free fatty acids are the main cause of type 2 diabetes, another auto-inflammatory disease (Boni-Schnetzler et al., 2008; Boni-Schnetzler et al., 2009). The expression of IL-1β was over one hundred-fold

higher in beta cells isolated from the islets of patients with type 2 diabetes compared to non diabetic patients (Boni-Schnetzler et al., 2008).

One of the best characterised inherited auto-inflammatory diseases is the Cryopyrin-Associated Periodic Syndrome (CAPS) (Hoffman et al., 2004; Masters et al., 2009). CAPS is characterised by unpredictable recurrent attacks of fever, redness associated with rash, and joint pain. This disease is caused by the mutations in the Nod-Like Receptor Pyrin domain-3 (NLRP-3) gene (French and Consortium, 1997). This mutation increases the activity of cryoprin which leads to over-production of active IL-1β (Richards et al 2001; Dowds et al., 2003).

IL-1 also plays a key role in local brain tissue reactions. The chronic over-expression of IL-1 in brain tissue and cerebrospinal fluid can also produce pathological reactions (Stanley and Griffin, 1990; Rothwell and Luheshi, 2000). In the CNS, IL-1 is produced and secreted by microglia. IL-1 elevation has been demonstrated in a diverse array of CNS diseases, such as acute brain injury or stroke (Griffin et al., 1993; Griffin et al., 1994). Augmented production of IL-1 has also been implicated in the pathogenesis of a number of chronic neuro-degenerative diseases such as Alzheimer's disease (AD), multiple sclerosis (MS), Down syndrome and human immunodeficiency virus (HIV)-associated dementia (Griffin et al., 1989; Rogers et al., 1992; Royston et al., 1992; Griffin et al., 1994; McGuinness et al., 1997; Allan et al., 2005; Simi et al., 2007).

1.5 The potential of anti-IL-1 therapeutics

Nature has placed specific “roadblocks” such as the IL-1Ra to reduce the effects of IL-1 and to control the inflammatory response. Therefore, therapies targeted to reduce the production or activities of IL-1 have an attractive future as new anti-inflammatory compounds (Ledford, 2007; Pelegrin, 2008). Several studies have established IL-1 as key cytokines in the progression of RA, and IL-

1Ra can reduce the symptoms (Beutler, 1999; Breedveld, 1999; Emery and Buch, 2002). Therefore, specific and selective inhibitors of the IL-1 pathway, such as antibodies to IL-1 for example, would be beneficial to the outcome of different inflammatory diseases (Pascual et al., 2005; Wu et al., 2007; Pelegrin, 2008; Ilowite et al., 2009). In animal models of RA, anti-IL-1 treatment reduced joint destruction and also abolished bone erosions of knee and ankle joints (Joosten et al., 1999).

To date, two large well-controlled studies in patients with RA approved that recombinant IL-1Ra is clinically effective in reducing joint destruction (Kay and Calabrese, 2004). IL-1Ra is also currently being developed as a treatment for stroke (Emsley et al., 2005). However, IL-1Ra has a short half-life in plasma and relatively poor brain penetration, so novel anti-IL-1 therapies are still being investigated (reviewed in Braddock and Quinn, 2004).

It has been shown that local production of IL-1 affects tumour growth and metastases in several human cancers as well as experimental models (Gemma et al., 2001; Liss et al., 2001; Saijo et al., 2002; Salven et al., 2002). In a murine model, hepatic metastases and tumour growth is inhibited by IL-1Ra (Chirivi et al., 1993). Over-expression of IL-1Ra in mice also had the same effect on tumour growth (Weinreich et al., 2003; Barr et al., 2004). The tumour growth and metastatic potential of human melanoma xenograft that produces IL-1 constitutively was also significantly inhibited by over expression or treatment with IL-1Ra (Elaraj et al., 2006). These results indicate that IL-1 is essential for the invasiveness of malignant cells.

In type 2 diabetes, using the recombinant form of IL-1Ra or a specific monoclonal antibody against IL-1β corrects dysfunctional beta-cell production of insulin and reduced IL-1β activity resulting in suppression of IL-1β mediated

inflammation in the microenvironment of the islet. Dysfunctional beta-cells are corrected and insulin production is increased (Donath et al., 2009).

The generation of anti-human IL-1α/β DVD-Ig™ molecules (dual variable domain immunoglobulin) that block both IL-1α and IL-1β but not IL-1Ra are also emerging as a potential anti-IL-1 therapy (Wu et al., 2009). Consequently, an improved understanding of the IL-1 system may allow the development of new drugs to inhibit IL-1 action.

1.6 Protein degradation

Continuous turn-over (synthesis and degradation) of proteins is vital for the functionality and viability of cells. It is very important that the cells recognise and degrade any unneeded or mis-folded proteins whose accumulation could be dangerous to the cell (Goldberg and St. John, 1976; Rechsteiner, 1987; Hershko and Ciechanover, 1992). Mis-regulation of protein degradation affects cell cycle, gene expression and responses to oxidative stress. The rate of degradation of individual proteins varies widely and depends on their half-lives, ranging from few minutes to weeks (Bohley, 1995).

Protein degradation in eukaryotic cells is carried out by two distinct proteolytic mechanisms: lysosomal and proteasomal. Lysosomes are rich in proteolytic enzymes and were considered to be the only site for protein breakdown in cells until 1978. However, studies with inhibitors of lysosomal acidification (weak bases) or lysosomal proteases (E64) established that lysosomes are mainly involved in the degradation of membrane-associated proteins or extracellular proteins and only 10-20% of total cytosolic protein (Glaumann and Ballard, 1987).

The presence of the proteasome was suggested by Etlinger and Goldberg studying erythrocytes, since erythrocytes have no lysosomes (Etlinger and Goldberg, 1977). The proteasome was discovered in these cells by Ciechanover

and Hershko when they were trying to isolate an unusual ATP dependent hydrolytic enzyme (Ciechanover and Hershko, 1978). The proteasome is an ATP dependent multi-catalytic proteolytic complex. It accounts for 80% breakdown of intracellular proteins (short and long lived) (Ciechanover and Hershko, 1978) in both stressed (Heinemeyer et al., 1991) and non-stressed cellular environment (reviewed in Rock and Goldberg, 1999). These two pathways of protein breakdown are summarised in figure 1.2.

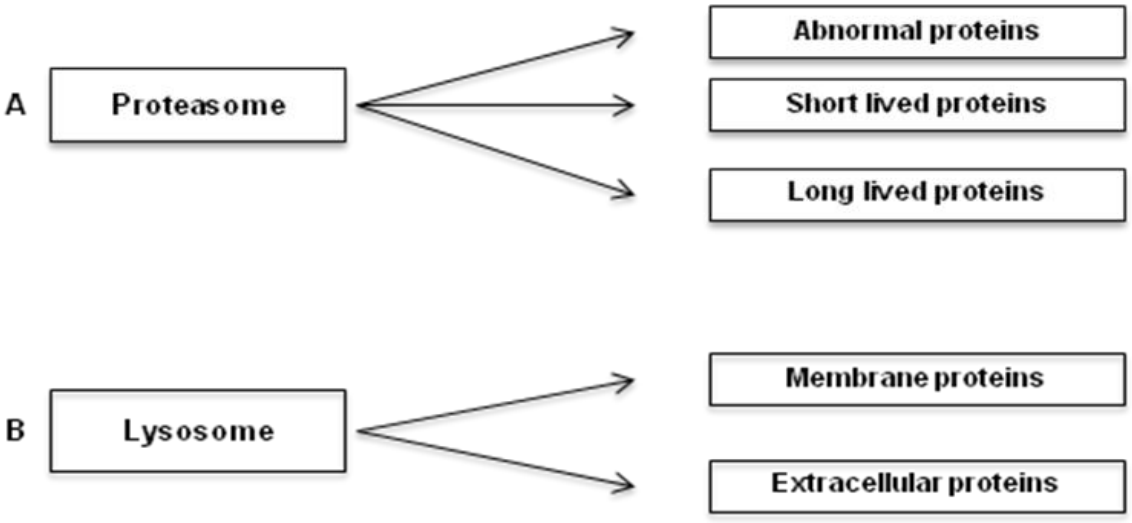

Figure 1.2 Two major pathways of protein breakdown in eukaryotic cells. (A) In mammalian cells, most proteins are degraded by the proteasome pathway (B). The breakdown of extracellular and membrane proteins is by the lysosome-endosomal pathway.

1.7 Proteasome

The proteasome is involved in the regulation of many basic cellular processes (Sakai et al., 2004) such as stress responses and apoptosis (Hilt and Wolf, 1996; Shinohara et al., 1996; Varshavsky, 1997; Chen et al., 2000; Naujokat and Hoffmann, 2002), proliferation (Naujokat and Hoffmann, 2002), signal transduction (Taylor and Jobin, 2005), metabolic regulation (Asher et al., 2005), immune surveillance (Strehl et al., 2005), differentiation (Bowerman and Kurz, 2006) and gene transcription (Collins and Tansey, 2006).

The proteasome is also present in simple primitive organisms, such as

eubacteria and archaeabacteria. The structure of the proteasome in these organisms is simple but proteolytically strong and regarded as the ancestor of the eukaryotic proteasome (Tanaka et al., 1989; Nangy et al., 1998). In eukaryotic cells, the proteasome is present in both the nucleus and cytoplasm and accounts for about 1% of total cell protein in mammalian cells (Hendil, 1988). The ratio of the proteasome in cytoplasm to the nucleus varies and depends on the status of the cells, with higher levels in proliferating and transformed cell lines than in quiescent cells (Kumatori et al., 1990).

1.7.1 Proteasome structure

The 26S proteasome is a large multi protein complex with a molecular mass of 2000 kDa. It consists of a barrel shaped 20S (700 kDa) core catalytic particle (CP) stacked by two 19S (900 kDa) regulatory particles (RP) (Orino et al., 1991; Peters et al., 1993; Walz et al., 1998). The structure and function of the proteasome is highly conserved in eukaryotes.

The functional proteolytic 20S proteasome is built up of four stacked heptameric rings arranged as two identical catalytic inner β-subunits and two structurally identical outer α rings (Löwe et al., 1995; Groll et al., 1997; Unno et al., 2002; Hu et al., 2005; Zhang et al., 2009). In higher organisms, the subunits are different (α1-α7 and β1-β7) (Zhang et al., 2009) whereas in lower organisms they are a single form (Löwe et al., 1995).

Structural and mutational studies of the yeast CP show that only three rings (β1, β2 and β5) inside the chamber have proteolytic activities, each with different substrate specificity (Groll et al., 1997; Heinemever et al., 1997; Groll et al., 1999; Jager et al., 1999). The substrate specificity is determined by the amino acid at position 45 in the β chains. Structural analysis of the β1 ring shows that it has caspase-1 like activity. It preferentially interacts with acidic amino acids like

glutamate (Hilt and Wolf, 1996; Dick et al., 1998). Glycine is the amino acid located at position 45 on the β2 ring. It preferentially cleaves after basic amino acids due to a spacious substrate pocket (trypsin like activity) (Groll et al., 1999; Heinemever et al., 1997). The chymotrypsin-like activity of the proteasome can be attributed to the β5 ring. The presence of methionine at position 45 minimises the size of substrate pocket, giving the preference to cleave neutral amino acids (Groll et al., 1997).

19S RP is composed of 19 subunits and is subdivided in two parts: a lid and a ring shaped base which binds directly to the 20S (Glickman et al., 1998). The lid consists of 9 subunits and has no ATPase activity (Rpn3, Rpn5-12). The base has 10 subunits and 6 of them (Rpt1-Rpt6) have ATPase activity while the other four have none (Rpn1, Rpn2, Rpn10 and Rpn13) (Glickman et al., 1994; Rubin et al., 1998; Glickman et al., 1998; Verma et al., 2000; Sone et al., 2004). Rpt subunits are involved in de-ubiquitination of the protein to be degraded. The structure of 26S proteasome is simplified in figure 1.3.

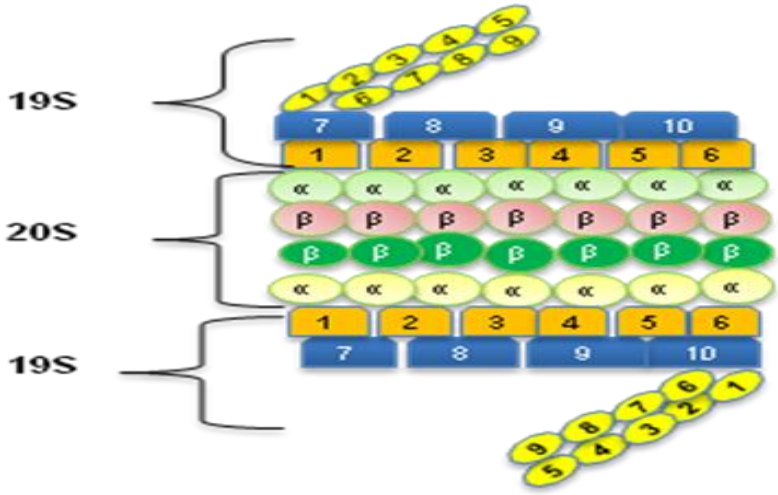

Figure 1.3 The simplified structure of eukaryotic 26S proteasome. 26S consists of a protease particle called 20S proteasome capped by two regulatory particles called 19S regulatory particles. 20S consists of four rings (αββα). Each ring consists of seven different subunits, only β1, β2 and β5 have protease activities. 19S cap consists of 19 subunits, ten of them in the base (6 have ATPase activity) and nine in the lid.

1.7.2 Ubiquitination

Apart from some exceptions (such as ornithine decarboxylase) (Murakami et al., 1992), almost all proteins degraded by 26S proteasome are tagged by a highly conserved small protein called ubiquitin (Ub) (8.5 kDa) (Wilkinson et al., 1980; Smith-Thomas et al., 1994; Hochestrasser, 1996; Hershko and Ciechanover, 1998). This pathway by which proteins are ubiquitinated and degraded by the proteasome is termed the ubiquitin-proteasome pathway (UPP).

Ubiquitination is an ATP-dependent process and involves three different enzymes (E1-E3) (Ciechanover et al., 1982). First step is the attachment of Ub to ubiquitin activating enzyme (E1) by a thioester bond (Sun, 2003). The second step involves translocation of activated Ub to an ubiquitin carrier enzyme (E2) also via a thioester bond. The third step is either direct transfer of the activated ubiquitin moiety to the substrate or ubiquitin ligase (E3) (Hershko et al., 1983). Repeated addition of Ub moieties onto the first Ub results in a poly-ubiquitinated substrate protein (Petroski and Deshaies, 2005). The minimum signal for targeting to the 26S proteasomal degradation is tetra-ubiquitin (Thrower et al., 2000; Adams, 2003). All these processes are summarised in figure 1.4.

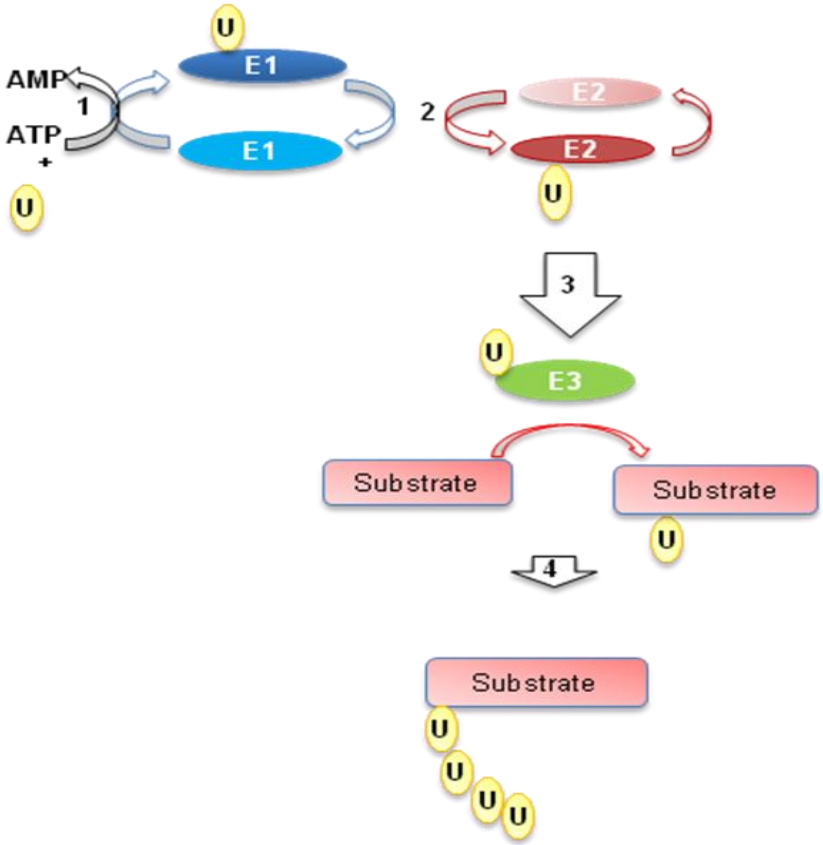

Figure 1.4 The simplified scheme of substrate ubiquitination. Ubiquitination involves 4 steps. Step 1: Ubiquitin activation by attaching to E1. Step 2: Transfer of Ubiquitin (Ub) from a ubiquitin activating enzyme (E1) via a thioester linkage to a ubiquitin carrier enzyme (E2). Step 3: E3 ubiquitin ligase which facilitates positioning and transfer of ubiquitin from the E2 directly onto the substrate and final step (4) ubiquitin chain elongation by conjugation of Ub to lysine residues of ubiquitin at position 48 (or alternatively Lys29 and 63) by an E3 ligase. Once the protein is poly-ubiquitinated it is transferred for ATP dependent substrate degradation in the 26S proteasome.

1.7.3 Proteasome function

The 20S core has a hollow cylindrical structure (160-100 Å) and provides an enclosed cavity through which proteins enter to be degraded. Openings at the two ends of the core allow the target protein to enter at one end and degraded short peptides to exit at the other end. This gating is under tight control of 19S RP the so-called "brain of the proteasome".

Recognition and removal of Ub from the tagged protein is carried out by Rpn11, a subunit in the lid of 19S (Verma et al., 2002). Genetic studies confirmed that Rpn11 mutation results in failure of de-ubiquitination and subsequently degradation of the protein (Verma et al., 2002; Yao and Cohen, 2002; Guterman

and Glickman, 2004). Once trapped, six ATPase subunits (Rpt1-Rpt6) within the base of 19S complex would form a pseudosymmetric ring complex around the substrate (Löwe et al., 1995; Groll et al., 1997; Larsen and Finley, 1997). As substrate is pushed or pulled through the narrow proteolytic chamber of the 20S cavity, the upstream globular domains destabilise and unfold (Navon and Goldberg, 2001; Smith et al., 2005). Once inside the 20S core particle, the β1, β2 and β5 rings start their different proteolytic functions and release of short peptides as well as reusable Ub (Glickman et al., 1998; Braun et al., 1999).

1.8 Proteasome controls the controllers

The UPP is critical for inflammatory responses, antigen presentation and the cell cycle. One of the first identified UPP substrates was inhibitory κB protein (IκB) (p65) which sequesters the transcription factor NF-κB (p50) in the cytoplasm of quiescent inflammatory cells (Palombella et al., 1994). Upon the stimulation of inflammatory cells, the Nt of IκB is phosphorylated at two conserved serine residues (Ser32 and Ser36) which is followed by the poly-ubiquitination at conserved lysine residues (Karin, 1999). The ubiquitinated P65 is targeted to the 26S proteasome and NF-κB is freed (Lenardo and Baltimore, 1989; Grilli et al., 1993; Palombella et al., 1994; Thanos and Maniatis, 1995; Baldwin, 1996). Released NF-κB translocates to the nucleus to exert its effects by up-regulating expression of many genes involved in the immune and inflammatory responses such as IL-1 (Leitman et al., 1992; Rhoades et al., 1992; Goldfeld et al., 1993; Kramer, 1995; Luo et al., 1996) and anti-apoptotic genes (Müller et al., 1993). Therefore, the activation of NF-κB can be inhibited by proteasome inhibitors (Sunwoo et al., 2001; Lövborg et al., 2006; Duan et al., 2007). The activation pathway of NF-κB activation is summarised in figure 1.5.

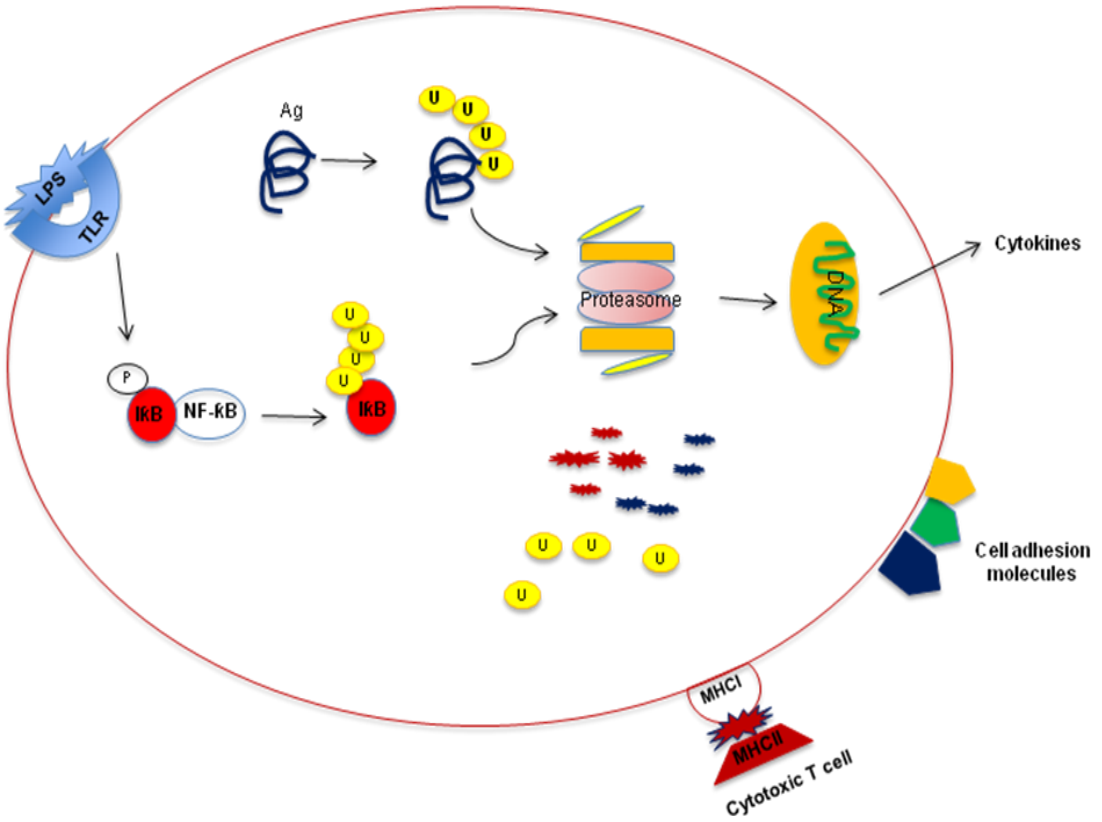

Figure 1.5 Proteasome pathways in immune system. Upon activation of Toll like receptors (TLR) by different stimuli IκB is phosphorylated by specific kinases and then ubiquitinated (U). The ubiquitinated IκB is targeted to proteasome and NF-κB released and translocated to the nucleus to activate transcription of different target genes. The synthesis of different cytokines and cell-adhesion molecules is increased by activation of the NF-κB pathway. Proteasome is also involved in degradation of the antigens. The degraded proteins will be presented on the major histocompatibility complex class I (MHCI) on the surface of infected cells to be recognised by MHCII on the surface of cytotoxic T cells.

The proteasome is also involved in the initiation of the immune response. Small degraded peptides by UPP derived from infected cells (virally or oncogenic transformants) are presented on the surface of the immune cells in combination with major histocompatibility complex class I (MHCI). Cytolytic CD8 T lymphocytes will be stimulated by these displayed peptides and eliminate the offending cell (Goldberg and Rock, 1992; Germain and Margulies, 1993; Townsend and Trowsdale, 1993) (Figure 1.5).

Another transcription factor, the tumour suppressor protein 53 (p53), is also regulated by UPP (Maki et al., 1996). p53 is phosphorylated and activated in response to cellular stress or Deoxy-Ribonucleic Acid (DNA) damage and this

causes its dissociation from its inhibitor MDM2. Once activated, p53 is no longer targeted for proteasomal degradation. It binds to specific DNA sequences and initiates transcription of genes and induces growth arrest, DNA repair or apoptosis (Vogelstein, 2000; Bratton and Cohen, 2001).

1.9 Proteasome activity and diseases

A functional proteasome system is essential for all eukaryotic cells since UPP is involved in many cellular regulatory functions. Therefore, any alteration in proteasome activities or its components influences cellular homoeostasis and results in pathological conditions.

Depression in activity or integrity of proteosomal enzymes results in the accumulation of abnormally folded proteins and formation of inclusion bodies. This causes development of neurodegenerative diseases such as Parkinson's disease (McNaught and Jenner, 2001), Huntington disease (Zhou et al., 2003) and Alzheimer disease (AD) (Keck et al., 2003; Oh et al., 2005). It has been shown that proteasome activity has an inverse relationship with aging (Reviewed in Layfield et al., 2005; Martinez-Vicente et al., 2005). Reduction of proteasome activity in the elderly leads to the pathogenesis of many diseases prevalent in this group of people. The most affected tissues are shown in figure 1.6. These diseases have been also extensively reviewed in Grillari et al., 2006.

The reduction of all three proteasome peptidase activities of the 20S proteasome has been found in eye lens nuclei of elderly individuals, which favours cataract formation (Zetterberg et al., 2003). Down-regulation of the proteasome in myocardial tissue reduces tolerance of the heart to ischaemia/reperfusion (Divald and Powell, 2006) and also accumulation of pro-apoptotic proteins that later induce apoptosis, cardiac dysfunction and consequently, increases the susceptibility of the heart to cardiovascular diseases (Tsukamoto et al., 2006). In

aged keratinocytes (Petropoulos et al., 2000) and human fibroblasts (Chondrogianni et al., 2003), the reduction in proteasomal peptidase activities (chymotrypsin-like) is coupled with increased levels of both oxidised and ubiquitinated proteins

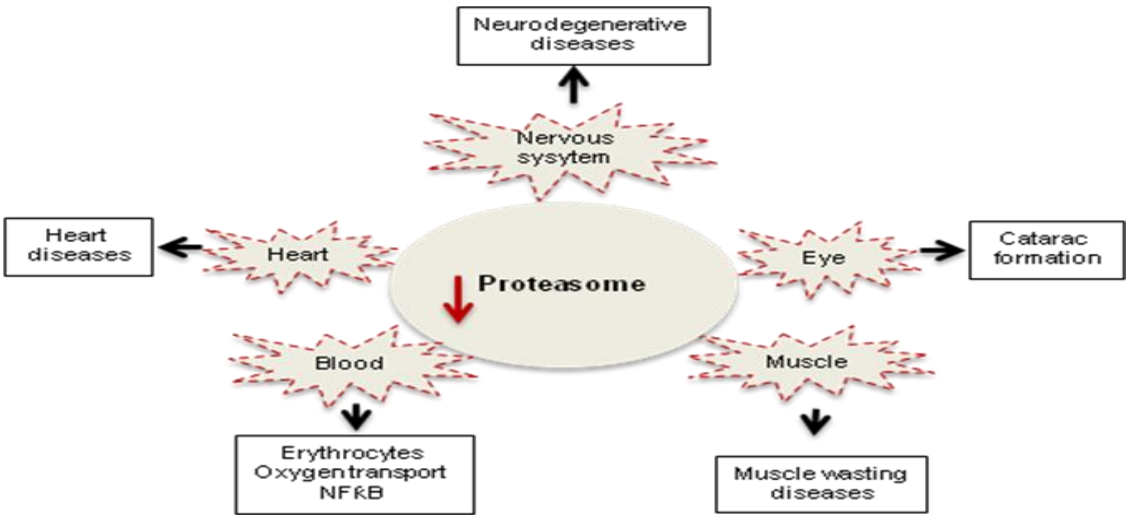

Figure 1.6 Decrease of proteasome activity affects different tissues. The activity of the proteasome is reduced in elderly people. The reduction of protein degradation affects different tissues such as nervous system, eye, liver and muscle.

The structural alterations of proteasome subunits may also contribute to the observed age-related decline of proteasome activity. The distribution and silver staining intensities of proteasome subunits were found to vary with age in human epidermis (Bulteau et al., 2000) and human lymphocytes (Carrard et al., 2003) as determined by two-dimensional gel electrophoresis of purified 20S proteasome. The decline of chymotrypsin-like activities in epidermis (Bulteau et al., 2000) and human lymphocytes (Carrard et al., 2003) causes the increase of oxidised and ubiquitinated proteins.

The UPP also plays an essential role in immune surveillance. The down-regulation of proteasome activity decreases the immune response by the reduction of proteasomal degradation of proteins into antigenic peptides. Down regulation of

proteasome expression in some tumour types such as renal carcinoma (Johnson et al., 1998; Meidenbauer et al., 2004) and viral infections such as HIV, leads to the escape of cells from immune surveillance and favours proliferation (Goldberg and Rock, 1992; Germain and Margulies, 1993; Restifo et al., 1993, Seliger et al., 1996; Delp et al., 2000; Ott et al., 2003).

Skeletal muscle atrophy is a hallmark of many systemic diseases such as diabetes (Price et al., 1996; Taillandier et al., 2003), cancer cachexia (Llovera et al., 1994; Temparis et al., 1994; Baracos et al., 1995), metabolic acidosis (Mitch, 1994) and sepsis (Hobler et al., 1999). The loss of muscle mass in these different states is due to up-regulation of UPP (Jagoe et al., 2001). It has been shown that the expression of mRNAs of many genes involved in protein degradation, including polyubiquitins, Ub fusion proteins, the Ub ligases, multiple but not all subunits of the 20S proteasome and its 19S regulator significantly increased in these four catabolic states (Flann et al., 1997; Lecker et al., 2004).

Higher expression of β1 and β5 subunits of proteasome was found in neurones, astrocytes and endothelial cells in the brain of AD patients (Mishto et al., 2006). This enhanced presence in aging brain and muscle tissue could reflect a persistent inflammation.

Different synthetic and natural proteasome activators or inhibitors have been used in different pathologies and present potential therapeutic properties (reviewed in Delcros et al., 2003). For example, proteasome-activating or modulating compounds could be more effective for neurodegenerative diseases, whereas proteasome inhibitors could be beneficial to induce apoptosis of cancer cells.

1.10 Major classes of proteasome inhibitors

Protein synthesis inhibitors have been used for a long time to establish protein function and turnover. The introduction of proteasome inhibitors has led to a similar and rapid analysis of protein turn-over in living cells. Any changes in intracellular protein turn-over by proteasome inhibitors, is a strong indication of proteasome-mediated degradation. Stronger evidence can be obtained by direct measurements of changes in the half-life of the protein and demonstration that the protein is stabilised after addition of the proteasome inhibitor. Synthetic and natural proteasome inhibitors that could selectively inhibit proteasomal degradative pathway are available. These inhibitors are usually short peptides with low molecular weight attached to a C-terminal pharmacophore. They can enter the cells readily and their pharmacophore interacts with a catalytic residue forming reversible or irreversible covalent adduct (Fenteany et al., 1995; Dick et al., 1996; Tsubuki et al., 1996; Mellgren, 1997; Adams et al., 1998).

There are different classes of proteasome inhibitors each affecting different active sites of the proteasome. The inhibitors affecting a chymotrypsin-like site are hydrophobic, and more permeable (Rock et al., 1994; Chen and Hochstrasser, 1996; Kisselev et al., 1999). In contrast, the trypsin-like or caspase-like inhibitors contain charged residues and are less permeable and therefore have less effect on overall proteolysis (Arendt and Hochstrasser, 1997; Heinemeyer et al., 1997; Kisselev et al., 1999).

1.10.1 Peptide aldehydes

The first developed and most widely used proteasome inhibitors are the peptide aldehyde class. These compounds are reversible inhibitors and also inhibit lysosomal and calcium activated proteases (Tsubuki et al., 1996; Mellgren, 1997). These compounds have fast dissociation rates. They enter the cells, bind the

proteasome and are oxidised into inactive acids and transport out of the cells rapidly. Therefore, they do not affect cell viability and growth (Rock et al., 1994; Lee and Goldberg, 1996). These inhibitors block the chymotrypsin-like proteolytic activity of the 26S proteasome without influencing its ATPase or isopeptidase activities (Groll et al., 1997). X-ray diffraction analysis has suggested a hemiacetyl complex is formed with the N-terminal threonine hydroxyl group of β-chains of the proteasome and the inhibitor (Salvesen and Nagase, 1989). The mutation of this threonine to Ala abolishes the activity of this enzyme (Groll et al., 1997). One of the best examples is ALLN (acetyl-Leu-Leu-norleucinal) (Vinitisky et al., 1992; Rock et al., 1994). Another useful aldehyde inhibitor is MG132 (Cbz-Leu-Leu-leucinal). Although these compounds are less specific, their availability and low cost make them good candidates for the study of proteasome functions in mammalian cells.

1.10.2 Peptide boronates

These compounds are highly selective and present 100 fold higher potency compared to aldehyde inhibitors (Adams et al., 1998). These compounds are considered as reversible proteasome inhibitors, but their dissociation rate is much slower than the aldehyde inhibitors. They form stable tetrahedral intermediates with the N-terminal threonine residues of the catalytically active proteasome β subunits (McCormack et al., 1997).

The combination of being metabolically stable, highly potent and selective make these compounds good drug candidates for the inhibition of proteasome activities. One of the best boronate inhibitors is the boronate analogue of MG132, MG262 (Z-Leu-Leu-Leu-boronate) which is 100-fold more potent than MG132 (Adams et al., 1998).

1.10.3 Non-peptide inhibitors

A naturally derived and more specific proteasome inhibitor is the antibiotic lactacystin (Fenteany et al., 1995; Dick et al., 1996). Lactacystin was originally isolated from the cultured broth of a *Streptomyces* strain by Omura and colleagues when they were trying to isolate microbial metabolites that induced differentiation of neuroblastoma using the Neuro 2A, murine neuroblastoma cell line. This antibiotic induced outgrowth of neurite-like structure in the Neuro 2A cell line (Omura et al., 1991).

Mammalian cells (Dick et al., 1997) and yeast (Lee and Goldberg, 1996) are not permeable to lactacystin. In aqueous solution (neutral pH) lactacystin spontaneously hydrolysed to its active form *clasto*-lactacystin β-lactone (β-lactone) which is cell permeable. β-lactone is a significantly more selective proteasome inhibitor than peptide aldehydes and also 20-fold more effective than lactacystin (Ostrowska et al., 1997; Geier et al., 1999). It can enter the cell and reacts with the proteasome's active site threonines resulting in the opening of the β-lactone ring and acylation of the proteasome's catalytic hydroxyl group (Dick et al., 1996; Dick et al., 1997). Both lactacystin and β-lactone block all of the β subunits proteaolytic activities (chymotryptic, tryptic-like and peptidylglutamyl) but with very different kinetics (Craiu et al., 1997). The mode of action has been elucidated from studies using radiolabeled synthetic lactacystin which rapidly and irreversibly inactivates the chymotryptic activity of 20S proteasome. This irreversible inhibition is due to covalent modification of the hydroxyl groups of the highly conserved amino-terminal threonine on the β5 subunits of the proteasome (Fenteany et al., 1995). Other proteolytic sites (the tryptic and peptidylglutamyl) of the proteasome are also reversibly inhibited but at much slower rates (Craiu et al., 1997; Fenteany et al.,

1995). The mechanism of proteasome inhibition by lactacystin is summarised in figure1.7.

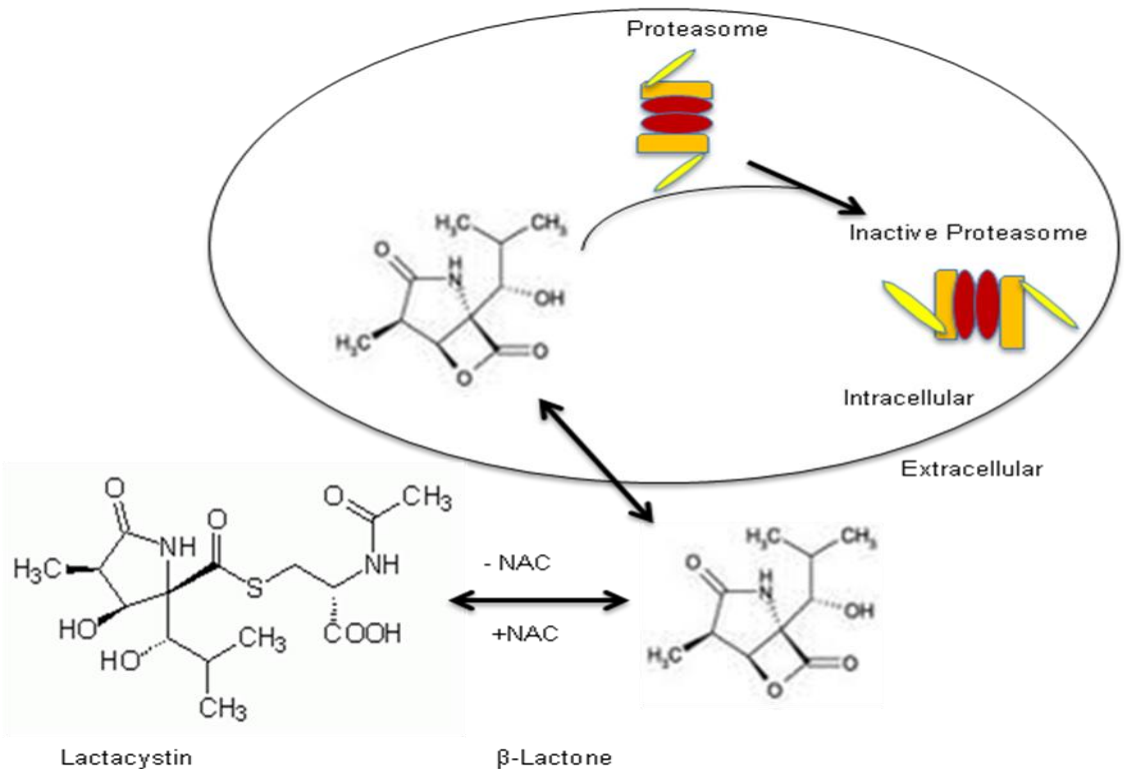

Figure 1.7 Mechanism of proteasome inhibition by lactacystin. In aqueous solution (neutral pH) lactacystin is spontaneously is hydrolysed to its active form, β-lactone which can easily enter cells. It reacts with hydroxyl group of the active site amino acid in proteasome and inactivates the proteasome.

1.11 Proteasome inhibitors: research tools

The inhibition of the UPP has profound effects on the modification and degradation of many highly regulatory eukaryotic proteins such as tumour suppressors, transcription factors and cytokines.

Mutation of p53 is common in many types of cancers and contributes to both tumour formation and drug resistance (Hollstein et al., 1991). Treatment of Rat-1 fibroblasts and pheochromocytoma (PC12) cells with proteasome inhibitors caused a stabilisation and accumulation of transcriptionally active p53, which is required for apoptosis (Lopes et al., 1997). In malignancies, such as human papilloma virus (HPV)-related cancers, the degradation of p53 is increased due to

increased activation of the UPP (Spataro et al., 1998). Restoration of p53 status by proteasome inhibitors could have therapeutic potential in these malignancies.

Defective apoptosis is involved in the pathogenesis of several diseases including cancers. UPP appears to be involved in inducing apoptosis (the major form of cell death) in proliferating cells and to be protective in quiescent or terminally differentiated cells (Drexler, 1997). In B cell chronic lymphocytic leukaemia (B-CLL), a low dosage of lactacystin increases apoptotic cell death in malignant lymphocytes obtained from patients with B-CLL compared to normal human lymphocytes (Masdehors et al., 1999). Treatment of human multiple myeloma (MM) and human squamous cell carcinoma (SCC) by another proteasome inhibitor, PS-341, also increased apoptosis by blocking the activation of NF-κB pathway (Hideshima et al., 2001; Sunwoo et al., 2001; Dudek et al., 2010).

The effect of proteasome inhibitors has been also studied in neurones and these reagents stabilise signals of survival and differentiation. Treatment of rat PC12 neuronal cells by β-lactone induced the neurite outgrowth elevated levels of ubiquitylated protein and stabilised Ub-dependent substrates (Obin et al., 1999). Consistent with this observation, addition of lactacystin at various concentrations to cultures containing the major myelin-producing cells in the CNS (oligodendroglial cell precursors) was found to induce their withdrawal from the cell cycle and induce their biochemical and morphological differentiation, with the appearance of extensive myelin-like sheets (Pasquini et al., 2003). The three classic proteolytic activities of the proteasome were also significantly decreased.

Blockage of proteolytic activity of the proteasome by MG132 and β-lactone, in the human monocytic cell line THP-1 causes stabilisation of intracellular pro-IL-1β levels and this leads to a corresponding increase in IL-1β and pro-IL-1β into

culture supernatants of activated monocytes (Moors and Mizel, 2000). MG132 prevents the degradation of IL-2 in the culture of mouse C57BL/6 spleen cells (Yu and Malek, 2001). Treatment of human umbilical vein endothelial cells by MG132 increased the expression of IL-6 mRNA and protein release. This effect could be reversed by actinomycin D, suggesting the transcriptional upregulation of IL-6 under proteasomal inhibition (Shibata et al., 2002). Inhibition of proteasome activity by different proteasome inhibitors causes a significant increase in release of IL-8 in different cells types such as human epithelial A549 cells and human embryonic kidney HEK293T (Wu et al., 2002), lung carcinoma cell line A549 and human monocyte cell line THP-1 (Gerber et al., 2004).

These experiments strongly suggest that the proteasome is an important factor in the regulation of pro-inflammatory cytokines and their receptors. These finding led us to investigate the effects of proteasome inhibitors on the stability and release of IL-1α and IL-1β in J774 and mouse bone marrow derived macrophages (BMDM) as a model. The effects of proteasome inhibitors on IL-1 expression and release may provide additional information for understanding their beneficial use in treatment of inflammatory diseases.

1.12 Aims

IL-1β is an active immunoregulator of the inflammation; therefore its production, activation and degradation are tightly regulated. The transcription of pro-IL-1β is upregulated upon activation of TLR by bacterial stimulus (such as LPS). Then, pro-IL-1β could follow two pathways, (1) it can be processed and secreted by activation of NLR and caspase-1 responding to a second stimulus (such as ATP) and the mature IL-1β corresponding to the Ct of the pro-IL-1β exerts its biological functions; or (2) in the absence of a second stimulus intracellular pro-IL-1β is degraded.

Until now the remaining Nt domain of pro-IL-1β has been regarded only as the conformational repressor of IL-1β activity, and it is not known if the 10 and 14 kDa N-terminus derived peptides after pro-IL-1β processing by caspase-1 have any immunoregulatory functions. Therefore the first objective of this study was designed to answer this question. The second objective focused in the degradation pathway of pro-IL-1β if there is no activation by second stimulus. The two aims of this study are summarised in figure 1.8.

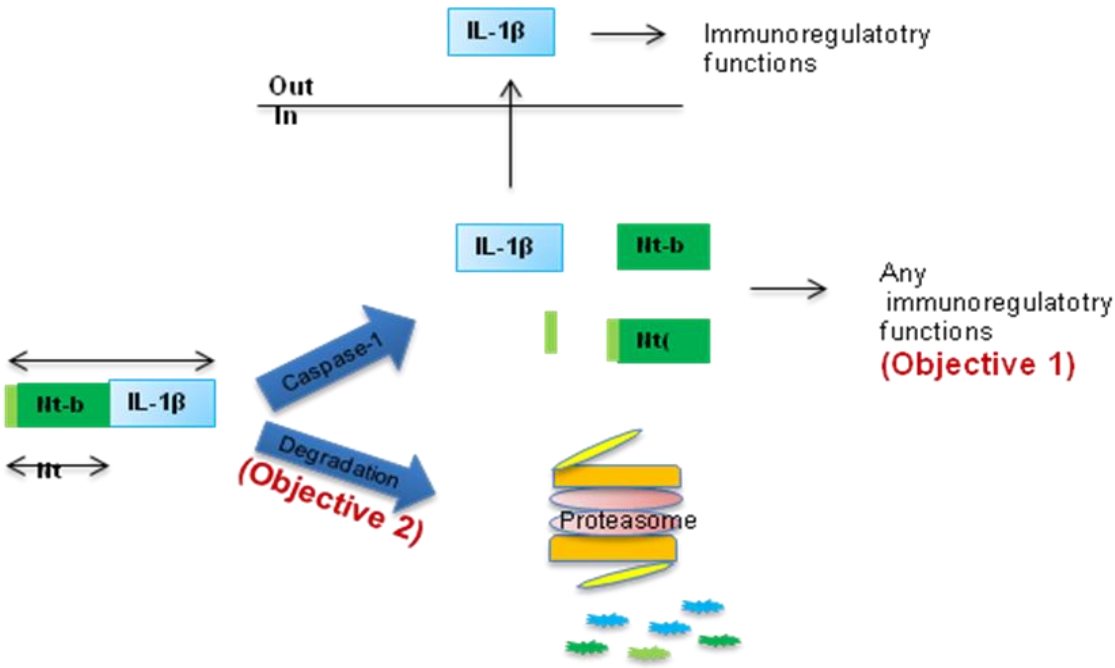

Figure 1.8 Schematic diagram to summarise the aims of this project. The processing of pro-IL-1β is carried out by caspase-1 upon activation of specific cytoplasmic receptors. Mature IL-1β binds to IL-1RI to exert its immunological functions. But until now the N-terminus of pro-IL-1β is regarded as a suppressor domain of pro-IL-1β. The first objective of this study was to find out if pro-IL-1β Nt has any immunolregulatory functions, whereas the second objective involved the degradation pathway for intracellular pro-IL-1β if there is no secondary stimulus to induce its processing.

This thesis comprises four experimental chapters, each describing experiments testing the following hypotheses:

- The N-terminus of pro-IL-1β has immune regulatory functions. In order to test this hypothesis, the N-terminus of pro-IL-1β was cloned and expressed in bacteria (chapter 3) and mammalian cells (chapter 4).

- The proteasome is involved in the degradation of IL-1 (chapter 5).
- IL-1 is tagged by a highly conserved ubiquitin protein before targeting it to the proteasome (chapter 5).
- The inhibition of the proteasome affects the stability and the release of IL-1 (chapter 6).

CHAPTER 2

Materials and Methods

2.1 Chemicals

All chemicals and reagents used in this work were purchased from Sigma Aldrich (UK), unless otherwise stated.

2.2 Bacterial expression

2.2.1 Bacterial strains, media and plasmids

The plasmid pET-22(+) (Novagen, UK) was used for sub-cloning of the Nt genes. pET-22(+) has an N-terminal 6x-Histidine tag (His-tag) upstream of restriction sites for *Nde*I and *Xho*I on the multiple cloning site (MCS). *Escherichia coli* (*E. coli*) strains JM109 and DH5-α (Invitrogen, UK) were used for transformation of human pro-IL-1β and its N-terminus (Nt) of IL-1β. *E. coli* BL21(DE3) (Novagene, USA) was used for protein expression of pro-IL-1β and IL-1β Nt proteins.

Bacteria were grown in Luria Bertani Medium (LB): 1% w/v peptone from casein, 0.5% w/v yeast extract, 17 mM NaCl pH 7.0 (Merck, UK), supplemented with 1.2% w/v agar for colony selection on plates. *E. coli* containing recombinant plasmids was selected by adding the antibiotic ampicillin (50 µg/ml) to the medium (Bioline, UK).

2.2.2 General sub-cloning methods

All DNA manipulations were carried out using standard techniques (Sambrook et al., 1989). Sub-cloning strategies (summarised in Figure 2.1) were designed for the production of 10 kDa N-terminus fragment (Nt-b), 14 kDa N-terminus (Nt) and pro-IL-1β. Polymerase chain reaction (PCR) primers (synthesised by Sigma Genosys, UK) were designed to maintain the reading frame throughout the fusion proteins. Primers were designed to add *Nde*I restriction site at the 5' end and *Xho*I site at the 3' end of constructs to facilitate

cloning into the MCS of linelarised pET-22(+). The summary of cloning steps is explained in figure 2.1. Details and sequence of the primers are given in table 2.1. The *Nde*I (CATATG) restriction site between 1329-1333 nucleotides of pro-IL-1β DNA was changed by designed mutagenic primers (see Table 2.1) but still coded for the same amino acid, proline. Following all sub-cloning steps, recombinant plasmids were transformed into competent *E. coli* JM109 (Invitrogen, UK), transformed bacteria were selected on LB-agar plates containing ampicillin (50 µg/ml). Bacterial colonies were screened for the presence of the appropriate recombinant plasmid by DNA isolation (Qiaspin MINIprep, Qiagen, UK) and restriction digest analysis. The presence of inserts in recombinant plasmids was confirmed by sequencing (Beckman Coulter Genomics, UK).

Gene	Primers (sequence from 5' to 3')
Mutagenic Primers	
Pro-IL-1β-*Nde*I	F-*Nde*I: GATGTCTGGT**CCT**TATGAACTGAA R-*Nde*I: TTCAGTTCATA**AGG**ACCAGACATC
Sub-cloning Primers	
His-pro-IL-1β	F1: CATATGGCAGAAGTACCT GAGCTCG R1: CTCGAGAGACACAAATTGCATGGTG
His-Nt	F1: CATATGGCAGAAGTACCT GAGCTCG R2: CTCGAGGTGCACATAAGCCTCGTTATCC
His-Nt-b	F2: CATATGGGCCCTAAACAGATGAAG R2: CTCGAGGTGCACATAAGCCTCGTTATCC

Table 2.1 Subcloning and mutagenetic primers. Forward (F) and Reverse (R) primers used in subcloning and site directed mutagenesis. Restriction enzyme sites are underlined and point mutation is in bold.

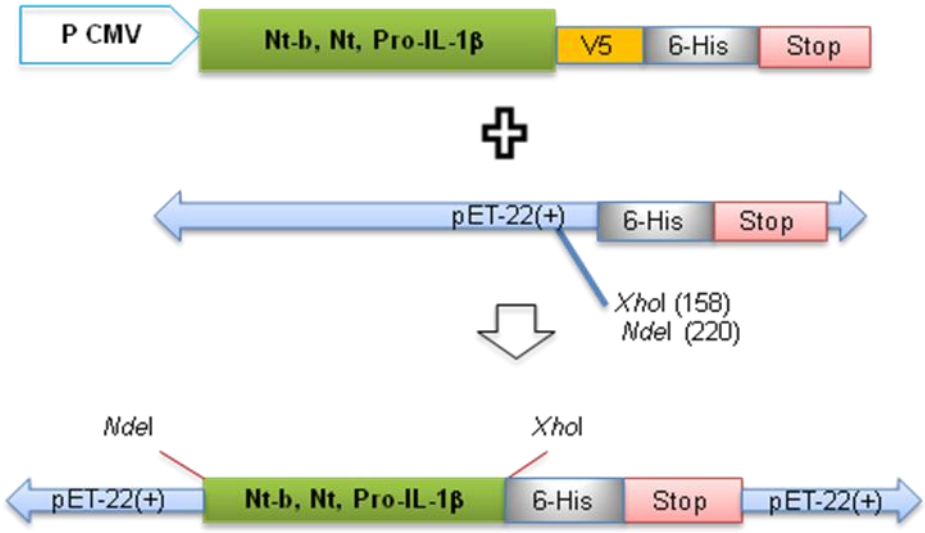

Figure 2.1 Cloning of Nt-b, Nt and pro-IL-1β into pET-22(+). The original DNA was amplified by PCR. Primers were designed to insert *Nde*I and *Xho*I at 5' and 3' termini of the genes, respectively. Before ligation, pET-22(+) vector and genes were double digested by *Nde*I and *Xho*I. Primers were designed to maintain the reading frame throughout the fusion proteins.

2.2.3 Bacterial expression constructs of Nt-b, Nt and pro-IL-1β

Amplifications were carried out in 25 µl volumes containing 0.5 µM of each primer, 5 µl 10x PCR buffer, 0.2 mM nucleotide (dATP, dCTP, dGTP, and dTTP, Invitrogen, UK), 2.5 U of Accuzyme DNA polymerase (Bioline, UK) and 10 ng plasmid DNA. PCR was carried out in a master gradient thermocycler (Techne TC-3000, UK). The gene amplification conditions were as follow: initial denaturing at 94ºC for 2 min, then 20 cycles consisting of 94ºC for 30 sec, 50ºC for different times depending on the size of DNA (first PCR of pro-IL-1β fragments, Nt-b and Nt: 1 min), 72ºC for 1 min and an additional polymerisation step at 72ºC for 7 min. The first PCR DNA products of pro-IL-1β were used directly as the template for a second round of amplification after melting at 80ºC for 5 min in a heating block. The second PCR of pro-IL-1β was set up as follows: initial denaturing at 94ºC for 2 min, then 20 cycles consisting of 94ºC for 30 sec, 50ºC for 2 min, 72ºC for 1 min and an additional polymerization step at 72ºC for 7 min.

The PCR products were purified by QIAQuick™ PCR column purification kit (Qiagen, Germany) according to the manufacturer's instructions. Five volumes of

Buffer PBI (Qiagen, Germany) was added to the PCR reaction, mixed and then placed in a QIAquick column and centrifuged for 60 sec. The column was washed by adding 0.75 ml PE buffer (Qiagen, Germany) and centrifuged for 1 min. The column was placed in a clean 1.5 ml micro-centrifuge and 50 µl water added to the centre of a column, left for 1 min and centrifuged for 1 min at 10000 x *g* (gravity x force). The purified PCR product was loaded on a 1% low melting point agarose gel (Invitrogen, UK), containing 0.5 µg/ml ethidium bromide, and run in modified Tris-acetate-EDTA (TAE) buffer (Millipore, UK) at 90 V for 1 h. The amplified bands containing the insert (Nt-b and Nt genes) were cut out using a clean razor. The extra gel was removed and the band stored in a new tube at -20ºC for later use. Both PCR products and vector were digested by *Nde*I and *Xho*I (Promega, UK) restriction enzymes as shown in table 2.2.

The restriction digests for vector and inserts were left for 4 and 5 h at 37ºC, respectively. In order to prevent re-ligation of sticky ends of digested vector, de-phosphorylation was carried out by adding alkaline phosphatase (AP, Promega) (1 µl) in the presence of 10x AP buffer (10 µl) made up to the total volume to 100 µl by addition of dH_2O and left for another 1 h at 37ºC. The digested products were run on 1% low melting point gel for 1 h at 90 V. The bands were cut from the gel and kept at -20ºC for ligation. A specific high molecular DNA marker (Invitrogen, UK) was used to quantify the amount of DNA for the subsequent ligation reaction. A ratio of 1:10 vector insert was used to increase ligation on the basis of the formula below:

$$\text{ng insert} = [25 \text{ ng Vector} \times \text{kb insert} \times 10] / \text{kb vector}$$

The reaction was set up in a sterile micro-centrifuge tube as shown in table 2.3.

Insert digestion	Quantity		pET-22(+) digestion	Quantity
Insert	45 (µl)		Vector	10 (µl)
Buffer D (10x)	6 (µl)		Buffer D (10 x)	2 (µl)
*Nde*I	10 U		*Nde*I	10 U
*Xho*I	10 U		*Xho*I	10 U
dH_2O	7 (µl)		dH_2O	6 (µl)
Total	60 (µl)		Total	20 (µl)

Table 2.2 Restriction digestion reactions of amplified fragments and pET-22(+) vector. The PCR products of inserts (Nt-b, Nt and pro-IL-1β) and pET-22(+) vector, were digested by *Nde*I and *Xho*I for 4 h and used for the ligation reaction. Each µl of enzyme represents 10 Units (U).

	Pro-IL-1β	Nt	Nt-b	Auto-ligation control
Ligase 10X buffer	2 µl	2 µl	2 µl	2 µl
Insert DNA (250 ng)	3.4 µl	2.53 µl	2.22 µl	----
Vector DNA (25 ng)	3.7 µl	3.7 µl	3.7 µl	3.7 µl
T4 DNA Ligase (Invitrogen, UK)	1 U	1 U	1 U	1 U
dH_2O	9.9 µl	10.77 µl	11.1 µl	13.3 µl
Total	20 µl	20 µl	20 µl	20 µl

Table 2.3 Ligation recipe for inserts and vector. Restriction digest products of Nt-b, Nt and pro-IL-1β) were ligated to digested pET-22(+) vector at 20ºC overnight by ligase. Each µl of enzyme represents 10 Units (U).

The ligation reaction mixtures were made up to 20 µl with dH_2O and incubated at 20ºC overnight. The ligation reactions were then heated at 70ºC and mixed with 2x cold sterile TCM buffer (TrisHCl 20 mM, $CaCl_2$ 20 mM, $MgCl_2$ 20 mM, pH 7.5). The mixture was added to the ice-thawed competent *E. coli* JM109 cells (Invitrogen, UK) and left on ice for 20 min. The cells were heat-shocked at 42ºC for 45 sec exactly and returned to the ice for 2 min. One ml of SOC (Super Optimal Culture, Invitrogen, UK) medium was added to each tube before incubation at 37ºC with vigorous shaking for 1 h. Following incubation, the cells were centrifuged at 2000 x *g* (low speed) for 10 min and resuspended in 100 µl of supernatant before being plated on LB agar containing ampicillin (50 µg/ml) and incubated overnight at 37ºC.

2.2.4 Screening of transformed colonies

Colonies were picked up with a sterile yellow tip swirled in 5 µl dH_2O and then used to inoculate to a LB agar plate containing ampicillin (50 µg/ml) and left at 37ºC for 7 h. The positive colonies were selected following PCR. PCR mix was prepared as shown in table 2.4 using Taq polymerase (Promega, UK).

Amplification was carried out by 35 cycles consisting of 94ºC for 30 sec, 50ºC for 30 sec, 72ºC for 30 sec after initially denaturing at 94ºC for 30 sec. Gel loading buffer was added to each reaction and analysed by agarose gel electrophoresis (1%) for 1 h at 100 V.

	Master Mix for pro-IL-1β (µl)	**Master Mix for Nt and Nt-b (µl)**
dH_2O	6.3	6.3
dNTPs	1.00	1.00
Primers (Table 2.1)	T7 (2)+R*Nde*I (2)	T7 (2)+R2 (2)
$MgCl_2$	1.6	1.6
Buffer 10x	2.00	2.00
Taq polymerase	0.1	0.1
Total	20.00	20.00

Table 2.4 PCR reactions for screening. The positive colonies were amplified by PCR 35 cycles consisting of 94ºC for 30 sec, 50ºC for 30 sec, 72ºC for 30 sec after initial denaturing at 94ºC for 30 sec.

2.2.5 DNA purification

A QIAprep Miniprep kit was used to purify plasmid DNA according to the manufacturer's instructions. Briefly, a bacterial colony was inoculated into a 10 ml starter culture containing LB broth and ampicillin (50 µg/ml), and shaken at 37ºC at 225-250 rpm overnight. One ml of this culture was centrifuged at 5000 x *g* for 10 min and the pellet was resuspended in Buffer P1 (RNAase) before buffer P2 (detergent) was added and the tubes gently inverted few times. Buffer N3 (guanidine hydrochloride and acetic acid) was then added and inverted gently. Following centrifugation for 10 min at 9000 x *g*, the supernatant was transferred to

a QIAprep spin column and centrifuged for 30 sec. The column was washed first by Buffer PB and then twice by PE. After each wash it was centrifuged for 30 sec to discard the flow through. The DNA was then eluted into 50 µl Buffer EB (10 mM Tris-HCl pH 8.5) or dH_2O by further centrifugation.

2.2.6 Restriction enzyme digestion

The identity of the purified plasmid was verified by performing restriction digest of constructs with different restriction enzymes. Restriction digest reaction mixtures were made up of 2 µg DNA sample, 2 µl of 10x buffer and 1 unit of each enzyme to be used. Promega (UK) or New England Biolabs (UK) enzymes were used. The detail of specific buffer for each enzyme is given in table 2.5. The reaction mixture was made up to 20 µl with dH_2O and incubated at 37ºC for 1 h.

Restriction enzyme	Supplier	Buffer
*Bbv*CI	New England Biolabs	NEB 4
*Eco*0109I	New England Biolabs	NEB 4
*Nde*I	Promega	Buffer D
*Xho*I	Promega	Buffer D
*BspE*I	New England Biolabs	NEB 3
*EcoR*V	Promega	Buffer D
*Xmn*I	New England Biolabs	NEB 2

Table 2.5 Restriction enzyme used in this study. The constructs were digested with different restriction enzymes.

2.2.7 Agarose gel electrophoresis

In order to visualise the purification and restriction digest products, the DNA samples were resolved using agarose gel electrophoresis. The gel was prepared by dissolving 1% (w/v) agarose (Invirtogen, UK) in TAE buffer (40 mM Tris acetate pH 8, 1 mM Ethylene Diaminetetra Acetic Acid (EDTA)) by heating in a microwave on full power for approximately one min. The solution was allowed to cool slightly

once the agarose was dissolved. 0.2 µg/ml ethidium bromide was added and gently mixed. Gels were cast using a Biorad Sub-Cell GT tank that was filled with TAE buffer once the gel was set. DNA samples were diluted by bromophenol blue loading buffer (0.25% w/v bromophenol blue, 0.25% w/v cyanol, 40% w/v sucrose) and loaded onto the gel along with a DNA ladder (Bioline, UK). Loaded gels were run at 100 V for 1 h or until the dye had moved two thirds of the length of the gel using a BioRad Power supply (UK). DNA bands were visualised by placing the gel on an ultraviolet transilluminator and photographed using an imaging system (Image station 4000 MM Pro, Kodak).

2.2.8 Sequencing of recombinant plasmid DNA

PCR fragments were purified using the QIAQuick^{TM} PCR column purification kit (Qiagen, Germany) and sent to Beckman Coulter Genomics, UK for sequencing. Alignments to analyze the sequences were performed using the Clustal X program (Thompson et al., 1997).

2.2.9 Plasmid transformation into *E. coli* competent cells

E. coli strain BL-21(DE3) was used for transformation by recombinant plasmids. Competent cells were thawed on ice for 5 min and then recombinant DNA was added and left on ice. After 5 min, the competent cells were heat shocked at 42ºC for 30 sec. Cells were placed on ice for another 5 min before adding 250 µl pre-warmed SOC medium to the cells. Cells were incubated at 37ºC with vigorous shaking (250 rpm) for 1 h. Positive transformants for *E. coli* strain BL-21(DE3) were selected by plating out 200 µl of the reaction on LB agar containing ampicillin (50 µg/ml) and grown overnight at 37ºC.

2.2.10 Induction conditions

An individual colony was selected and used to inoculate 1 ml LB containing ampicillin (50 µg/ml) and grown overnight at 37ºC with vigorous shaking. After 16 h, 10 ml fresh LB medium was inoculated with 1 ml of overnight culture and then grown at 37ºC with shaking until an optical density at 600 nm (OD_{600}) of between 0.7-0.8 was reached. Protein expression was induced by addition of different concentrations (1-5 mM) of isopropyl-β-thiogalactopyranoside (IPTG, Promega, UK). The cultures were grown overnight at 37ºC with shaking at 250 rpm. At the end of the induction periods, the cultures were chilled on ice before being harvested by centrifugation at 4ºC for 15 min at 10000 x *g*. Each cell pellet was frozen at -80ºC for future experiments.

2.2.11 Expression conditions

Expression cultures were set up as explained in section 2.2.10. Each culture was induced with IPTG (2 mM). The cultures were grown at two temperatures: 22 and 28ºC for different time points (1 to 5 h) with shaking at 250 rpm. Samples of 1 ml were taken at each time point in the production phase and centrifuged immediately at 10000 x *g* at 4ºC for 15 min. Pellets were stored at -80ºC for future analysis.

2.2.12 Large-scale expression cultures

Three 2.5 litre flasks containing 500 ml LB were inoculated with 25 ml overnight culture and grown under shaking at 37ºC until the OD_{600} of between 0.7-0.8 was reached. The expression was started by adding IPTG to a final concentration of 2 mM for three cultures of Nt-b, Nt and pro-IL-1β. The temperature was reduced to 22ºC for pro-IL-1β and was grown for 2 h with vigorous shaking. Nt-b and Nt cultures were grown at 28ºC for 2 and 4 h,

respectively with shaking. After the appropriate time points the cells were harvested by centrifugation at 10000 x *g* for 15 min at 4ºC. The pellets were washed with ice-cold PBS, centrifuged and were stored at -80ºC for future experiments.

2.2.13 Solubilisation and purification of expressed proteins

The frozen cell pellets were thawed on ice and re-suspended in lysozyme based Bugbuster® protein extraction reagent (Novagen, UK). The cells were fractionated into soluble and insoluble material according to the manufacturer's protocol. The lysate was solubilised at room temperature (RT) with gentle agitation for 30 min before centrifugation at 10000 x *g* for 30 min at 4ºC. The supernatant was used for the next step of the purification.

2.2.14 Purification by immobilised metal affinity chromatography (IMAC)

The His-Tag coding sequence present in pET-22(+) (140-157 encoding nucleotides) was the target for the initial capture using immobilised metal affinity chromatography (IMAC) using sepharose beads ligated to cobalt metal ions (Co^{2+}) (Clontech, UK). 20 µl of bed volume beads were equilibrated with washing buffer (20 mM sodium phosphate buffer, 0.5 M NaCl, 30 mM imidazole, pH 7.4) for 10 min at 4ºC. After three washes, the clarified cell lysate was applied to the equilibrated beads and left at 4ºC for 30 min. The beads were washed with wash buffer 4 times for 15 min at 4ºC. Protein was eluted with 10x bed volume at different concentrations of imidazole in 20 mM sodium phosphate buffer, 0.5 M NaCl, pH 7.4. Protein purification was monitored by apparent molecular weight on SDS-PAGE (Section 2.2.18) followed by silver staining (section 2.2.19). The supernatant containing desired protein was either stored at -80ºC or used for another purification step.

2.2.15 Size exclusion chromatography (SEC)

Pooled fractions containing recombinant protein were applied to Superdex 75 columns (Amersham Pharmacia Biotech, UK) equilibrated in 50 mM Tris, pH 8.0. The collected fractions were assayed by SDS–PAGE (Section 2.2.18) and those containing the protein of interest were pooled. The column was washed with 2x column volumes (V_c) of 0.1 M NaOH between cycles to ensure removal of trace contaminants. Between different protein samples, columns were cleaned with 1.0 M NaOH to remove endotoxin and prevent cross-contamination between samples.

2.2.16 Anion-exchange chromatography (AEC)

Fractions from IMAC or SEC were further purified and concentrated by application to a HiTrap miniQ column (Amersham Pharmacia Biotech, UK) equilibrated with 10x V_c of 50 mM Tris, pH 8.0. The column was washed with 10x V_c 50 mM Tris, pH 8.0. The protein was loaded at a rate of 3 ml per min. Then the column was washed with 10x V_c 50 mM Tris, pH 8.0. The protein was eluted by using a 10x V_c linear gradient from 0 to 1 M NaCl in 50 mM Tris, pH 8.0 at rate of 5 ml per min. Fractions were assayed by SDS-PAGE and those containing the protein of interest were pooled and either stored at -80ºC or used for another purification step.

2.2.17 Bicinchoninic acid (BCA) assay

Protein concentration was determined using the BCA protein assay (Pierce, USA), according to the manufacturer's instructions. The assay takes advantage of the reduction of Cu^{2+} in the reaction buffer to Cu^{+} by sample proteins, and the subsequent chelation of Cu^{+} by BCA to produce a purple product. The amount of coloured product was quantified by reading absorbance at 570 nm (plate reader from Dynatech Laboratories, USA). Absolute protein concentrations in samples

were calculated by the method of Bradford compared to bovine serum albumin (BSA) as standard curve (Bradford, 1976).

2.2.18 Sodium dodecyl sulfate-polyacrylamide gel electrophoresis (SDS-PAGE)

Sample buffer (10% w/v SDS, 50% v/v glycerol, 400 mM Tris-HCl pH 6.8, 0.025% w/v bromophenol blue, 5% v/v β-mercaptoethanol) was added (1:5 v/v) to recombinant proteins or cell lysates and boiled at 95ºC for 5 min before being centrifuged. Supernatants alongside protein standards (Biorad, UK) were resolved on mini-gels with a resolving layer (15% Acrylamide/Bis-acrylamide (30%/0.8 w/v) solution, 0.375 M Tris pH 8.8, 0.1% SDS, 0.05 ammonium persulphate, 0.05% TEMED (N,N,N',N'-tetramethylethylenediamine)) and a stacking layer (4% Acrylamide/Bis-acrylamide (30%/0.8 w/v) solution (Biorad, UK), 0.13 M Tris pH 6.8, 0.1% SDS, 0.05% ammonium persulphate, 0.05% TEMED). Gels were run in a Biorad Mini-electrophoresis tank in SDS running buffer (25 mM Tris pH 8.3, 192 mM glycine, 0.1% SDS) at a constant voltage of 200 V for 1 h.

2.2.19 Coomassie blue staining

After electrophoresis, gels were stained in Coomassie blue staining solution (45% methanol, 45% dH_2O, 10% acetic acid, 0.25% w/v Coomassie brilliant blue) (Biorad, UK) for 1 h with agitation. Gels were then rinsed briefly in dH_2O and destained in several changes of destaining solution (45% methanol, 45% deionized water, 10% acetic acid) until the background blue colour had disappeared. Destained gels were stored in distilled water prior to drying.

2.2.20 Silver staining

Immediately after gel electrophoresis, gels were silver stained according to manufacturers' instructions (GE Healthcare, UK). In order to eliminate the

interfering substances, gels were placed in fixing solution (30% ethanol, 10% acetic acid and 50% dH_2O) from 2 to 16 h. Gels were washed 3 times with dH_2O for 5 min. Gels were transferred to sensitizing solution (10% ethanol, 5% w/v sodium thiosulphate and 2.5% w/v glutaraldehyde) for 30 min to enhance both sensitivity and contrast. After three times 10 min washes with dH_2O, gels were placed in silver solution (silver nitrate 2.5% w/v) for 20 min. Gels were washed again 2 times briefly before being placed in developing solution (sodium carbonate 6%, formaldehyde 37% w/v) for 2 to 5 min with vigorous shaking until the staining was sufficient. The bands would appear at the places where the reduction of the silver ion into visible metallic silver takes place. Staining was terminated by stop solution (MeOH 50%, acetic acid 12%) for 10 min. Gels were washed with dH_2O three times for 5 min to ensure removal of stopping solution and put in preserving solution (Glycerol 87% w/w) for 20 min.

2.2.21 Western blot analysis

After SDS-PAGE, proteins were transferred onto a sheet of nitrocellulose membrane (BioRad, UK) and run for 1 h at 100 V using BioRad mini trans blotter. Non-specific antibody binding to the membranes was blocked by incubation in 5% fat-free dried milk (w/v) in Tween-Tris-buffered saline (TTBS) (1 M Tris, 5 M NaCl, pH 7.5, 0.2% Tween 20 (v/v)) for 1 h at RT or 4ºC overnight. Membranes were washed four times over 10 min with TTBS, and immunoblotted with appropriate primary antibody (Table 2.6) in TTBS containing 5% skimmed milk for 2 h at RT or 4ºC overnight. After several washes with TTBS, primary antibodies were detected by incubation with appropriate horseradish peroxidase conjugated secondary antibody (Dako, UK, 1 h, RT). Membranes were then washed several times again, and visualised by enhanced chemiluminescence (ECL, Amersham) according to the manufacturer's instructions. The equal loading of protein was monitored by

actin blotting. Primary and secondary antibodies used for different Western blot detections are listed in table 2.6.

1^{ry} Antibody (1: 1000)	**Supplier**	**2^{ry} Antibody** (1:2000)	**Supplier**
Anti-His	Novagen, UK	Goat anti-rabbit- IgG-HRP	DAKO, UK
Anti-IL-1α	R&D Systems, UK	Rabbit anti-goat-IgG-HRP	DAKO, UK
Anti-myc	Invitrogen, UK	Rabbit anti-mouse-IgG -HRP	DAKO, UK
Anti-V5	Invitrogen, UK	Rabbit anti-mouse-IgG -HRP	DAKO, UK
Anti-IL-1β	NIBSC*, UK	Sheep anti-mouse-IgG -HRP	DAKO, UK
Anti-Ubiquitin	Calbiochem, UK	Goat anti-rabbit-IgG-HRP	DAKO, UK

Table 2.6 Primary (1^{ry}) and secondary (2^{ry}) antibodies used for Western blot. The blots were incubated with 1^{ry} antibodies and then the proteins were detected by incubation with appropriate horseradish peroxidase (HRP) conjugated with 2^{ry} antibody. *: National Institute for Biological Standards and Control (NIBSC).

2.3 Mammalian protein expression

2.3.1 Cell cultures

All cells were cultured in a humidified incubator at 37ºC with 5% CO_2. Cell lines were passaged every 3-5 days depending on confluency of cells. Cell lines and primary cells were maintained in Dulbecco's modified eagle medium (DMEM, Invitrogen, UK, with 4.5 g/l glucose and L-glutamine) supplemented with 1% Penicillin/streptomycin antibiotic solution (P/S, 100 µg/ml streptomycin and 100 IU penicillin, Cambrex Bio Science, Belgium), and 10% (v/v) of foetal calf serum (FCS, PAA Laboratories, UK).

2.3.2 Cell lines

HEK293T (human embryonic kidney fibroblast) and COS-7 (African green monkey kidney fibroblast) cells were grown until 80-90% confluency. They were seeded at density of 1 million of cells per ml in 35 mm diameter petri dishes. The cells were then kept in DMEM containing 10% FCS v/v and 1% P/S v/v overnight in an incubator to be used for transfection next day.

2.3.3 Production of SP-Nt-b-Myc and SP-Nt-Myc constructs

The full-length sequence encoding for human Nt-b and Nt fragments was amplified by PCR from original vectors pEM7 and pEM5, respectively. SP and myc-tag genes were amplified from two other vectors called pEM57 and pPP68, respectively. Table 2.7 shows the primers used for the construction of the chimeric gene.

Amplifications were carried out in 25 µl as explained in section 2.2.3. The first cycle of PCR for all genes was at 94ºC for 2 min. The PCR programs for second cycle of amplification are summarized in table 2.8.

Primer name	Polarity	Sequence
P1 (T7 promoter)	**Sense**	5'-TAATACGACTCACTATAGGG-3'
P2-Nt-b	**Antisense**	5'-GCCCATTCCCTGACCATGCCA-3'
P2-Nt	**Antisense**	5'-TGCCATTCCCTGACCATGCCAAGC-3'
P3-Nt-b	**Sense**	5'-CAGGGAATGGGCCCTAAACAGATG-3'
P3-Nt	**Sense**	5'-CAG GGAATGGCAGAAGTACCTGAG-3'
P4-Nt and P4-Nt-b	**Antisense**	5'-TTG TTC GTG CAC ATA AGC CTC-3'
P5-Nt-b	**Sense**	5'-GTGCACGAACAAAAACTTATTTCTG-3'
P5-Nt	**Sense**	5'-GTGCACGAACAAAAACTTATTTCTG-3'
P6 (BGHR)	**Antisense**	5'-TAGAAGGCACAGTCGAGG-3'

Table 2.7 List of designed primers used for mammalian constructs. Sequence of designed primers for PCR amplification of SP, Nt-b, Nt and myc.

Gene	Primers	Nucleotides	2nd cycle
Nt-b	P3-Nt-b and P4	276	94°C 30 sec,50°C 40 sec, 72°C 40 sec
Nt	P3-Nt and P4	356	94°C 30 sec, 50°C 30 sec, 72°C 45 sec
SP	T7 and P2	137	94°C 30 sec, 50°C 30 sec, 72°C 30 sec
Myc	P5 and BGHR	100	94°C 30 sec,50°C 30 sec, 72°C 30 sec

Table 2.8 Amplification of Nt-b, Nt, SP and myc genes. Nt, Nt-b, SP and myc genes were amplified using specific designed Primers (Table 2.7) using PCR program**.**

The third cycle (extension cycle) was set for an extra 7 min at 72ºC. PCR reactions were purified and used for 1st and 2nd fusion PCRs. SP-Nt-b-Myc and SP-Nt-Myc constructs were made by double fusion PCR (Amberg et al., 1995) as shown in figure 4.1. SP (MGPGVLLLLLVATAWHGQG) and c-myc tag (EQKLISEEDL) were introduced in frame at the 5'- and 3'- end of the Nt-b and Nt genes by fusion PCR using designed overlapping primers before cloning into pcDNA3.1(+) vector. First fusion was carried out by fusion of SP at the 5' of Nt-b and Nt genes. P1 (T7) was used as the forward primer for both SP-Nt-b and SP-Nt and the P4-Nt/Nt-b was used as reverse primer. The PCR conditions were set up as: one cycle of 94ºC for 2 min, 20 cycles consisting of 94ºC for 30 sec, 50ºC 30 sec, 72ºC 60 sec (1 Kb/ 2 min) and extension cycle of 72ºC for 7 min. The second fusion was performed by fusion of myc tag at the 3' end of the first purified fusion PCR products (SP-Nt-b and SP-Nt). T7 and BGHR primers were used for this second fusion PCR as forward and backward primers, respectively. The PCR was programmed as one cycle of 94ºC 2 min, 20 cycles of 94ºC 30 sec, 50ºC 30 sec, 70 sec (for SP-Nt-b-myc) and 72ºC 80 sec (for SP-Nt-myc). The final extension cycle was set for 7 min at 72ºC. The PCR products were purified by QIAQuick™ PCR column purification kit (section 2.2.5). The purified PCR product was analysed on 1% agarose gel.

2.3.4 Transfection of mammalian cells

COS-7 and HEK293T cells (80-90% confluent) were transfected using Lipofectamine™ 2000 (Invitrogen, UK) according to manufacturer's instructions. One day before transfection, cells were seeded at the indicated density onto 6 well plates and kept at 37ºC in a CO_2 incubator overnight. 1 µg of DNA and 3 µl Lipofectamine™ 2000 were diluted gently in 100 µl of Opti-MEM® I Reduced Serum Medium (Invitrogen, UK) in two separate eppendorfs. The dilutions were

kept at RT for 5 min. It is very important to keep Lipofectamine: plasmids ratio constant as transfection efficiency depends on this ratio. Diluted DNA and diluted Lipofectamine™ 2000 (total volume of 200 µl) were combined and mixed gently before incubation for 20 min at RT. 200 µl of diluted complexes were added to each well containing 0.8 ml of Opti-MEM® I Reduced Serum Medium and mixed gently on a rocking plate. After 5 h another 600 µl Opti-MEM® I Reduced Serum Medium was added to each well. The cells were incubated at 37ºC in a CO_2 incubator for 16, 24, 48 and 72 h after transfection. Following this, protein expression was assessed in lysates and concentrated supernatants of transfected HEK293T and COS-7 cell lines after 24-72 h.

2.3.5 Cell lysate preparation

Cells were lysed by incubation in lysis buffer (200 mM HEPES, 100 mM NaCl, 5 mM EDTA, 1% NP-40 (v/v)) with protease inhibitors (Roche, UK) for 15 min at 4ºC. Adherent cells were scraped into the lysis buffer, and lysates were vortexed before clearing of debris by centrifugation (10000 x *g*, 15 min at 4ºC). Supernatants were removed, concentrated through a 10 kDa cut-off column (Millipore, UK) and analysed directly by Western blot as described in section 2.2.18.

2.4 RNA isolation and reverse transcriptase PCR (RT PCR)

2.4.1 RNA extraction and quantification

RNA was extracted from confluent COS-7 cell cultures in 6-well plates. Medium was removed from the wells. Cells were lysed by adding 1 ml TRIzol® Reagent (Invitrogen, UK) directly into each well and the cell lysate were passed through a pipette several times. The homogenised samples were incubated for 5 min on ice to allow separation of nucleoprotein complexes. TRIzol extracts were

then transferred to new tubes before the addition of 200 µl chloroform. Samples were shaken vigorously by hand for 15 sec, and then incubated for 3 min at RT. RNAs (the aqueous colourless upper phase) were separated from phenol-chloroform phase (lower red organic phase) by centrifugation of the sample at 12000 x *g* for 20 min at 4ºC. The aqueous phase was transferred to a new tube. RNAs were precipitated by incubation with 1 ml isopropanol for 15 min at RT. Precipitated RNA was pelleted by centrifugation at 12000 x *g* for 15 min at 4ºC. The RNA pellet was then washed sequentially with 70% and 100% v/v ethanol, dried, and re-suspended in 20 µl RNase-free water.

The purity and concentration of RNA samples was assessed using an ND-1000 spectrophotometer and ND-1000 v3.1.0 software (Nanodrop Technologies, USA). At least 50 µg RNA was purified from each well of COS-7 cells, and all samples had an A260/280 ratio ≥ 1.85, indicating that the preparations were almost free from protein contamination.

2.4.2 DNA extraction

DNA was extracted from the remaining interphase and organic phase. 100% ethanol (in a ratio of 1:3; ethanol to TRIzol®) was added and mixed by inversion. The samples were stored at 30ºC for 2-3 min before centrifugation at 2000 x *g* for 5 min at 4ºC. The precipitated DNA pellet was washed twice by washing solution (0.1 M sodium citrate in 10% ethanol) and kept for 30 min at 22ºC in washing buffer after every wash. Then, the DNA pellet was collected after centrifugation at 2000 x *g* for 5 min at 4ºC. The DNA was kept in 75% ethanol (1.5-2 ml ethanol per 1 ml TRIzol® reagent) for 20 min at 22ºC. The DNA was pelleted after centrifugation at 2000 x *g* for 5 min at 4ºC. The DNA was air dried for 15 min and then dissolved in 8 mM NaOH stored at 4ºC until use.

2.4.3 Reverse transcription (RT)

RNA reverse transcription (RT) was performed according to the Advantage RT-for-PCR kit protocol (Clontech, UK). 1 µg COS-7 RNA was incubated with 1 µg DNAase at R/T for 15 min. DNAse was inactivated by 25 mM EDTA. 1.6 µM oligo $(dT)_{18}$ primer was added and diluted with 12.5 µl RNase-free water. In order to denature RNA, the mixture was incubated for 10 min at 70ºC and chilled rapidly to prevent reformation of secondary structures. 200 U MMLV reverse transcriptase, 1x reaction buffer, 500 µM deoxynucleotide triphosphates (dNTPs) (Invitrogen, UK) and 20 U recombinant RNase inhibitor ((Invitrogen, UK) were added to the reaction mix prior to incubation for 1 h at 37ºC. RT was then stopped by heating the mixture to 70ºC for 15 min, followed dilution to 100 µl with RNase-free water.

2.4.4 PCR

50 ng cDNA of pro-IL-1β, Nt and Nt-b were PCR amplified using primers specific for desired genes (Table 2.1). The *β-actin* gene was also amplified using specifc primers for *β-actin* gene.

PCR reactions were made up with 2x Biomix Red (Bioline), containing dNTPs, Taq DNA polymerase and reaction buffer. This was diluted to 1x with primers (0.4 µM), cDNA and DNase/RNase-free water. Reactions were run on a thermal cycler (Labnet International, UK). The gene amplification conditions were as follows: initial denaturing at 94ºC for 5 min prior to cDNA amplification over 30 cycles consisting of denaturing at 94ºC for 1 min, annealing at 60ºC for 1 min and extention at 72ºC for 3 min. Finally an additional extension step of PCR products for a further 5 min (72ºC) prior to separation on 1% agarose gels was performed. DNA bands were visualised on a UV transilluminator and images captured using a digital camera (Canon, UK).

2.5 Endogenous expression of IL-1

2.5.1 Mouse macrophages (J774A.1)

The mouse macrophage J774A.1 (J774) cell line was grown in DMEM supplemented with 10% FCS and 1% P/S at 37ºC in a humidified incubator containing 5% CO_2. These cells were plated in 24 or 48 well plates at a density of $1x10^6$ cells/ml and allowed to adhere at 37ºC in incubator overnight. Thereafter the medium was replaced with fresh medium and cells were stimulated as described.

2.5.2 Mouse bone marrow derived macrophages (BMDMs)

All experiments were carried out under the regulations of the U.K. Animal Scientific Procedures Act of 1986. Bone marrow derived macrophages (BMDMs) were prepared as reported previously (Handel-Fernandez, 2000) from femur and tibia bones of male C57BL/6 mice (8-10 week of age) that were sacrificed by an overdose of CO_2. All excess tissues from femur and tibia were removed. The bones were immobilised and separated by placing the knee joint in scissors and gently wiggled one bone whilst applying pressure with the scissors. The ends of the bone were cut and bone marrow washed out with 70% DMEM supplemented with 10% FCS, 100 U/ml penicillin, and 100 µg/ml streptomycin, and 30% of L929 cell supernatant which contain macrophage-stimulating factor (differentiation media). The bone marrow cells were resuspended in 10ml per bone of differentiation media. A further 30 ml differentiation media was added and the cells were distributed between a T75 flask (10 ml cells) and a T225 flask (30 ml cells), and incubated at 37ºC. After 3 days 5 ml/bone of the same media was added. After 6-9 days, the resulting BMDMs were detached with PBS containing 5 mM EDTA and 4 mg/ml lidocaine, replated into 48-well plates (at a density of $1x10^6$ cells/ml) containing DMEM with 10% FBS and 1% P/S and used the next day.

2.5.3 LPS treatments

Where applicable, endogenous IL-1 expression was induced by treating J774 or BMDM cells with 1 µg/ml LPS (*E. coli*, O26:B6, Sigma Aldrich) or phosphate buffered saline (PBS) as a control for different time points.

2.5.4 Cyclohexamide (CHX) treatments

For protein stability studies, cells were treated with 5 µg/ml cyclohexamide (CHX) or Dimethylsulfoxide (DMSO) as a control, for the desired time points.

2.5.5 Protease inhibitor treatments

The stock solution of proteasome inhibitors ALLN (acetyl-leu-leu-norleucinal), MG262 (Z-Leu-Leu-Leu-boronate) and β-lactone (*clasto*-lactacystin β-lactone) were prepared by dissolving in DMSO to a concentration of 10 mM. The LPS-stimulated cells were treated with relevant proteasome inhibitors at concentrations of 0, 1, 3, 10 and 50 µM for 2 and 4 h.

2.5.6 IL-1 release

Stimulated J774 and BMDMs were incubated for 1 h with nigericin (10 µM) and ATP (5 mM), respectively. The amount of IL-1 in the supernatant was measured by ELISA (see section 2.4.8 for details).

2.5.7 Lactate dehydrogenase assay

Lactate dehydrogenase (LDH) activity was measured in cell culture medium using the Cytotoxicity Detection Assay (Promega, UK), according to manufacturer's instructions. Upon the damage of the plasma membrane LDH is released into the cell culture medium. The cytotoxicity assay is based on the conversion of a tetrazolium salt into a red formazan product by LDH. The intensity of the generated colour correlates directly with the amount of LDH in the sample

as a result of cell death. LDH activity was quantified by plate reader at OD 490 nm (Synergy HT, Biotech).

2.5.8 Enzyme-linked immunosorbent assay (ELISA)

Enzyme-linked immunosorbent assays (ELISAs) were applied for the quantification of a vast diversity of small molecules. All incubations were performed at RT and on a microplate table-top shaker unless stated otherwise. Microtiter plates (Sigma M5785-1CS Nunc-ImmunoTM plate, UK) were coated with 100 ng/well immobilised rat anti-mouse (capture antibody) IL-1α (R&D Systems, UK) or IL-1β (R&D Systems, UK) in PBS overnight. The wells were washed four times with phosphate buffered saline (PBS, pH 7.4) containing 0.05% Tween 20 (T-PBS). Then, non specific binding sites were blocked with PBS containing 1% BSA (v/w) (blocking buffer) for 1 h. The samples and standards (recombinant mouse IL-1α or lL-1β, (R&D Systems, UK)) were added after plates were washed 4 times with T-PBS and incubated at RT for 2 h or overnight at 4ºC. This was followed by 4 washes with T-PBS. 2.5 ng of biotinylated goat anti-mouse IL-1α or anti-mouse IL-1β (detection Ab, R&D Systems, UK) was added to each well and left for 1 h on a shaker. After 4 washes, streptavidin–horseradish peroxidase conjugate (Dako UK, Cambridge, UK) was applied for 30 min as a 1:20000 dilution in blocking buffer. Finally, the plates were washed 4 times with T-PBS and developed with substrate solution by mixing 1:1 Reagent A (H_2O_2) and Reagent B (Tetramethylbenzidine (TMB)) (R&D Systems, UK) for 20 min. The colorimetric reaction was stopped by the addition of 1 M sulfuric acid (H_2SO_4). The optical density was measured at 450 nm using a microplate reader (Synergy HT, Biotech) immediately after adding of 1 M H_2SO_4. In order to correct any optical imperfections in the plate, the absorbance reading was also done at 570 nm and

subtracted from reading at 450 nm. Readings made only at 450 nm without correction may be higher and less accurate.

2.6 Immunoprecipitation (IP)

2.6.1 Cell lysis preparation for IP

Cells were lysed on ice for 15 min in lysis buffer (50 mM HEPES (pH 7.5), 5 mM EDTA, 150 mM NaCl and 1% Triton X-100 detergent, 10mM N-ethylmaleimide and cocktail of protease inhibitors (Calbiochem) before they were scraped. All cellular debris were removed by centrifugation (15 min, 14000 x *g*, 4ºC). The supernatant was transferred to a new pre-cooled eppendorf tube and kept as the cytoplasmic fraction.

2.6.2 IP of IL-1β protein

The cytoplasmic fraction of the cells was collected as described in section 2.5.1 and added to pre-washed (wash buffer: 50 mM HEPES (pH 7.5), 5 mM EDTA, 150 mM NaCl and 1% Triton X-100 detergent) Protein G agarose (Merck, UK) and incubated at 4ºC for 2 h on an orbital shaker. Cell lysate was removed from Protein G beads by centrifugation at 10000 x *g* for 5 min at 4ºC and added to 1.5 µg of IL-1β at 4ºC for 3 h on a shaker. Cell lysate was incubated with anti-mouse IL-1β at 4ºC for 4 h on an orbital shaker. The immune-complex was captured by adding cell lysate-antibody complex to pre-washed Protein G agarose and left rocking gently at 4ºC for 2 h or overnight. The affinity matrix was washed with lysis buffer and prepared for SDS-PAGE and Western blot analysis as explained in section 2.2.18 and 2.2.21.

2.7 Enrichment of Ubiquitinated protein

Cytoplasmic fractions of the cells (0.5 mg/ml) were collected as explained in section 2.6.1 and added to 40 µl suspended polyubiquitin affinity beads

(Calbiochem, UK), and left rotating at 4ºC for 4 h. The beads were washed three times with 1 ml of wash buffer (50 mM HEPES (pH 7.5), 5 mM EDTA, 150 mM NaCl and 1% Triton X-100 detergent). The affinity matrix was suspended in 40 µl of 2x gel loading buffer (250 mM Tris, HCl, pH 6.8, 4% SDS, 10% β-mercaptoethanol, 20% glycerol and bromophenol blue) and boiled at 95ºC for 5 min before centrifugation at 12000 x *g* for 1 min. The supernatant was applied to 12-15% SDS-PAGE (Section 2.2.18) and further Western blot analysis for IL-1β and IL-1α expression was performed (Section 2.2.21).

2.8 Statistical Analysis

All statistical analyses were performed using Prism version 5.00 for Windows, from GraphPad Software (www.graphpad.com). Comparisons between means of treated groups were performed using one way analysis of variance (ANOVA), followed by Bonferroni multiple comparison post-hoc test to identify individual differences. Dose response IL-1 release data was fitted to a bell shaped curve, to account for both the potentiation and inhibitory effects. Dose response cell death was fitted to a sigmoidal dose response curve, as this was the closest fit to the data available. All data are expressed as mean ± standard deviation (s.d) of the values obtained from at least three independent experiments. A value of $p < 0.05$ was considered statistically significant. The half-life of the protein was calculated using non-linear fit followed by one phase exponential decay.

2.9 Prediction of ubiquitinated proteins

The amino acid sequence of pro-IL-1α and pro-IL-1β were entered into a web based bioinformatics programme called UbPred (www.ubpred.org). This programme predicts potential ubiuitination sites based on proteomics studies (Hitchcock, et al., 2003; Peng, et al., 2003).

CHAPTER 3

Cloning, expression and purification of pro-IL-1β and N-terminus fragments in bacterial cells

3.1 Introduction

Pro-IL-1β N-terminus fragments result after sequential caspase-1 processing at Asp27 and Asp116 to produce mature IL-1β, which corresponds to C-terminus (Figure 3.1) (Kostura et al., 1989; Sleath et al., 1990). Although mature IL-1β has been the subject of extensive research, little attention has been paid to the N-terminus by-products of the IL-1β precursor. The main objective of this chapter was the cloning of N-terminus fragments of pro-IL-1β into a bacterial expression vector for their subsequent expression and purification.

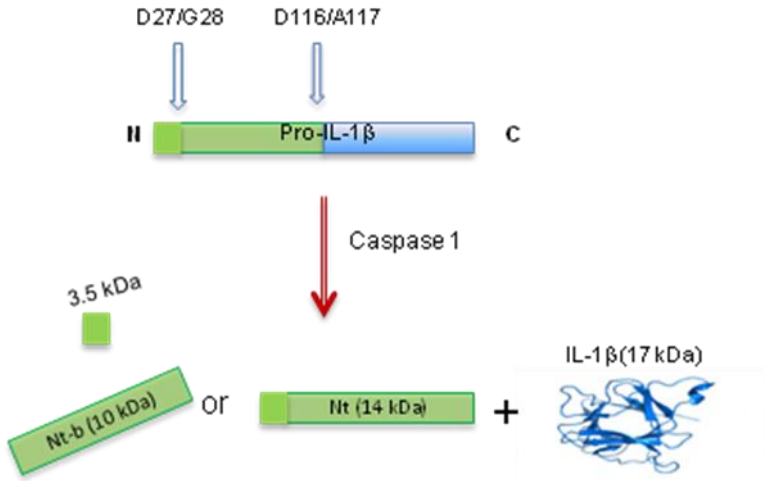

Figure 3.1 Pro-interleukin-1β (pro-IL-1β) processing by caspase-1. The two caspase-1 cleavage sites on pro-IL-1β are between Asp27/Gly28 and Asp116/Ala117 (blue arrows). The products for the cleavage scenario are represented as smaller blocks (3.5 kDa, 10 kDa (Nt-b) and 14 kDa (Nt)), and the final mature protein as the actual three-dimensional structure shown in blue (IL-1β, 17 kDa). Nt-b (10 kDa) and Nt (14 kDa) are represented in green.

3.2 Cloning of pro-IL-1β N-terminus fragments

Human pro-IL-1β N-terminus DNA coding fragments were amplified by PCR using specific oligonucleotides F1, F2, R1 and R2 (Table 2.1) from a vector (pEM7) containing the full coding sequence for pro-IL-1β. F1 and R2 oligonucleotides (Table 2.1) amplified the full pro-IL-1β N-terminus from Met1 to the second caspase-1 processing site at Asp116, this fragment coded for a predicted protein of 14 kDa (“Nt”) (Figure 3.1). Oligonucleotides F2 and R2 (Table 2.1) amplified an intermediate fragment of the pro-IL-1β N-terminus corresponding

to the section between the two caspase-1 processing sites (from Asp27 to Asp116), this fragment coded for a predicted protein of 10 kDa ("Nt-b") (Figure 3.1). Oligonucleotide F2 incorporated an ATG starting codon at the 5' end of Nt-b (Table 2.1). In addition we also amplified the full length pro-IL-1β to use as a negative control in future experiments using the oligonucleotides F1 and R1 (Table 2.1). A point mutation was introduced in the pro-IL-1β coding sequence by two-step overlapping PCR to change an internal *Nde*I restriction site, since this restriction enzyme was used in subsequent cloning steps. Oligonucleotides F-*Nde*I and R-*Nde*I changed the nucleotide sequence CCATAT to CCTTAT in the pro-IL-1β sequence without affecting the amino acid coding frame, and eliminated the internal *Nde*I restriction site (Table 2.1). Oligonucleotides F1, F2, R1 and R2 incorporated *Nde*I and *Xho*I restriction sides into either side of the amplified fragments (Table 2.1) to use in future cloning steps.

The PCR products encoding full length pro-IL-1β, Nt-b and Nt were purified and resolved on a 1% agarose gel with ethidium bromide, and correct amplification was confirmed under UV transillumination (Figures 3.2 and 3.3). The amplification products corresponding to the 1st and 2nd overlapping PCR reactions to mutate *Nde*I site on pro-IL-1β are also shown in figure 3.2. The fragments corresponded to the expected sizes, 430 bp and 400 bp for 1st pro-IL-1β PCR and 800 bp for 2nd overlapped PCR to get full pro-IL-1β, 353 bp for Nt and 281 bp for Nt-b, (Figures 3.2 and 3.3).

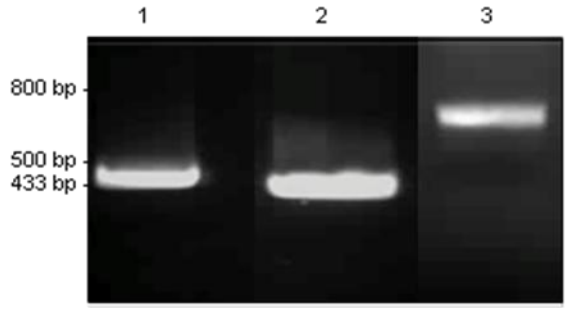

Figure 3.2 Characterisation of the 1st and 2nd PCR of pro-IL-1β products running on a low melting point 1% agarose gel. Lane 1: 433 bp (primers F1 and R-*Nde*I, 1st part of pro-IL-1β) and lane 2: 400 bp (primers F-*Nde*I and R1, 2nd part of pro-IL-1β), show the products of 1st PCR. Lane 3: 800 bp (primers F1 and R1, full length of pro-IL-1β), 2nd PCR product after PCR column purification.

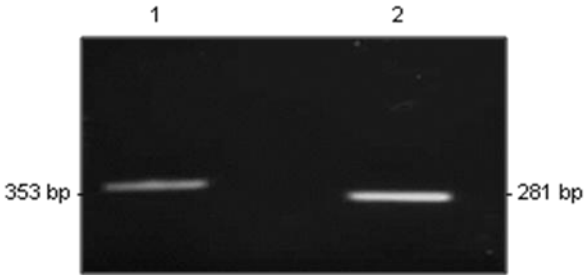

Figure 3.3 PCR products of Nt and Nt-b on 1% agarose gel. Nucleotides were amplified by PCR. Each product was purified by Qiagene PCR column purification and small amount run on 1% agarose gel. Lane 1: 353 bp (primers F2 and R1, Nt) and lane 2: 281 bp (primers F2 and R2, Nt-b).

Amplified products were cloned into the bacterial expression vector pET-22(+). Since pET-22(+) is a low-copy vector, we used two common *E. coli* strains (JM109 and DH5-α) to select the strain which gives the greatest amount of vector. Both competent strains were transformed with 10 ng of pET-22(+), grown in 5 ml of LB with ampicillin, and plasmid was purified by commercial mini-preps. To check whether the purified vector was correct, we digested with different restriction enzymes (*Nde*I*, Xho*I*, BspE*I*, EcoR*V*, Eco*0109I *and Xmn*I). The fragments obtained after digestion were resolved on a 1% agarose gel and corresponded to the expected sizes. Digestion resulted in clearer fragments from the vector purified from the *E. coli* JM109 strain suggesting more DNA (Figure 3.4); therefore we selected *E. coli* JM109 strain for future cloning steps.

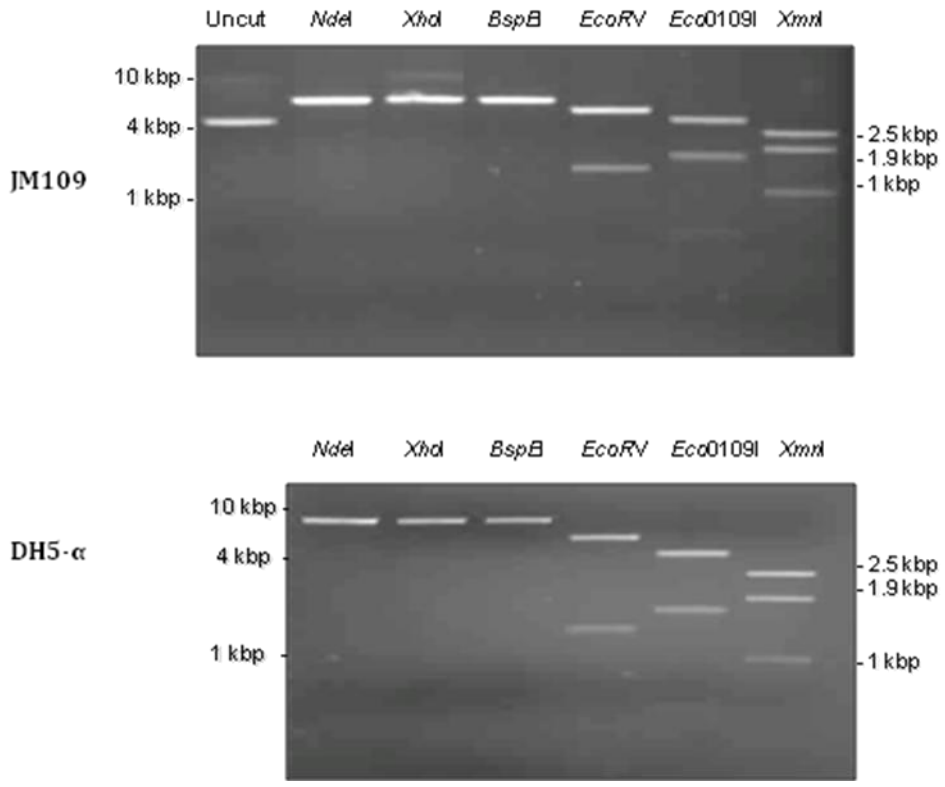

Figure 3.4 Restriction digests of transformed pET-22(+) into two *E. coli* strains JM109 (top) and DH5-α (bottom). Mini-prep DNA purification was performed after transformation of pET-22(+) into *E. coli* strains JM109 (top) and DH5-α (bottom), 5 ng plasmid DNA was incubated with 5 units of each restriction enzyme at 37ºC for 60 min. DNA fragments were separated on 1% agarose gel stained with ethidium bromide.

Amplified fragments and vector were digested by *Nde*I and *Xho*I. In order to prevent auto-ligation of the vector, after digestion it was dephosphorylated using AP and was finally purified by running the reaction mix on a low melting point agarose gel. The desired products were extracted from the gel after quantification and used for ligation (see materials and methods). Ligation reactions were transformed into *E. coli* JM109 competent cells and seeded into LB ampicillin plates. Colonies were screened by PCR for correct insertion of the three different inserts (pro-IL-1β, Nt and Nt-b) using oligonucleotides F1 and R1 for pro-IL-1β, F1 and R2 for Nt, F2 and R2 for Nt-b (Table 2.1) and then resolved on 1% agarose gel with ethidium bromide. There were 5 positive colonies for Nt-b construct (out of 25 screened), one for Nt (out of 12 screened) and 5 for pro-IL-1β (out of 134 screened) as shown in figures 3.5, 3.6 and 3.7, respectively.

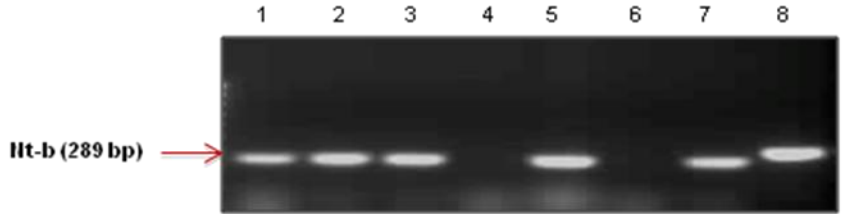

Figure 3.5 Analysis of 7 colonies randomly selected from the library of Nt-b construct cloned into *E. coli* JM109. Selected colonies were amplified by PCR. Lanes 1 to 7 were selected colonies from agar plate and lane 8 is the positive control Nt-pcDNA3.1(+) vector (pEM5). There are 5 positive colonies with the expected size (289 bp) as shown by red arrow.

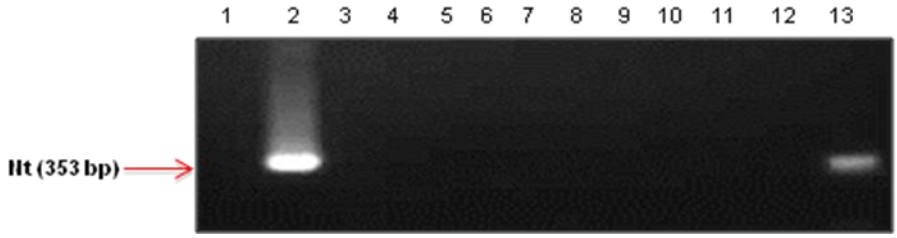

Figure 3.6 Analysis of 11 colonies randomly selected from the library of Nt construct cloned into *E. coli* JM109. Selected colonies were amplified by PCR. Lane 1 is dH_2O and lane 2 is the positive control Nt-pcDNA3.1(+) vector (pEM5), lanes 3-13 selected colonies from agar plate. There is only one positive colony**.** Red arrow shows single positive colony for Nt (353 bp) (lane 13).

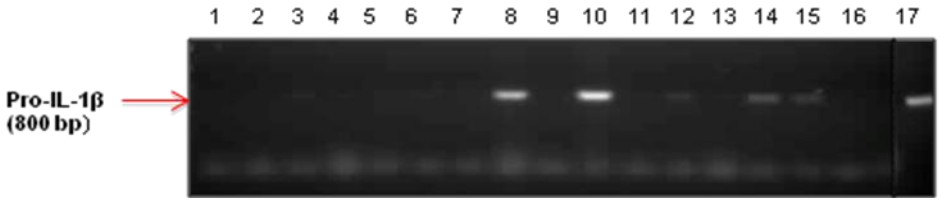

Figure 3.7 Analysis of 15 colonies randomly selected from the library of pro-IL-1β construct cloned into *E. coli* JM109. Selected colonies were amplified by PCR. Lanes 1-15 are selected colonies from agar plate, lane 16 is dH_2O and lane 17 is the positive control pro-IL-1β-pcDNA3.1(+) vector (pEM7). There were five positive colonies (red arrow). Colonies 8 and 10 used for mini-prep purification.

The recombinant plasmids from positive colonies were purified by mini-prep and digested using different restriction enzyme combinations. The resulting fragments were resolved by 1% agarose gel electrophoresis with ethidium bromide and visualised under an UV lamp. All restriction reactions resulted in fragments of the expected sizes for the different vectors.

In order to confirm the insertion of Nt-b fragment into the plasmid, the cloned Nt-b was digested with *Bbv*CI restriction enzyme since empty vector has no

*Bbv*CI restriction site. Double digestion of Nt-b construct by *Xho*I/*Nde*I and also *Xho*I/*Xba*I resulted in two fragments of 5.3 kbp and 270 or 310 bp respectively, which confirms the correct orientation of the insert (Figure 3.8).

Digestion of Nt construct with *Eco*01091 resulted in three different sized products (3325, 1674 and 847 bp), which differentiate it from the empty pET-22(+) vector (3325, 1674 and 494 bp) (Figure 3.9, lanes 2 and 3). The presence and correct orientation of Nt sequence in pET-22(+)-Nt construct was checked with single restriction digest by *Bbv*CI and double digestion by *Nde*I/*Xho*I, respectively (Figure 3.9, lanes 4 and 5). Digestion with *Bbv*CI resulted in a single product (Figure 3.9, lane 4). Double digestion with *Nde*I/*Xho*I resulted in two products corresponding to the vector (5.3 kbp) and the Nt insert (347 bp) (Figure 3.9, lane 5).

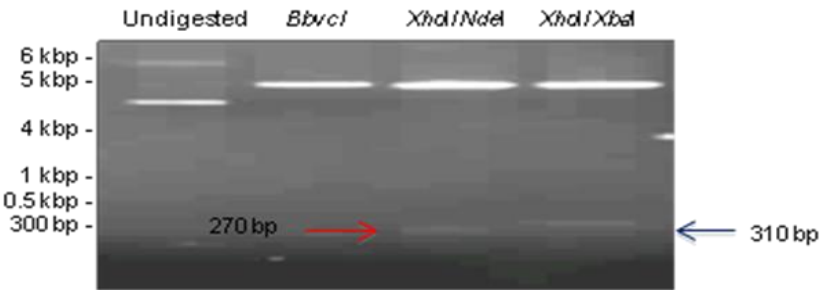

Figure 3.8 Restriction digest of Nt-b construct. Agarose gel stained with ethidium bromide showing restriction analysis of Nt-b plasmid undigested (lane 1), digested with *Bbv*CI (lane2) and double digested with *Xho*I and *Nde*I (lane 3) which resulted in linear plasmid (5.3 kbp) and 270 bp fragment (red arrow). A second double digestion of Nt-b construct with *Xho*I and *Xba*I (lane 4) produced linear plasmid (5.3 kbp) and 310 bp fragment (blue arrow). The size of all fragments are as expected and confirms correct orientation of the insert.

The restriction digest of the pro-IL-1β vector also confirmed the correct insertion of pro-IL-1β into pET-22(+). Single and double restriction reactions revealed fragments of the expected sizes for the correct cloning. Restriction digest by *Xmn*I produced the expected fragments (4.2 and 1.9 kbp). The presence of the insert was also confirmed by *Bbv*CI digest (obtaining a single expected fragment

of 5.6 kbp) and *Eco*0109I restriction digest produced three expected fragments (2.8, 1.6 and 1.4 kbp) (Figure 3.10).

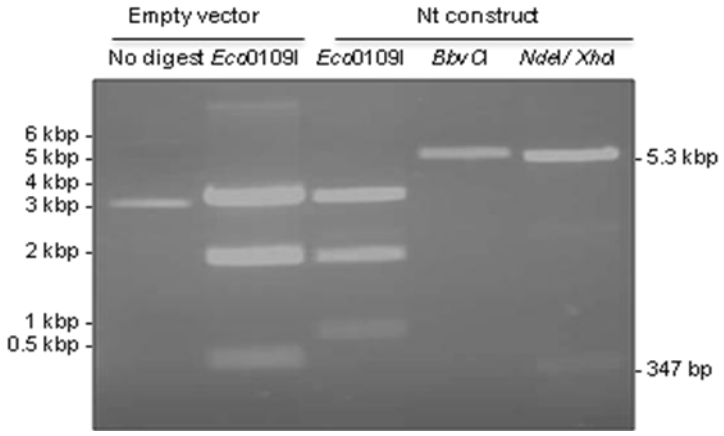

Figure 3.9 Restriction digest of Nt construct. Agarose gel stained with ethidium bromide showing restriction analysis of empty pET-22(+) (lane 2) or Nt vector (lanes 1, 3-5) digested with different restriction enzymes. Lane 1: uncut Nt vector, lane 2: restriction digest of empty pET-22(+) with *Eco*O109I, lane 3: restriction digest of Nt construct with *Eco*O109I, lane 4: Nt vector digested with *Bbv*CI (5.7 kbp) and lane 5: Nt vector double digested with *Nde*I/*Xho*I (5.3 kbp and 347 bp). All fragments correspond to the expected sizes and confirms correct orientation of the insert.

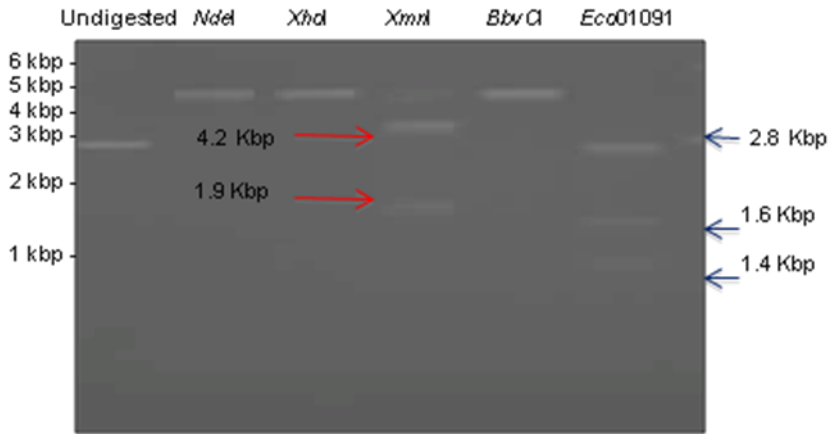

Figure 3.10 Restriction digest of pro-IL-1β construct. Agarose gel stained with ethidium bromide showing restriction analysis of pro-IL-1β vector digested with different restriction enzymes as follow: uncut DNA,: *Nde*I, *Xho*I, *Xmn*I (resulted two expected fragments: 4.2 Kb and 1.9 Kb, red arrows), *Bbv*CI and *Eco*O109I (resulted three expected fragments: 2.8 Kb, 1.6 Kb and 1.4 Kb, blue arrows).

The correct nucleotide sequence of the cloned genes into pET-22(+) was analysed by automatic sequencing across the full length, using the universal primer T7 and intermediate specific primers. The sequencing confirmed that the ATG start codon of the cloned fragments were in frame with the 6x His-Tag and the stop codon (Figure 3.11).

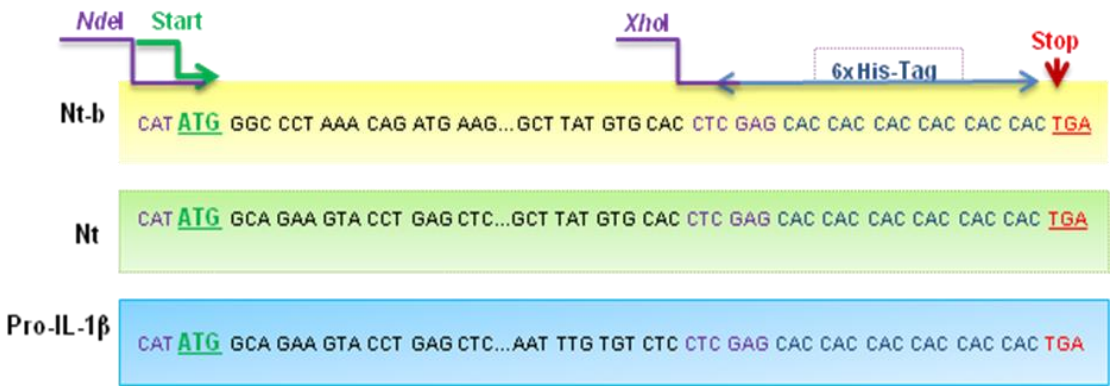

Figure 3.11 DNA sequence of Nt-b, Nt and pro-IL-1β genes cloned into pET-22(+). The construction of pET-22(+)-Nt-b (yellow panel), pET-22(+)-Nt (green panel) and pET-22(+)-pro-IL-1β (blue panel). It shows the genes ligated between the *Nde*I and *Xho*I restriction sites and the gene is in frame with the 6xHis-tag and the TGA stop codon.

3.3 Bacterial expression of pro-IL-1β N-terminus fragments

The recombinant pET-22(+) plasmids Nt-b, Nt and pro-IL-1β were transformed into the *E. coli* expression strain BL21(DE3). Colonies were selected and small cultures were set up to express and elute these recombinant proteins by taking advantage of the His-tag. Subsequently larger scale expression cultures of selected colonies were grown. Based on calculated molecular weights, sizes of the expressed proteins were expected to be approximately 10, 14, and 31 kDa for Nt-b, Nt and pro-IL-1β proteins, respectively.

Small cultures of *E. coli* BL21(DE3) transformed with Nt-b, Nt and pro-IL-1β expression vectors were prepared. Recombinant protein expression was induced using different concentrations of IPTG (1 to 5 mM) for 4 or 16 h at 37ºC. The size of the expressed Nt-b, Nt and pro-IL-1β proteins were as predicted (Figures 3.12, 3.13 and 3.14). Signals were absent in any of the lanes loaded with un-induced bacteria (0 mM IPTG) or IPTG treated bacteria transformed with empty pET-22(+) vector. We chose 2 mM IPTG as the optimal concentration to induce expression for all future experiments.

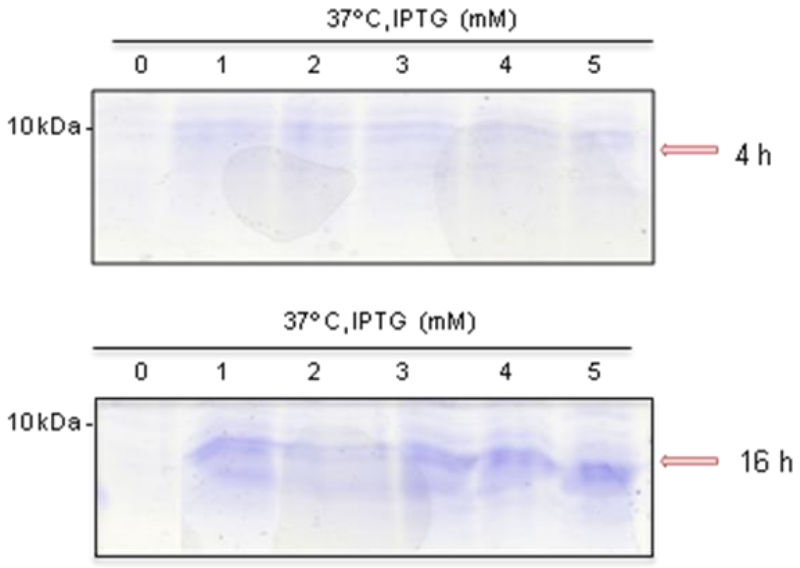

Figure 3.12 Coomassie blue staining of pro-IL-1β Nt-b bacterial expression at 37ºC. SDS-PAGE of transformed *E. coli* BL21(DE3) cells with Nt-b expression vector induced at 37ºC by different concentration of IPTG (1 to 5 mM) for 4 h (top panel) and 16 h (bottom panel). The red arrows show expressed IL-1β Nt-b protein (10 kDa).

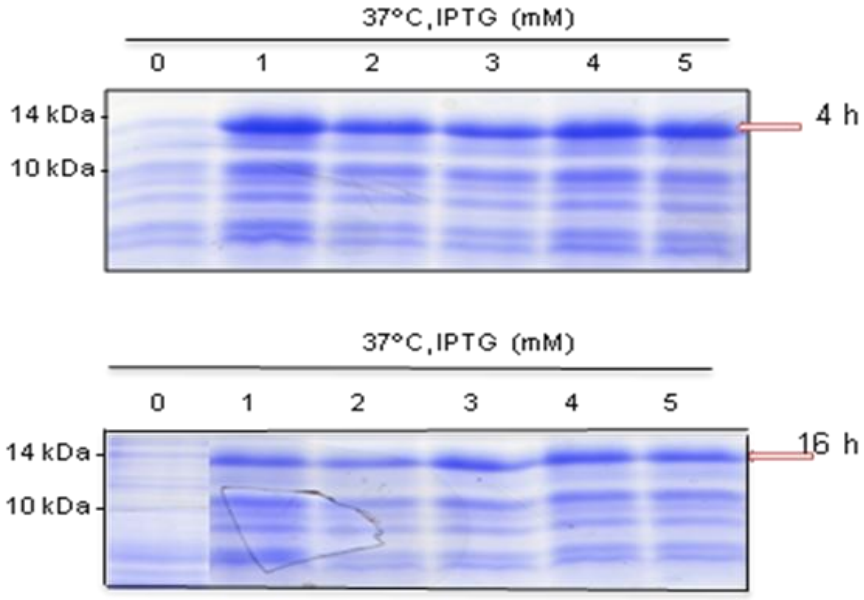

Figure 3.13 Coomassie blue staining of pro-IL-1β Nt bacterial expression at 37ºC. SDS-PAGE of transformed *E. coli* BL21(DE3) cells with Nt expression vector induced at 37ºC by different concentration of IPTG (1 to 5 mM) for 4 h (top panel) and 16 h (bottom panel). The red arrows show expressed IL-1β Nt protein (14 kDa).

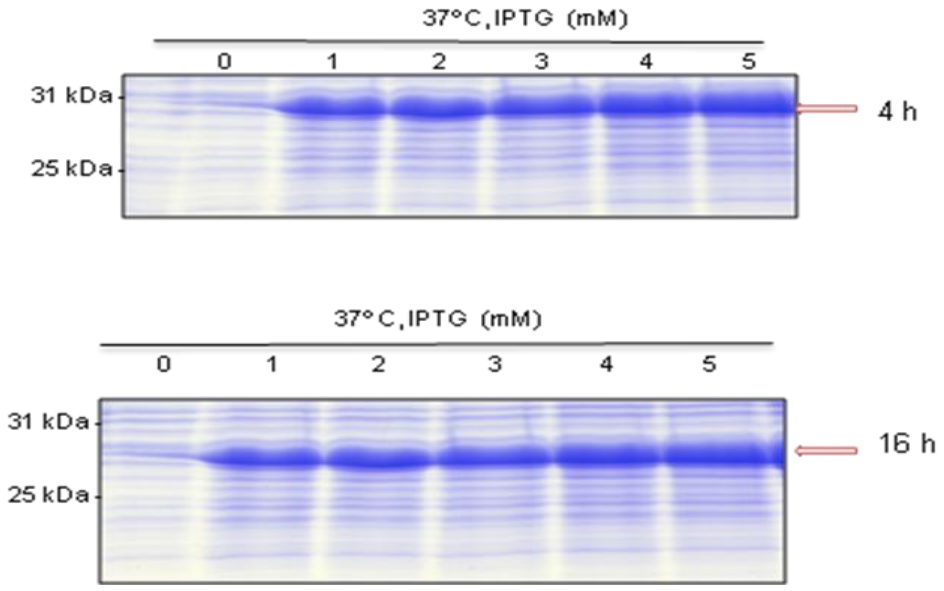

Figure 3.14 Coomassie blue staining of pro-IL-1β bacterial expression at 37ºC. SDS-PAGE of transformed *E. coli* BL21(DE3) cells with pro-IL-1β expression vector induced at 37ºC by different concentration of IPTG (1 to 5 mM) for 4 h (top panel) and 16 h (bottom panel). The red arrows show expressed pro-IL-1β protein (31 kDa).

We next optimised the time and temperature expression conditions using 2 mM IPTG. The best-optimised expression conditions were found to be different for the three proteins. Coomassie blue staining of bacteria lysates transformed with pro-IL-1β Nt-b vector and induced by different IPTG concentrations (Figure 3.12) did not show significant expression differences of Nt-b protein, therefore the samples were Western blotted with an anti-His antibody (see materials and methods for details). The highest expression was achieved by 2 mM IPTG for 4 h (Figure 3.15).

After induction with 2 mM IPTG for 1 to 4 h at 37ºC, cells were harvested by centrifugation. Bacteria were then lysed to solubilise the expressed proteins. The expressed protein remained in the bacterial pellet as inclusion bodies for both Nt-b and Nt expressed proteins (Figures 3.15 and 3.16).

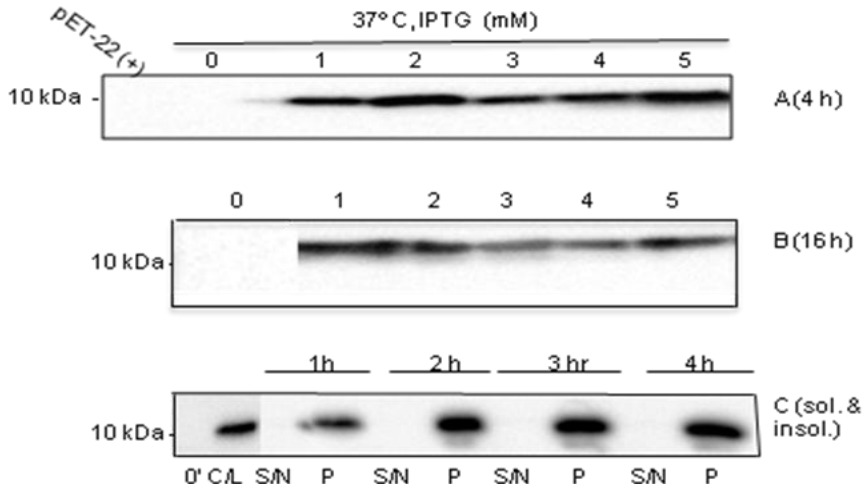

Figure 3.15 Anti-His Western blot of pro-IL-1β Nt-b bacterial expression at 37ºC. Panel A and B show anti-His signals of total lysates from transformed *E. coli* BL21(DE3) with Nt-b expression vector induced at 37ºC by different concentration of IPTG (1 to 5 mM) for 4 (A) and 16 (B) h. Panel C shows the soluble and insoluble fractions of the expressed Nt-b by 2 mM IPTG for different times (1 to 4 h). All Nt-b protein was in the insoluble (insol.) pellet (P) and no soluble (Sol) protein was obtained in supernatant (S/N).

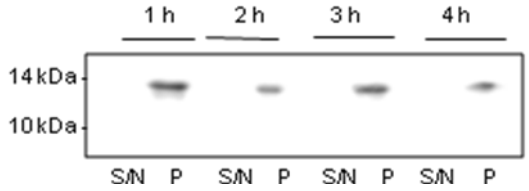

Figure 3.16 Anti-His Western blot analysis of the solubility of pro-IL-1β Nt expression at 37ºC. The panel shows the anti-His signal of the soluble (S/N) and insoluble (P) lysate fractions of the expressed Nt by 2 mM IPTG for different times (1 to 4 h) at 37ºC. No soluble protein was found in the supernatant (S/N) and all expressed pro-IL-1β Nt remained in the pellet (P) fraction.

In order to increase the recovery of soluble protein, the induction of pro-IL-1β Nt-b was performed at two lower temperatures 22 and 28ºC. One ml samples of the cell culture were taken at different time points. The bacteria were solubilised and western blotted with an anti-His antibody as explained in Materials and Methods (Figure 3.17). Expression was achieved at all time points at 28ºC compared to 22ºC where proteins were expressed only after 5 h of induction (Figure 3.17, A and B). At 28ºC maximum solubility was achieved after 2 h induction although most of the expressed protein remained in the pellet fraction as inclusion bodies. At later times all expressed protein remained in the pellet fraction (Figure 3.17, C and D). Next, we expressed Nt protein at 22ºC (Figure 3.18) or

28ºC (Figure 3.19) and solubilised protein was detected by Western blot. In comparison, the highest expression and solubility for Nt was obtained at 28ºC after 4 h induction with 2mM IPTG (Figure 3.19).

Expression and solubility of pro-IL-1β was investigated after induction at 22ºC (Figure 3.20). The protein expression peaked at 4 and 5 h after induction, but at those time points presented maximum protein degradation. The maximum expression of soluble pro-IL-1β protein with minimum degradation was achieved using 2 mM IPTG for 2 or 6 h at 22ºC (Figure 3.20). However, for practical reasons we chose 2 h of induction for future experiments.

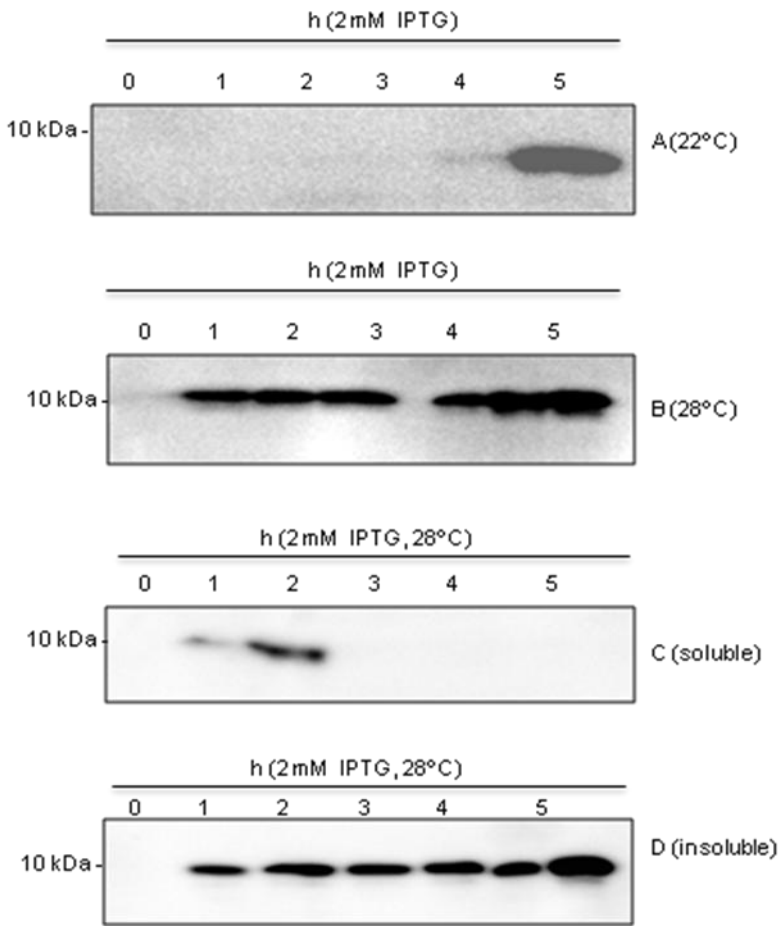

Figure 3.17 Anti-His Western blot analysis of the expression and solubility of pro-IL-1β Nt-b at 28ºC. Panels A and B show the anti-His signal of bacterial lysates uninduced (0) and induced with 2 mM IPTG for different times as indicated (1 to 5 h) at 22ºC (panel A) and 28ºC (panel B). Panel C and D show soluble fractions of Nt-b protein after expression was induced at 28ºC by 2 mM IPTG. Soluble and insoluble fractions are shown in panel C and D, respectively. Solubility was achieved only after 2 h induction.

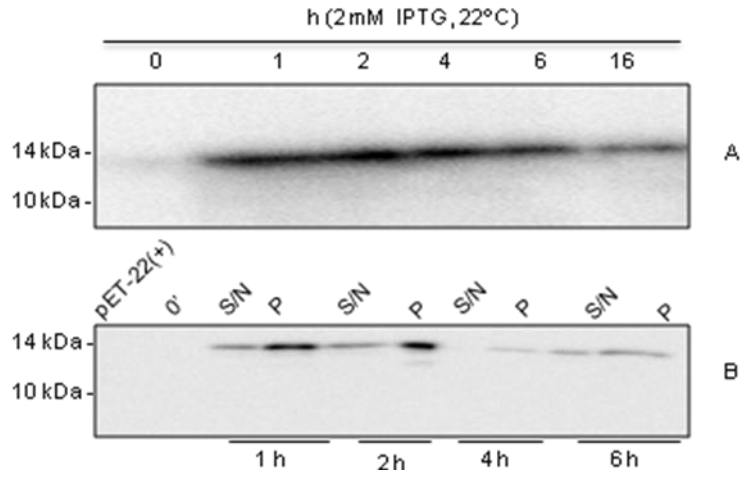

Figure 3.18 Anti-His Western blot analysis of the expression and solubility of pro-IL-1β Nt at 22ºC. Top panel shows the anti-His signal of bacterial lysates uninduced (0) and induced with 2 mM IPTG for different times as indicated (1, 2, 4, 6 and 16 h) at 22ºC. Bottom panel shows soluble (S/N) and insoluble fractions (P) of Nt protein after expression induced at 22ºC by 2 mM IPTG. Solubility was maximum after 1 and 2 h induction. No expression was found in uninduced culture (0) or in bacteria transformed with the empty vector pET-22(+).

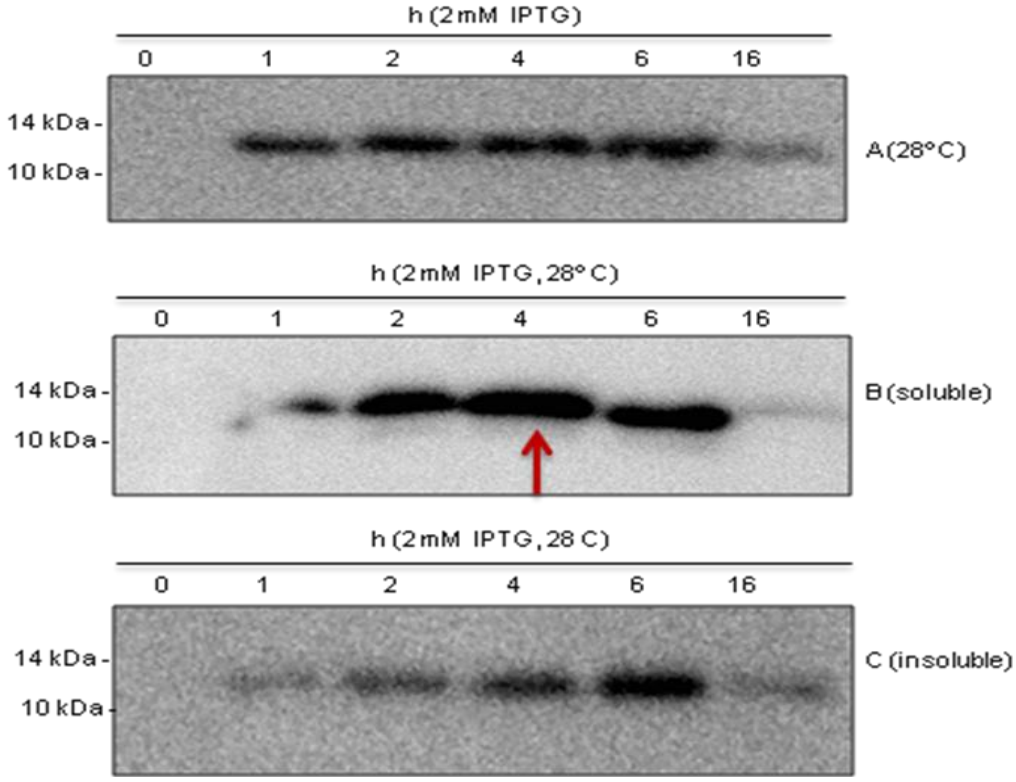

Figure 3.19 Anti-His Western blot analysis of the expression and solubility of pro-IL-1β Nt at 28ºC. Panel A shows the anti-His signal of total bacterial lysates uninduced (0) and induced with 2 mM IPTG for different times as indicated (1, 2, 4, 6 and 16 h) at 28ºC. Panel B and C show Nt protein expression induced at 28ºC by 2 mM IPTG. Soluble and insoluble fractions are shown in panel B and C respectively. The highest solubility was achieved after 4 h induction (red arrow on panel B). No expression was seen in un-induced culture (lane 0).

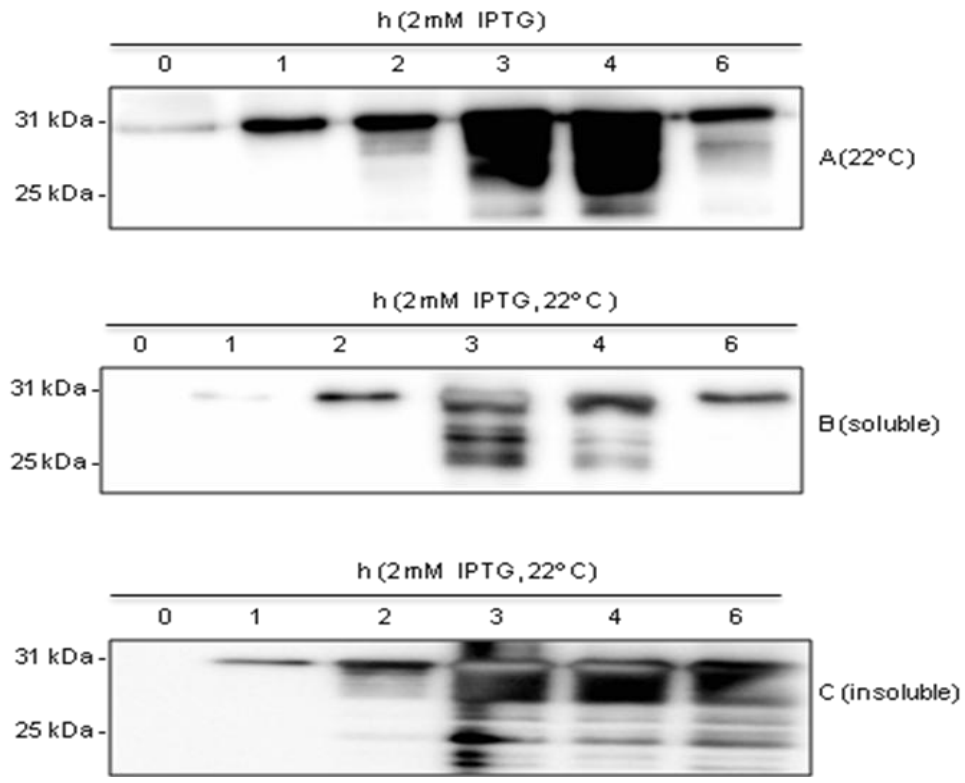

Figure 3.20 Anti-IL-1β Western blot analysis of the expression and solubility of pro-IL-1β at 22ºC. Panel A shows the anti-His signal of total bacterial lysates uninduced (0) and induced with 2 mM IPTG for different times as indicated (1 to 6 h) at 22ºC. Panel B and C show pro-IL-1β protein expression induced at 22ºC by 2 mM IPTG. Soluble and insoluble fractions are shown in panel B and C respectively. The highest solubility was achieved after 4 h induction. No expression was seen in un-induced culture (lane 0).

The optimal conditions for induction, expression and elution of recombinant Nt-b, Nt and pro-IL1β proteins are summaried in table 3.1.

Protein	**IPTG** (mM)	**Time** (h)	**Temperature** (ºC)	**Imidazole** (mM)
Nt-b	2	2	28	300
Nt	2	4	28	300
Pro-IL-1β	2	2	22	300

Table 3.1 Optimal conditions for the expression and purification of Nt-b, Nt and pro-IL-1β.

3.4 Purification of recombinant pro-IL-1β N-terminus fragments

3.4.1 Purification of recombinant proteins using immobilised metal affinity chromatography (IMAC)

Immobilised metal affinity chromatography (IMAC) is a fast, inexpensive, and popular method to purify recombinant proteins from heterogeneous cellular lysates (Porath et al., 1975). IMAC takes advantage of the strong, specific and reversible interaction of certain amino acid side chains (such as tryptophan, cysteine, and especially, histidine) with immobilised transition metals (Ni^{2+}, Co^{2+} or Zn^{2+}). Briefly, the protein of interest is engineered to contain a small repetitive tag of Histidines on the N- or C-terminus. The recombinant protein is exposed to immobilised metal ions ligated to sepharose beads. After binding, the beads are washed and the target protein is eluted, usually with imidazole. IMAC is a reputable separation method standing alongside techniques such as size exclusion chromatography (SEC) and ion exchange chromatography such as AEC (Hochuli et al., 1987).

Purification of pro-IL-1β N-terminus fragments and pro-IL-1β was initially performed utilising Co^{2+} based IMAC techniques. Small-scale purification of pro-IL-1β was started by growing a culture of 10 ml at the conditions for optimal solubilisation.

Nt-b and Nt proteins were induced at optimal conditions (Table 3.1). Cells were harvested, solubilised and then mixed with 20 µl of bed volume equilibrated beads for 30 min. After washing, elution was achieved by incubation at different concentrations of imidazole for 30 min at 4ºC. Highest elution rate for both Nt and Nt-b proteins was achieved by 300 mM imidazole incubated after 30 min at 4ºC (Figures 3.21 and 3.22).

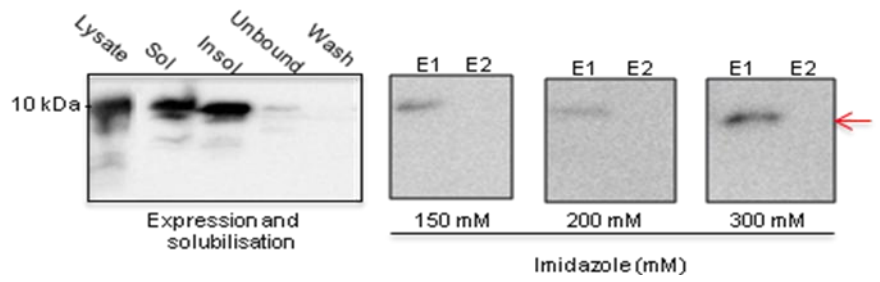

Figure 3.21 Anti-His western blot of eluted pro-IL-1β Nt-b after adding to IMAC. The solubilised protein was added to the equilibrated Co^{2+} Talon resins (IMAC) for 30 min at 4°C. The proteins were eluted by different concentrations of imidazole, 150 mM imidazole, 200 mM imidazole and 300 mM imidazole. Two consecutive elutions (E1 & E2) for the different concentrations of imidazole were performed to obtain maximum protein recovery. Maximum recovery was achieved using 300 mM imidazole (red arrow).

Expression of pro-IL-1β protein was induced using optimal conditions (Table 3.1). Elution was achieved using the same protocol as explained for Nt fragments. The highest concentration of imidazole (300 mM) resulted in the highest recovery of protein (Figure 3.23).

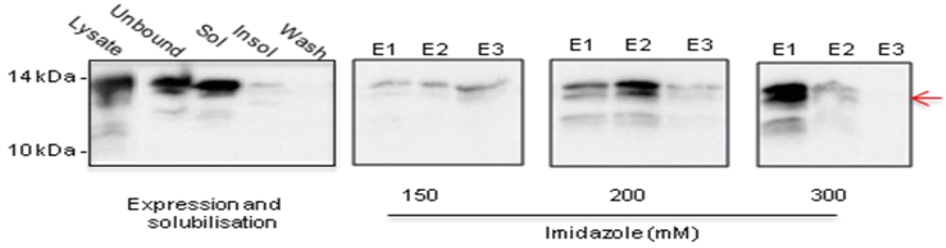

Figure 3.22 Anti-His Western blot of eluted pro-IL-1β Nt after adding to IMAC. The solubilised protein was added to the equilibrated Co^{2+} Talon resins for 30 min at 4ºC. The proteins were eluted by different concentrations of imidazole: 150 mM, 200 mM and 300 mM. Three consecutive elutions (E1 to E3) for the different concentrations of imidazole were performed to obtain maximum protein recovery. Maximum recovery was achieved using 300 mM imidazole (red arrow).

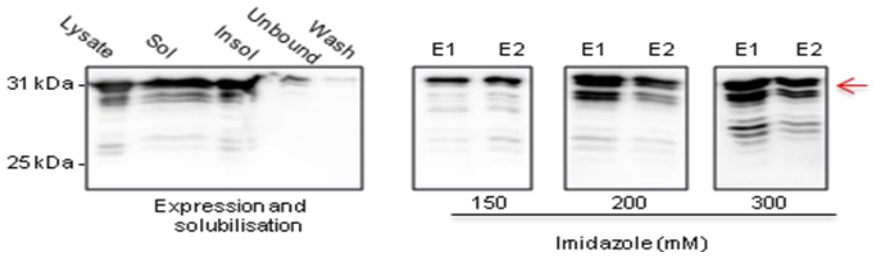

Figure 3.23 Anti-IL-1β Western blot of eluted pro-IL-1β after adding to IMAC. The solubilised protein was added to the equilibrated Co^{2+} Talon resins for 30 min at 4ºC. The proteins were eluted by different concentrations of imidazole: 150 mM (A), 200 mM (B) and 300 mM (C). Two consecutive elutions (E1 and E2) for the different concentrations of imidazole were performed to obtain maximum protein recovery. Maximum recovery was achieved using 300 mM imidazole (red arrow).

In order to increase the purity of the eluted proteins, solubilised lysates were passed through different size cut-off filters to remove bacterial proteins with a molecular mass higher or lower than our desired target proteins. 30 and 50 kDa cut-off filters were used for Nt fragments and pro-IL-1β, respectively. However, these cut-off filters made no significant difference to the recovery of the eluted fraction and most of the recombinant proteins did not pass through the filter. As shown in figure 3.24, only half of the 10 kDa Nt-b protein passed through the 30 kDa cut-off filter. Almost all of Nt (14 kDa) and pro-IL-1β (31 kDa) protein remained in the greater than 30 and 50 kDa fraction, respectively (Figure 3.24).

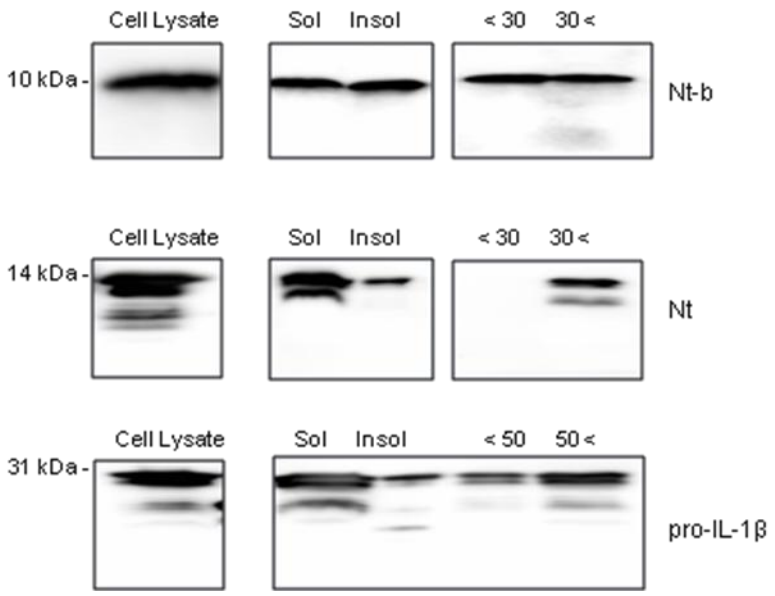

Figure 3.24 Anti-IL-1β Western blot of soluble pro-IL-1β and anti-His Western blot of N-terminus fragments. Soluble fractions were passed through 30 and 50 kDa cut-off filters as indicated. Most of Nt-b expressed protein did not pass through the 30 kDa cut-off filter (top panel). None of Nt protein was passed through the 30 kDa cut-off filter (medium panel). Pro-IL-1β was highly retained in the 50 kDa cut-off filter fraction (bottom panel).

3.4.2 Purification of recombinant proteins using anion exchange chromatography (AEC) and size exclusion chromatography (SEC)

Column chromatography is used to separate organic compounds on the basis of their charge and size. It consists of two phases: mobile (proteins to be separated) and stationary (glass beads or resin) through which mobile phase

travels at different rates. In anion exchange chromatography (AEC) the molecules are separated on the basis of their charge since the resin of the column has a positive charge so it would bind to negatively charged molecules. A high salt buffer is used to elute the desired protein from the column after contaminant proteins are removed by extensive washing. In SEC the molecules are removed on the basis of their size. Microscopic glass beads with tiny holes are packed into column. Once the sample is passed through the column, the molecules that are smaller than the holes get retained in the beads. Thus smaller molecules move more slowly through the column than bigger ones.

Once optimal Co^{2+} Talon elution conditions were established (Table 3.1), we checked the purity of the eluted fractions by Coomassie blue or silver staining on 15% SDS-PAGE electrophoresed gels. As shown in figure 3.25 (panel A) elution of pro-IL-1β from the Co^{2+} Talon column with imidazole (E1 and E2) also carries other contaminant bacterial proteins.

In order to increase the purity, second column (AEC and/or SEC) were applied. Bacterial expression of pro-IL-1β from 50 ml cultures was induced and eluted from Talon columns following optimal conditions (Table 3.1) and followed by AEC. As shown in figure 3.25 (panels A and B), the eluted protein did come off the column in waste fractions of the miniQ^{TM} AEC column (fractions A13 to A15 and B1 to B4).

Since pro-IL-1β was eluted in the waste fraction, we decided to apply first a SEC column (Superdex 75). Figure 3.26 shows anti-His western blot (C) and silver staining (D) of A2-A13 eluted fractions. Almost all eluted proteins were in A3 and A4 fractions. These fractions also corresponded with the waste fractions of the column. In order to see if it is possible to recover the protein, these fractions were applied to AEC column (mini Q) (Figure 3.27). Although most of the protein was

lost during the purification steps, some was eluted in the B1 and B2 fractions of the mini Q column but with some other contaminant bacterial proteins (Figure 3.27).

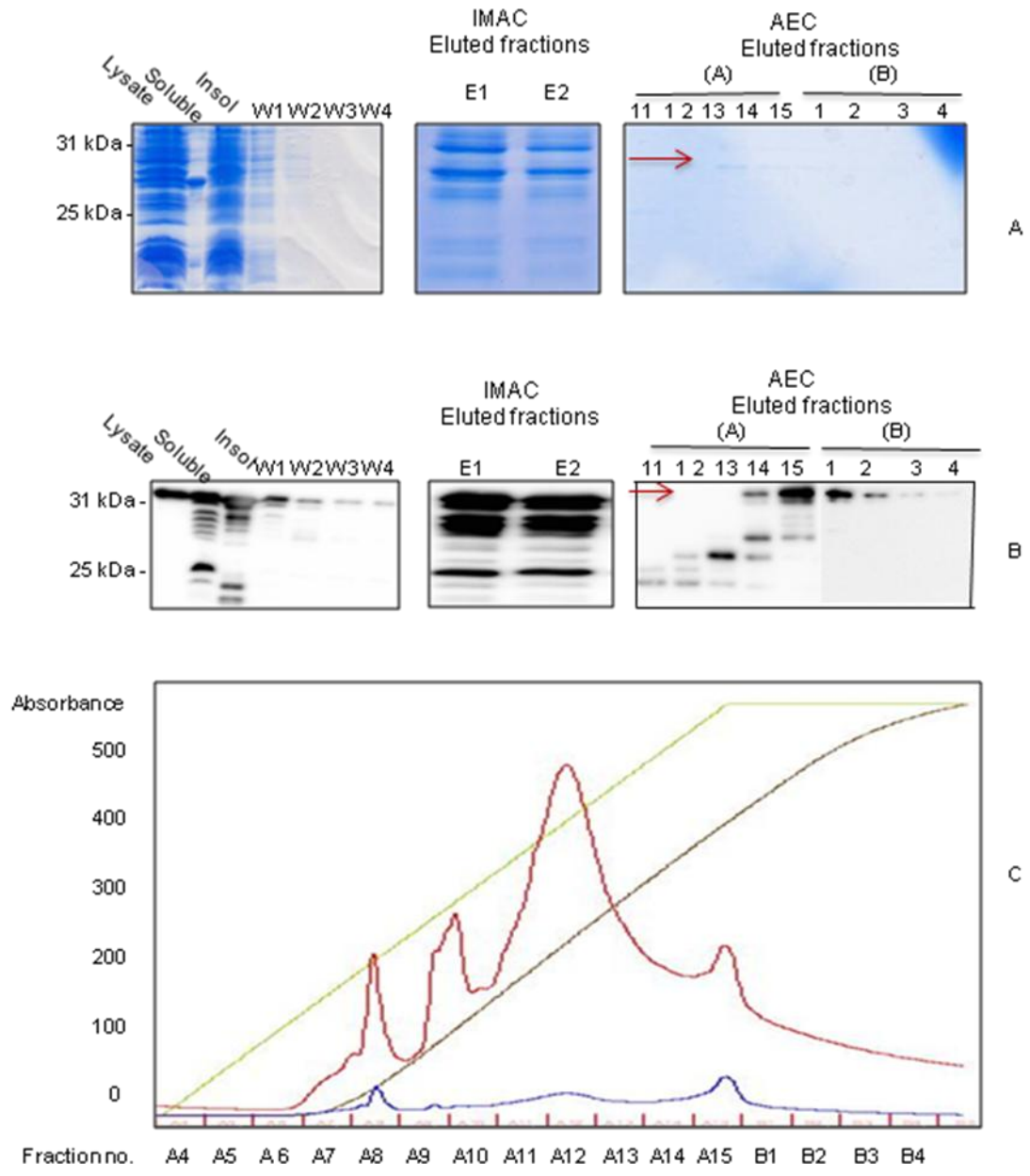

Figure 3.25 HPLC (miniQ) profile of Co^{2+} Talon column eluted pro-IL-1β. The eluted fractions (E1 and E2) from Co^{2+} Talon resins were added to an equilibrated miniQ column. Coomassie blue staining (panel A) and anti-IL-1β Western blot (panel B) of eluted fractions from Co^{2+} Talon resins (E1 and E2) and the eluted fractions (A13 to A15 and B1 to B4) of mini-Q column. Panel C shows the HPLC elution profile of mini-Q column eluted fractions A13 to A15 and B1 to B4. Blue line shows absorbance at 280 nm, red line absorbance at 254 nm, green line is the pressure and brown line is the salt concentrations (panel C). All pro-IL-1β was found in fractions A13-A15 which corresponds to the non-specific waste elutions. Red arrow shows eluted protein.

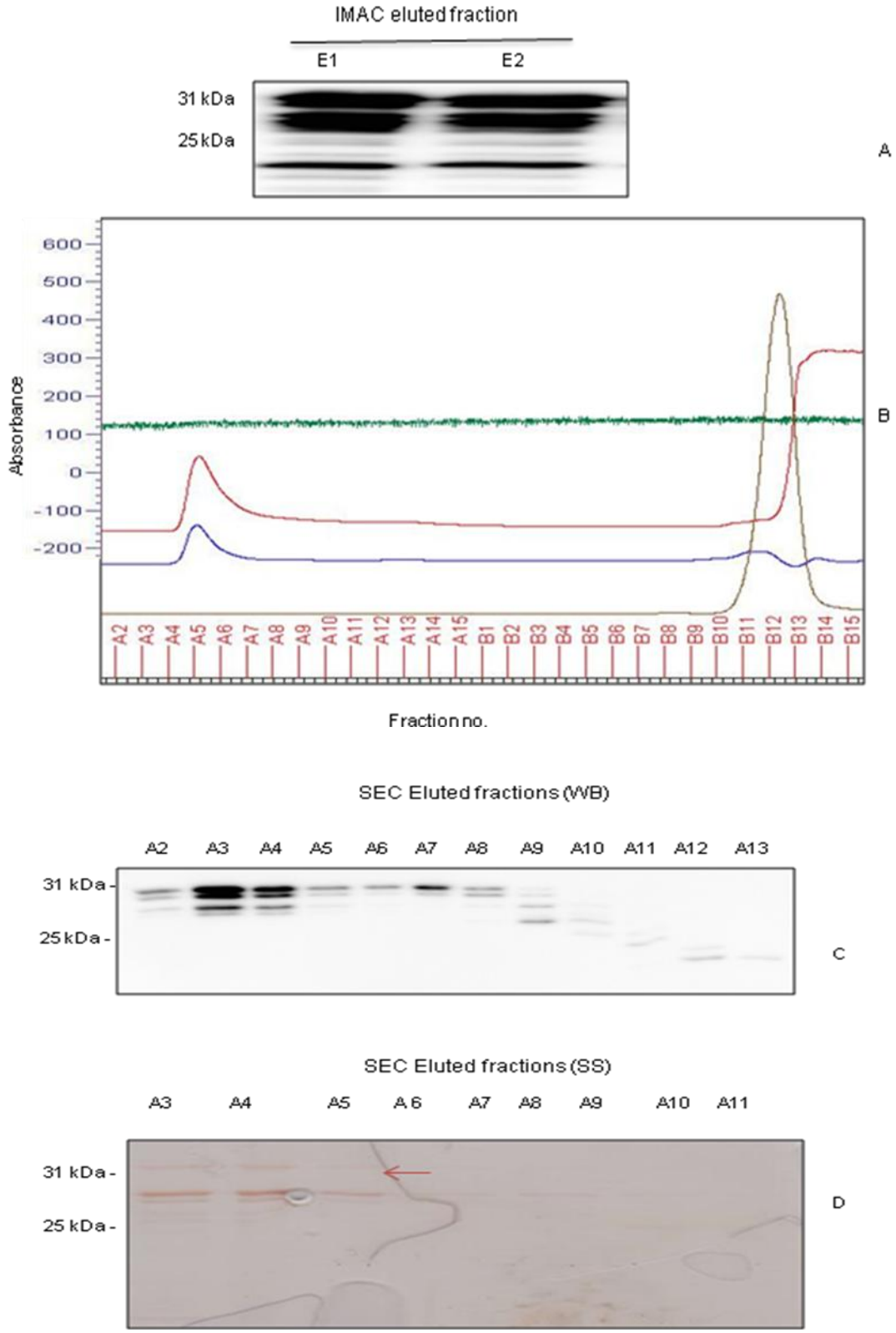

Figure 3.26 SEC profile of Co^{2+} Talon column eluted pro-IL-1β. The eluted fractions from Co^{2+} Talon resins (E1 and E2) (A) were fractionated by SEC (Superdex 75 column). Panel B shows the SEC elution profile of the pro-IL-1β. Blue line represent absorbance at 280 nm and red line absorbance at 254 nm, green line shows pressure and brown line conductivity (B). Anti-IL-1β Western blot (WB) analysis (C) of eluted protein from A2 to A8 fractions (highest protein was found in A3 and A4 fractions). Silver staining (SS) (D) demonstrate contaminant proteins in A3-A5 fractions (red arrow).

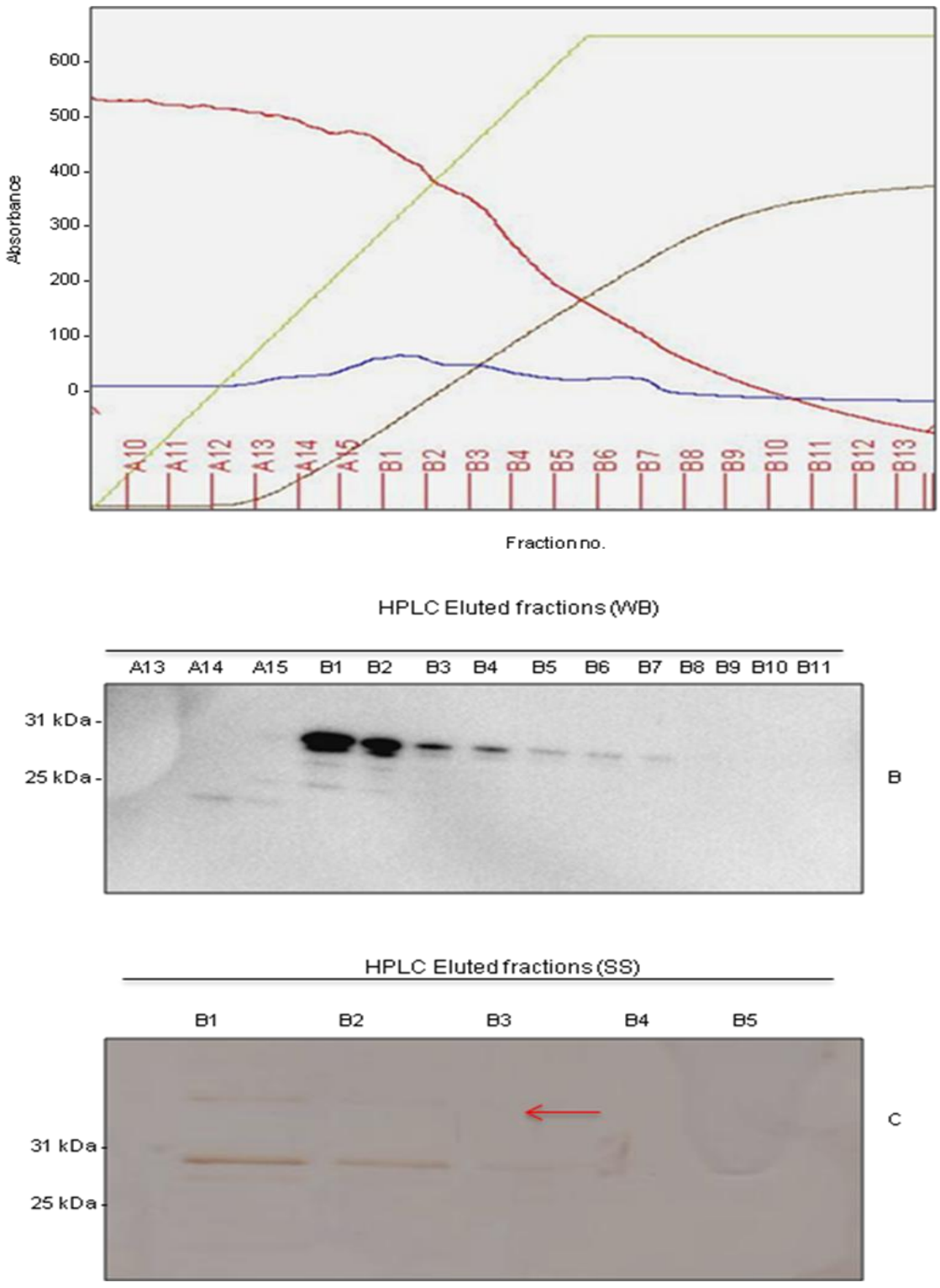

Figure 3.27 HPLC (miniQ) profile of pro-IL-1β protein after SEC. Co^{2+} Talon column eluted pro-IL-1β fractions (E1 and E2) were fractionated by SEC (Superdex 75 column). A3 and A4 fractions were applied to mini-Q Column for further purification. Panel A shows the result of AEC (red line is absorbance at 254 nm, blue line absorbance at 280 nm, yellow line salt concentration and brown line conductivity). Anti-IL1β Western blot (WB) analysis (B) of eluted protein from A13 to A15 and B1 to B11 fractions show that the pro-IL-1β protein was eluted in B1 to B7 fractions (highest elution in B1 and B2). Silver staining (SS) (C) demonstrate a contaminant protein in B1-B3 fractions (red arrow).

The same protocol was applied to pro-IL-1β Nt protein. After optimal expression and elution from Co^{2+} Talon resins (Table 3.1 and Figure 3.28, panel B), the initial imidazole eluted fractions (E1 and E2) were pulled and applied onto Superdex SEC column. As demonstrated by Western blot and SDS-PAGE silver staining the pro-IL1-β Nt protein was recovered at early fractions of elution (A2 to A4) (Figure 3.28, panels B-D). A clear higher mass protein (approximately 20 kDa) was also purified from fractions A2-A4 together with Nt protein. In order to increase purity these fractions were applied to a min-Q AEC column (Figure 3.29). However, as demonstrated by Western blot almost all of the protein was lost during second AEC column purification (Figure 3.29).

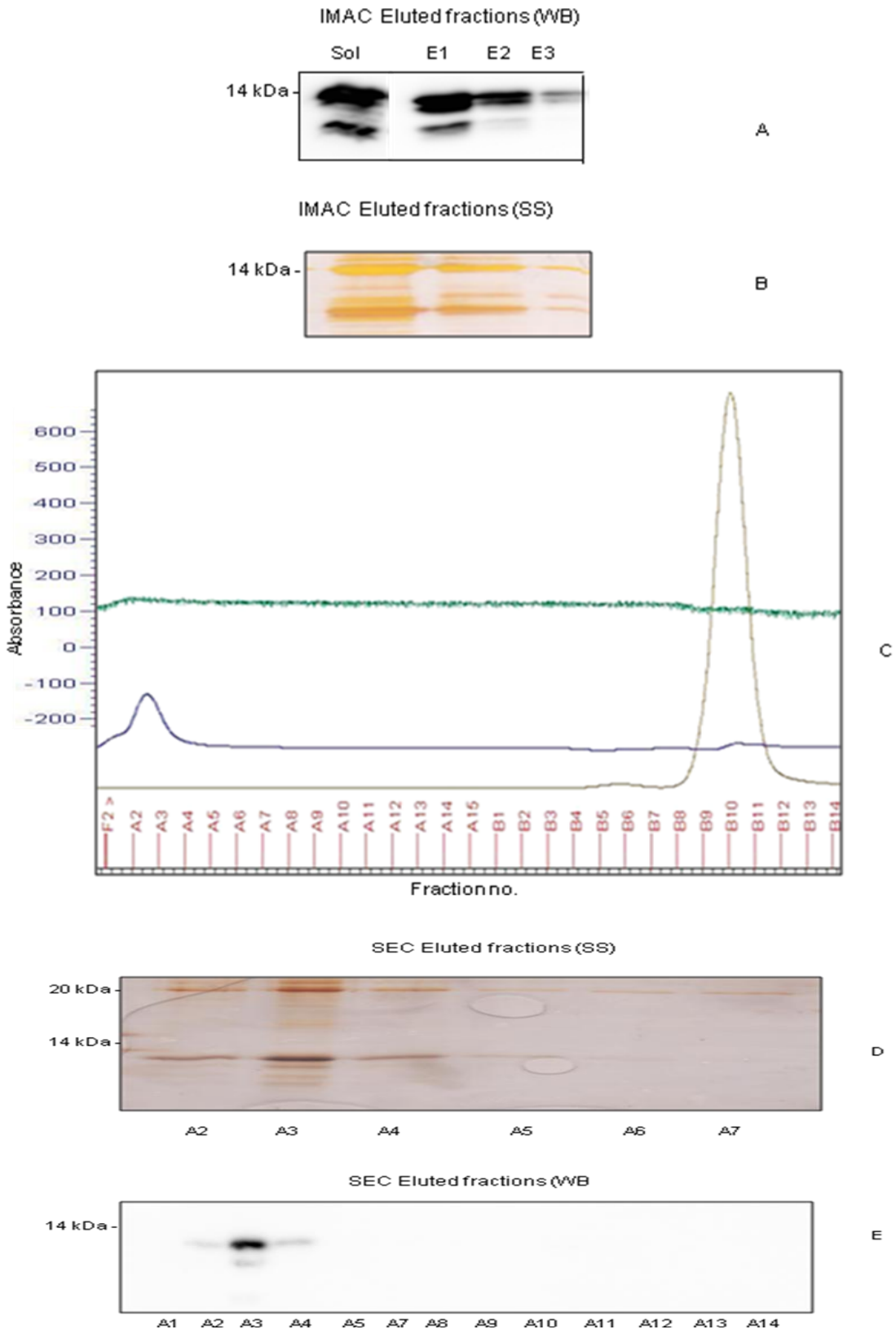

Figure 3.28 SEC profile of Co^{2+} Talon column eluted pro-IL-1β Nt. The imidazole eluted fractions (E1 and E2) (A) were fractionated by SEC (Superdex 75 column) (B). Blue line represents absorbance at 280 nm, green line pressure and brown line conductivity. The purity of fractions was analysed by silver staining (SS) (C). Nt protein was eluted in fraction A2-A4 in combination with a contaminant protein (about 20 kDa). The presence of Nt protein in fractions A2 to A4 was also confirmed by Anti-His Western blot (WB) (D).

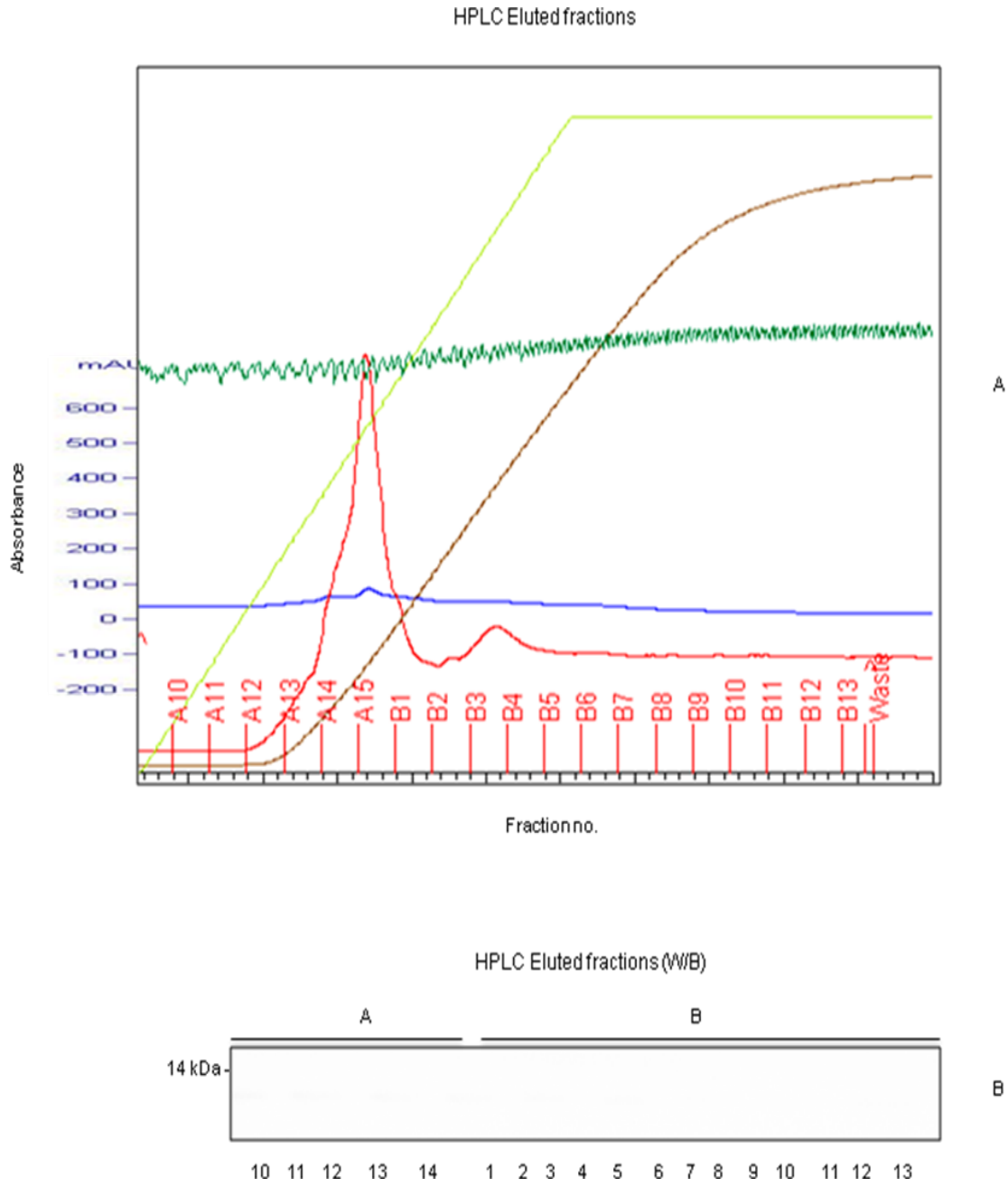

Figure 3.29 HPLC (miniQ) profile of pro-IL-1β Nt protein from SEC (fractions A2-A4). Panel A shows the result of AEC (red line is absorbance at 254 nm, blue line absorbance at 280 nm, brown line conductivity and green line pressure). Anti-His Western blot (W/B) (panel B) shows that pro-IL-1β Nt protein was not eluted in any fractions after AEC second column.

3.5 Summary

The N-terminus fragments and full-length of pro-IL-1β were cloned in IPTG inducible bacterial expression vectors and produced as His-tagged proteins in *E. coli* BL-21(DE3) strain. All proteins were purified by Co^{2+} Talon affinity chromatography followed by SEC and/or AEC in order to increase their purity. However, the proteins were not purified to high homogeneity. Pro-IL-1β always co-purified with a higher mass protein and Nt protein always co-purified with several other contaminating bacterial proteins. Because of the impurity, we were not able to use these proteins for further experiments since we planned to look at inflammatory responses and contaminating bacterial proteins would prevent any reliable interpretation of the data. Because of the limitation of our engineered bacterial expression system, we were pursuaded to clone and express these genes in mammalian expression vectors (chapter 4).

CHAPTER 4

Cloning and expression of pro-IL-1β N-terminus fragments in mammalian cells

4.1 Introduction

In this chapter we used mammalian expression systems as opposed to bacterial expression systems in order to exclude any chance of bacterial endotoxins contaminating our samples. The effect of such bacterial endotoxins could mask the possible immunoregulatory effect of pro-IL-1β Nt fragments on macrophages, since endotoxins are strong activators of these cells. In order to compensate for the lower production of recombinant protein in mammalian expression systems, we designed a strategy where the recombinant Nt-b and Nt proteins were fused to the signal peptide (SP) of colony stimulating factor (CSF)-1 at their N-terminus. With this strategy we could isolate the recombinant protein from the culture supernatants, which is a much simpler protein environment compared with complex cellular extracts. After protein expression the SP would be cleaved in the ER and thus absent in the mature secreted protein. This approach has been successfully used in our lab to export other cytoplasmic proteins, such as the Apoptosis-associated Speck-like protein containing a Caspase-activating recruiting domain (ASC). In addition, we will introduce a C-terminus myc epitope (myc) in our new pro-IL-1β Nt constructions to aid detection by Western blot.

4.2 Construction of SP-Nt-b-Myc and SP-Nt-Myc expression vectors

The vector used to generate the recombinant plasmids for pro-IL-1β Nt fragments was derived from the mammalian expression vector, pcDNA3.1(+). This vector has the human cytomegalo virus (CMV) immediate-early promoter that allows high level expression of the gene in a wide range of mammalian cells (Liu et al., 1997). The 5'-upstream SP, 3'-downstream myc tag, Nt-b and Nt fragments were generated by independent PCRs using specific overlapping primers. SP sequence was amplified from the vector pEM57, which contained the full

sequence of mouse CSF-1, using the primers T7 and P2-Nt-b or P2-Nt (Table 2.7). The myc tag sequence was amplified from the vector pPP68, which contained the human sequence of pannexin-1 followed by the c-myc tag using the primers P5-Nt-b/P5-Nt and P6 (Table 2.7). The Nt-b and Nt sequences were amplified separately using primers P5-Nt-b or P5-Nt in combination with BGHR (Table 2.7) from pEM7 and pEM5, respectively (Figure 4.1). All these amplified fragments were resolved on 1% low melting point agarose gels and extracted for subsequent sub-cloning (Figure 4.2). The size of all initial PCR fragments were as expected: SP: 100 bp; Myc: 135 bp; Nt-b: 276 bp; and Nt: 356 bp) (Figure 4.2).

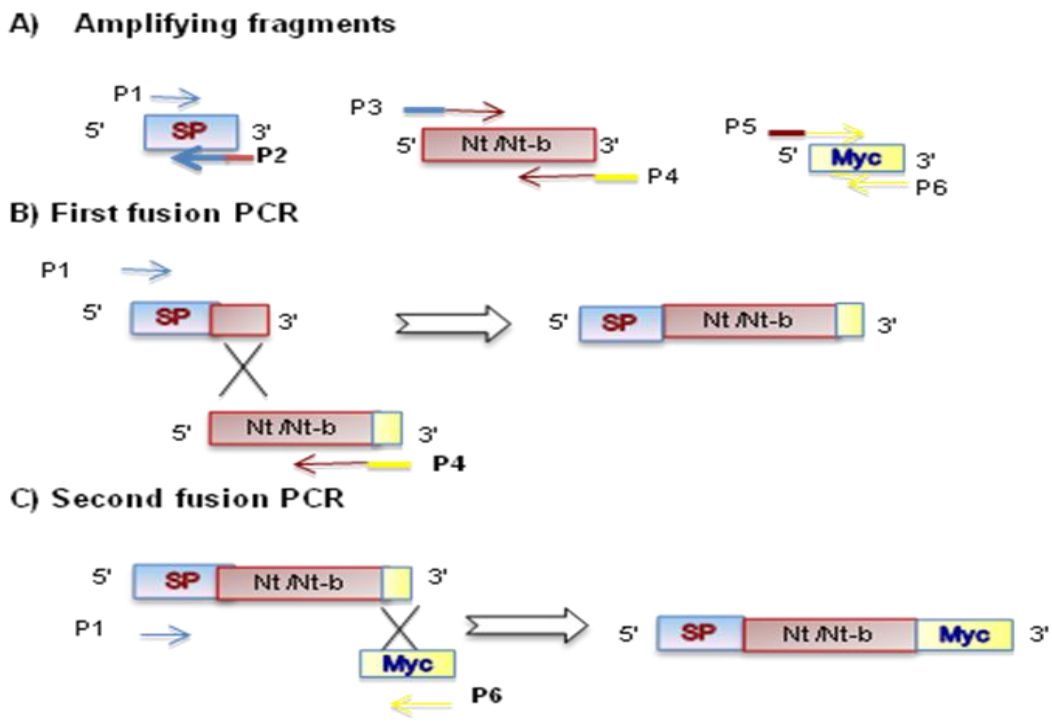

Figure 4.1 Diagram of PCR-based construction of the SP-Nt-b/Nt-Myc vector. A) Corresponding genes were amplified from original plasmids (SP: pEM57, Nt: pEM5, Nt-b: pEM7 and myc tag: pPP68) by different PCRs. The overlapping homology on the ends of the PCR fragments was generated by amplification of 5'- and 3'-flanking regions with designed primers specific for the sequence of the target fusion fragment. **B)** The 5'- and 3'-flanking regions are joined to Nt-b or Nt and using flanking primers for each of the two fragments which resulted in first fusion PCR. **C)** The final PCR product was amplified with the outermost primers P1 and P6 (second fusion PCR). Second fusion PCR product can be directly used to transfect COS-7 or HEK cells.

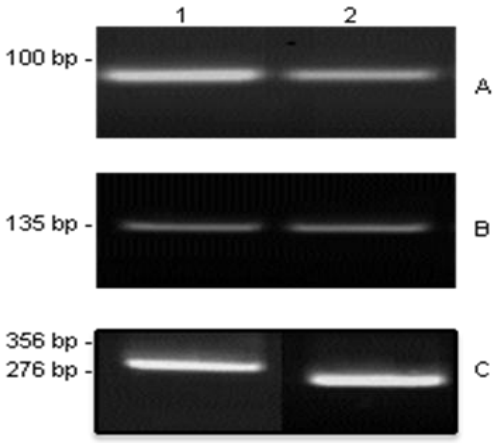

Figure 4.2 PCR amplification of SP (A), myc tag (B) and pro-IL-1β Nt fragments (C). Lane 1 shows the amplified products for Nt-b constructs and Lane 2 shows the amplified products for Nt-b constructs. The products of these PCR were used to generate the Nt construction.

These PCR products were first used to fuse the SP to pro-IL-1β Nt sequences by overlapping PCR with T7 and P4 Nt or P4 Nt-b primers (Table 2.3) and resolved on 1% low melting point agarose gel. The sizes of the different fusion products were as expected, 408 bp for SP-Nt-b and 485 bp for SP-Nt (Figure 4.3). The amplification products were excised from the gel and used in subsequent overlapping PCR to incorporate the myc epitope sequence obtained before (Figure 4.2) using the T7 and BGHR primers (Table 2.3). Final generation of SP-Nt-b-myc and SP-Nt-myc sequences was confirmed by resolving purified PCR reactions on 1% agarose gel. The sizes of the different fragments were as expected: 566 bp and 643 bp for SP-Nt-b-myc and SP-Nt-myc, respectively (Figure 4.4).

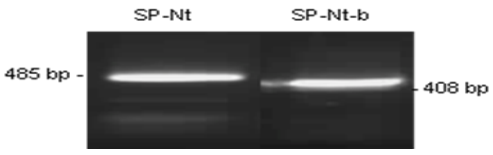

Figure 4.3 Generating a SP at 5' upstream of Nt and Nt-b by PCR. The first fusion PCR products of SP (5'-upstream) with Nt and Nt-b were generated in frame sequences by designed primers. The resultant 1st fusion products, SP-Nt and SP-Nt-b corresponded to desired sizes, 485 and 408 bp, respectively.

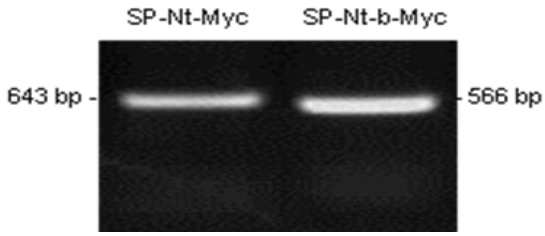

Figure 4.4 Generating a myc tag at 3' downstream of Nt and Nt-b by PCR. The products of 1st fusion PCR, SP-Nt (485 bp) and SP-Nt-b (408 bp) were used to fuse myc tag at their C-terminus by designed primers. The generated SP-Nt-myc and SP-Nt-b-myc corresponded to desired sizes, 643 and 566 bp, respectively.

The purified PCR products and the host vector (pcDNA3.1(+)) were digested by *Hind*III restriction enzyme, since there was a unique *Hind*III restriction enzyme within the multiple cloning site of the vector and on the flanking sequences of SP-Nt-myc and SP-Nt-b-myc generated fragments. After digestion, the vector was de-phosphorylated in order to prevent re-ligation and used for subsequent ligation with *Hind*III digested SP-Nt-myc and SP-Nt-b-myc fragments. Ligation reactions were transformed into *E. coli* JM109 competent cells and seeded into LB ampicillin plates. Ten ampicillin resistant colonies were screened by PCR amplification of constructs using oligonucleotides T7 and BGHR. PCR products were resolved on 1% agarose gel. There were 5 positive colonies for SP-Nt-b-myc construct and 9 positive colonies for SP-Nt-myc (Figure 4.5).

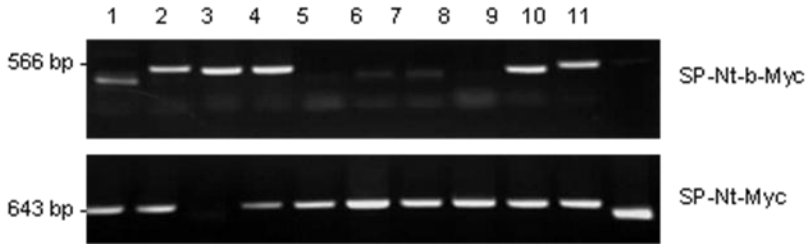

Figure 4.5 Screening of randomly selected colonies from the library of SP-Nt-b-Myc (A) and SP-Nt-myc (B) constructs after transformation into *E. coli* JM109. Selected colonies were amplified by PCR and run on agarose gel stained with ethidium bromide. The size of the fragments is as expected for SP-Nt-b-Myc (566 bp) and the SP-Nt-myc (643 bp). Lane 11 in lower panel was used as positive control (pEM4).

One colony containing the SP-Nt-b was purified by mini-prep. Digestion of purified plasmids with *BbvC*I confirmed insertion of the gene of interest into the vector, since there is only one *BbvC*I restriction site in the Nt sequence which is absent in the pcDNA3.1(+) sequence (Figure 4.6). The orientation of the inserts was further confirmed by *Hind*III restriction digestion, which resulted in three expected products of 5.6 kbp, 556 bp and 643 bp (Figure 4.6).

Finally, the correct nucleotide sequence of the cloned genes was confirmed by automated sequencing across the full length of the recombinant vectors, using the universal primer T7 and intermediate specific primers P4, P5 and BGHR (Table 2.3). The nucleotide sequences of the cloned genes were identical to the expected sequence. The sequencing also confirmed that the cloned fragments were in frame with the start codon, signal peptide, the genes of interest, myc tag and stop codon (Figures 4.7 and 4.8).

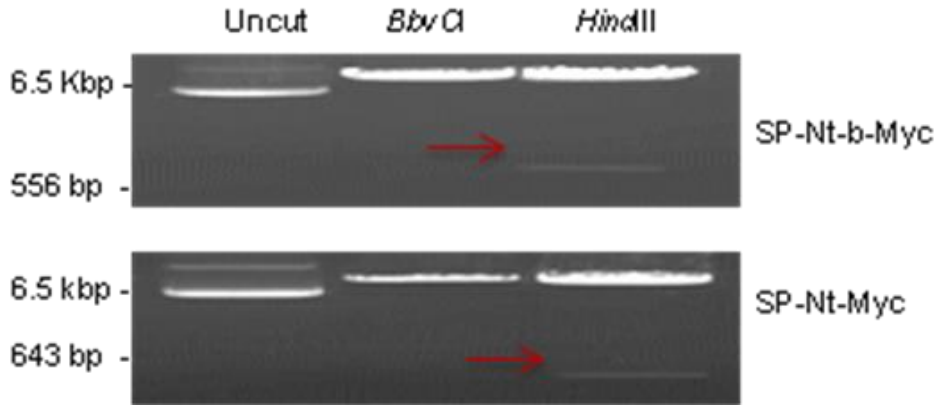

Figure 4.6 Restriction digestions of SP-Nt-b-myc and SP-Nt-myc genes after cloning into the pcDNA3.1(+) expression vector. The figure shows uncut plasmid, *BbvC*I and *Hind*III restriction reaction of SP-Nt-b-myc (top) or SP-Nt-myc (bottom) cloned into pcDNA3.1(+) vector, respectively. Red arrow denotes the small fragment of 556 bp and 643 bp after *Hind*III restriction reaction of SP-Nt-b-myc and SP-Nt-myc genes.

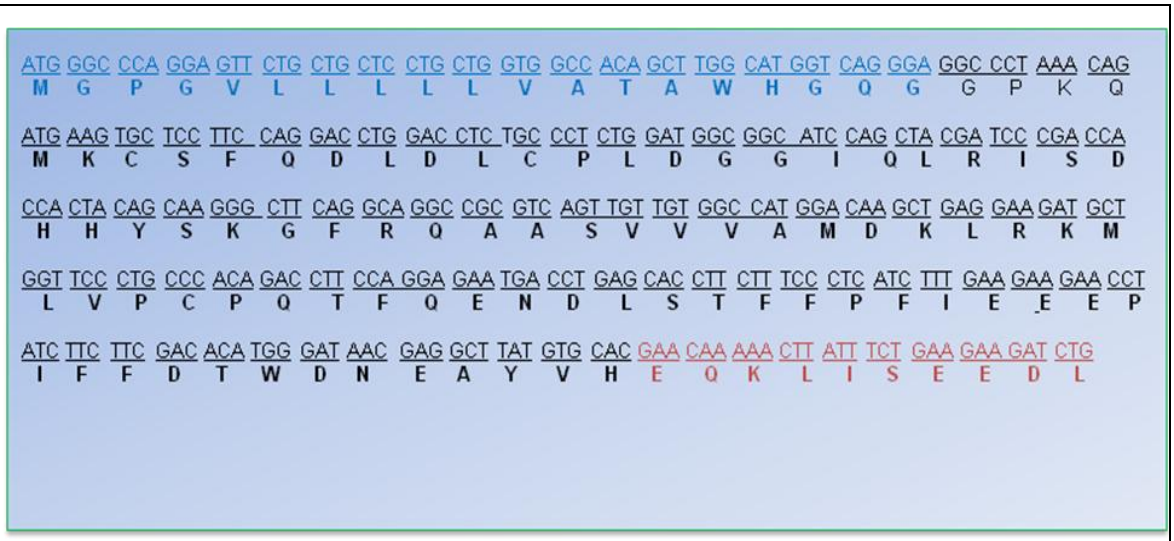

Figure 4.7 DNA and protein sequence alignment of SP-Nt-b myc genes cloned into pcDNA3.1(+). DNA sequence shows the genes are in frame with start codon (ATG), the SP (in blue), Nt-b gene (in black) and myc tag (in red). The protein sequence is as predicted (B).

Figure 4.8 DNA and protein sequence alignment of SP-Nt-myc genes cloned into pcDNA 3.1(+). DNA sequence shows the genes are in frame with start codon (ATG), the SP (in blue), Nt gene (in black) and myc tag (in red). The protein sequence is as predicted (B).

4.3 Transfection into mammalian cell lines

We next assessed expression and release of Nt proteins in mammalian cells. Constructs were transfected into human embryonic kidney (HEK293T) and monkey kidney (COS-7) cell lines seeded at a density of 5×10^5 cells/well in six-

well plates, and were 70-80% confluent on the day of transfection. Transfection was performed with different amounts (1-4 µg) of plasmid DNA using Lipofectamine™2000 according to the manufacturer's instructions. The expression and release of Nt-b and Nt was analysed at protein levels by an anti-myc Western blot.

Initially the expression of Nt-b and Nt proteins was assessed in lysates of transfected HEK293T and COS-7 cell lines 24-72 h after transfection. However, no anti-myc signal was found by Western blot in the lysates or in the concentrated media of transfected HEK293T or COS-7 cells for the expected molecular size of Nt or Nt-b (Figures 4.9 and 4.10). A strong signal in the lysates of cells transfected with a Pannexin-1-myc vector (used as a positive control) was detected corresponding to the expected size of this protein (50-55 kDa). These data suggest that the lack of signals for the new constructions was not due to transfection or an antibody detection problem.

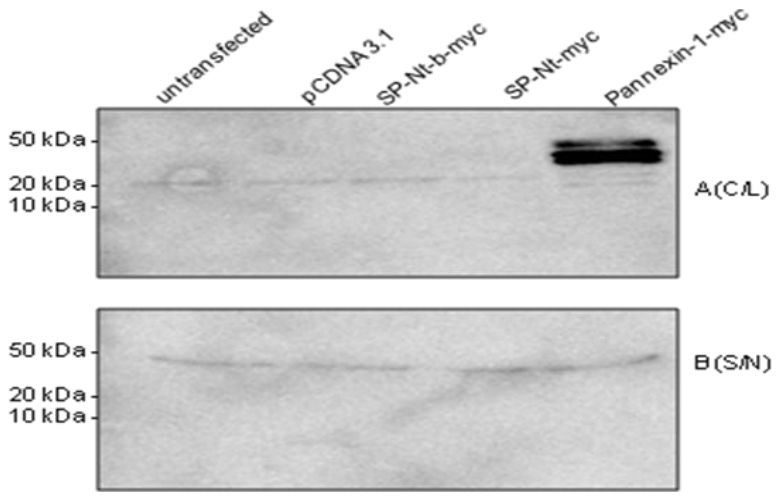

Figure 4.9. Anti-myc Western blot for HEK293T. The figure represents anti-myc Western blot of cell lysates (C/L) (A) or concentrated supernatants (S/N) (B) of untransfected cells (lane 1) or transfected with mock plasmid (pcDNA3.1(+), lane 2)), SP-Nt-b-myc (lane 3), SP-Nt-myc (lane 4) and Pannexin-1-myc (lane 5) (positive control). The results are representative of four independent transfections.

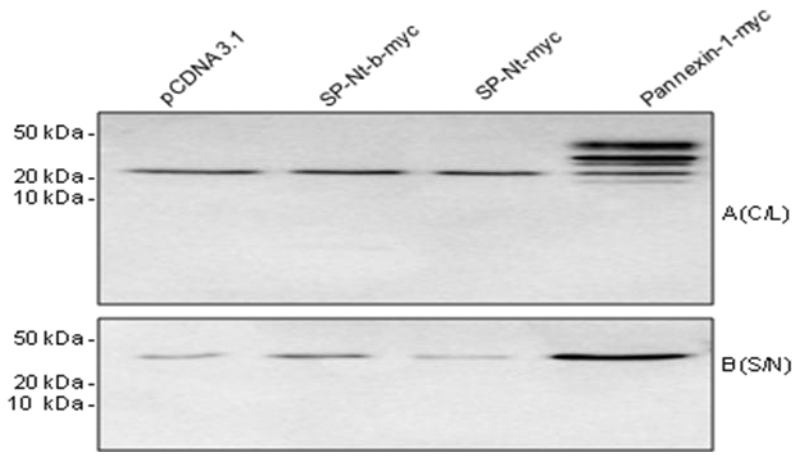

Figure 4.10 Anti-myc Western blot for COS-7. The figure shows anti-myc Western blot of cell lysates (A) or concentrated supernatants (B) of mock plasmid pcDNA3.1(+) or transfected with SP-Nt-b-myc, SP-Nt-myc or Pannexin-1-myc (Panx-1) (positive control). The results are representative of four independent transfections.

Due to the small size of the expected recombinant Nt and Nt-b proteins and the apparent difficulty in expressing them in mammalian cell lines, we did not know if the lack of expression was due to a problem with the newly created vectors containing the signal peptide. Transfection and expression of the already validated original starting vectors lacking the SP (pro-IL-1β-V5, Nt-V5 and Nt-b-V5) was used to set up transfection conditions. After 48 h transfection into COS-7 cells, anti V5 Western blot of the lysates revealed a specific signal for pro-IL-1β-V5 (31 kDa) and SP-ASC-V5 (used as a positive control A). The release of a 25 kDa protein can be detected in the concentrated supernatant which corresponds to the release of the ASC protein with SP (Figure 4.11, panel B). However, no specific anti-V5 signal was found for the transfected constructs Nt-b-V5 (10 kDa) or Nt-V5 (14 kDa), suggesting that the expression of these small proteins does not occur in the conditions used (Figure 4.11, panel A).

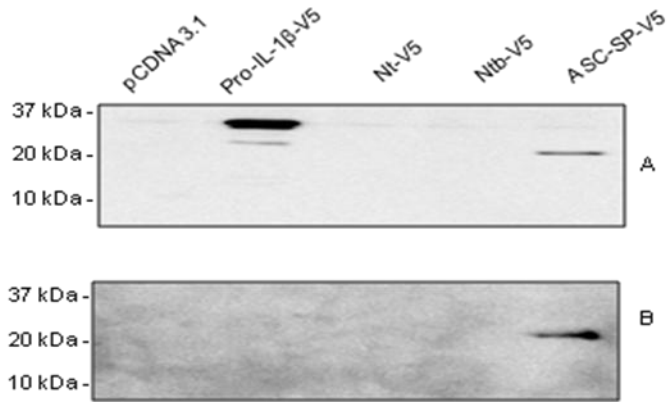

Figure 4.11 Anti-V5 Western blot for COS-7 cell line. The figure shows anti-V5 Western blot of the lysates (A) or concentrated supernatants (B) transfected with mock plasmid (pcDNA3.1(+)), pro-IL-1β-V5, Nt-b-V5 , Nt-V5 , or SP-ASC-V5. The results are representative of three independent transfections.

We next asked if the Nt and Nt-b plasmids were getting into the cell and if they were expressed at transcript levels in the conditions used. Isolation of total DNA and RNA was performed from transfected cells and PCR or RT-PCR revealed that all plasmids were getting into the cells, but only pro-IL-1β was expressed at transcript level (Figure 4.12).

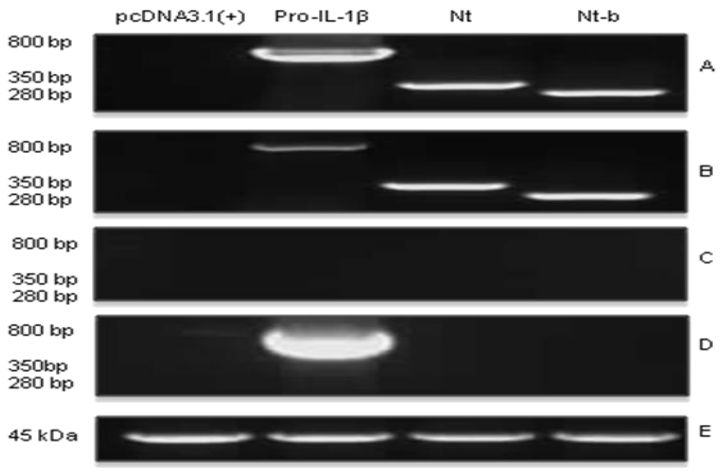

Figure 4.12 PCR (A and B) and RT-PCR (C-E) for control plasmids (A) or COS-7 cell extracts (B-E) transfected with pcDNA3.1(+) (mock), pro-IL-1β-V5, Nt-V5 or Nt-b-V5 constructions. Panel A shows the PCR of original purified plasmids. Panel B shows PCR from extracted DNA from COS-7 cells, panel C shows negative RT-PCR, panel D shows RT-PCR for IL-1 and panel E shows β-actin. Only pro-IL-1β RNA was detected and confirms the sole expression of pro-IL-1β in COS-7 (D). The results are representative of three independent transfections.

4.4 Summary

The N-terminus fragments were cloned into the pcDNA3.1(+) plasmid. The new constructs were used to transfect two mammalian cell lines: Human Embryonic Kidney (HEK) 293K cells and monkey kidney cells (COS-7). The correct introduction of plasmid DNA into the cells and the expression of messenger RNA and protein were assessed. No transcript or protein expression was observed in either of the new constructs, despite normal transfection of vector DNA into the cell. As a control we obtained expression of full pro-IL-1β. Lack of pro-IL-1 Nt fragment expression in mammalian cells could be due to their small size (10 and 14 kDa). Having had no expression of these proteins we were not able to use these constructs for further experiments to check its activity on immune cells.

Because of the limitation of our engineered bacterial and mammalian expression systems to express and purify enough amounts of active protein, we developed another study to investigate additional important aspects of IL-1, its expression and degradation (chapter 5).

CHAPTER 5

Stability of IL-1

5.1 Introduction

Controlling the turn-over of cellular proteins is fundamental for the proper functioning of the cells. The main pathway for intracellular degradation is via the proteasome (Rock and Craiu, 1997). It has been reported that aberrant function of the proteasome is related to many acute and chronic neurodegenerative diseases (reviewed in Burkhardt and Dahlmann, 2007). Over the years, procedures to determine protein degradative pathways in cultured eukaryotic cells have been established. This chapter describes the degradation pathway of IL-1α and IL-1β in cultured mouse J774 macrophages. The objectives of this study were to test the hypothesis that cytosolic IL-1α and IL-1β are degraded by proteasome.

5.2 Endogenous expression of IL-1 in J774 cells

Characterisation of IL-1α and IL-1β expression was performed in mouse J774 macrophage cells. Cells were stimulated with 1 µg/ml LPS for various periods of time: 1, 2, 4, 6, 8, 16 and 24 h. Cell death was measured by analysis of lactate dehydrogenase (LDH) release into supernatants. Cell death was not significant at any of the time points tested (Figure 5.1). The effects of LPS on IL-1 gene expression were determined by Western blot of cell lysates. The results suggested that both IL-1α and IL-1β proteins had different expression profiles. It was evident that IL-1α expression was up-regulated at the later stages (from 4 h), whereas IL-1β expression occurred at earlier time points (from 2 h) and was subsequently down-regulated more quickly (Figure 5.2).

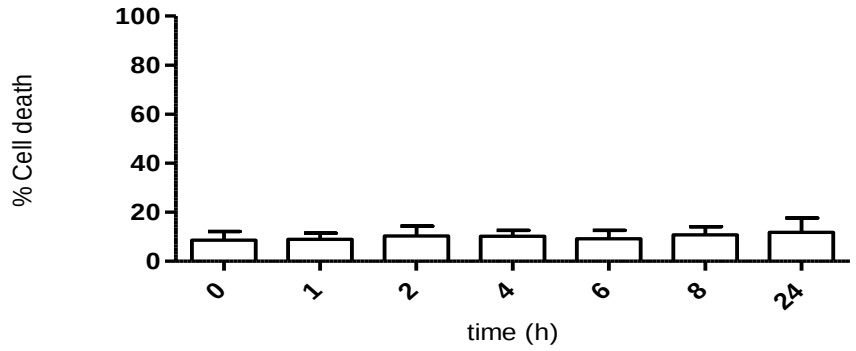

Figure 5.1 Cell death of stimulatedJ774 cells stimulated with LPS (1 µg/ml) for different time points. J774 cells were stimulated with LPS (1 µg/ml) for different time points as shown in figure. Cell death was assessed by measuring LDH release into the culture medium and normalised to total cellular LDH content. Data shown are mean ± s.d. of three independent experiments. No significant cell death in any time points of LPS treatment was seen compared to control. One-way ANOVA with post-hoc Bonferroni multiple comparisons test.

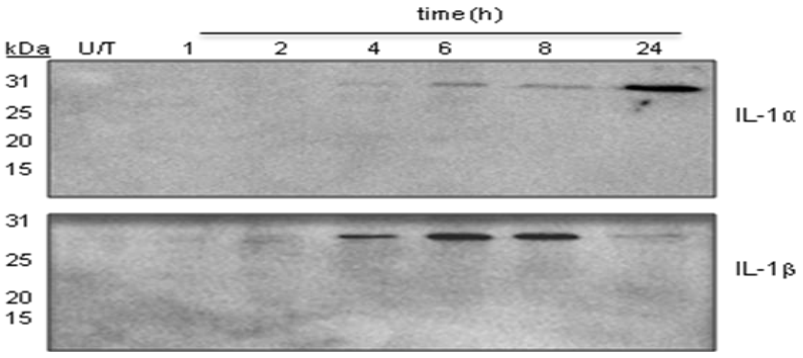

Figure 5.2 Anti-IL-1 Western blot expressions of IL-1α and IL-1β in stimulated J774 cells. J774 cells were stimulated with LPS (1 µg/ml) for different periods of time as shown in figure. Cell lysates of stimulated J774 cells were blotted with anti-IL-1α or anti-IL-1β antibodies. Maximum expression was achieved after 24 h for IL-1α and after 6 h for IL-1β. Three independent experiments confirmed the same result.

Because of the different expression patterns for IL-1α and IL-1β, we also measured cytokine expression at 16, 24 and 48 h after LPS treatment to establish a suitable expression time point for both proteins for future experiments. LDH analysis of supernatants showed that 48 h LPS treatment was toxic to the cells (35% at 48 h compared to 15% cell death at other times) (Figure 5.3). Both ELISA (Figure 5.4) and Western blot analysis (Figure 5.5) of cell lysates confirmed that 16 h stimulation was sufficient for a good expression level for both proteins.

In order to check if stimulation of the J774 cells by LPS (1 µg/ml) caused any release or processing of IL-1 proteins into the culture media, supernatants were also analysed for the presence of IL-1 by Western blot. No release or processing of either IL-1α or IL-1β protein was detected (Figure 5.5). Therefore, in all subsequent experiments, IL-1α and IL-1β expression was induced in J774 cells by 16 h stimulation with LPS (1 µg/ml).

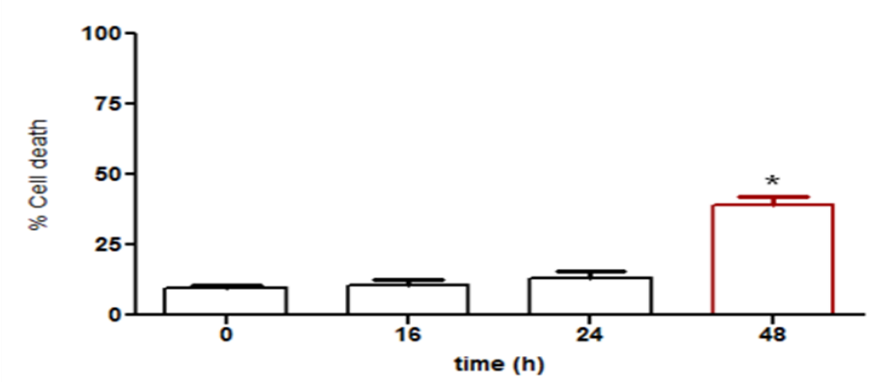

Figure 5.3 LDH release of stimulated J774 cells with LPS (1 µg/ml) for 16 and 48 h. J774 cells were stimulated with LPS (1 µg/ml) for different time points. Cell death was assessed by measuring LDH release into the culture medium and normalised to total cellular LDH content. Data shown are mean ± s.d. of three independent experiments. LDH release after 48 h of LPS treatment was the only time point significant comparing to control treatment (0 LPS) (* $p < 0.05$), one-way ANOVA with post-hoc Bonferroni multiple comparison test.

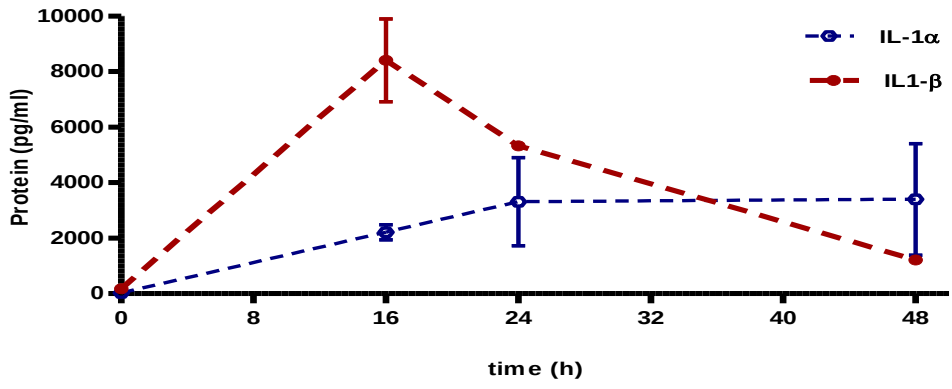

Figure 5.4 Expression of IL-1α and IL-1β in stimulated J774 cells. Cells were stimulated with LPS (1 µg/ml) for different time points and IL-1 levels measured by ELISA. The expression pattern of IL-1α and IL-1β was different, with maximum expression at 24 and 16 h stimulation for IL-1α and IL-1β, respectively. Data are the mean ± s.d. of three separate experiments.

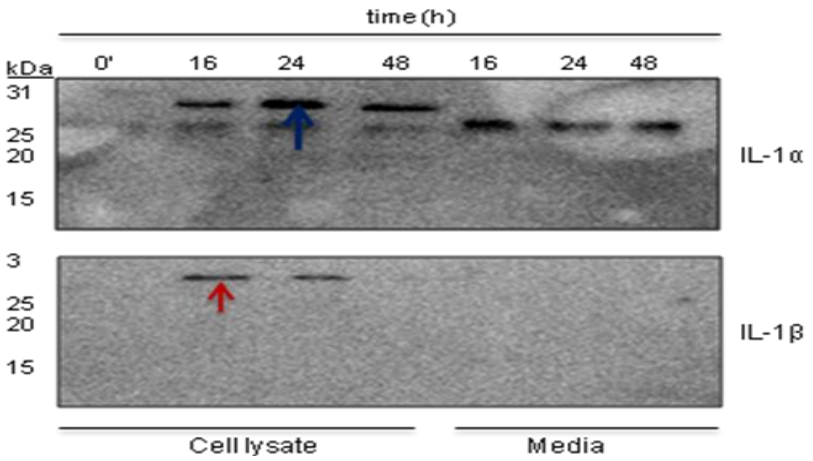

Figure 5.5 Anti-IL-1 Western blot expression and release of IL-1α and IL-1β in stimulated J774 cells. J774 cells were stimulated with LPS (1 µg/ml) for 16, 24 and 48 h. Cell lysates and media of stimulated J774 cells were blotted with anti-IL-1α and anti-IL-1β antibodies. Maximum expression for IL-1α (blue arrow) after 24 h and for IL-1β (red arrow) after 16 h. No processing or release of IL-1α and IL-1β was observed. The lower band in IL-1α blot shows the non specific binding.

5.3 Optimising cyclohexamide (CHX) treatment in stimulated J774 cells

In order to be able to measure the stability of IL-1 in J774 cells, further protein synthesis was blocked using cyclohexamide (CHX). J774 cells were stimulated (1 µg/ml LPS, 16 h) and then incubated in medium alone (control), medium containing DMSO (vehicle) and medium containing CHX (5 µg/ml) from 1 to 8 h. The incubation was stopped at indicated time points. LDH analysis of media showed no significant cell death up to 5 h of CHX treatment (Figure 5.6). However, longer incubations increased cell death significantly (at 6 h cell death increased from 10% to 30%, and at 8 h from 15% to 40% compared to control or DMSO treated cells) (Figure 5.6).

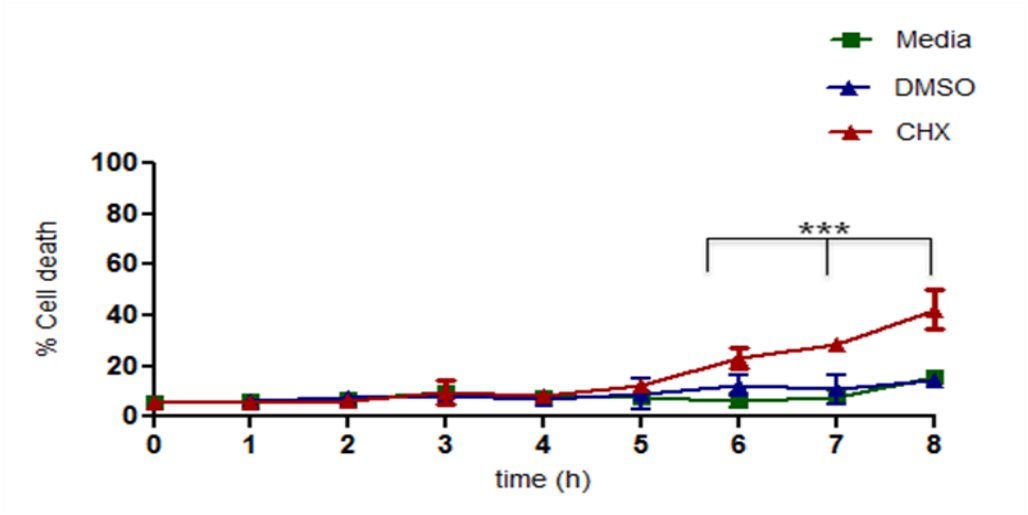

Figure 5.6 Cytotoxicity of cyclohexamide (CHX). J774 cells were stimulated with LPS (1 µg/ml, 16 h) and then incubated with CHX (5 µg/ml) from 1 to 8 h. LDH analysis of media shows that incubation of the cells with CHX (5 µg/ml) more than 5 h increased cell death significantly. Data are the mean ± s.d. of three separate experiments. LDH release after 6 h of CHX treatment was significant when compared to control treatment (0 CHX) (*** $p < 0.001$), one-way ANOVA with post-hoc Bonferroni multiple comparison test.

5.4 Half-life of IL-1 in J774 cells

In order to measure the rate of protein turn-over due to intracellular degradation and to establish the half-life of IL-1, LPS-stimulated J774 cells were treated with media only, media with DMSO and media with CHX from 30 min to 5 h. The cells were lysed and the levels of IL-1α and IL-1β proteins were determined by ELISA. IL-1 levels were normalised to cytokine levels after 16 h expression. As shown in figures 5.7 and 5.8, both proteins were degraded in a very similar pattern. There was not much degradation up to 2 h and DMSO had no effect on the degradation rate compared to media only.

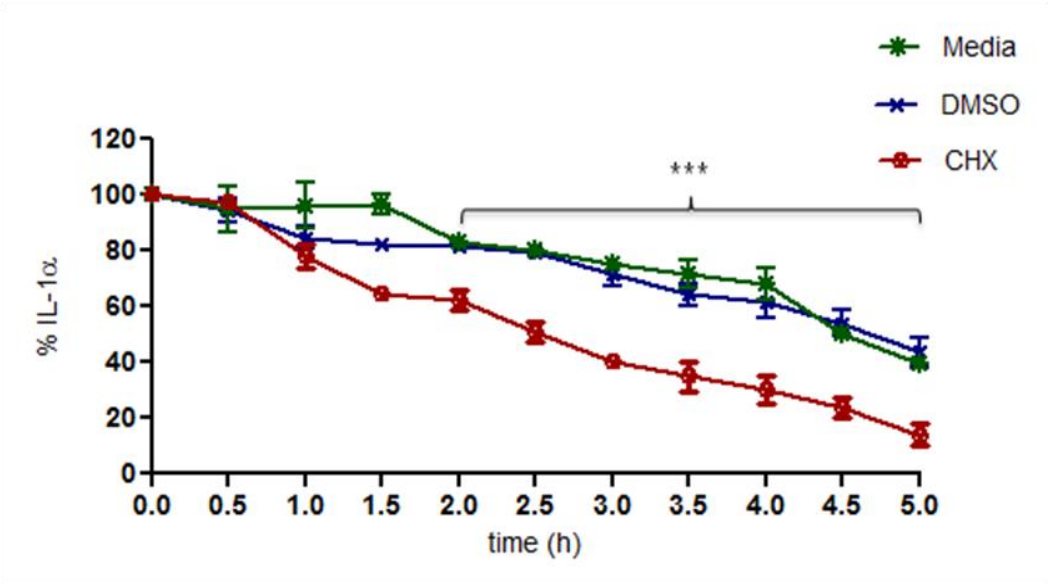

Figure 5.7 Effect of CHX on accumulation of IL-1α protein in J774 cells. J774 cells were stimulated with 1 µg/ml LPS for 16 h and then incubated with medium alone, DMSO (vehicle, same volume used for solubilising CHX) and CHX (5 µg/ml) for up to 5 h. Cells were harvested every 30 min. The amount of protein was measured by ELISA at each time point and normalised to levels of IL-1α after 16 h of LPS treatment (time 0). As shown in figure, there was not much degradation up to 1 h. Only 10% of protein was left after 5 h of CHX treatment. DMSO had no effect on degradation of IL-1α comparing to media alone. Data represents mean ± s.d of three independent experiments. ***: $p < 0.001$ vs control (DMSO only), one-way ANOVA with post-hoc Bonferroni multiple comparison test.

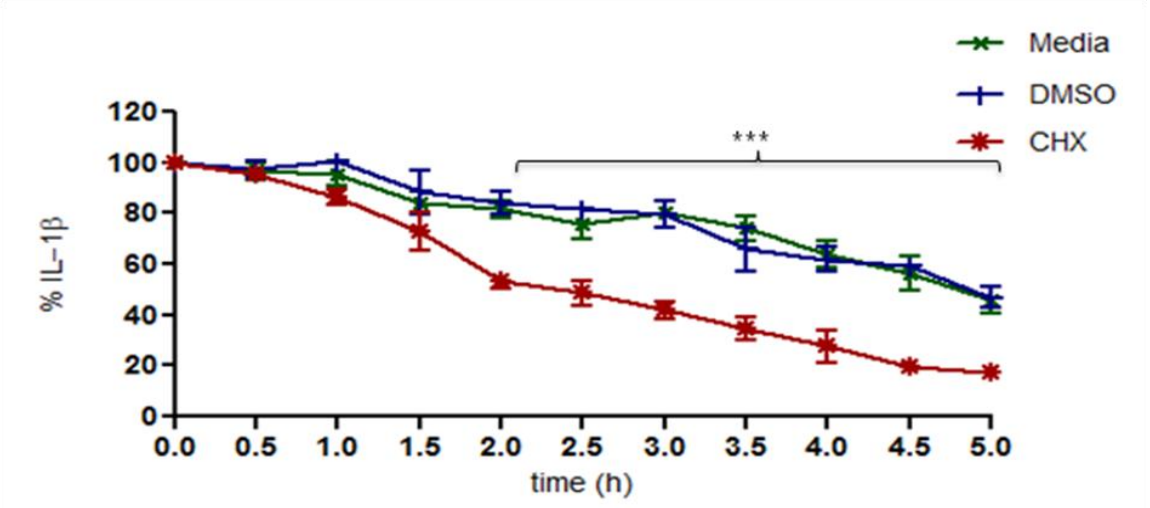

Figure 5.8 Effect of cyclohexamide (CHX) on accumulation of IL-1β protein in J774 cells. J774 cells were stimulated with LPS (1 µg/ml, 16 h) and then incubated with medium alone, DMSO (vehicle, same volume used for solubilising CHX) and CHX (5 µg/ml) for up to 5 h. Cells were harvested every 30 min. Protein levels were normalised to levels of IL-1β after 16 h LPS treatment (time 0). As shown in figure, there was not much degradation up to 1 h. Only 10% of protein is left after 5 h of CHX treatment. DMSO has no effect on degradation of IL-1β comparing to media alone. Data represents mean ± s.d of three independent experiments. ***: $p < 0.001$ vs control (DMSO only), one-way ANOVA with post-hoc Bonferroni multiple comparison test.

The relative half-life of IL-1α and IL-1β was measured using statistical analysis (non linear regression followed by one phase exponential decay). IL-1α had a half-life of 4 ± 0.35 h and IL-1β had a half-life of 4 h ± 0.23 h in J774 cells (Figure 5.9).

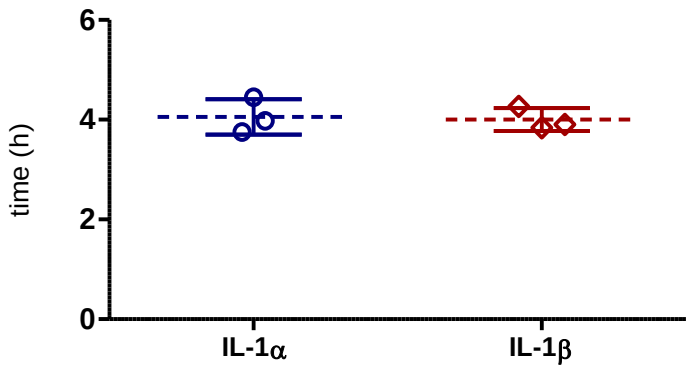

Figure 5.9 Half-life of IL-1α and IL-1β proteins. Both IL-1α and IL-1β have similar half-life in J774 cells. Data is representative of three independent experiments. The half-life was calculated using non-linear fit, followed by one phase exponential decay.

5.5 Degradation of IL-1

Previous studies have shown that if degradation is under the control of the proteasome pathway, the presence of proteasome inhibitors could increase the half-life of the protein (Moors and Mizel, 2000). In order to determine whether the proteasome degrades IL-1α and IL-1β in J774 cells, LPS-stimulated cells (1 µg/ml, 16 h) were incubated with CHX (5 µg/ml) for two time points: 2 and 4 h. The result showed that CHX significantly reduced protein synthesis after 2 and 4 h compared to non-treated cells (Figures 5.10 and 5.11). After 2 h incubation, the level of IL-1α was reduced from 95% following DMSO treatment to 70% following CHX treatment. Further reduction in protein synthesis was seen after 4 h treatment, a reduction from 60% following DMSO treatment to 20% following CHX treatment (Figure 5.10). A very similar pattern was observed for IL-1β; after 2 h DMSO

incubation 10% of protein was degraded whereas in CHX treated 40% degradation was observed. After 4 h of CHX treatment 80% of protein was degraded compared to only 30% degradation in DMSO treated cells (Figure 5.11).

It could be concluded that 2 and 4 h CHX treatment had a significant effect on protein synthesis. Therefore, these time points could be used for the next steps to study the stability of IL-1 in J774 cells.

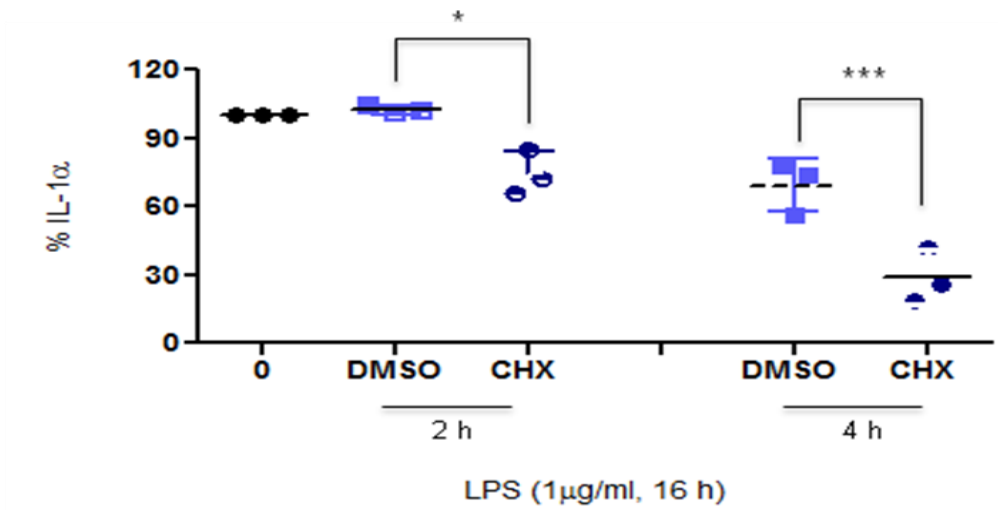

Figure 5.10 CHX effect on the level of IL-1α in stimulated J774 cells. Stimulated cells were incubated with CHX (5 µg/ml) for 2 and 4 h. The amount of protein was determined by ELISA. Incubation of J774 cells with CHX had a significant effect on IL-1α levels. CHX treatment reduced the amount of protein after 2 (from 90% to 70%) and 4 h (from 60% in control to only 20%) comparing to control (DMSO only). *: $p < 0.05$ vs control (DMSO only), and ***: $p < 0.001$ vs control (DMSO only), one-way ANOVA with post-hoc Bonferroni multiple comparison test.

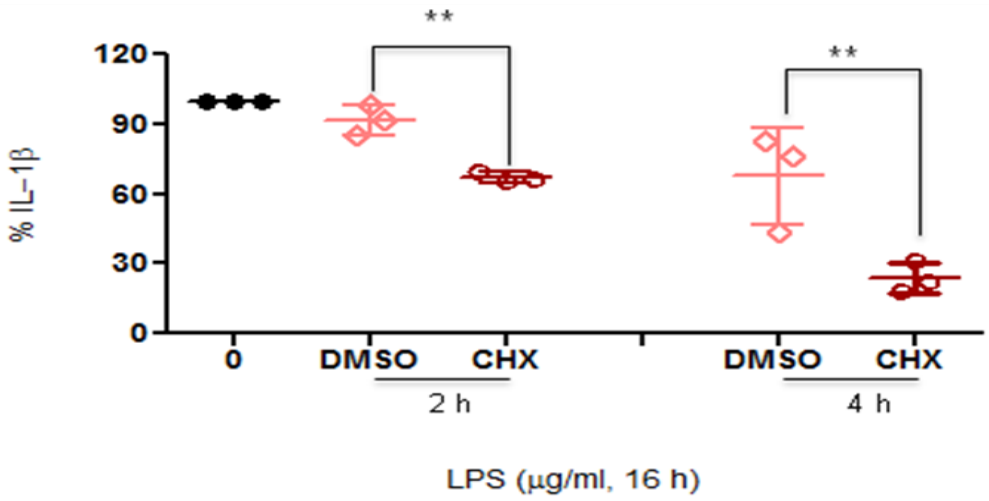

Figure 5.11 CHX effect on the level of IL-1β in stimulated J774 cells. Stimulated cells were incubated with CHX for 2 and 4 h. The amount of protein was determined by ELISA. Incubation of J774 cells with CHX had a significant effect on IL-1β levels. CHX treatment reduced the amount of protein after 2 (from 95% in control to 70%) and 4 h (from 70% in control to only 20%) comparing to control (DMSO only). **: $p < 0.01$ vs control (DMSO only), one-way ANOVA with post-hoc Bonferroni multiple comparison test.

5.5.1 Effect of ALLN on the stability of IL-1

In an initial experiment, the established proteasome inhibitor ALLN (acetyl-leu-leu-norleucinal) (Rock et al., 1994; Vinitisky et al., 1992) was used to investigate whether the proteasome was involved in the turn-over of IL-1 proteins in J774 cells. Stimulated cells were incubated with CHX alone and CHX in combination with different concentrations of ALLN (1, 3, 10, 30 and 50 µM) for 2 and 4 h. The cytotoxicity of the inhibitor was assessed by LDH release into supernatant of treated cells compared to control (untreated cells). The level of both IL-1α and IL-1β proteins in lysed cells was measured by ELISA.

LDH analysis of supernatant of treated cells showed no significant cell death with any concentration of ALLN in combination with CHX compared to CHX only treatment (Figure 5.12). Despite a significant effect of 2 h CHX treatment on the level of IL-1α and IL-1β proteins (Figures 5.10 and 5.11), the 2 h CHX and ALLN treatment had no effect on the stability of either IL-1 proteins. The stability of

both the IL-1α and IL-1β proteins was affected by ALLN at the 4 h time point as shown in figures 5.13 and 5.14. As the concentration of ALLN was increased the stability of IL-1α was enhanced using concentrations higher than 3 μM, with maximum stability at higher concentrations (30 and 50 μM) (Figure 5.13). In contrast, the significant effect for IL-1β was observed at higher concentrations, 30 and 50 μM (Figure 5.14).

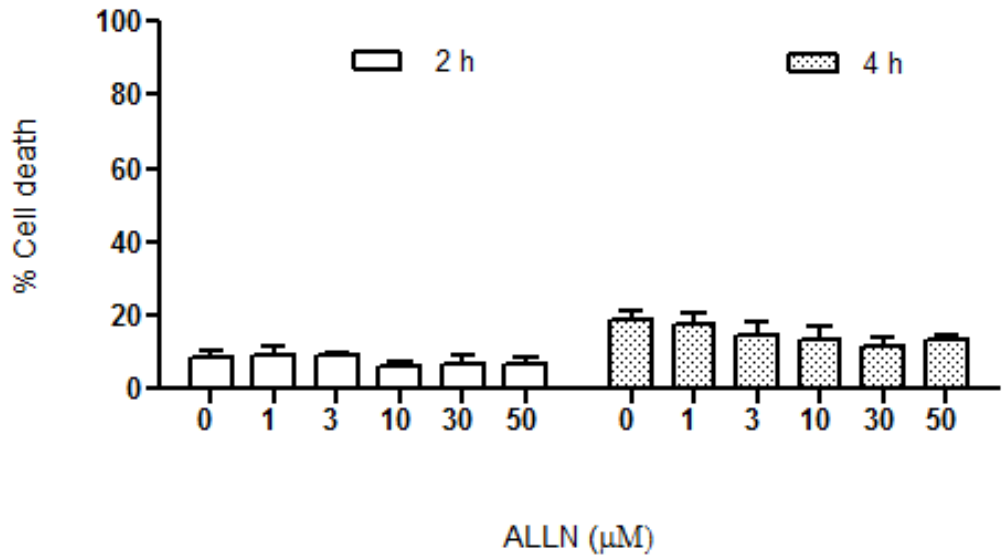

Figure 5.12 LDH release from stimulated J774 cells (LPS 1 μg/ml, 16 h) after ALLN treatment. Stimulated J774 cells were treated with different concentrations of ALLN and CHX (5 μg/ml). Cell death was assessed by measuring LDH release into the culture medium and normalised to total cellular LDH content. Data shown are mean ± s.d. of three independent experiments. No significant cell death was observed at any treatments comparing to control (0 μM treatment). One-way ANOVA with post-hoc Bonferroni multiple comparisons test.

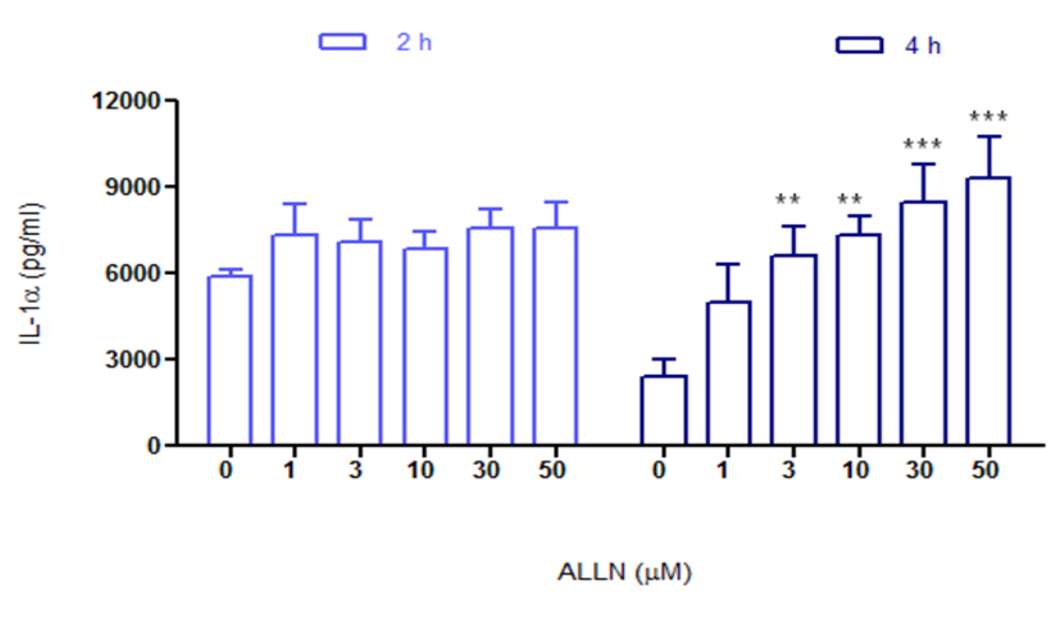

Figure 5.13 The effect of ALLN on stability of IL-1α. Stimulated J774 cells (LPS 1 μg/ml, 16 h) were treated with increasing concentrations of ALLN in combination with CHX for 2 and 4 h. The result shows ALLN increased the stability of IL-1α after 4 h at higher concentrations (30 and 50 μM) but had no effect after 2 h. Data represents mean ± s.d of three independent experiments. **: $p < 0.01$, and ***: $p < 0.001$ vs control, one-way ANOVA with post-hoc Bonferroni multiple comparisons test.

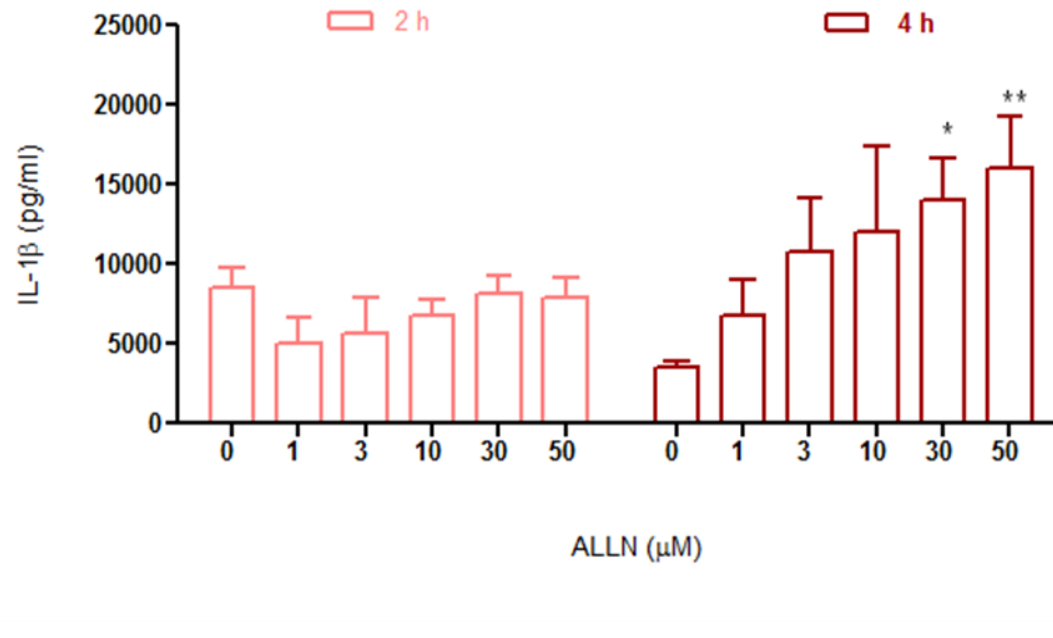

Figure 5.14 The effect of ALLN on stability of IL-1β. Stimulated J774 cells (LPS 1 μg/ml, 16 h) were treated with increasing concentrations of ALLN in combination with CHX for 2 and 4 h. The result shows ALLN increased the stability of IL-1β after 4 h at higher concentrations (30 and 50 μM) but no effect after 2 h. Data represents mean ± s.d of three independent experiments. *: $p < 0.05$, and **: $p < 0.01$ vs control, one-way ANOVA with post-hoc Bonferroni multiple comparison test.

5.5.2 Effect of MG262 on the stability of IL-1

We also investigated whether a more potent and specific proteasome inhibitor, MG262 (Adams et al., 1998) would be more effective on the stability of IL-1 in J774 cells. LDH analysis of supernatant showed no significant cell death in any treatments compared to non-treated cells (Figure 5.15).

ELISA analysis of lysates of LPS-stimulated J774 cells treated with CHX shows that application of MG262 had a time-dependent effect on the stability of IL-1 (Figures 5.16 and 5.17). The inhibition of proteasome activity by MG262 for 2 h had no effect on the stability of either IL-1α or IL-1β whereas 4 h treatment had a significant effect (Figures 5.16 and 5.17). A significant increase in the IL-1α concentration was observed in the lysates of J774 cells treated with 3 μM of MG262 after 4 h compared with non-treated cells (Figure 5.16). In contrast, higher concentrations of MG262 (10 μM) were needed to significantly stabilise IL-1β (Figure 5.17). The maximum stability of both IL-1α and IL-1β was established at 10 μM concentration of the drug; however there was not much increase at higher concentrations (30 and 50 μM).

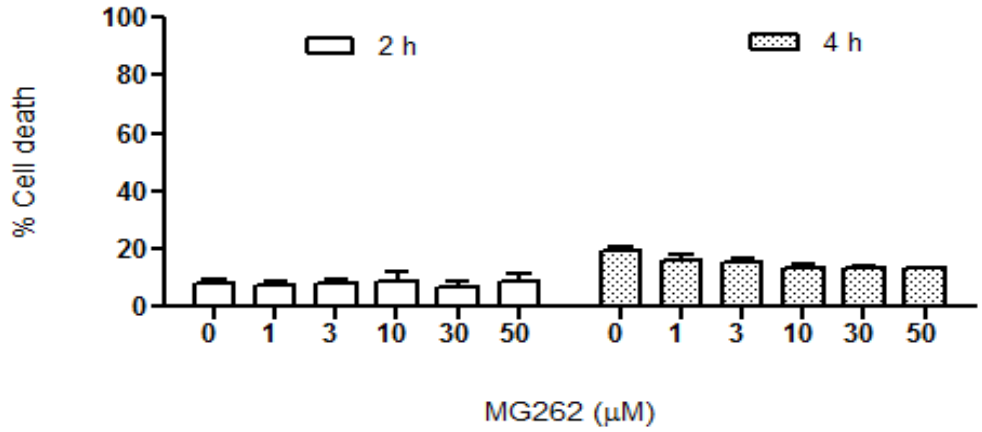

Figure 5.15 LDH release from LPS-stimulated J774 cells after MG262 treatment. Stimulated J774 cells (LPS 1 µg/ml, 16 h) were treated with different concentrations of MG262 and CHX (5 µg/ml). Cell death was assessed by measuring LDH release into the culture medium and normalised to total cellular LDH content. Data shown are mean ± s.d. of three independent experiments. No significant cell death was observed at any treatment compared to control (0 µM treatment). One-way ANOVA with post-hoc Bonferroni multiple comparisons test.

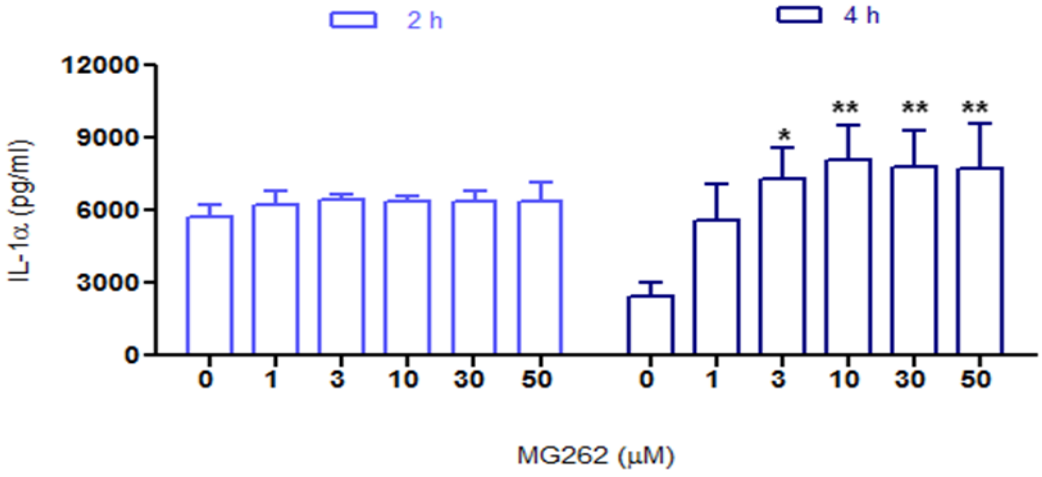

Figure 5.16 The effect of MG262 on stability of IL-1α. Stimulated J774 cells (LPS 1 µg/ml, 16 h) were treated with increasing concentrations of MG262 in combination with CHX for 2 and 4 h. The result shows MG262 increased the stability of IL-1α after 4 h in a concentration dependent manner but had no effect after 2 h. Data shows that even a low concentration (3 µM) of MG262 significantly increased the half-life of IL-1α. Data represents mean ± s.d. of three independent experiments. *: $p < 0.05$, and **: $p < 0.01$ vs control, one-way ANOVA with post-hoc Bonferroni multiple comparison test.

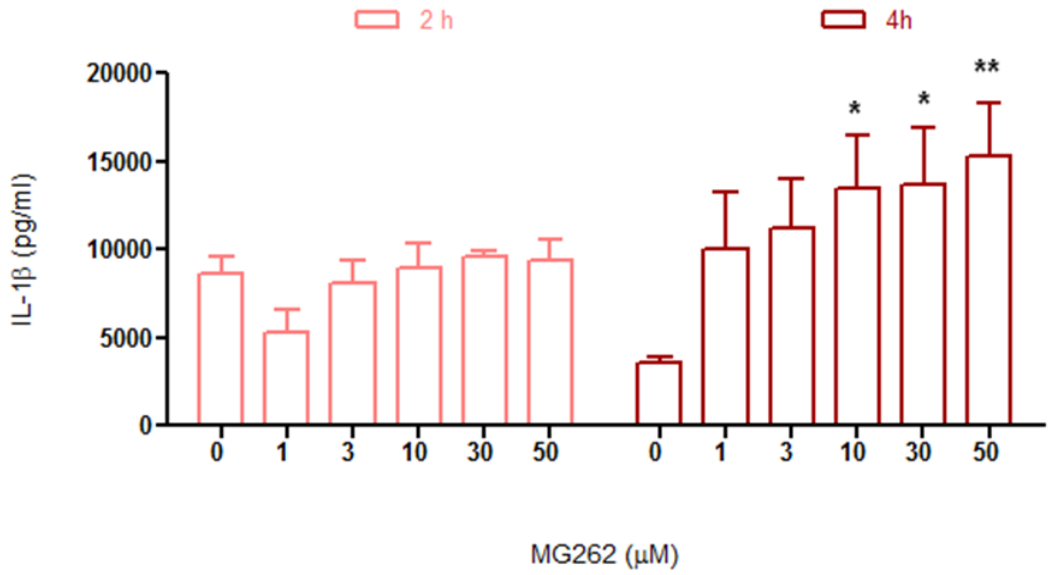

Figure 5.17 The effect of MG262 on stability of IL-1β. Stimulated J774 cells (LPS 1 μg/ml, 16 h) were treated with increasing concentratiosn of MG262 in combination with CHX for 2 and 4 h. The result shows MG262 increased the stability of IL-1β after 4 h in a concentration dependent way but had no effect after 2 h. Data shows that 3 μM of MG262 significantly increased the half-life of IL-1β. Data represents mean ± s.d. of three independent experiments. *: $p < 0.05$, and **: $p < 0.01$ vs control, one-way ANOVA with post-hoc Bonferroni multiple comparison test.

5.5.3 Effect of β-lactone on the stability of IL-1

β-lactone is an irreversible and more specific proteasome inhibitor than MG262 and ALLN (Fenteany et al., 1995; Dick et al., 1996; Groll et al., 1997). Therefore, we also used this proteasome inhibitor to study the stability of IL-1 in J774 cells.

J774 cells were treated as explained earlier (sections 4.4.1 and 4.4.2). LDH analysis of supernatant showed no significant cell death in any treatments compared to non-treated cells (Figure 5.18).

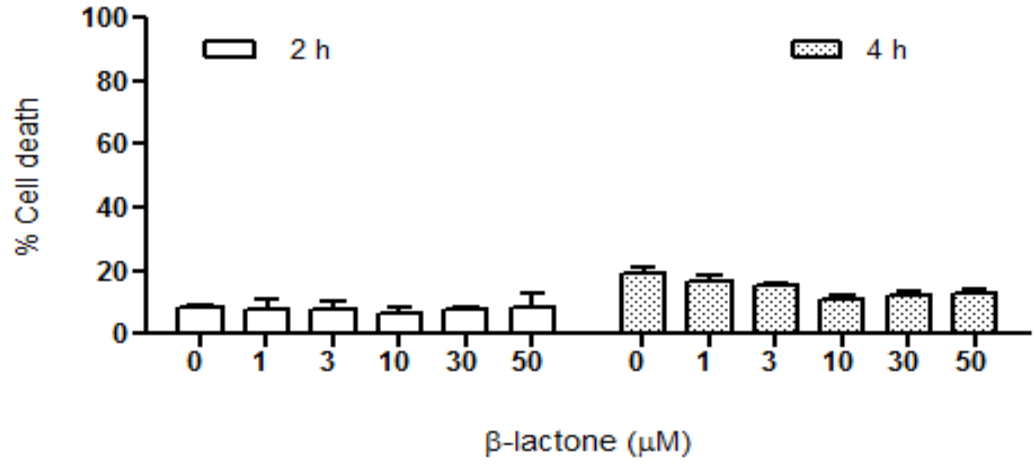

Figure 5.18 LDH release from stimulated J774 cells (LPS 1 μg/ml for 16 h) after β-lactone treatment. Stimulated J774 cells were treated with different concentration of β-lactone and a single concentration of CHX (5 μg/ml). Cell death was assessed by measuring LDH release into the culture medium and normalised to total cellular LDH content. Data shown are mean ± s.d. of three independent experiments. No significant cell death was observed at any treatments compared to control (0). One-way ANOVA with post-hoc Bonferroni multiple comparisons test.

ELISA analysis of lysates from CHX treated LPS-stimulated J774 cells showed that β-lactone treatment after 2 h had no effect on IL-1 stability whereas 4 h treatment had a concentration dependent effect (Figures 5.16 and 5.17). Low concentration of β-lactone (1 μM) had a significant effect on increasing the stability of IL-1α (Figure 5.19), and the maximum stability was reached at 10 μM (Figure 5.19). In contrast, a higher concentration of β-lactone was required to give a significant increase in the stability of IL-1β (Figure 5.12). These results suggest that the degradation of both IL-1α and IL-1β in J774 cells is proteasome-mediated.

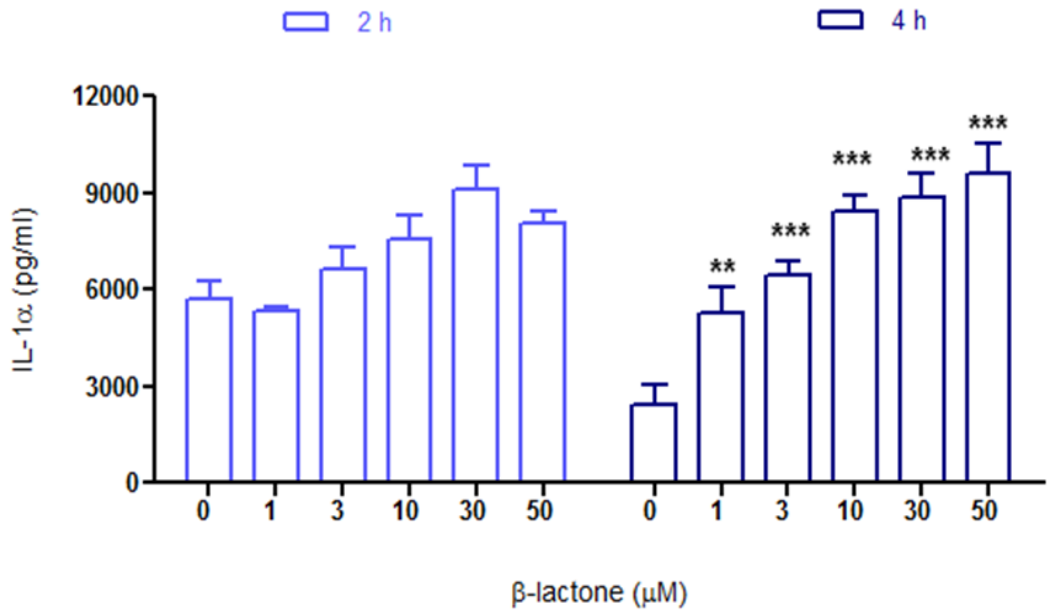

Figure 5.19 The effect of β-lactone on stability of IL-1α. Stimulated J774 cells (LPS 1 μg/ml, 16 h) were treated with increasing concentrations of β-lactone in combination with CHX for 2 and 4 h. The result shows β-lactone increased the stability of IL-1α after 4 h in a concentration dependent manner but had no effect after 2 h. Data shows that even a low concentration (1 μM) of β-lactone significantly increased the half-life of IL-1α. Data represents mean ± s.d. of three independent experiments. **: $p < 0.01$, and ***: $p < 0.001$ vs control, one-way ANOVA with post-hoc Bonferroni multiple comparison test.

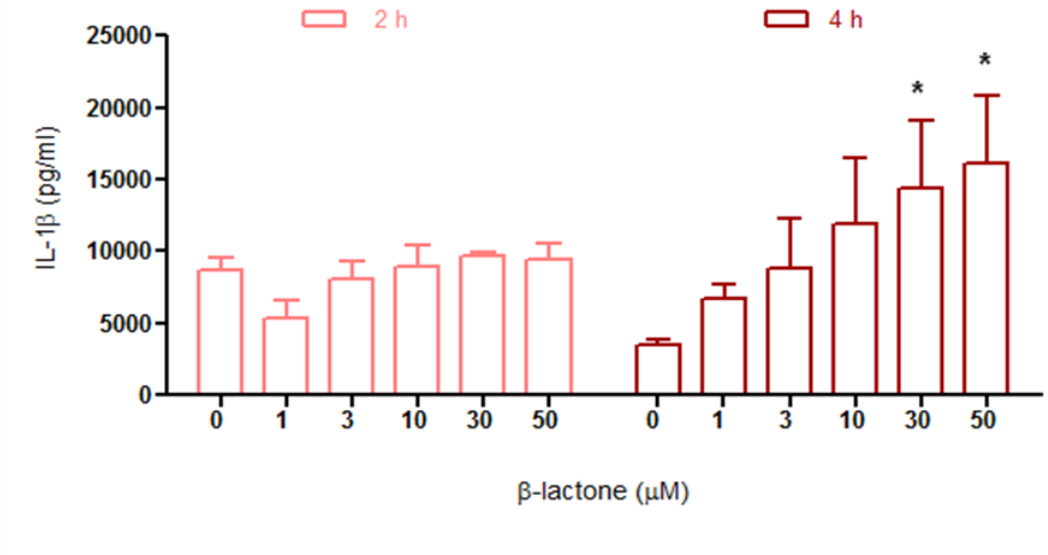

Figure 5.20 The effect of β-lactone on stability of IL-1β. Stimulated J774 cells (LPS 1 μg/ml, 16 h) were treated with increasing concentrations of β-lactone in combination with CHX for 2 and 4 h. The result shows β-lactone increased the stability of IL-1β after 4 h at high concentrations (30 and 50 μM) but had no effect after 2 h. Data represents mean ± s.d of three independent experiments. *: $p < 0.05$ vs control, one-way ANOVA with post-hoc Bonferroni multiple comparison test.

5.6 Ubiquitination of IL-1

Having established that proteasome inhibitors increased the stability of both IL-1α and IL-1β in J774 cells, and because proteasome targets need to be ubiquitinated, our next aim was to investigate if these cytokines were tagged by ubiquitin (Ub).

The bioinformatics programme (www.ubpred.org) predicted 4 and 2 potential ubiquitination sites on IL-1α and IL-1β, respectively (Figure 5.21) (Hitchcock, et al., 2003; Peng, et al., 2003).

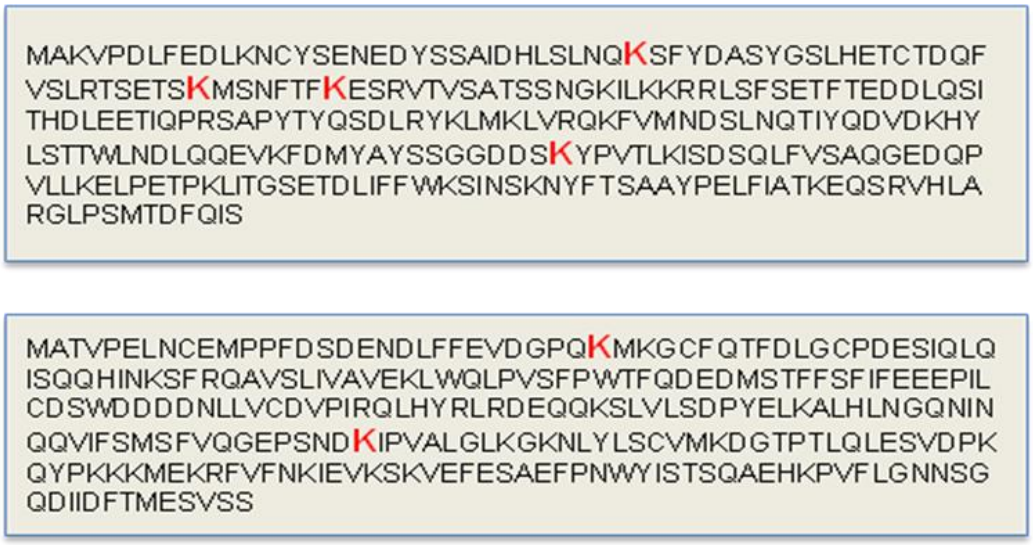

Figure 5.21 Computer predictions of ubiquitination sites. Computer prediction shows there are 4 and 2 potential ubiquitination sites (red bold letters) in IL-1α (top panel) and IL-1β (bottom panel).

To determine the involvement of ubiquitination in degradation of IL-1α and IL-1β, LPS (1 µg/ml, 16 h) stimulated J774 cells treated with β-lactone (30 µM), CHX (5 µg/ml) or both for 4 h. Cell lysates were prepared as explained in section 2.6.2 and added to agarose beads comprised of Glutathione S-transferase (GST)-fusion protein containing a Ub associated protein (Calbiochem, UK). The complex was incubated at 4ºC for 4 h, washed 3 times briefly and the ubiquitin-enriched fraction collected in loading buffer. The ubiquitination of IL-1α and IL-1β was

determined by Western blot of the recovery fraction with anti-IL-1α and anti-IL-1β. The results suggest that both IL-1α and IL-1β are tagged by ubiquitin before destined for the degradation by the proteasome (Figures 5.22 and 5.23). Treatment of stimulated J774 cells with β-lactone increased the enrichment of both IL-1α and IL-1β because of increasing the stability of these cytokines (Figure 5.22 and 5.23). The inhibition of further protein synthesis by CHX had the reverse effect less enrichment (Figures 5.22 and 5.23).

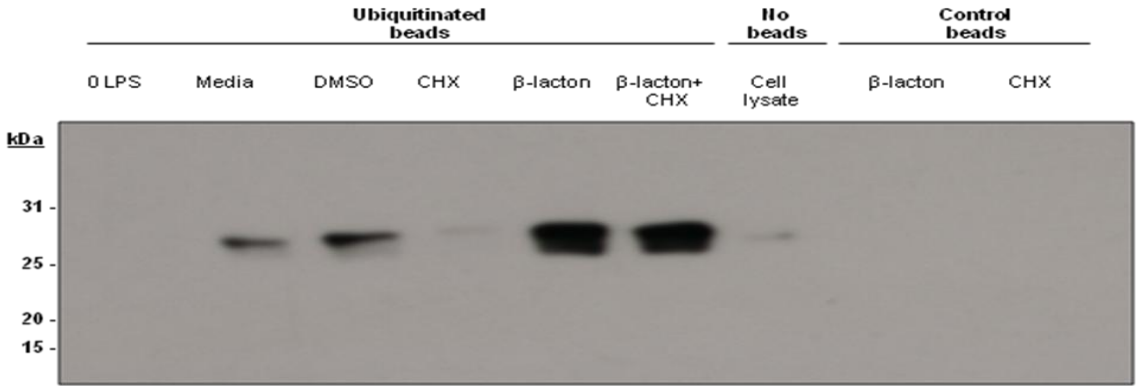

Figure 5.22 Ubiquitination of IL-1α. Stimulated J774 cells (LPS 1 μg/ml, 16 h) were incubated with β-lactone with or without CHX for 4 h. Cell lysates were added to GST-ubiquitin-associated agarose beads and then subjected SDS-PAGE and immunoblotted with anti-IL-1α antibodies. IL-1α was not detected in control beads.

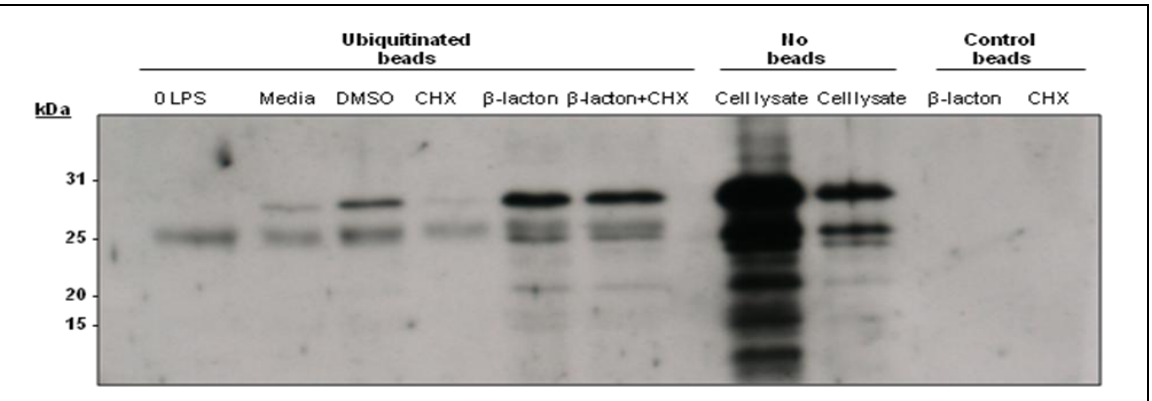

Figure 5.23 Ubiquitination of IL-1β. Stimulated J774 cells (LPS 1 μg/ml, 16 h) were incubated with β-lactone with or without CHX for 4 h. Cell lysates were added to GST-ubiquitin-associated agarose beads and then subjected to SDS-PAGE and immunoblotted with anti-IL-1β antibodies. IL-1β was not detected in control beads.

5.7 Summary

Expression of IL-1α and IL-1β was stimulated in J774 macrophage cells by LPS (1 µg/ml) for different periods of time. A good level of expression for both proteins was achieved after 16 h LPS treatment. The turn-over of IL-1α and IL-1β proteins in stimulated J774 cell was studied by blocking further protein synthesis with CHX (5 µg/ml). The half-life of IL-1α and IL-1β was worked out to be 4 h. In order to establish the degradation pathway for these proteins, different proteasome inhibitors (ALLN, MG262 and β-lactone), with different concentrations were incubated with stimulated J774 cells in the presence of CHX for 2 and 4 h. All three inhibitors increased the stability of both IL-1α and IL-1β in a time and concentration dependent manner.

The enrichment of IL-1α and IL-1β after inhibition of proteasome function with β-lactone in stimulated J774 cells suggests the ubiquitination of both IL-1α and IL-1β.

These results suggest that the proteasome is involved in the degradation of both IL-1α and IL-1β proteins and that both are tagged by ubiquitin before degradation under our experimental conditions. On the basis of these results, we went on to study if proteasome inhibitors increase the release of IL-1α and IL-1β in stimulated J774 cells (chapter 6).

CHAPTER 6

Effect of proteasome inhibition on the release of IL-1

6.1 Introduction

The release of IL-1α and IL-1β from leukocytes has a broad range of effects on immune and non immune cells (Dinarello, 1998). Their release induces fever, hypotension, and the production of other pro-inflammatory mediators (Crown et al., 1991; Nemunaitis et al., 1994). Therefore, it is important to understand the regulatory factors that control IL-1 release by inflammatory monocytes and macrophages. Previous studies have shown that proteasome inhibitors increase the release of IL-1β in activated human monocytes (Moor and Mizels, 2000). The aim of this chapter was to study the effect of intracellular IL-1α and IL-1β levels on the release of IL-1α and IL-1β in J774 macrophages and primary cultures of mouse bone marrow derived macrophages (BMDMs).

6.2 Release of IL-1 in J774 cells

6.2.1 Effect of proteasome inhibitors on the release of IL-1α in J774 cells

Having established that proteasome inhibitors (ALLN, MG262 and β-lactone) stabilise IL-1α and IL-1β in LPS-stimulated J774 cells in a time and concentration dependent manner (chapter 5), our next goal was to investigate whether proteasome inhibition alters the release of IL-1α and IL-1β from J774 cells.

J774 cells were stimulated with LPS (1 µg/ml, 16 h) and then incubated with three proteasome inhibitors (ALLN (50 µM), MG262 (30 µM) or β-lactone (30 µM)) alone or with CHX (5 µg/ml) for 4 h. The release of IL-1α was stimulated by incubation of the cells with the potassium ionophore nigericin (10 µM, 1 h). Supernatants were collected, cell death and IL-1 levels were analysed by LDH assay and ELISA, respectively.

LDH results showed that incubation of stimulated J774 cells with vehicle or nigericin did not induce significant LDH release into culture supernatants, indicating that the increase in IL-1 is not due to toxicity of used proteasome inhibitors (Figure 6.1).

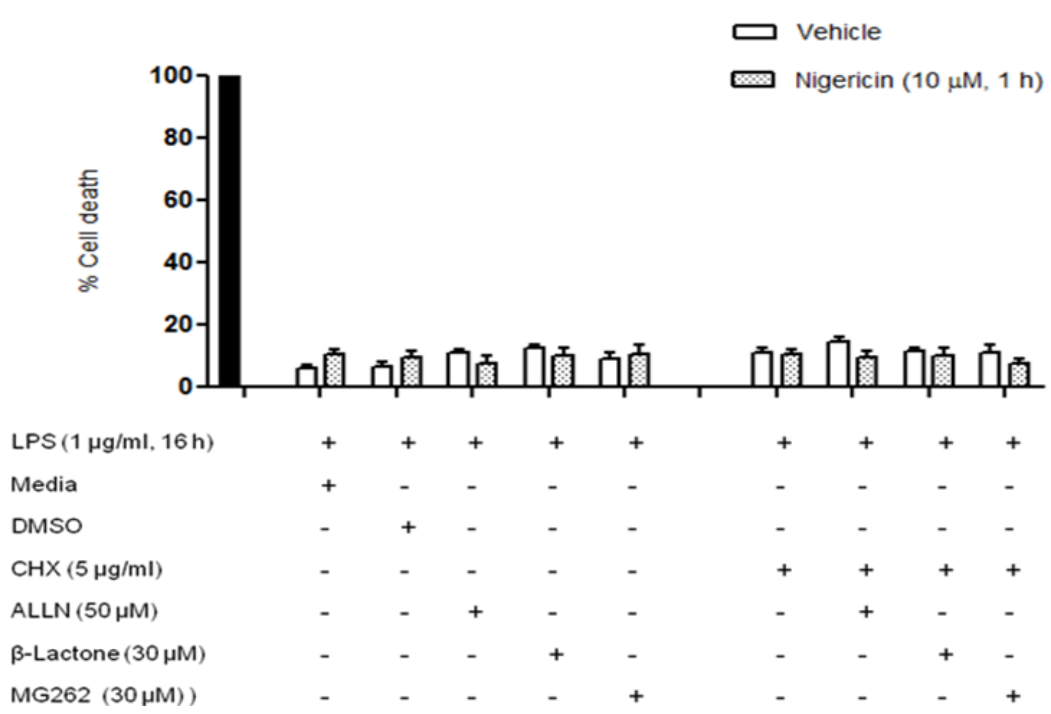

Figure 6.1 The effect of proteasome inhibitors on LDH release. Stimulated J774 cells (LPS 1 µg/ml, 16 h) were treated with different proteasome inhibitors (ALLN (50 µM), MG262 (30 µM) and β-lactone (30 µM)) in the presence or absence of CHX (5 µg/ml) for 4 h. Cells were treated with nigericin and vehicle. Cell death was assessed by measuring LDH release into the culture medium and normalised to total cellular LDH content (black bar). Data shown are mean ± s.d. of three independent experiments. There was no significant cell death associated with any of the treatments when compared to the control (no nigericin), one-way ANOVA with post-hoc Bonferroni multiple comparison test.

As shown in figure 6.2, the exposure of LPS-stimulated J774 cells to nigericin, caused a rapid release of IL-1α into the media while the release in control cultures (no nigericin) was negligible. Treatment of the cells with the proteasome inhibitors for 4 h did not increase IL-1α release compared to untreated. Once protein synthesis was stopped by CHX, nigericin failed to induce IL-1α release, since it was likely degraded. However, the addition of proteasome

inhibitors to CHX treated cells prevented the degradation of IL-1α and allowed secretion in response to nigericin to be restored (Figure 6.3).

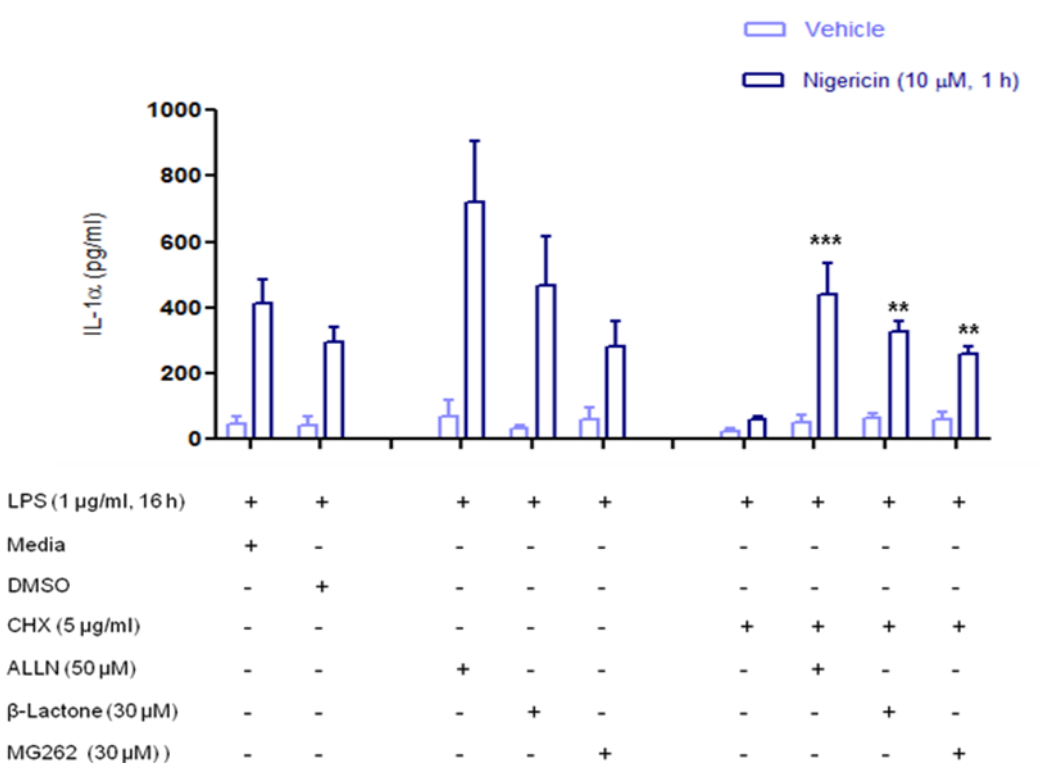

Figure 6.2 The effect of proteasome inhibitors on the release of IL-1α. J774 cells stimulated with LPS (1 µg/ml, 16 h), were treated with different proteasome inhibitors (ALLN (50 µM, β-lactone (30 µM) and MG262 (30 µM)) in the presence or absence of CHX (5 µg/ml) for 4 h. The release of IL-1α was stimulated by nigericin (10 µM, 1 h). IL-1α was measured by ELISA. Data represents mean ± s.d. of three independent experiments. **: $p < 0.005$, and ***: $p < 0.001$ vs control (CHX only treated), one-way ANOVA with post-hoc Bonferroni multiple comparison test.

6.2.2 Effects of proteasome inhibitors on the release of IL-1β in J774 cells

We next investigated the effect of proteasome inhibitors on IL-1β release. The same protocol was followed, as explained in section 6.2. As shown in figure 6.3, nigericin treatment also significantly increased the release of IL-1β in LPS-stimulated J774 cells. However, proteasome inhibitors did not have any effect on the release of IL-1β in J774 cells compared to non-treated. Once protein synthesis was stopped by CHX, nigericin failed to induce IL-1β release, since it was likely degraded. However, the addition of proteasome inhibitors to CHX treated cells

prevented the degradation of IL-1β and allowed secretion in response to nigericin to be restored.

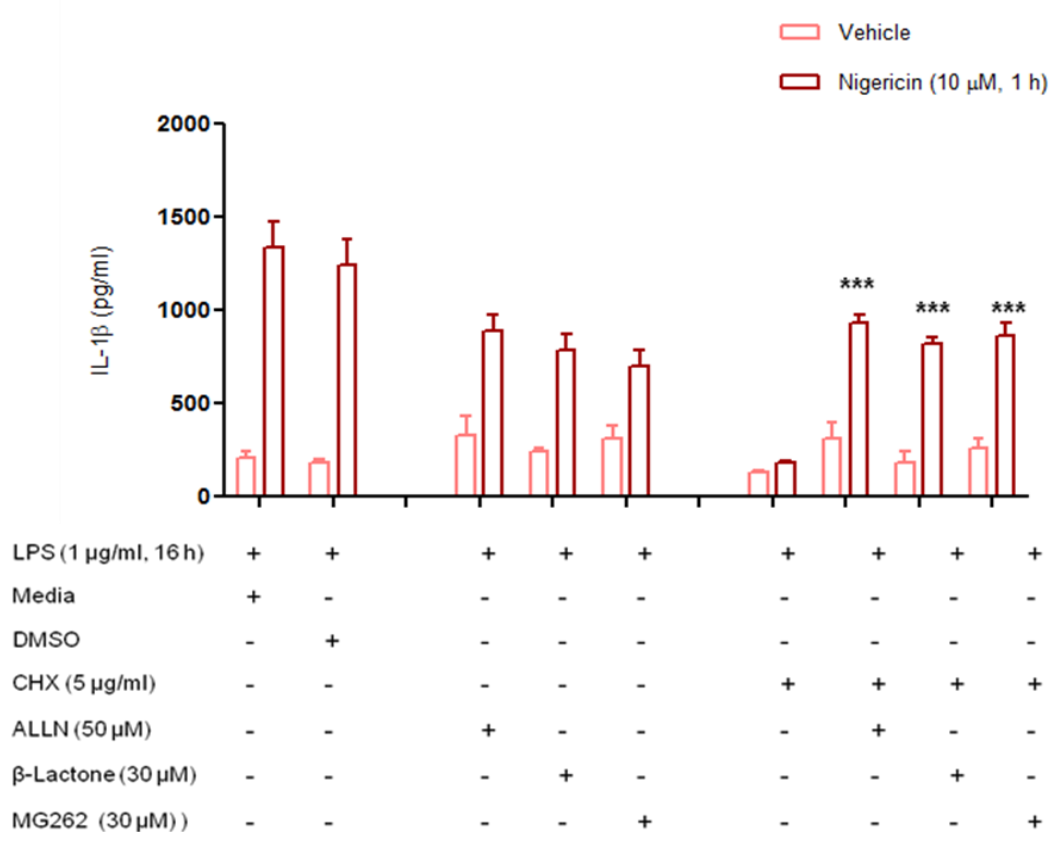

Figure 6.3 The effect of proteasome inhibitors on the release of IL-1β. J774 cells stimulated with LPS (1 μg/ml, 16 h), were treated with different proteasome inhibitors (ALLN (50 μM), β-lactone (30 μM) and MG262 (30 μM)) in the presence or absence of CHX (5 μg/ml) for 4 h. The release of IL-1β was stimulated by nigericin (10 μM) for 1 h. IL-1β was measured by ELISA. Data represents mean ± s.d of three independent experiments. ***: $p < 0.001$ versus control (CHX treated), one-way ANOVA with post-hoc Bonferroni multiple comparison test.

6.3 Stability of IL-1 in bone marrow derived macrophages (BMDMs)

6.3.1 Degradation of IL-1α in BMDMs

Having obtained evidence that the proteasome is involved in degradation of IL-1 in J774 cells, it was important to analyse the regulation of IL-1 turn-over in primary mouse, bone marrow derived macrophages (BMDMs).

As with J774 cells, IL-1α and IL-1β expression in BMDMs was stimulated by LPS (1 μg/ml, 16 h) and different treatments were applied. Cell death was

measured by analysis of LDH release into media. Stimulation of BMDMs with LPS and proteasome inhibitors did not cause cell death. However, CHX alone or in combination with all three proteasome inhibitors seemed to increase cell death in BMDMs compared to non-treated (media with DMSO) although only CHX treatment was statistically significant (Figure 6.4).

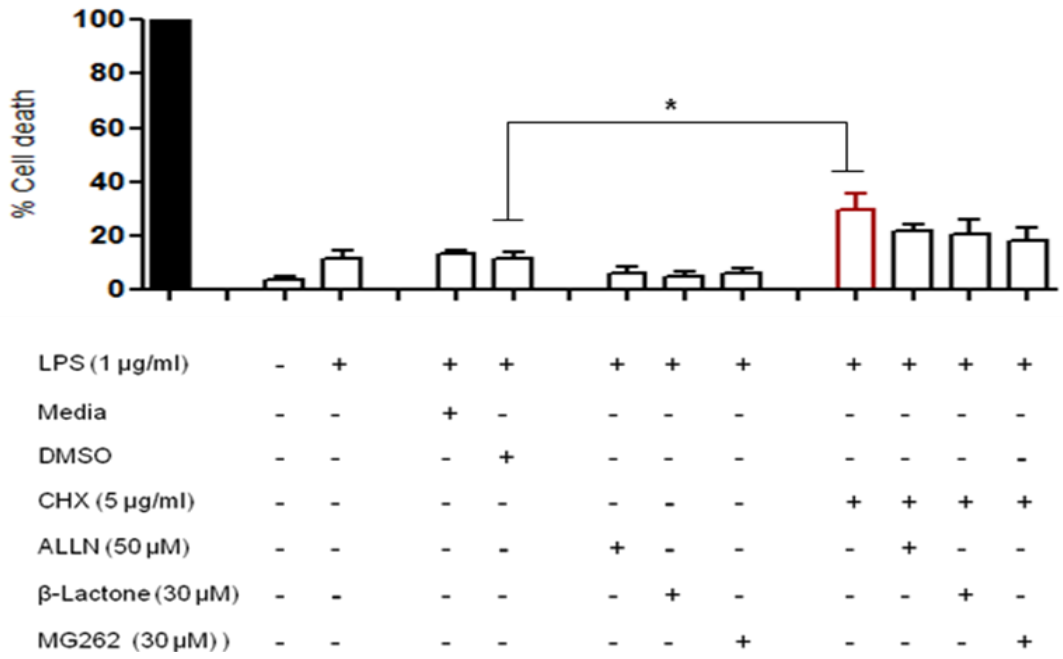

Figure 6.4 LDH release of stimulated BMDMs (LPS 1 µg/ml). LPS-stimulated BMDMs (1 µg/ml, 16 h) were treated with different proteasome inhibitors ALLN (50 µM), β-lactone (30 µM) and MG262 (30 µM) in the presence or absence of CHX (5 µg/ml) for 4 h. Cell death was assessed by measuring LDH release into the culture medium and normalised to total cellular LDH content (black bar). Proteasome inhibitor treatments did not increase cell death compared to control (DMSO only). CHX alone and in combination with proteasome inhibitor treatments increased cell death compared to control (DMSO only). Data shown are mean ± s.d of four independent experiments. *: $p < 0.05$ vs control (DMSO), one-way ANOVA with post-hoc Bonferroni multiple comparison test.

The effects of LPS on IL-1 gene expression were determined by ELISA of cell lysates. The results showed that stimulation of BMDMs with LPS significantly increased the expression of both IL-1α and IL-1β proteins (Figures 6.5 and 6.6, respectively). In order to see if proteasome inhibitors increased the stability of IL-1α in BMDMs, LPS-stimulated BMDMs were treated with media only, DMSO, CHX

alone (5 µg/ml) or in combination with three proteasome inhibitors ALLN (50 µM), β-lactone (30 µM) and MG262 (30 µM) for 4 h. The cells were lysed and the amount of IL-1α was determined by ELISA. As shown in figure 6.5, most of the expressed protein was degraded after 4 h and CHX treatment did not have significant effect on the levels of IL-1α compared to non-treated (DMSO). However, all three proteasome inhibitors had a significant effect on the stability of IL-1α protein (Figure 6.5).

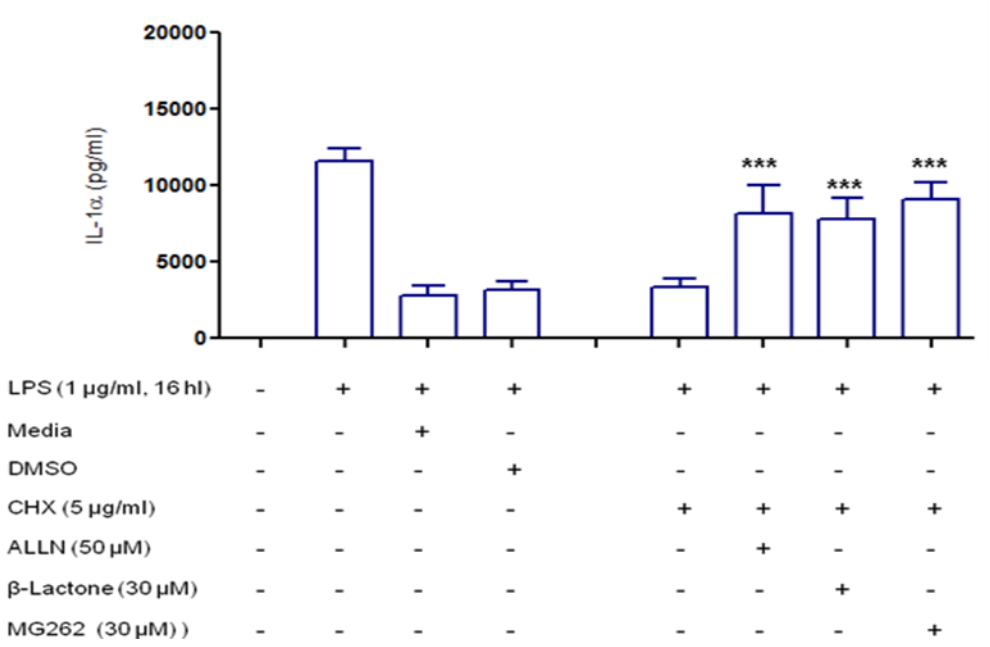

Figure 6.5 The effect of proteasome inhibitors on the stability of IL-1α in BMDMs. LPS-stimulated BMDMs (1 µg/ml, 16 h) were treated with different proteasome inhibitors, ALLN (50 µM), β-lactone (30 µM) and MG262 (30 µM), in combination with CHX (5 µg/ml) for 4 h. Cells were lysed and the amount of IL-1α was determined by ELISA. The results show all three proteasome inhibitors increased the stability of IL-1α after 4 h. Data represents mean ± s.d of four independent experiments. ***: $p < 0.001$ versus control (CHX), one-way ANOVA with post-hoc Bonferroni multiple comparison test.

6.3.2 Release of IL-1α in BMDMs

We next determined the effect that stabilising intracellular IL-1α levels had on the release of IL-1α into supernatants of LPS-stimulated BMDMs. LPS-stimulated BMDMs were exposed to ATP (5 mM) for 1 h after proteasome inhibitor treatments and also in combination with CHX. IL-1α levels were measured before

ATP treatment. As shown in figure 6.6, proteasome inhibitors did not have any effect on release of IL-1α. However, once cells were treated with proteasome inhibitors in combination with CHX or CHX alone, the release of IL-1α increased significantly compared to non-treated cells (media or media with DMSO) (Figure 6.6). This is consistent with LDH leakage over the 4 h period of exposure of BMDMs to CHX alone or in combination with different proteasome inhibitors over the same period of exposure (Figure 6.4).

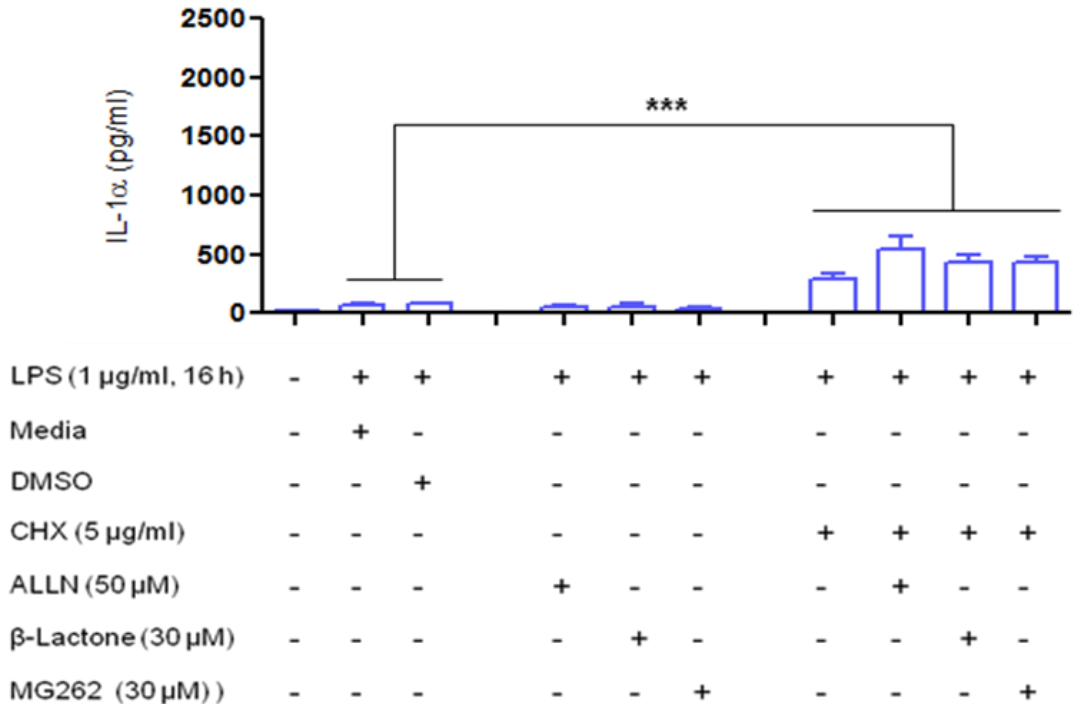

Figure 6.6 The effect of proteasome inhibitors on release of IL-1α in the absence of ATP. LPS-stimulated BMDMs (1 µg/ml, 16 h) were treated with different proteasome inhibitors ALLN (50 µM), β-lactone (30 µM) and MG262 (30 µM) in the presence or absence of CHX (5 µg/ml) for 4 h. Supernatants were removed and the amount of IL-1α was measured by ELISA. The data showed CHX and proteasome inhibitors increased the release of IL-1α compared to non treated cultures (media or media with DMSO). Data represents mean ± s.d. of four independent experiments. ***: $p < 0.001$ vs control, one-way ANOVA with post-hoc Bonferroni multiple comparison test.

In order to study the effect of proteasome inhibitors on release of IL-1α, LPS-treated BMDMs were stimulated with 5 mM ATP for 1 h. The exposure of LPS-stimulated BMDMs to ATP did not cause significant release of IL-1α into the

media compared to non-ATP treated cultures (Figure 6.7). However, the treatment of the BMDMs with the ALLN and β-lactone proteasome inhibitors for 4 h did increase ATP-induced IL-1α release compared to media or DMSO. In contrast, MG262 did not have any effect on the release of IL-1α in BMDMs compared to non-treated macrophages (Figure 6.7). However, proteasome inhibitors did not have any effect on the release of IL-1α once the protein synthesis was stopped by CHX (Figure 6.7).

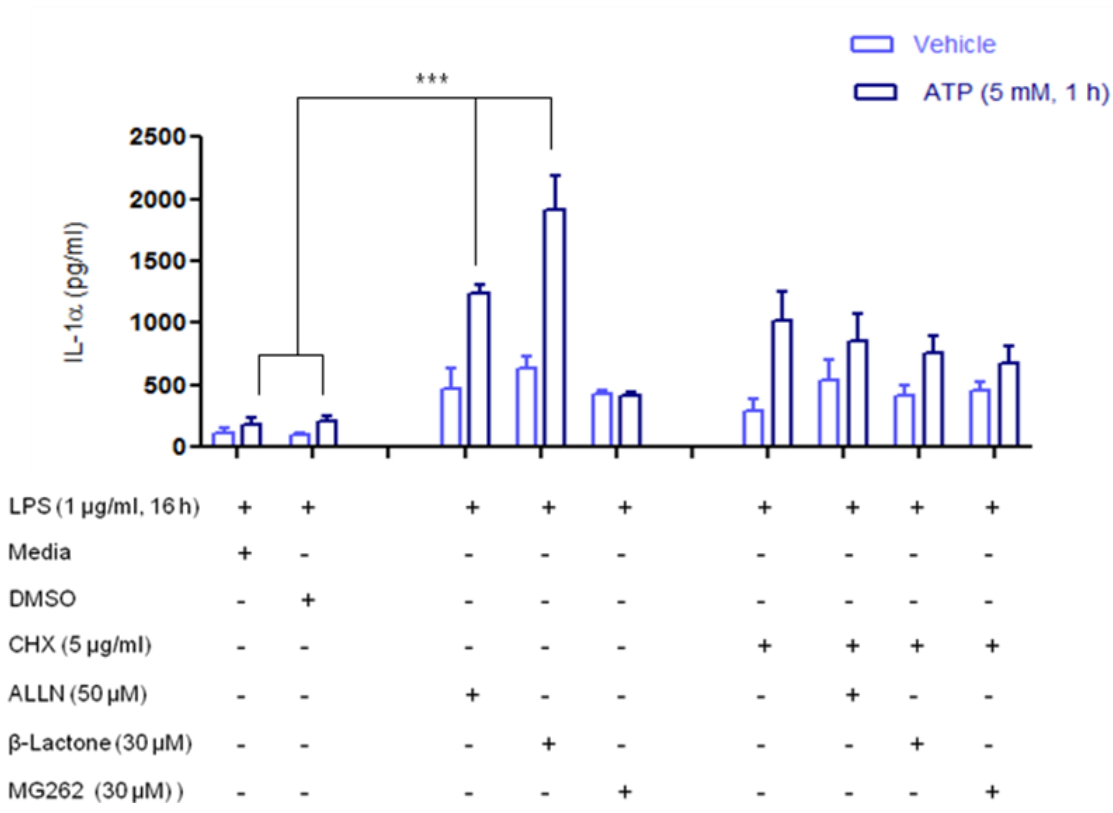

Figure 6.7 The effect of proteasome inhibitors on release of IL-1α in BMDMs. LPS-stimulated BMDMs (1 µg/ml, 16 h), were treated with different proteasome inhibitors (ALLN (50 µM), β-lactone (30 µM) and MG262 (30 µM) in combination with CHX for 4 h. The release of IL-1α was stimulated by incubation of the cells with ATP (5 mM, 1 h). ELISA results show that ATP did increase the release of IL-1α in the presence of ALLN and β-lactone. Data represents mean ± s.d. of four independent experiments. ***: $p < 0.001$ vs control, one-way ANOVA with post-hoc Bonferroni multiple comparison test.

6.3.3 Degradation of IL-1β in BMDMs

Expression and stability of IL-1β was also determined as explained in section 6.3.1. As shown in figure 6.8, all three proteasome inhibitors significantly increased the stability of IL-1β in BMDMs compared to CHX treated cultures.

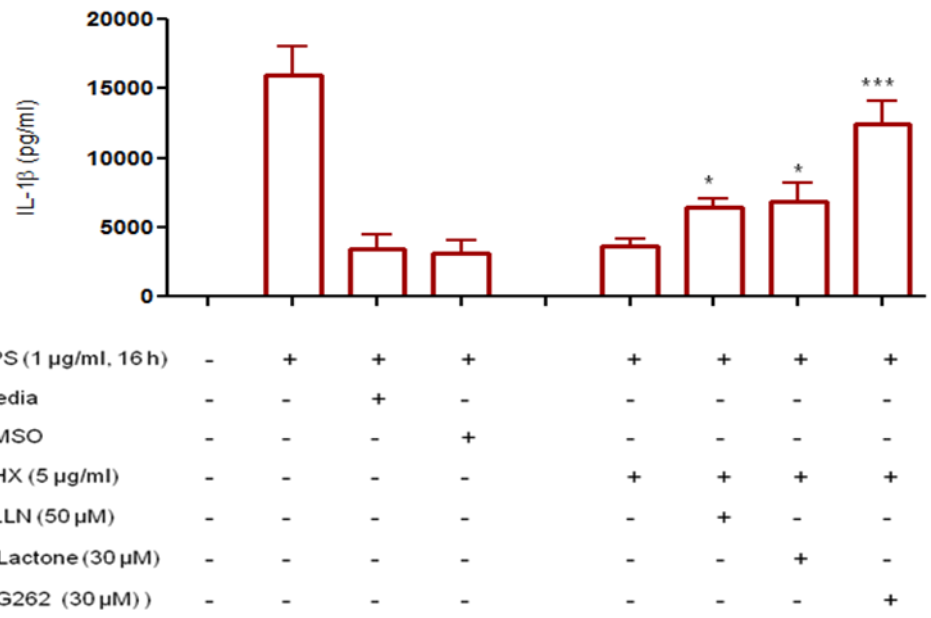

Figure 6.8 The effect of proteasome inhibitors on stability of IL-1β in BMDMs. LPS-stimulated BMDMs (1 µg/ml, 16 h), were treated with different proteasome inhibitors, ALLN (50 µM), β-lactone (30 µM) and MG262 (30 µM), in combination with CHX (5 µg/ml) for 4 h. The cells were lysed and amount of IL-1β was determined by ELISA. The result shows all proteasome inhibitors increased the stability of IL-1β, after 4 h. Data represents mean ± s.d. of four independent experiments. *: $p < 0.05$ *** and $p < 0.001$ vs control (CHX), one-way ANOVA with post-hoc Bonferroni multiple comparison test.

6.3.4 Release of IL-1β in BMDMs

We also determined the effect of stabilising intracellular IL-1β on the levels of cytokine released into the media. IL-1β levels before ATP treatment were measured by ELISA. As with IL-1α, CHX and proteasome inhibitor treatments significantly increased the release of IL-1β into the media compared to non treated cells (media or DMSO) (Figure 6.9).

Treatment of the BMDMs with ATP, induced only very small amounts of IL-1β release into media compared to non treated cultures (no ATP) (Figure 6.10).

However, and contrary to IL-1α, once protein synthesis was inhibited by CHX, the addition of proteasome inhibitors increased the release of IL-1β (Figure 6.10). The treatment of the BMDMs with the β-lactone increased ATP-induced IL-1β release compared to non-treated (media or DMSO). In contrast, ALLN and MG262 did not have any effect on the release of IL-1β in BMDMs compared to non-treated (Figure 6.10).

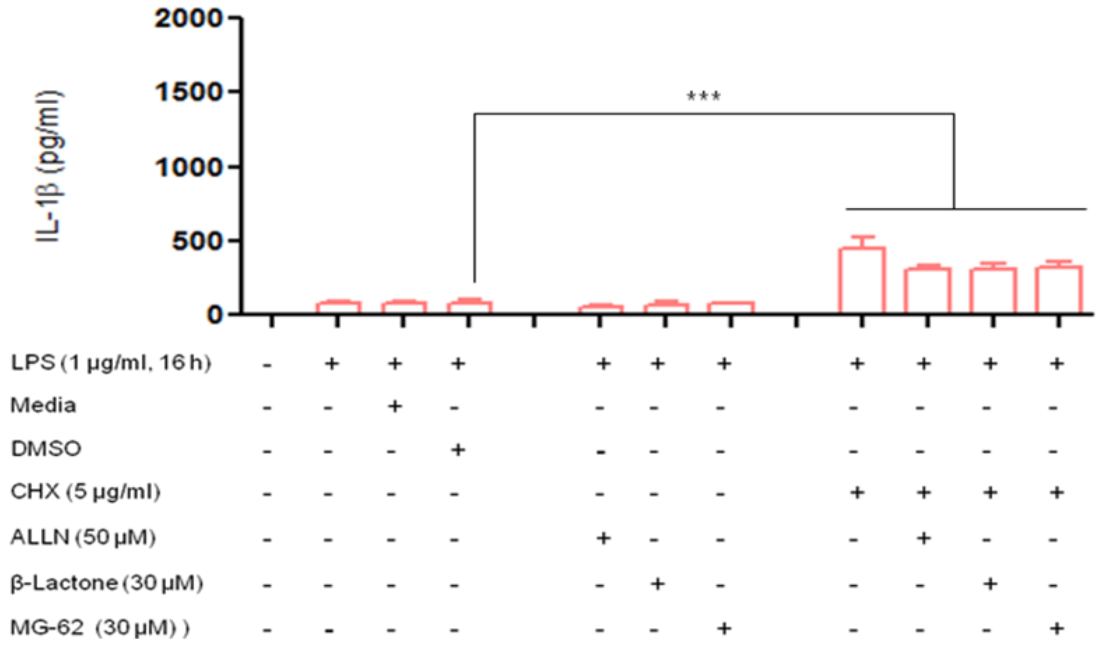

Figure 6.9 The effect of proteasome inhibitors on release of IL-1β in the absence of ATP. LPS-stimulated BMDMs (1 µg/ml, 16 h) were treated with different proteasome inhibitors (ALLN (50 µM), β-lactone (30 µM) and MG262 (30 µM)) in combination with CHX (5 µg/ml) for 4 h. Supernatants were removed and release of IL-1β was measured by ELISA. The results show proteasome inhibitors did not have any effect on the release of IL-1β. In contrast CHX alone or in combination with proteasome inhibitors increased the release of IL-1β significantly compared to non treated cultures (Media or media with DMSO). Data represents mean ± s.d. of four independent experiments. ***: $p < 0.001$ vs control, one-way ANOVA with post-hoc Bonferroni multiple comparison test.

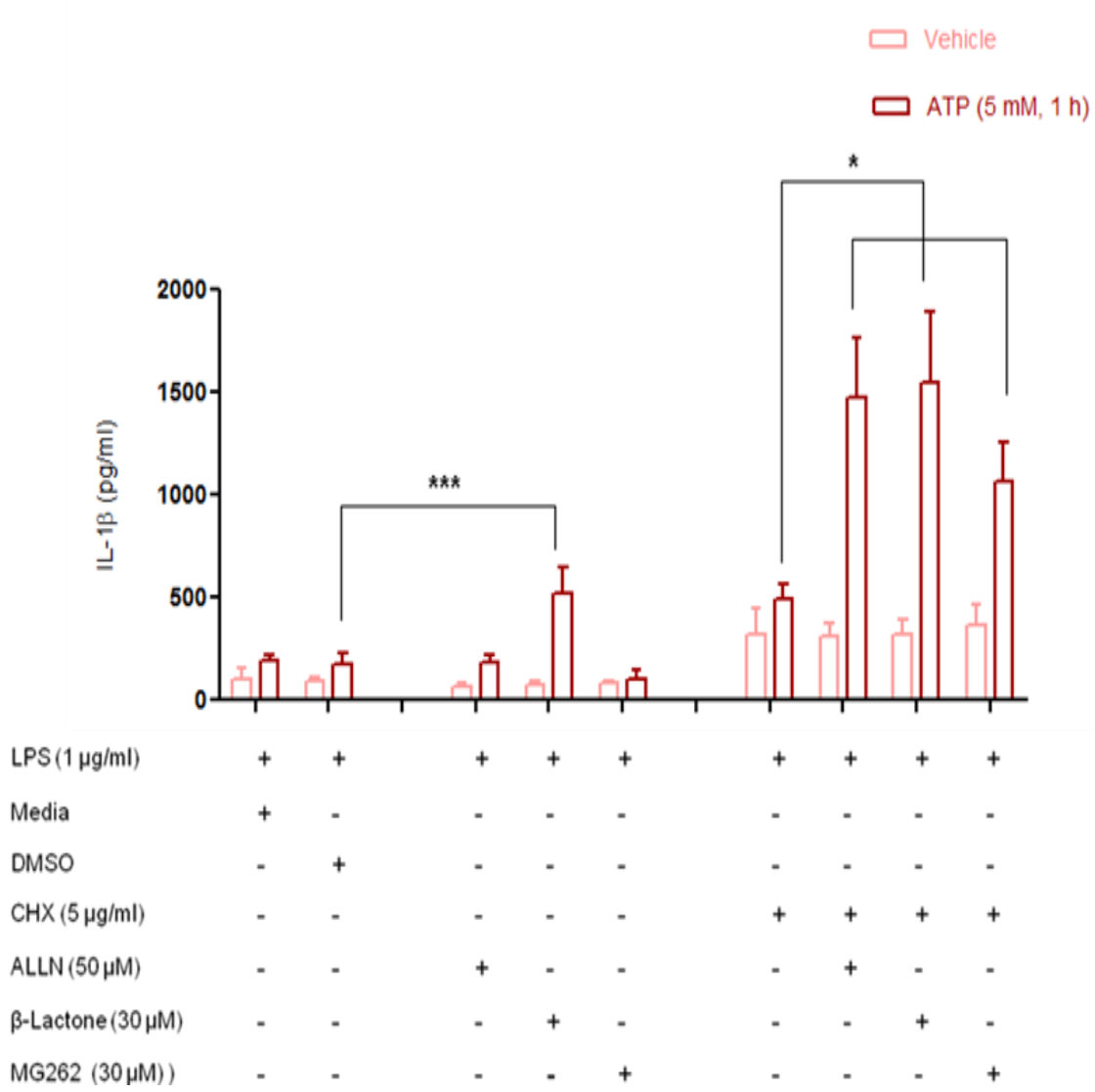

Figure 6.10 The effect of proteasome inhibitors on release of IL-1β in BMDMs. LPS-stimulated BMDMs (1 µg/ml, 16 h) were treated with different proteasome inhibitors, ALLN (50 µM), β-lactone (30 µM) and MG262 (30 µM), in combination with CHX (5 µg/ml) for 4 h. Release of IL-1β was subsequently stimulated with ATP (5 mM, 1 h). The results show 4 h incubation of stimulated BMDM with proteasome inhibitors in combination with CHX did increase the release of IL-1β compared to CHX treatments. Only β-lactone did increase the release of IL-1β compared to media or DMSO treated. Data represents mean ± s.d. of four independent experiments. *: $p < 0.05$ and ***: $p < 0.001$ vs control, one-way ANOVA with post-hoc Bonferroni multiple comparison test.

6.4 Summary

J774 cells and BMDMs were stimulated by LPS (1 µg/ml, 16 h). Cells were subsequently incubated with three proteasome inhibitors alone (ALLN (50 µM), β-lactone (30 µM) and MG262 (30 µM)) or in combination with CHX (5 µg/ml) for 4 h. The release of IL-1α and IL-1β was induced by incubation with nigericin (10 µM, 1 h) in J774s and with ATP (5 mM, 1 h) in BMDMs.

In J774 cells, nigericin increased release of both IL-1α and IL-1β. Despite the protection of IL-1α and IL-1β from degradation by all three proteasome inhibitors, no significant increase of IL-1α and IL-1β was observed. Once further protein synthesis was stopped by CHX, secretion of IL-1α and IL-1β was increased significantly.

In BMDMs, all three proteasome inhibitors increased the stability of IL-1α and IL-1β. β-lactone had a significant effect on release of both IL-1α and IL-1β. ALLN increased the release of IL-1α. In contrast, MG262 had no effect on release of either of IL-1α or IL-1β.

These results demonstrate that proteasome mediated degradation of intracellular IL-1α and IL-1β serves to restrict the intracellular amount of IL-1α and IL-1β in activated monocytes and macrophages.

CHAPTER 7:

Discussion

7.1 Introduction

The multifunctional IL-1α and IL-1β proteins, both key mediators of inflammation, are translated as 31 kDa precursors. The processing of these pro-forms by cellular proteases results in the production of a 17 kDa C-terminal fragment (Ct) and a 14 kDa N-terminal fragment (Nt) (Dinarello, 1996). There is evidence that the Nt of pro-IL-1α has biological functions (reviewed in Chapter 1), whereas no biological activity have been discovered for the Nt of pro-IL-1β.

The characterisation of the biological activities of the Nt of pro-IL-1β require *in vitro* expression studies. The first part of the work presented in this thesis attempted to engineer expression of recombinant human pro-IL-1β Nt fragments: Nt-b (10 kDa) and Nt (14 kDa) (chapters 3 and 4). Although engineered protein expression has been used as a scientific tool to study the function of proteins, there are limitations of the applicability of this technique and the expression of different proteins needs to be tightly optimised. A specific expression system with particular conditions might be suitable for one protein but not for another. Therefore, there is no guarantee of a high yield of pure recombinant product. The yields and purity of recombinant proteins depends on a large number of factors such as expression vector, amino acid sequence, solubility, or the size of the desired protein. Because of the limitations of this technique, we were not able to yield pure recombinant proteins. In this study, we also investigated the expression and degradation of endogenous IL-1 in the mouse macrophage J774 cell line and in primary mouse bone marrow derived macrophages (BMDMs) (chapters 5 and 6).

7.2 Bacterial expression system

E. coli is the most widely used prokaryotic system for the expression of mammalian recombinant proteins because it can express proteins in large

quantities and it is easy, cheap, grows quickly and is easy to manipulate. However, many mammalian recombinant proteins are poorly expressed in *E. coli* due to a number of technical limitations, including poor solubility and inefficient translation due to codon bias and protein folding (Ikemura, 1981; Dong et al., 1996). Protein solubility can be affected by numerous factors, including vector design, solubilising detergents and lysis method (reviewed by Baneyx, 1999).

Successful expression of the recombinant pro-IL-1β and its N-terminus fragments (Nt and Nt-b) in bacterial *E. coli* BL-21(DE3) strain was achieved at 37ºC, even though all of the synthesised protein was sequestered in insoluble inactive aggregates called inclusion bodies. The formation of inclusion bodies is one of the main drawbacks of expression of mammalian proteins in bacteria (Frankel et al., 1991; Frangioni et al., 1993; Mirzahoseini et al., 2003; Mirzahoseini et al., 2009; Alibolandi et al., 2010). This would be due to the intermolecular association of hydrophobic domains during folding. The bacterial outer membrane proteins would fragment and display hydrophobic and anionic surfaces that then act as a trap for exposed hydrophobic or cationic surfaces on the expressed protein and leads to miss folding of proteins (Baneyx and Mujacic, 2004).

On the other hand, the use of temperatures lower than the ones used for *E. coli* culture (37ºC) results in higher yields and also improves biological activity of the soluble protein, even for proteins that are difficult to express (Baldwin, 1986; Strandberg and Enfors, 1991; Schellman, 1997; Betts and King, 1998; Ferrer et al., 2004; Pope et al., 2004; Scharnagl et al., 2005). Temperatures of 20-30ºC are often used for optimal solubility of the recombinant protein although the rate of expression usually decreases (Miksch et al., 1997; Fang and Ewald 2004; Leon et al., 2004; Yuan et al., 2004). At temperatures below 30ºC, the recombinant protein is often able to fold properly and thus remain soluble (Vera et al., 2007).

Expression of our recombinant proteins at lower temperatures (22 and 28ºC) proved that lower temperatures increase the solubility of the proteins.

In order to purify the soluble recombinant proteins, one-step affinity purification, Co^{2+} based IMAC technique, was employed under native conditions. The His-tag encoded in our recombinant proteins facilitated the purification by Co^{2+} resin. This one step purification did not eliminate all the non-specific contaminating proteins. Co-purification of bacterial proteins is a common problem and limits the effectiveness of this approach (Thain et al., 1996; Rohman and Harrison-Lavoie, 2000). Recombinant proteins were co-purified with bacterial proteins to an extent that was not acceptable for our future applications that required pure protein. To address this limitation, we optimised simple purification procedures such as elution by increasing washes and using different concentrations of imidazole, or passing the eluted proteins through 30 and 50 kDa cut-off columns. However, these approaches did not increase the yield of pure proteins.

Due to the limitations of single-step Co^{2+} based IMAC purification, we performed extra purification strategies based on iso-electric points (AEC) and molecular weights (SEC) of our recombinant proteins. Previous studies have shown that these two additional steps may effectively remove contaminating proteins (Viljoen, 1982; Colangeli et al., 1998). SEC was selected as the purification step between IMAC and AEC since it provided the highest resolution from contaminants prior to AEC.

The eluted recombinant proteins (Nt and pro-IL-1β) from Co^{2+} resin were added first to SEC to separate proteins on the basis of size. Almost all of the proteins came off the column in early eluted fractions. This could suggest the formation of very large aggregates of recombinant proteins which were trapped in

the external volume of the column. The SEC column consists of porous beads and large molecules do not pass through the pores and equilibrate with the external volume (between the beads and the internal volume), whereas small molecules pass the pores and equilibrate with the internal volume. Therefore, large protein molecules are excluded from the internal column volume and emerge in the first fractions from the column. Molecules that can access the internal volume emerge in later fractions according to their size.

As explained in chapter 3, eluted fractions from SEC containing the recombinant proteins were applied to AEC. For both pro-IL-1β and Nt, these were the A2-A4 fractions of SEC. Pro-IL-1β containing fractions still co-eluted with some other contaminant bacterial proteins after SEC and in the case of Nt, almost all the recombinant protein was lost after AEC. In conclusion, it was not possible to achieve high purity Nt IL-1β recombinant proteins by Co^{2+}-based IMAC purification followed by SEC and AEC.

7.3 Mammalian protein expression

In order to overcome the limitations of recombinant protein expression in *E. coli*, different mammalian cell lines, such as HEK293T and COS, have been used (Geisse et al., 1996; Cazalla et al., 2005). These mammalian systems also have their own drawbacks, such as decreased expression levels, much slower growth rates, and higher cost. Successful expression does not solely depend on the cell line, but also on the expression vectors used. Mammalian protein expression vectors contain signal sequences required for transcription and translation of the target protein (i.e., promoter elements, polyadenylation sites, etc.). The use of selectable markers and sequences encoding epitope tags that are recognised by specific antibodies facilitate the subsequent analysis of protein expression and

function at later stages (Schneider et al., 1995; Puig et al., 1998; Uzzau et al., 2001).

In addition to the expression plasmid, other factors such as the transfection procedures, efficiency of plasmid uptake and its integration at a high transcriptionally active site, affect the rate of protein expression. This is accomplished through the use of specific vectors which contain the coding sequences of the proteins to be studied, and which can then be introduced into cells by a variety of methods (Geng and Carstens, 2006).

7.3.1 Mammalian cell lines

We chose the human embryonic kidney (HEK293T) and monkey kidney (COS-7) cell lines to express our recombinant proteins for several reasons. These cell lines are popular due to their high transfection efficiencies. Additionally, CMV promoter, commonly used for protein expression in eukaryotic systems, is highly active in these cells and provides efficient expression (Liu et al., 1997). Moreover the presence of large T-antigen allows episomal amplification of the vector (which contains the SV40 origin of replication). Therefore, the presence of a highly active promoter combined with the episomal amplification of the expression vector is expected to maximize the level of expression of recombinant proteins in this cell type.

Transfection of cultured mammalian cells with the sequences for Nt-b or Nt, led to localisation of expressed Nt-b or Nt proteins mainly in cellular extracts. In order to overcome this problem, we also constructed Nt-b and Nt vectors with a 19 amino acids long signal SP added to the N-terminal of Nt-b and Nt sequence. In this way, we could target the recombinant protein to the culture supernatant, which is a much simpler protein environment compared with complex cellular extracts.

Despite all these considerations (like bacterial expression system), it is not guaranteed that the protein of interest is going to be expressed and released. Moreover, the reasons for these differences are not well understood and can be determined only by trial and error. Therefore, choosing the optimum vector for a given protein and assay system can be an empirical and time-consuming endeavour. Undoubtedly, such factors as the identity of the cell line, the gene of interest, the biological readout, as well as others all contribute to variability in the usefulness of the vector.

7.3.2 Expression of recombinant proteins

The two cell lines, HEK293T and COS-7, were transfected with our engineered plasmids (SP-Nt/Nt-b-myc). Expression of the proteins was monitored by Western blot using myc antibody. Unfortunately, despite taking into account all the considerations and using a straightforward protocol, recombinant proteins were not expressed in either of mammalian cells used. Limitations could be both in the level of plasmid DNA uptake by the cells during transfection and/or in the expression rate itself (transcription/translation). Transfection of a pannexin-1-myc expression vector as a positive control in HEK293T cell line showed this protein was expressed, ruling out a problem in the transfection/detection protocol. The transfection of the same positive control protein in COS-7 gave a similar result.

In order to check whether the lack of expression was due to the vectors, COS-7 cells were transfected with the original starting vectors without signal peptide, Nt-V5, Nt-b-V5, as well as pro-IL-1β-V5. The expression was monitored by taking advantage of a V5 antibody. Unfortunately, we found no expression for the transfected constructs Nt-b-V5 (10 kDa) or Nt-V5 (14 kDa), despite the positive expression of pro-IL-1β (31 kDa) and SP-ASC-V5 (25 kDa). The release of the 25

kDa protein encoding a fusion between ASC and the SP was detected in the concentrated supernatant.

PCR for the vector from transfected cells showed that the IL-1β Nt-b and Nt plasmids were getting into the cell, but RT-PCR confirmed that only pro-IL-1β was expressed at transcript level. It could be suggested that IL-1β Nt-b and Nt mRNA are degraded very rapidly due to their small size, resulting in limited or no translation. Small RNAs could block translation by binding to ribosome binding sites or get degraded by inducing the endoribonuclease (Prévost et al., 2011). In conclusion, it was not possible to express IL-1β Nt-b and Nt recombinant proteins in mammalian systems under the conditions used.

7.4 Endogenous expression of IL-1α and IL-1β

In order to focus on the impact of protein stability on the regulation of IL-1α and IL-1β production, LPS (1 μg/ml) was used to promote expression of endogeneous IL-1α and IL-1β without inducing processing or release of either form (Chin and Kostura, 1993). This approach would allow us to determine the rate of degradation of IL-1 in the cytosol.

The kinetics of IL-1α and IL-1β expression are related to the inflammatory response induced by LPS. The expression pattern of IL-1α and IL-1β in stimulated J774 cells was different but consistent with previous studies (Auron and Webb, 1994). The appearance of IL-1α in J774 cells is delayed until 4 h of LPS-stimulated macrophages and remained low until 8 h, with maximum accumulation at 24 h. In contrast, the high level of IL-1β in stimulated J774 cells is transient. The expression of IL-1β in response to LPS was rapid, appeared in the cells after 2 h stimulation reaching its maximum level at 18 h when it began to decline (Figure 5.4). This result would suggest that the expression of IL-1α and IL-1β in stimulated J774 cells is controlled at different sites (Auron and Webb, 1994).

The difference in expression of IL-1α and IL-1β could in part be due to the difference in the kinetics with which the proteins would be secreted after second stimulus (Hazuda et al., 1988). The difference in kinetics of IL-1α and IL-1β release has been demonstrated by two other groups using the mouse macrophage cell line P388D1 (Giri et al., 1985) and human peripheral blood monocytes (Hazuda et al., 1988). In stimulated P388D1 cells and human monocytes, the release of IL-1α is delayed until 12.5 h and 10 h after LPS activation, respectively. Whereas IL-1β is secreted after 2 h in both cell types (Giri et al., 1985; Hazuda et al., 1988).

7.5 Half-life of IL-1

Proteins are continuously synthesised and degraded in the cell. A delicate balance of two pathways determines the half-life of a cytosolic protein. The main intracellular degradation pathway for the intracellular short-lived proteins is the proteasome (Hershko and Ciechanover, 1998), although there are some exceptions (Blagosklonny et al., 1999). Cytosolic proteins have very different half - lives, ranging from a few min (example: ornithine decarboxylase) to more than two weeks (example: phosphoglycerate kinase) (Persson et al., 1984; Rogers et al., 1986). Other factors such as biological function, primary sequence (especially N-terminal residues), tertiary structure, post-translational modification and location in the cell, also determine the half-life of a protein (Dice, 1987).

The half-life of IL-1 in J774 cells was about 4 h under our experimental conditions. Another study has shown a similar half-life for intracellular IL-1β protein (3 h) in the human monocytic cell line, THP-1 (Moors and Mizel, 2000). The rate of IL-1α and IL-1β accumulation and degradation are critical factors that dictate availability of these cytokines for processing and release by activated monocytes.

The relatively short half-life of IL-1α and IL-1β in J774 cells (4 h) would explain the importance of their regulation.

7.6 Effect of proteasome inhibitors on the stability of IL-1

The proteasome system has important roles in regulating the expression levels of important signal transduction molecules involved in immune responses (Rockwell et al., 2000; Nakayama et al., 2001; Yamamoto and Gaynor, 2001). The best known example involves the attenuation of NF-κB activation which after degradation of an inhibitor protein, IκBα, allows NF-κB to translocate into the nuclei of cells and activate the genes that encode pro-inflammatory cytokines (Duffey et al., 1999; Hosseini et al., 2001). Activation of NF-κB has been implicated in expression of many inflammatory cytokines, including IL-1α and IL-1β (Dinarello, 1991; Yamamoto and Gaynor, 2001).

Manipulation of the proteasomal system may offer a means of regulating levels of pro-inflammatory cytokines, which would be an anti-inflammatory strategy for related diseases (Elliott and Zollner, 2003). The rationale to consider proteasome inhibitors as potential anti-inflammatory agents for treatment of the inflammatory diseases correlates with their potency to inhibit NF-κB activation (Duffey et al., 1999; Hass et al., 1998; Hosseini et al., 2001; Ortiz-Lazareno et al., 2008) consequently prevents the expression of many inflammatory cytokines. Therefore, the discovery of new anti-inflammatory drugs based on proteasome inhibition would be very advantageous for treatment of different inflammatory diseases (Meng et al., 1999).

The effects of proteasome inhibitors on the stability and release of different inflammatory cytokines have extensively been studied in the last two decades (Read et al., 1995; Weber et al., 1995; Pierce et al., 1996; Conner et al., 1997; Meng et al., 1999; Wu et al., 2002; Shall et al., 2004). One of the main aims of this

work was to study the effects of proteasome inhibitors on IL-1α and IL-1β stability and their release in J774 cells and primary bone marrow derived macrophages (BMDMs).

Previous studies have shown that proteasome inhibition results in prevention of IκB degradation and attenuation of NF-κB nuclear translocation (Malinin et al., 1997; Karin and Greten, 2005). In our study, LPS was used to induce the expression of IL-1α and IL-1β before treatment with the different proteasome inhibitors. Treatment with different proteasome inhibitors showed no toxic effect on LPS-stimulated J774 cells and BMDMs despite reports of their cytotoxicity on various cell types (Drexler, 1997; Meriin et al., 1998; Moors and Mizel, 2000). Three different proteasome inhibitors at different concentrations and two different time points (2 and 4 h) were used in stimulated J774 cells. ALLN and MG262 are less potent proteasome inhibitors and also block calpain and cathepsin proteases (Kisselev et al., 2001).

LPS stimulation increased the expression of IL-1α and IL-1β in J774 cells and BMDMs. Once further protein synthesis was stopped with CHX for 2 h, a 'fast' reduction in levels of IL-1α and IL-1β was seen independent of proteasome. These data suggest that translational attenuation plays an important role in regulating the amount of intracellular proteins (Cowan and Morley, 2004; Rahmani et al., 2005). 2 h incubation of stimulated J774 cells with different concentrations of proteasome inhibitors in combination with CHX had no effect on stability of either IL-1α or IL-1β.

Proteasome degradation pathways could be another control point for intracellular protein levels. As shown in our study, after blocking protein synthesis with CHX for 4 h, the levels of IL-1α and IL-1β become stable upon treatment with proteasome inhibitors. Treatment of stimulated J774 cells with ALLN (3 μM, 4 h)

was enough to increase the stability of IL-1α significantly. However, ALLN had less of an effect on IL-1β stability since a 10 fold higher concentration of ALLN was needed to have a significant increase on stability of IL-1β. MG262 was more potent than ALLN with respect to IL-1β stability. Lower concentrations of MG262 were required to increase IL-1β stability significantly. In contrast, the highly specific proteasome inhibitor β-lactone which has no effect on serine proteases, cysteine proteases, trypsin and chymotrypsin, even at long exposure times (Fenteany et al., 1995) had a greater effect on the stability of IL-1α compared to ALLN and MG262. Concentrations as low as 1 μM of β-lactone stabilised intracellular IL-1α levels more than two fold in LPS-stimulated J774 cells. Higher concentrations of β-lactone were required to increase the stability of IL-1β.

The effects of these proteasome inhibitors on stability of IL-1α and IL-1β were also studied in BMDMs. All three proteasome inhibitors increased the stability of IL-1α and IL-1β after 4 h incubation compared to non-treated samples (Chapter 6). Stabilisation of IL-1α and IL-1β *in vitro* by proteasome inhibitors support our hypothesis that the proteasome is involved in IL-1α and IL-1β degradation.

However, the concentration of IL-1α and IL-1β was reduced significantly in CHX and vehicle treated cells (DMSO). This could be due to the fact that the half-life of IL-1α and IL-1β might be shorter in BMDMs. The conditions should be optimised for BMDMs as the experimental conditions for J774 cells were used for these cells.

The results of this study suggest that the proteasome degradation pathway serves as an important regulatory mechanism for the production of IL-1α and IL-1β (Moors and Mizel, 2000; Imai et al., 2003). The proteasome system restricts intracellular levels of these proteins and consequently their processing and

release. However, we cannot exclude the possibilities that other degradation pathways may also participate in the degradation of IL-1α and IL-1β (Tsubuki et al., 1996; Mellgren, 1997; Ding et al., 2007; Harris et al., 2011). Other studies have shown that IL-1β can be degraded by autophagy, another major intracellular degradation system (Harris et al., 2011). These two cellular degradation systems are functionally coupled (Ding and Yin, 2008). Suppression of one pathway activates the other one. Proteasome inhibition induces autophagy. Autophagy purges polyubiquitinated protein aggregates induced by proteasome inhibitors. Therefore, cells are protected from the toxicity of proteasome inhibitors (Ding and Yin, 2008).

7.7 Ubiquitination of IL-1α and IL-1β

Ubiquitination, the covalent addition of a chain of a small but highly conserved protein ubiquitin (Ub) to one of their lysine residues, is a key post-translational modification to target proteins to the proteasome (Voges et al., 1999). Ubiquitination could affect protein stability, cellular localisation, and biological activity. Many different human diseases such as various types of cancer, neurodegeneration, and metabolic disorders are associated with alterations in proteasome system (reviewed in chapter 1). The detection of altered or normal ubiquitination of target proteins may provide a better understanding of the pathogenesis of these diseases.

Development of several epitope-tagged Ub affinity components allows for the detection of endogenous poly-Ub proteins in different cells (Young, et al., 1998; Wilkinson, et al., 2001; Hicke et al., 2005; Dikic et al., 2009; Shi et al., 2010; Xu et al., 2010). Because of the relatively low cellular abundance, ubiquitinated substrates have to be enriched to be identified. Computational prediction shows

there are 4 lysine residues in IL-1α and 2 in IL-1β with potential to be ubiquitinated.

The enrichment of IL-1α and IL-1β with an ubiquitin enrichment kit after inhibition of proteasome function with β-lactone in stimulated J774 cells suggested the ubiquitination of these cytokines. In order to confirm these results we tried to immunoprecipitate (IP) IL-1α and IL-1β and try to detect ubiquitination of these cytokines by anti-ubiquitin Western blotting. No specific bands were observed. The IP protocol used for this purpose (chapter 2, section 2.6.3) only showed non-covalently interacting proteins (results not shown).

7.8 Effect of proteasome inhibitors on release of IL-1

The release of IL-1α and IL-1β requires two steps, which are usually controlled by different stimuli. The first step drives gene transcription and intracellular accumulation of IL-1 and the second step activates IL-1 processing and release (Perregaux and Gabel, 1998). Therefore, the production of these cytokines is tightly regulated. In the absence of a second stimulus, most of the newly synthesised product remains unprocessed in the cytosol or is degraded within the cell (Ferrari et al., 2006). Mechanisms involved in these processes are poorly known (Nickel, 2003; Prudovsky et al., 2003).

The release of IL-1 was stimulated with nigericin (10 µM, 1 h) in J774 cells and ATP (5 mM, 1 h) in BMDMs after different treatments. Both nigericin and ATP were able to induce the release of IL-1α and IL-1β from stimulated J774 cells and BMDMs, respectively (Chapter 6). Under our experimental conditions proteasome inhibitors had no effect on the release of either IL-1α or IL-1β in stimulated J774 cells when compared to DMSO only. The fact that no effect on release of IL-1 was observed in LPS-treated cells after treatment with proteasome inhibitors suggests that the proteasome specifically targets intracellular IL-1 for degradation. However,

the release of IL-1α and IL-1β significantly increased in these cells treated with proteasome inhibitors and CHX when compared to CHX alone treated cells due to the higher levels of intracellular protein.

In BMDMs, β-lactone increased the release of both IL-1α and IL-1β compared to controls, but ALLN only increased the release of IL-1α. Enhancement of IL-1 release by ALLN and β-lactone was not related to the cytotoxic effect of proteasome inhibition. This data is supported by previous work demonstrating a similar increase of IL-1β by β-lactone in primary human monocytes in the absence of LDH release into culture supernatants (Moors and Mizel, 2000). The combination of proteasome inhibitors and CHX increased the release of IL-1β in BMDMs, although this increase could be due to the cytotoxicity of CHX in BMDMs. In agreement with other studies, these data suggest that the proteasome limits the amount of the cytokine available for the processing and secretion upon monocyte/macrophage activation (Moors and Mizel, 2000).

7.9 Summary

- Bacterial and mammalian expression systems have an important role to play in the production of recombinant protein molecules. In summary, the cDNA fragment encoding Nt-b and Nt were amplified using PCR to be used for transformation or transfection of specific vectors. The vectors pET-22(+) and pcDNA3.1(+) were used to construct the recombinant bacterial and eukaryotic expression vector, respectively. Using transgenic technology, the eukaryotic cells (such as HEK293 and COS-7) were transfected and the expression monitored by taking advantage of a specific tag. However, using these protocols we were not successful to produce the purified proteins for further studies.
- The proteasome pathway is the main mechanism for intracellular degradation, has controversial roles on immune responses by regulating pro-

inflammatory cytokines (Rockwell et al., 2000; Nakayama et al., 2001; Yamamoto, and Gaynor, 2001). J774 cells and BMDMs were stimulated by LPS (1 µg/ml, 16 h). This stimulation resulted in expression of IL-1α and IL-1β. Treatment of LPS-stimulated J774 cells and BMDMs *in vitro* with different proteasome inhibitors (ALLN, MG262 and β-lactone) increased the stability of intracellular IL-1α and IL-1β in a time and concentration dependent manner. The enrichment of IL-1α and IL-1β in stimulated J774 cells after inhibition of proteasome function with β-lactone suggest ubiquitination of both IL-1α and IL-1β before they are targeted to the proteasome (Figure 7.1). This result could suggest that the proteasome may control inflammation through the degradation of IL-1α and IL-1β. Therefore, proteasome inhibitors may have a possible role in the treatment of inflammatory diseases (Elliott and Zollner, 2003).

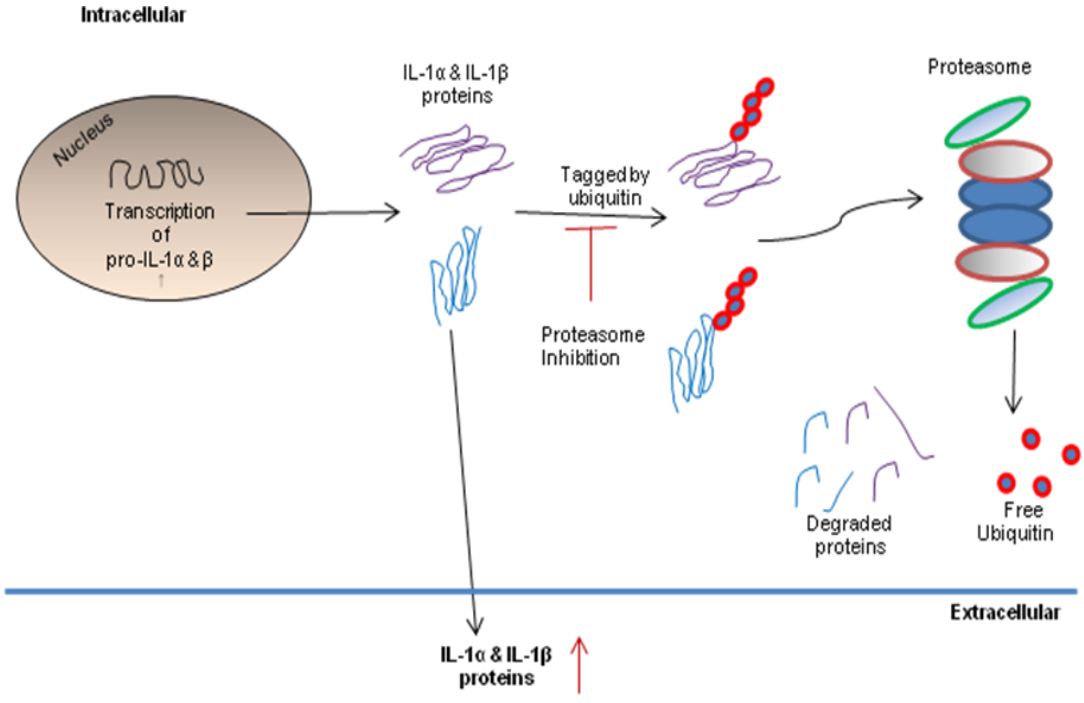

Figure 7.1 Proposed degradation pathways for IL-1α and IL-1β in activated macrophages. Pro-forms of IL-1α and IL-1β are transcribed in response to different stimuli. The extra intracellular IL-1α and IL-1β are tagged by Ub and destined to proteasome to be degraded.

Our observations are important because both inflammatory and autoimmune diseases, such as rheumatoid arthritis, intestinal inflammatory disease, MS and asthma, are often associated with the active participation of monocytic cells and with the deregulated expression and degradation of pro-inflammatory cytokines which influence a plethora of cellular functions (Fang and Mark, 2006; Garton et al., 2006). This deregulation results in accumulation of toxic proteins due to change of proteolytic systems (Ross and Poirier, 2005).

7.10 Future work

Despite the failure to purify the Nt fragments of pro-IL-1β protein under our experimental conditions, due to the limitations of expression systems used, it is possible to obtain Nt-b protein by either purification of pro-IL-1β from macrophage lysates or IP using over-expression system. Nt-b fragments could be obtained after an *in vitro* caspase-1 cleavage assay and pulling down both caspase-1 and mature Ct IL-1β. A specific Ab could be developed by purification of Nt-b from IP supernatants. The immunological functions of Nt-b could be further studied using this antibody.

Although the inhibitors used in this study showed inhibition of the proteasomal degradation pathway, it is also possible that these inhibitors might also affect non-proteasomal pathways of protein degradation such as the lysosomal or autophagy pathway. Thus, the real contribution of these pathways (which should include cytosolic and organelle proteases) to the degradation of truly short-lived proteins would require further studies with specific inhibitors of these various proteases.

The degree of ubiquitination of the protein of interest can be assessed by comparing the ratio of ubiquitinated/unmodified target protein in several experimental conditions. In order to make sure that ubiquitination is specific to IL-

1α and β, it is necessary to detect ubiquitination by IP of IL-1α and IL-1β followed by anti-ubiquitin Western blotting. It is necessary to optimise the IP protocol used for IL-1β (chapter 2, section 2.6.3). Different stringent conditions for cell lysis, IP and washing buffers could be used to improve the protocol (Didier et al., 2003; Xiong et al., 2009). Protein deubiquitination could be prevented by addition of different deubiquitinating enzyme inhibitors such as N-ethylmaleimide to all buffers during the experimental procedures (Laney and Hochsetrasser, 2002).

CHAPTER 8:

References

Adams J. The proteasome: structure, function, and role in the cell. Cancer Treatment Review 2003; 29: 3-9.

Adams J., Behnke M., Chen S., Cruickshank A.A., Dick L.R., Grenier L., Klunder J.M., Ma Y.T., Plamondon L. and Stein R.L. Potent and selective inhibitors of the proteasome: dipeptidyl boronic acids. Bio-organic Medical Chemistry Letters 1998; 8: 333-338.

Alibolandi M., Mirzahoseini M., Abad M.A.K. and Movahed M.A. High level expression of human basic fibroblast growth factor in *Escherichia coli*: evaluating the effect of the GC content and rare codons within the first 13 codons. Journal of Biotechnology 2010; 9: 2456-2462.

Allan S.M., Tyrrell P.J. and Rothwell N.J. Interleukin-1 and neuronal injury. Nature Reviews Immunology 2005; 5: 629-640.

Andrei C., Dazzi C., Lotti L., Torrisi M.R., Chimini G. and Rubartelli A. The secretory route of the leaderless protein interleukin-1β involves exocytosis of endolysosome related vesicles. Molecular Biology of Cell 1999; 10: 1463-1475.

Arend W.P., Gordon D.F., Wood W.M., Janson R.W., Joslin F.G. and Jameel S. IL-1β production in cultured human monocytes is regulated at multiple levels. Journal of Immunology 1989; 143: 118-126.

Arendt A.C. and Hochstrasser M. Identification of the yeast 20S proteasome catalytic centres and subunit interactions required for active-site formation. Proceeding National Academy of Science USA 1997; 94: 7156-7161.

Asher G., Bercovich Z., Tsvetkov P., Shaul Y. and Kahana C. 20S proteasomal degradation of ornithine decarboxylase is regulated by NQO1. Molecular Cell Biology 2005; 17: 645-655.

Auron P.E. and Webb A.C. Interleukin-1: a gene expression system regulated at multiple levels. European Cytokine Network 1994; 5: 573-592.

Auron P.E., Webb A.C., Rosenwasser L.J., Muccl S.F., Rich A., Wolff S.M. and Dinarelli C.A. Nucleotide sequence of human monocyte interleukin 1 precursor cDNA. Science 1984; 81: 7907-7911.

Baldwin A.S. The NF-κB and IκB proteins: New discoveries and insights. Annual Review of Immunology 1996; 14: 649-681.

Baldwin R.L. Temperature dependence of the hydrophobic interaction in protein folding. Proceedings National Academy of Science USA 1986; 83: 8069-8072.

Baneyx F. Recombinant protein expression in *Escherichia coli*. Current Opinion in Biotechnology, 1999; 10: 411-421.

Baneyx F. and Mujacic M. Recombinant protein folding and misfolding in *Escherichia coli.* National Biotechnology 2004; 22: 1399-1408.

Bar D., Apte R.N., Voronov E., Dinarello C.A. and Cohen S.A. Continuous delivery system of IL-1 receptor antagonist reduces angiogenesis and inhibits tumor development. FASEB Journal 2004; 18: 161-163.

Baracos V.E., DeVivo C., Hoyle D.H.R. and Goldberg A.L. Activation of the ATP-ubiquitin-proteasome pathway in skeletal muscle of cachectic rats bearing a hepatoma. American journal of Physiology 1995; 268: 996-1006.

Betts S.D. and King J. Cold rescue of the thermolabile tailspike intermediate at the junction between productive folding and off-pathway aggregation protein. Science 1998; 7: 1516-1523.

Beutler B.A. The role of tumor necrosis factor in health and disease. Journal of Rheumatology 1999; 26: 16-21.

Bianco F., Pravettoni E., Colombo A., Schenk U., Möller T., Matteoli M. and Verderio C. Astrocyte-derived ATP induces vesicle shedding and IL-1β release from microglia. Journal of Immunology 2005; 174: 7268-7277.

Blagosklonny M.V., An W.G., Melillo G., Nguyen P., Trepel J.B. and Neckers L.M. Regulation of BRCA1 by protein degradation. Oncogene 1999; 18: 6460-6468.

Bohley. The fates of proteins in cells. Nature 1995; 82: 544-550.

Boni-Schnetzler M., Boller S. and Debray S. Free fatty acids induce a pro-inflammatory response in islets via the abundantly expressed interleukin-1 receptor I. Endocrinology 2009; 150: 5218-5229.

Boni-Schnetzler M., Thorne J. and Parnaud G. Increased interleukin (IL)-1β messenger ribonucleic acid expression in beta-cells of individuals with type 2 diabetes and regulation of IL-1β in human islets by glucose and auto-stimulation. Journal of Clinical Endocrinology Metabolism 2008; 93: 4065-4074.

Bowerman B. and Kurz T. Degrade to create: developmental requirements for ubiquitin-mediated proteolysis during early C.elegans embryogenesis. Development 2006; 133: 773-784.

Braddock M. and Quinn A. Targeting IL-1 in inflammatory disease: new opportunities for therapeutic intervention. Nature Reviews Drug Discovery 2004; 3: 330-339.

Bradford M. A rapid and sensitive method for the quantitation of microgram quantities of protein utilizing the principle of protein-dye binding. Annual Biochemistry 1976; 72: 248-254.

Bratton S.B. and Cohen G.M. Apoptotic death sensor: an organelle's alter ego? Trends Pharmacological Science 2001; 22: 306-315.

Braun B.C., Glickman M., Kraft R., Dahlmann B. and Kloetzel P.M. The base of the proteasome regulatory particle exhibits chaperone-like activity. National Cell Biology 1999; 1: 221-226.

Breedveld F.C. Future trends in the treatment of rheumatoid arthritis: cytokine targets. Rheumatology 1999; 38: 11-13.

Bulteau A.L., Petropoulos I. and Friguet B. Age-related alterations of proteasome structure and function in aging epidermis. Journal of Biological Sciences and Medical Sciences 2000; 35: 767-777.

Burkhardt D. Role of proteasomes in disease. Biochemistry 2007; 8: 1-12.

Carrard G., Dieu M., Raes M., Toussaint O. and Friguet B. Impact of ageing on human proteasome structure and function in human lymphocytes. International Journal of Biochemistry and Cell Biology 2003; 35: 728-739.

Carruth L.M., Demczuk S. and Mizel S.B. Involvement of a calpain-like protease in the processing of the murine interleukin-1α precursor. Journal of Biological Chemistry 1991; 266: 12162-12170.

Cazalla D., Sanford J.R. and Caceres J.F. A rapid and efficient protocol to purify biologically active recombinant proteins from mammalian cells. Protein Expression Purification 2005; 42: 54-58.

Chamberlain J., Evans D., King A., Dewberry R., Dower S., Crossman D. and Francis S. Interleukin-1β and signalling of interleukin-1 in vascular wall and circulating cells modulates the extent of neointima formation in mice. American Journal of Pathology 2006; 168: 1396-1403.

Chen F., Chang D., Goh M., Klibanov S.A. and Ljungman M. Role of p53 in Cell Cycle Regulation and apoptosis following exposure to proteasome inhibitors. Cell growth and differentiation 2000; 11: 239-246.

Chen P. and Hochstrasser M. Autocatalytic subunit processing couples active site formation in the 20S proteasome to completion of assembly. Cell 1996; 86: 961-972.

Chin J. and Kostura M.J. Dissociation of IL-1β synthesis and secretion in human blood monocytes stimulated with bacterial cell wall products. Journal of Immunology 1993; 151: 5574-5585.

Chirivi R.G., Garofalo A., Padura I.M., Mantovani A. and Giavazzi R. Interleukin 1 receptor antagonist inhibits the augmentation of metastasis induced by interleukin 1 or

lipopolysaccharide in a human melanoma/nude mouse system. Cancer Research 1993; 53: 5051-5044.

Chondrogianni N., Stratford F.L.L., Trougakos I.P., Friguet B., Rivett A.J. and Gonos E.S. Central role of the proteasome in senescence and survival of human fibroblasts. Journal of Biological Chemistry 2003; 278: 28026-28037.

Ciechanover A. The Ubiquitin-Proteasome Proteolytic Pathway. Cell 1994; 79: 13-21.

Ciechanover A., Elias S., Heller H. and Hershko A. "Covalent affinity" purification of ubiquitin-activating enzyme. Journal of Biological Chemistry 1982; 257(5): 2537-2542.

Ciechanover A., Hod Y. and Hershko A. A heat-stable polypeptide component of an ATP-dependent proteolytic system from erythrocytes. Biochemical and Biophysical Research Communications 1978; 81: 1100-1105.

Colangeli R., Heijbel A., Williams A.M., Manca C., Chan J., Lyashchenko K. and Gennaro M.L. Three-step purification of lipopolysaccharide-free, polyhistidine-tagged recombinant antigens of Mycobacterium tuberculosis. Journal of Chromatography Biomedical Sciences and Applications 1998; 223-235.

Collins G.A. and Tansey W.P. The proteasome: a utility tool for transcription? Current Opinion in Genetics and Development 2006; 16: 197-202.

Colotta F., Re F., Muzio M., Bertini R. and Polentarutti N. Interleukin-1 type II receptor: a decoy target for IL-1 that is regulated by IL-4. Science 1993; 261: 472-475.

Conner E.M., Brand S., Davis J.M., Laroux F.S., Palombella V.J., Fuseler J.W., Kang D.Y., Wolf R.E. and Grisham M.B. Proteasome inhibition attenuates nitric oxide synthase expression, VCAM-1 transcription and the development of chronic colitis. Journal of Pharmacology and Experimental Therapeutics 1997; 282: 1615-1622.

Cowan J.L. and Morley S.J. The proteasome inhibitor, MG132, promotes the re-programming of translation in C2C12 myoblasts and facilitates the association of hsp25 with the eIF4F complex. European Journal of Biochemistry 2004; 271: 3596-3611.

Craiu A., Gaczynska M., Akopian T., Gramm C.F., Fenteany G., Goldberg A.L. and Rock K.L. Lactacystin and *clasto*-lactacystin β-lactone modify multiple proteasome β-subunits and inhibit intracellular protein degradation and major histocompatibility complex class I antigen presentation. Journal of Biological Chemistry 1997; 272: 13437-13445.

Crown J., Jakubowski A., Kemeny N., Gordon, M., Gasparetto C., Wong G., Sheridan C., Toner G., Meisenberg B., Botet J., Applewhite J., Sinha S., Moore M., Kelsen D., Guhles W. and Gabrilove J. A phase I trial of recombinant human interleukin-1β alone and in combination with myelosuppressive doses of 5-fluorouracil in patients with gastrointestinal cancer. Blood 1991; 78: 1420-1427.

Delcros J.G., Floc'h M.B., Prigent C. and Arlot-Bonnemains Y. Proteasome Inhibitors as Therapeutic Agents: Current and Future Strategies. Current Medicinal Chemistry 2003; 10: 479-503.

Delp K., Momburg F., Hilmes C., Huber C. and Seliger B. Functional deficiencies of components of the MHC class I antigen pathway in human tumours of epithelial origin. Bone Marrow Transplant 2000; 25: S88-S95.

Dice J.F. Molecular determinants of protein half-lives in eukaryotic cells 1987; 1: 349-357.

Dick L.R., Cruikshank A.A., Destree A.T., Grenier L., Mc-Cormack T.A., Melandri F.D., Nunes S.L., Palombella V.J., Parent L.A., Plamondon L. and Stein R.L. Mechanistic studies on the inactivation of the proteasome by lactacystin in cultured cells. Journal of Biological Chemistry 1997; 272: 182-188.

Dick L.R., Cruikshank A.A., Grenier L., Melandri F.D., Nunes S.L. and Stein R.L. Mechanistic studies on the inactivation of the proteasome by lactacystin a central role for *clasto-lactacystin* β-lactone. Journal of Biological Chemistry 1996; 271: 7273-7276.

Dick T.P., Nussbaum A.K., Deeg M., Heinemeyer W., Groll M., Schirle, W., Keilholz M., Stevanovic S., Wolf D.H, Huber R., Rammensee H.G. and Schild H. Contribution of proteasomal beta-subunits to the cleavage of peptide substrates analyzed with yeast mutants. Journal of Biological Chemistry 1998; 273: 25637-25646.

Didier C., Broday L., Bhoumik A., Israeli S., Takahashi S., Nakayama K., Thomas S.M., Turner C.E., Henderson S., Sabe H. and Ronai Z. RNF5, a RING finger protein that regulates cell motility by targeting paxillin ubiquitination and altered localization. Molecular Cell Biology 2003; 23: 5331-5345.

Dikic I., Wakatsuki S. and Walters K.J. Ubiquitin-binding domains from structures to functions. Nature Reviews Molecular Cell Biology 2009; 10: 659-671.

Dinarello C.A. Interleukin 1 and interleukin 1 antagonist. Blood 1991; 77:1627-1652.

Dinarello C.A. Biologic basis for interleukin-1 in disease. Blood 1996; 87: 2095-2147.

Dinarello C.A. Interleukin-1. In The Cytokine Handbook 1998; Press: 35-72.

Dinarello C.A. Biology of interleukin 1. FASEB Journal 1998; 2: 108-115.

Dinarello C.A. Interleukin-1 beta, interleukin-18 and the interleulin-1 beta converting enzyme. Annual New York Acadmy of Science 1998; 856: 1-11.

Dinarello C.A. Interleukin-1 in the pathogenesis and treatment of inflammatory diseases. Blood 2010; 117(14): 3720-3732.

Ding W.X., Ni H.M., Gao W., Yoshimori T., Stolz D.B., Ron D. and Yin X.M. Linking of autophagy to ubiquitin-proteasome system is important for the regulation of endoplasmic reticulum stress and cell viability. American Journal of Pathology 2007; 171: 513-524.

Ding W.X. and Yin X.M. Sorting, recognition and activation of the misfolded protein degradation pathways through macroautophagy and the proteasome. Autophagy 2008; 4: 141-150.

Divald A. and Powell S.R. Proteasome mediates removal of proteins oxidized during myocardial ischemia. Free Radical Biology and Medicine 2006; 40: 156-164.

Donath M.Y., Weder C. and Brunner A. XOMA052, a potential disease modifying anti-1L-1β antibody, shows sustained HbA1c reductions 3 months after a single injection with no increases in safety parameters in subjects with Type 2 diabetes. Diabetes 2009; 58-67.

Dong H., Nilsson L. and Kurland C.G. Co-variation of tRNA abundance and codon usage in *Escherichia coli* at different growth rates. Journal of Molecular Biology 1996; 260: 649-663.

Dowds T.A., Masumoto J., Chen F.F., Ogura Y., Inohara N. and Nunez G. Regulation of cryopyrin/Pypaf1 signaling by pyrin, the familial Mediterranean fever gene product. Biochemistry Biophysics Research Communication 2003; 302: 575-580.

Drexler H.C. Activation of the cell death program by inhibition of proteasome function. Proceedings National Academy of Science USA 1997; 94: 855-860.

Duan J., Friedman J., Nottingham L., Chen Z., Ara G. and Van Waes C. Nuclear factor-kappaB p65 small interfering RNA or proteasome inhibitor bortezomib sensitizes head and neck squamous cell carcinomas to classic histone deacetylase inhibitors and novel histone deacetylase inhibitor PXD101. Molecular Cancer Therapy 2007; 6: 37-50.

Dudek S.E., Luig C., Pauli E.K., Schubert U. and Ludwig S. The clinically approved proteasome inhibitor PS-341 efficiently blocks influenza A virus and vesicular stomatitis virus propagation by establishing an antiviral state. Journal of Virology 2010; 84: 9439-9451.

Duff G.W. Interleukin 1 and fever. British Journal of Rheumatology 1985; 24: 12-14.

Duffey D.C., Chen Z., Dong G., Ondrey F.G., Wolf J.S., Brown K., Siebenlist U. and Van Waes C. Expression of a dominant-negative mutant inhibitor-kappa B alpha of nuclear factor-kappa B in human head and neck squamous cell carcinoma inhibits survival, pro-inflammatory cytokine expression, and tumor growth *in vivo*. Cancer Research 1999; 59: 3468-3474.

Dunn E., Sims J.E., Nicklin M.J. and O'Neill L.A. Annotating genes with potential roles in the immune system: six new members of the IL-1 family. Trends in Immunology 2001; 22: 533-536.

Elaraj D.M., Weinreich D.M. and Varghese S. The role of interleukin 1 in growth and metastasis of human cancer xenografts. Clinical Cancer Research 2006; 12: 1088-1096.

Elliott P.J. and Zollner T.M. Proteasome inhibition: a new anti-inflammatory strategy. Journal of Molecular Medicine 2003; 81: 235-245.

Emery P. and Buch M. Treating rheumatoid arthritis with tumour necrosis factor blockade. British Medical Journal 2002; 324: 312-313.

Emsley H.C., Smith C.J., Georgiou R.F., Vail A., Hopkins S.J. and Rothwell N.J. A randomised phase II study of interleukin-1 receptor antagonist in acute stroke patients. Journal of Neurology, Neurosurgery and Psychiatry 2005; 76: 1366-1372.

Etlinger J.D. and Goldberg A.L. A soluble ATP-dependent proteolytic system responsible for the degradation of abnormal proteins in erythrocytes. Proceedings of the National Academy of Sciences USA 1977; 74: 54-58.

Fang J. and Ewald D. Expression cloned cDNA for 10-deacetylbaccatin III-10-O-acetyltransferase in *Escherichia coli*: a comparative study of three fusion systems. Protein Expression Purification 2004; 35: 17-24.

Fang L.S. and Mark A.B. NF-κB activation as a patholoical mechanism of septic shock and inflammation. American Journal Physiology Lung Cell Molecular Physiology 2006; 290: L622-645.

Fenteany G., Robert F., Standaert R.F., Lane W.S., Choi S., Corey E.J. and Schreiber S.L. Inhibition of proteasome activities and subunit-specific amino-terminal Threonine modification by lactacystin. Science 1995; 268: 726-731.

Ferrari D., Pizzirani C., Adinolfi E., Lemoli R.M., Curti A., Idzko M.l., Panther E. and Virgilio F.D. The P2X7 receptor: a key player in IL-1 processing and release. Journal of Immunology 2006; 176: 3877-3883.

Ferrer M., Chernikova T.N., Timmis K.N. and Golyshin P.N. Expression of a temperature-sensitive esterase in a novel chaperone-based *Escherichia coli* strain. Applied and Environmental Microbiology 2004; 70: 4499-4504.

Flann S., Hawkes R.B., Riederer B.M., Rider C.C. and Beesley P.W. Changes in ubiquitin in dendrite outgrowth and differentiation. Neuroscience 1997; 81: 173-187.

Frangioni J.V. and Neel B.G. Solubilization and purification of enzymatically active glutathione S-transferase (pGEX) fusion proteins. Annual Biochemistry 1993; 210: 179-187.

Frankel S., Sohn R. and Leinwand L. Use of sarkosyl in generating soluble protein after bacterial expression. Proceedings of National Academy of Science USA 1991; 88: 1192-1196.

French F. and Consortium M.F. A candidate gene for familial Mediterranean fever. Nature Genetics 1997; 17: 25-31.

Fuhlbrigge C., Fine D., Unanue R. and Chaplin D. Expression of membrane interleukin 1 by fibroblasts transfected with murine pro interleukin 1α cDNA. Proceedings National Academy of Science USA 1988; 85: 5649-5557.

Garton K.J., Gough P.J. and Raines E.W. Emerging roles for ectodomain shedding in the regulation of inflammatory responses. Journal of Leukocyte Biology 2006; 79: 1105-1116.

Geier E., Pfeifer G., Wilm M., Lucchiari-Hartz M., Baumeister W., Eichmann K. and Niedermann G. A giant protease with potential to substitute for some functions of the proteasome. Science 1999; 283: 978-981.

Geisse S., Gram H., Kleuser B. and Kocher H.P. Eukaryotic expression systems: a comparison. Protein Expression Purification 1996; 8: 271-282.

Gemma A., Takenaka K. and Hosoya Y. Altered expression of several genes in highly metastatic subpopulations of a human pulmonary adenocarcinoma cell line. European Journal of Cancer 2001; 37: 1554-1561.

Geng J. and Carstens R.P. Two methods for improved purification of full-length mammalian proteins that have poor expression and/or solubility using standard *Escherichia coli* procedures. Protein Expression and Purification 2006; 48: 142-150.

Gerber A., Heimburg A., Reisenauer A., Wille A., Welte T. and Bühling F. Proteasome inhibitors modulate chemokine production in lung epithelial and monocytic cells. European Respiratory Journal 2004; 24: 40-48.

Germain R.N. and Margulies D.H. The biochemistry and cell biology of antigen processing and presentation. Annual Review of Immunology 1993; 11: 403-450.

Giri J., Lomedico P.T. and Mizel S.B. Studies on the synthesis and secretion of interleukin 1. Journal of Immunology 1985; 134: 343-349.

Glaumann H. and Ballard F.J. Lysosomes: their role in protein breakdown. Academic Press, New York 1987.

Glickman M.H., Rubin D.M., Coux O., Wefes I. and Pfeifer A. A subcomplex of the proteasome regulatory particle required for ubiquitin conjugate degradation and related to the COP9-signalosome and eIF3. Cell 1994; 94: 615-623.

Glickman M.H., Rubin D.M., Fried V.A. and Finley D. The regulatory particle of the *Saccharomyces cerevisiae* proteasome. Molecular Cell Biology 1998; 18: 3149-3162.

Goldberg A. and St. John A. Intracellular protein degradation in mammalian and bacterial cells. Annual Review of Biochemistry 1976; 45: 747-803.

Goldberg A.L. and Rock K.L. Proteolysis, porteasomes and antigen presentation. Nature 1992; 357: 379-379.

Goldfeld A.E., McCaffrey P.G., Strominger J.L. and Rao A. Identification of a novel cyclosporin-sensitive element in the human tumor necrosis a gene promoter. Journal of Experimental Medicine 1993; 178: 1365-1379.

Greenfeder S.A., Nunes P., Kwee L., Labow M., Chizzonite R.A. and Ju G. Molecular cloning and characterization of a second subunit of the interleukin-1 receptor complex. Journal of Biological Chemistry 1995; 270: 13757-13765.

Grenfell S., Smithers N., Witham S., Shaw A., Graber P. and Solari R. Analysis of mutations in the putative nuclear localization sequence of interleukin-1 beta. Journal of Biochemistry 1991; 280: 111-116.

Griffin W.S.T., Sheng J.G., Gentleman S.M., Graham D.I., Mrak R.E. and Roberts G.W. Microglial interleukin-1 alpha expression in human head injury: correlations with neuronal and neuritic beta-amyloid precursor protein expression. Neuroscience Letters 1994; 176(2): 133-136.

Griffin W.S.T., Stanley L.C., Fedoroff S., Juurlink B.H.J., Doucette R. and Burkholder G. Glial activation as a common denominator in neuro-degenerative disease: a hypothesis in neuropathophysiology. Editors Biology and Pathology of Astrocyte-Neuron Interactions, Altschul Symposium Series 1993; 2: 359-382.

Griffin W.S.T., Stanley L.C., Ling C., White L., MacLeod V., Perrot L.J., White C.L. and Araoz C. Brain interleukin-1 and S-100 immunoreactivity are elevated in Down syndrome and Alzheimer disease. Proceedings National Academy of Science USA 1989; 86: 7611-7615.

Grillari j., Katinger H. and Voglaue R. Aging and the ubiquitinome: Traditional and non-traditional functions of ubiquitin in aging cells and tissues. Experimental Gerontology 2006; 41: 1067-1079.

Grilli M., Chiu J.J.S. and Lenardo M. JNF-κB and Rel: participants in a multiform transcriptional regulatory system. International Review of Cytology 1993; 143: 1-62.

Groll M., Ditzel L., Lowe J., Stock D., Bochtler M., Bartunik H.D. and Huber R. Structure of 20S proteasome from yeast at 2.4 Å resolution. Nature 1997; 386: 463-471.

Groll M., Heinemeyer W., Jager S., Ullrich T., Bochtler M., Wolf D.H. and Huber R. The catalytic sites of 20S proteasomes and their role in subunit maturation: a mutational and crystallographic study. Proceedings National Academy of Science USA 1999; 96: 10976-10983.

Guterman A. and Glickman M.H. Complementary roles for Rpn11 and Ubp6 in de-ubiquitination and proteolysis by the proteasome. Journal of Biological Chemistry 2004; 279: 1729-1738.

Harris J., Hartman M., Roche C., Zeng S.G., O'She A., Sharp F.A., Lambe E.M., Creagh E.M, Golenbock D.T., Tschopp J., Kornfeld H., Fitzgerald K.A. and Lavelle Ed.C. Autophagy controls IL-1β secretion by targeting pro-IL-1β for degradation. The Journal of Biological Chemistry 2011; 11: 9587-9597.

Hass M., Page S., Page M., Neumann F.J., Marx N., Adam M., Löms Ziegler-Heitbrock H.W., Neumeier D. and Brand K. Effect of proteasome inhibitors on monocytic IκB-α and β depletion, NF-κB activation, and cytokine production. Journal of Leukocyte Biology 1998; 63: 395-404.

Hazuda D.J., Lees J.C. and Young P.R. The kinetics of interleukin-1 secretion from activated monocytes. Differences between interleukin-1α and interleukin-1β. The Journal of Biological Chemistry 1988; 263: 8473-8479.

Heguy A., Baldari C., Bush K., Nagele R., Newton R.C., Robb R.J., Horuk R., Telford J.L. and Melli M. Internalization and nuclear localization of interleukin-1 are not sufficient for function. Cell Growth Differentiation 1991; 2: 311-315.

Heinemeyer W., Fischer M., Krimmer T., Stachon U. and Wolf D.H. The active sites of the eukaryotic 20S proteasome and their involvement in subunit precursor processing. Journal of Biological Chemistry 1997; 272: 25200-25209.

Heinemeyer W., Kleinschmidt J.A., Saidowsky J., Escher C. and Wolf D.H. Proteinase yscE, the yeast proteasome/multicatalytic-multifunctional proteinase: Mutants unravel its function in stress proteolysis and uncover its necessity for cell survival. EMBO Journal 1991; 10: 555-562.

Hendil K.B. The 19 S multicatalytic 'prosome' proteinase is a constitutive enzyme in HeLa cells. Biochemistry. International 1988; 17: 471-477.

Hershko A. and Ciechanover A. The ubiquitin system for protein degradation. Annual Review of Biochemistry 1992; 61: 761-807.

Hershko A. and Ciechanover A. The ubiquitin system. Annual Review of Biochemistry 1998; 67: 425-480.

Hershko A., Heller H., Elias S. and Ciechanover A. Components of ubiquitin-protein ligase system. Journal of Biological Chemistry 1983; 258: 8206-8214.

Hicke L., Schubert H.L. and Hill C.P. Ubiquitin-binding domains. Nature Reviews Molecular Cell Biology 2005; 6: 610-621.

Hideshima T., Richardson P., Chauhan D., Palombella V.J., Elliott P.J, Adams J. and Anderson K.C. The proteasome inhibitor PS-341 inhibits growth, induces apoptosis, and overcomes drug resistance in human multiple myeloma cells. Cancer Research 2001; 61: 3071-3076.

Hilt W. and Wolf D.H. Proteasomes: destruction as a programme. Trends in Biochemical Science 1996; 21: 96-102.

Hitchcock A.L., Auld K., Gygi S.P. and Silver P.A. A subset of membrane-associated proteins is ubiquitinated in response to mutations in the endoplasmic reticulum degradation machinery. Proceedings National Academy of Science 2003; 28: 12735-40.

Hobler S.C., Williams A., Fischer D., Wang J.J., Sun X., Fischer J.E., Monaco J.J. and Hasselgren P.O. Activity and expression of the 20S proteasome are increased in skeletal muscle during sepsis. American Journal of Physiology 1999; 277: R434-R440.

Hochestrasser M. Ubiquitin-dependent protein degradation. Annual Review of Genetics. 1996; 30: 405-439.

Hochuli E., Dobeli H. and Schacher A. New metal chelate adsorbent selective for proteins and peptides containing neighboring histidine residues. Journal of Chromatography 1987; 411: 177-184.

Hoffman H.M., Rosengren S., Boyle D.L., Boyle D.L., Cho J.Y., Nayar J., Mueller J.L., Anderson J.P., Wanderer A.A. and Firestein G.S. Prevention of cold-associated acute inflammation in familial cold auto-inflammatory syndrome by interleukin-1 receptor antagonist. The Lancet 2004; 364 (9447): 1779-1785.

Hollstein M., Sidransky D., Vogelstein B. and Harris C.C. p53 mutations in human cancers. Science 1991; 253: 49-53.

Horai R., Asano M., Sudo K., Kanuka H., Suzuki M., Nishihara M., Takahashi M. and Iwakura Y. Production of mice deficient in genes for interleukin (IL)-1α, IL-1β, and IL-1 receptor antagonist shows that IL-1β is crucial in turpentine-induced fever development and glucocorticoid secretion. Journal of Experinemtal Medicine 1998; 187: 1463-1470.

Hosseini H., Andre P., Lefevre N., Viala N., Walzer T.,Peschanski M. and Lotteau V. Protection against experimental autoimmune encephalomyelitis by a proteasome modulator. Journal of Neuro-immunology 2001; 118: 233-244.

Hu B., Wang S., Zhang Y., Feghali C.A., Dingman J.R. and Wright T.M. A nuclear target for interleukin-1α: Interaction with the growth suppressor necdin modulates proliferation and collagen expression. Proceedings National Academy of Science USA 2003; 100: 10008-10013.

Hu G., Lin G., Wang M., Dick L., Xu R.M., Nathan C. and Li H. Structure of the Mycobacterium tuberculosis proteasome and mechanism of inhibition by a peptidyl boronate. Molecular Microbiology 2005; 59: 1417-1428.

Ihle J.N. Cytokine receptor signalling. Nature 1995; 377(6550): 591-594.

Ikemura T. Correlation between the abundance of *Escherichia coli* transfer RNAs and the occurrence of the respective codons in its protein genes. Journal of Molecular Biology 1981; 146 (1): 1-21.

Ilowite N., Porras O., Reiff A., Rudge S., Punaro M., Martin A., Allen R., Harville T., Sun Y.N., Bevirt T., Aras G. and Appleton B. Anakinra in the treatment of polyarticular-course juvenile rheumatoid arthritis: safety and preliminary efficacy results of a randomized multicenter study. Clinical Rheumatology 2009; 28: 129-137.

Imai J., Yashiroda H., Maruya M., Yahara I. and Tanaka K. Proteasomes and molecular chaperones: cellular machinery responsible for folding and destruction of unfolded proteins. Cell Cycle 2003; 2: 585-590.

Jager S., Groll M., Huber R., Wolf D.H. and Heinemeyer W. Proteasome beta-type subunits: unequal roles of propeptides in core particle maturation and a hierarchy of active site function. Journal of Molecular Biology 1999; 291: 997-1013.

Jagoe T. and Goldberg L. What do we really know about the ubiquitin-proteasome pathway in muscle atrophy? Current Opinion Clinical Nutrition and Metabolic Care 2001; 4: 183-190.

Johnson A., France J., Sy M.S. and Harding C.V. Down-regulation of the transporter for antigen presentation, proteasome subunits, and class I major histocompatibility complex in tumor cell lines. Cancer Research 1998; 58: 3660-3667.

Joosten L.A., Helsen M.M., Saxne T., van de Loo F.A., Heinegard D. and van den Berg W.B. IL-1 alpha/beta blockade prevents cartilage and bone destruction in murine type II collagen induced arthritis, whereas TNF alpha blockade only ameliorates joint inflammation. Journal of Immunology 1999; 163: 5049-5055.

Karin M. How NF-κB is activated: the role of the IκB kinase (IKK) complex. Oncogene 1999; 18: 6867-6874.

Karin M. The beginning of the end: IκB kinase (IKK) and NF-κB activation. Journal of Biological Chemistry 1999; 274: 27339-27342.

Karin M. and Greten R.F. NF-κB: Linking inflammation and immunity to cancer development and progression. National Review of Immunology 2005; 5: 749-759.

Kavita U. and Mizel S.B. Differential sensitivity of interleukin-1α and β precursor proteins to cleavage by calpain, a calcium-dependent protease. Journal of Biological Chemistry 1995; 270: 27758-27765.

Kay J. and Calabrese L. The role of interleukin-1 in the pathogenesis of rheumatoid arthritis. Rheumatology 2004; 4 (3): 2-9.

Keatings V.M., Collins P.D., Scott D.M. and Barnes P.J. Differences in interleukin 8 and tumor necrosis factor α in induced sputum from patients with chronic obstructive pulmonary disease or asthma. American Journal of American Journal of Respiratory and Critical Care Medicine 1996; 153: 530-534.

Keck S., Nitsch R., Grune T. and Ullrich O. Proteasome inhibition by paired helical filament-tau in brains of patients with Alzheimer's disease. Journal of Neurochemistry 2003; 85: 115-122.

Kisselev A.F., Akopian T.N., Woo K.M. and Goldberg A.L. The sizes of peptides generated from protein by mammalian 26S and 20S proteasomes: implications for understanding the degradative mechanism and antigen presentation. Journal of Biological Chemistry 1999; 274: 3363-3371.

Kisselev A.F. and Goldberg A.L. Proteasome inhibitors: from research tools to drug candidates. Chemical Biology 2001; 8: 739-758.

Kirii H., Niwa T., Yamada Y., Wada H., Saito K., Iwakura Y., Asano M., Moriwaki H. and Seishima M. Lack of interleukin-1β decreases the severity of atherosclerosis in ApoE-deficient mice. Arteriosclerosis Thrombosis and Vascular Biology 2003; 23: 656-660.

Kishimoto T., Taga T. and Akira S. Cytokine signal transduction. Cell 1994; 76: 253-262.

Kobayashi Y., Oppenheim J.J. and Matsushima K. Calcium-dependent binding of phosphorylated human pre-interleukin 1 alpha to phospholipids. Journal of Biochemistry 1990; 107: 666-670.

Kobayashi Y., Yamamoto K., Saido T., Kawasaki H., Oppenheim J. and Matsushima K. Identification of calcium-activated neutral protease as a processing enzyme of human interleukin 1α. Proceedings of National Academy of Science 1990; 87: 5548-5552.

Kostura M.J., Tocci G., Limjuco G., Chin J., Cameron P., Hillman A.G., Chartrain N.A. and Schmidt J.A. Identification of a monocyte specific pre-interleukin 1β convertase activity.

Proceedings National Academy of Science USA 1989; 86: 5227-5235.

Kramer B., Machleidt T., Wiegmann K. and Krönke M. Super antigen induced transcriptional activation of the human TNF gene promoter in T cells. Journal of Inflammation 1995; 45: 183-192.

Kramer B., Wiegmann K. and Krönke M. Regulation of the human TNF promoter by the transcription factor Ets. Journal of Biological Chemistry 1995; 270: 6577-6583.

Kumatori A., Tanaka K., Inamura N., Sone S., Ogura T., Matsumoto T., Tachikawa T., Shin S. and Ichihara A. Abnormally high expression of proteasomes in human leukemic cells. Proceedings of the National Academy of Sciences USA 1990; 87: 7071-7075.

Laney J.D. and Hochsetrasser M. Unit 14.5 Analysis of Protein Ubiquitination. Current Protocols in Protein Science 2002; 14 (5): 1-11.

Larsen C.N. and Finley D. Protein translocation channels in the proteasome and other proteases. Cell 1997; 91: 431-434.

Layfield R., Lowe J. and Bedford L. The ubiquitin-proteasome system and neuro-degenerative disorders. Essays in Biochemistry 2005; 41: 157-171.

Lecker S., Jagoe R.T., Gilbert A., Gomes M., Baracos V., Bailey J., Price S.R., Mitch W.E. and Goldberg A.L. Multiple types of skeletal muscle atrophy involve a common program of changes in gene expression. FASEB Journal 2004; 18: 39-51.

Ledford H. Fever pitch. Nature 2007; 450: 600-601.

Lee D.H. and Goldberg A.L. Selective inhibitors of the proteasome-dependent and vacuolar pathways of protein degradation in *Saccharomyces cerevisiae*. Journal of Biological Chemistry 1996; 271: 27280-27284.

Lee D.H. and Goldberg A.L. Proteasome inhibitors: valuable new tools for cell biologists. Trends Cell Biology 1998; 8: 397-403.

Leitman D.C., Mackow E.R., Williams T., Baxter J.D. and West B.L. The core promoter region of the tumor necrosis factor a gene confers phorbol ester responsiveness to upstream transcriptional activators. Molecular Cell Biology 1992; 12: 1352-1356.

Lenardo M.J. and Baltimore D. NF-κB: a pleiotropic mediator of inducible and tissue-specific gene control. Cell 1989; 58: 227-229.

Leon R.G., Munier-Lehmann H., Barzu O., Baudin-Creuza V., Pietri R., Lopez-Garriga J. and Cadilla C.L. High-level production of recombinant sulfide-reactive hemoglobin I from Lucina pectinata in *Escherichia coli*. High yields of fully functional holoprotein synthesis in the BL25 *E. coli* strain. Protein Expression Purification 2004; 38: 184-195.

Lepe-Zuniga J.L. and Gery I. Production of intra- and extracellular interleukin-1 (IL-1) by human monocytes. Clinical Immunology and Immunopathology 1984; 31: 222-230.

Levine J.S. Bronchial epithelial cell-cytokine interactions in airway inflammation. Journal of Investigative Medicine 1995; 43: 241-249.

Liss C., Fekete M.J., Hasina R., Lam C.D. and Lingen M.W. Paracrine angiogenic loop between head-and-neck squamous-cell carcinomas and macrophages. International Journal of Cancer 2001; 93: 781-785.

Liu Z., Cashion L.M. and Twu J.J. A systematic comparison of relative promoter/enhancer activities in mammalian cell lines. Annual Biochemistry 1997; 246: 150-152.

Llovera M., Garcia-Martinez C., Agell N., Marzabal M., Lopez-Soriano F.J. and Argiles J.M. Ubiquitin gene expression is increased in skeletal muscle of tumour-bearing rats. FEBS Letters 1994; 338: 311-318.

Lopes U.G., Erhardt P., Yao R. and Cooper G.M. p53-dependent induction of apoptosis by proteasome inhibitors. Journal of Biological Chemistry 1997; 272: 12893-12896.

Lopez-Castejon G. and Brough D. Understanding the mechanism of IL-1β secretion. Cytokine Growth Factor Review 2011; 22(4): 189-195.

Lövborg H., Öberg F., Rickardson L., Gullbo J., Nygren P. and Larsson R. Inhibition of proteasome activity, nuclear factor-κB translocation and cell survival by the anti-alcoholism drug disulfiram. International Journal of Cancer 2006; 118: 1577-1580.

Löwe J., Stock D., Ditzel L., Groll M. and Huber R. Crystal Structure of the 20S Proteasome from thermoplasma from the archaeon T. acidophilum at 3.4 Å resolution. Science 1995; 268: 533-539.

Luheshi N.M., Rothwell N.J. and Brough D. The dynamics and mechanisms of interleukin-1α and β nuclear import. Traffic 2009; 10(1): 16-25.

Luo C., Burgeon E., Carew J.A., McCaffrey P.G., Badalian T.M., Lane W.S., Hogan P.G. and Rao A. Recombinant NFAT1 (NFATp) is regulated by calcineurin in T cells and mediates transcription of several cytokine genes. Molecular Cell Biology 1996; 16: 3955-3966.

McCormack T., Baumeister W., Grenier L., Moomaw C., Plamondon L., Pramanik B., Slaughter C., Soucy F., Stein R., Zuhl F. and Dick L. Active site-directed inhibitors of Rhodococcus 20S proteasome.Kinetics and mechanism. Journal of Biological Chemistry 1997; 272:26103-26109

MacKenzie A., Wilson H.L., Kiss-Toth E., Dower S.K., North R.A. and Surprenant A. Rapid secretion of interleukin-1β by microvesicle shedding. Immunity 2001; 115: 825-835.

Maier J., Statuto M. and Ragnotti G. Endogeneous interleukin 1α must be transported to the nucleus to exert its activity in human endothelial cells. Molecular and Cellular Biology 1994; 14(3): 1845-1851.

Maki C.G., Huibregtse J.M. and Howley P.M. *In vivo* ubiquitination and proteasome-mediated degradation of p53. Cancer Research 1996; 56: 2649-2654.

Malinin N.L., Boldin M.P., Kovalenko A.V. and Wallach D. MAP3K-related kinase involved in NF-κB induction by TNF, CD95 and IL-1. Nature 1997; 401: 82-85.

Mandinova A., Soldi R., Graziani I., Bagala C., Bellum S., Landriscina M., Tarantini F., Prudovsky I. and Maciag T. S100A13 mediates the copper-dependent stress-induced release of IL-1alpha from both human U937 and murine NIH 3T3 cells. Journal of Cell Science 2003; 116: 2687-2696.

March J., Mosley B., Larsen A., Cerretti D., Braedt G., Price V., Gillis S. Henney C., Kronheim S.R, Grabstein K., Conlon J., Hopp T. and Cosman D. Cloning, sequence and expression of two distinct human interleukin-1 complementary DNAs. Nature 1985: 315:641.

Mariathasan S. and Monack D.M. Inflammasome adaptors and sensors: intracellular regulators of infection and inflammation. National Review of Immunology 2007; 7: 31-40.

Martinez-Vicente M., Sovak G. and Cuervo A.M. Protein degradation and aging. Experimental Gerontology 2005; 40: 622-633.

Martinon F., Burns K. and Tschopp J. The inflammasome: a molecular platform triggering activation of inflammatory caspases and processing of pro-IL-1β. Molecular Cell 2002; 10: 417-426.

Martinon F. and Tschopp J. Inflammatory caspases: linking an intracellular innate immune system to autoinflammatory diseases. Cell 2004; 117: 561-574.

Martinon F. and Tschopp J. NLRs join TLRs as innate sensors of pathogens. Trends in Immunology 2005; 26: 447-455.

Masdehors P., Satoshi O., Merle-Béral H., Frank M., Cosset JM., Dumont J., Magdelénat H. and Delic J. Increased sensitivity of CLL-derived lymphocytes to apoptotic death activation by the proteasome-specific inhibitor lactacystin. Journal of Haematology 1999; 105: 752-757.

Masters S.L., Simon A., Aksentijevich I. and Kastner D.L. Horror autoinflammaticus: the molecular pathophysiology of autoinflammatory disease. Annual Review of Immunology 2009; 27: 621-668.

Matsushima K., Taguchi M., Kovacs E.J., Young H.A. and Oppenheim J.J. Intracellular localization of human monocyte associated interleukin 1 (IL-1) activity and release of biologically active IL-1 from monocytes by trypsin and plasmin. Journal of Immunology 1986; 136: 2883-2891.

McGuinness M.C., Powers J.M., Bias W.B., Schmeckpeper B.J., Segal A.H., Gowda V.C., Wesselingh S.L., Berger J., Griffin D.E. and Smith K.D. Human leukocyte antigens and cytokine expression in cerebral inflammatory demyelinative lesions of X-linked adreno leukodystrophy and multiple sclerosis. Journal of Neuro-immunology 1997; 75: 174-182.

McMahon C.J., Slack J.L., Mosley B., Cosman D., Lupton S.D., Brunton L., Grubin C., M.Wignall J., Jenkins N., Brannan C.I., Copeland N.G., Huebner K., McMahon G.A., Garfinkel S., Prudovsky I., Hu X. and Maciag T. Intracellular precursor interleukin (IL)-1α, but not mature IL-1α is able to regulate human endothelial cell migration *in vitro*. Journal of Biological Chemistry 1997; 272: 28202-28205.

McNaught K.S.P. and Jenner P. Proteasomal function is impaired in substantia nigra in Parkinson's disease. Neuroscience Letters 2001; 297: 191-194.

Meidenbauer N., Zippelius A., Pittet M.J., Laumer M., Vogl S., Heymann J., Rehli M., Seliger B., Schwarz S. and Le-Gal F.A. High frequency of functionally active Melan-A-specific T cells in a patient with progressive immunoproteasome-deficient melanoma. Cancer Research 2004; 64: 6319-6326.

Mellgren R.L. Specificities of cell permeant peptidyl inhibitors for the proteinase activities of mu-calpain and the 20S proteasome. Journal of Biological Chemistry 1997; 272: 29899-29903.

Meng L., Mohan R., Kwok B.H.B., Elofsson M., Sin V. and Crews C.M. Epoxomicin, a potent and selective proteasome inhibitor, exhibits in vivo anti-inflammatory activity. Proceedings National Academy of Science USA 1999; 96: 10403-10408.

Meriin A.B., Gabai, V.L., Yaglom J., Shifrin V.I. and Sherman, M.Y. Proteasome inhibitors activate stress kinases and induce hsp72. Journal of Biological Chemistry 1998; 273: 6373-6379.

Miksch G., Neitzel R., Fiedler E., Friehs K. and Flaschel E. Extracellular production of a hybrid beta-glucanase from Bacillus by *Escherichia coli* under different cultivation conditions in shaking cultures and bioreactors. Applied Microbiology and Biotechnology 1997; 47: 120-126.

Mirzahoseini A., Omumi B. and Omidinia E. Investigation of reasons that imply the diminished inclusion bodies in *E. coli*. Journal of Sciences of Islamic Republic of Iran 2003; 14: 113-119.

Mirzahoseini M. and Alibolandi M. Stability of recombinant proteins in *Escherichia coli*: the effect of co-expression of five different chaperone sets. Journal of Sciences of Islamic Republic of Iran 2009; 20: 305-310.

Mishto M., Bellavista E., Santoro A., Stolzing A., Ligorio C., Nacmias B., Spazzafumo L., Chiapelli M., Licastro F. and Sorbi S. Immunoproteasome and LMP2 polymorphism in aged and Alzheimer's disease brains. Neurobiology Aging 2006; 27: 54-66.

Mitch W.E., Medina R., Grieber S., May C., England B.K., Price S.R., Bailey J.L. and Goldberg A.L. Metabolic acidosis stimulates muscle protein degradation by activating the adenosin triphosphate-dependent pathway involving ubiquitin and proteasomes. Journal of Clinical Investigation 1994; 93: 2127-2133.

Moors M.A. and Mizel S.B. Proteasome-mediated regulation of interleukin-1β turn-over and export in human monocytes. Journal of Leukocyte Biology 2000; 68: 131-136.

Mosley B., Urdal D.L., Prickett A., Larsen D., Cossman P. J.; Conlon S. and Dower S.K. The interleukin-1 receptor binds the human interleukin-1α precursor but not the interleukin-1β precursor. Journal of Biological Chemistry 1987; 262: 2941-2944.

Müller M., Ziegler-Heitbrock L. and Baeuerle A. Nuclear factor kappa B, a mediator of lipopolysaccharide effects. Immunobiology 1993; 187: 233-256.

Murakami Y., Matsufuji S., Kameji T., Hayashi S., Igarashi K., Tamura T., Tanaka K. and Ichihara A. Ornithine decarboxylase is degraded by the 26S proteasome without ubiquination. Nature 1992; 6404: 597-599.

Muruve D.A., trilli V.P., Zaiss K.A., White W.R., Clark S.A., Ross P.J., Parks R.J. and Tschopp J. The inflammasome recognizes cytosolic microbial and host DNA and triggers an innate immune response. Nature 2008; 452: 103-107.

Murzin A.G., Lesk A.M. and Chothia C. β-Trefoil fold. Patterns of structure and sequence in the Kunitz inhibitors interleukins-1α and 1β and fibroblast growth factors. Journal of Molecular Biology 1992; 223: 531-543.

Nakayama K., Furusu A., Xu Q., Konta T. and Kitamura M. Unexpected transcriptional induction of monocyte chemoattractant protein 1 by proteasome inhibition: involvement of the c-jun N-terminal kinase-activator protein 1 pathway. Journal of Immunology 2001; 167: 1145-1150.

Nangy I., Tamura T., Vanderleyden J., Baumeister W. and De Mot R. The 20S proteasome of *Streptomyces coelicolor*. Journal of Bacteriology 1998; 180: 5448-5453.

Naujokat C. and Hoffmann S. Role and function of the 26S proteasome in proliferation and apoptosis. Laboratory Investigation 2002; 82: 965-980.

Navon A. and Goldberg A.L. Proteins are unfolded on the surface of the ATPase ring before transport into the proteasomes. Molecular Cell Biology 2001; 8: 1339-1349.

Nemunaitis J., Appelbaum F.R., Lilleby K., Buhles W.C., Rosenfeld C., Zeigler Z.R., Shadduck R.K., Singer J.W., Meyer W. and Buckner C.D. Phase I study of recombinant interleukin-1 beta in patients undergoing autologous bone marrow transplant for acute myelogenous leukemia. Blood 1994; 83: 3473-3479.

Nickel W. The mystery of non-classical protein secretion. A current view on cargo proteins and potential export routes. European Journal of Biochemistry 2003; 270: 2109-2119.

Nicola N.A. (ed) Guidebook to cytokines and their receptors 1994; Sambrook and Tooze, Oxford.

Obin M., Mesco E., Gong X., Haasi A.L., Joseph J. and Taylor A. Neurite Outgrowth in PC12 Cells distinguishing the roles of ubiquitylation and ubiquitin-dependent proteolysis. The Journal of Biological Chemistry 1999; 274 (17): 11789-11795.

Oh S., Hong H.S., Hwang E., Sim H.J., Lee W., Shin S.J. and Mook-Jung I. Amyloid peptide attenuates the proteasome activity in neuronal cells. Mechanisms of Aging Development 2005; 126: 1292-1299.

Olofsson P.S., Sheikine Y., Jatta K., Ghaderi M., Samnegard A., Eriksson P. and Sirsjö A. A functional interleukin-1 receptor antagonist polymorphism influences atherosclerosis development. The interleukin-1β: interleukin-1 receptor antagonist balance in atherosclerosis. Circulation Journal 2009; 73: 1531-1536.

Omura S., Fujimoto T., Otoguro K., Matsuzaki K., Moriguchi R., Tanaka H. and Sasaka Y. Lactacystin, a novel microbial metabolite, induces neurogenesis of neuroblastoma cells. Journal of Antibiotics 1991; 44: 113-116.

Oppenheim J., Kovacs E., Matsushima K. and Durum S. There is more than one interleukin-1. Immunology Today 1986; 7: 45-56.

Orino E., Tanaka K., Tamura T., Sone S., Ogura T. and Ichihara A. ATP-dependent reversible association of proteasomes with multiple protein components to form 26S complexes that degrade ubiqultinated proteins in human HL-60 cells. FEBS Letters 1991; 284: 206-210.

Ortiz-Lazareno P.C., Hernandez-Flores G., Dominguez-Rodriguez J.R., Lerma-Diaz J.M., Jave-Suarez L.F., Aguilar-Lemarroy A., Gomez-Contreras P.C., Scott-Algara D. and Bravo-Cuellar A. MG132 proteasome inhibitor modulates pro-inflammatory cytokines

production and expression of their receptors in U937 cells: involvement of nuclear factor-κB and activator protein-1. Immunology 2008; 124(4): 534-541.

Ostrowska H., Wojcik C., Omura S. and Worowski K. Lactacystin, a specific inhibitor of the proteasome, inhibits human platelet lysosomal cathepsin A-like enzyme. Biochemistry and Biophysical Research Communications 1997; 234: 729-732.

Ott D.E., Coren L.V., Sowder R.C., Adams J. and Schubert U. Retroviruses have differing requirements for proteasome function in budding process. Journal of Virology 2003; 77: 3384-3393.

Palmer G., Trolliet S., Talabot-Ayer D., Mezin F., Magne D. and Gabay C. Pre-interleukin-1α expression reduces cell growth and increases interleukin-6 production in SaOS-2 osteosarcoma cells: differential inhibitory effect of interleukin-1 receptor antagonist (icIL-1Ra1). Cytokine 2005; 31: 153-160.

Palombella V.J., Rando O.J., Goldberg A.L. and Maniatis T. The ubiquitin-proteasome pathway is required for processing the NF-κB precursor protein and the activation of NF-κB. Cell 1994; 78: 773-785.

Pascual V., Allantaz F., Arce E., Punaro M. and Banchereau J. Role of interleukin-1 (IL-1) in the pathogenesis of systemic onset juvenile idiopathic arthritis and clinical response to IL-1 blockade. Journal of Experimental Medicine 2005; 201(9):1479-1486.

Pasquini L.A., Paez P.M., Moreno M.A., Pasquini J.M. and Soto E.F. Inhibition of the proteasome by lactacystin enhances oligodendroglial cell differentiation. The Journal of Neuroscience 2003; 23(11): 4635-4644.

Pelegrin P. Targeting interleukin-1 signaling in chronic inflammation: Focus on P2X7 receptor and Pannexin-1. Drug News Perspect 2008; 21(8): 424-433.

Peng J., Schwartz D., Elias J.E., Thoreen C.C., Cheng D., Marsischky G., Roelofs J., Finley D. and Gygi S.P. A proteomics approach to understanding protein ubiquitination. National Biotechnology 2003; 21: 921-926.

Perregaux D.G and Gabel C.A. Interleukin-1β maturation and release in response to ATP and nigericin. Evidence that potassium depletion mediated by these agents is a necesary and common feature of their activity. Journal of Biological Chemistry 1994; 269: 15195-15203.

Perregaux D.G. and Gabel C.A. Post-translational processing of murine IL-1: evidence that ATP-induced release of IL-1 alpha and IL-1 beta occurs via a similar mechanism. The Journal of Immunology 1998; 160: 2469-2477.

Persson L., Seely J.E. and Pegg A.E. Investigation of structure and rate of synthesis of ornithine decarboxylase protein in mouse kidney. Biochemistry 1984; 23: 3777-3783.

Peters J.M., Cejka Z., Harris J.R., Kleinschmidt J.A. and Baumeister W. Structural features of the 26S proteasome complex. Journal of Molecular Biology 1993; 234: 932-937.

Petropoulos I., Conconi M. and Friguet B. Increase of oxidatively modified protein is associated with a decrease of proteasome activity and content in aging epidermal cells. Journal of Gerontology 2000; 55: B220-B227.

Petroski M.D. and Deshaies R.J. Mechanism of lysine 48-linked ubiquitin-chain synthesis by the cullin-RING ubiquitin-ligase complex SCF-Cdc34. Cell 2005; 123: 1107-1120.

Pierce J.W., Read M.A., Ding H., Luscinskas F.W. and Collins T. Salicylates inhibit I kappa B-alpha phosphorylation, endothelial-leukocyte adhesion molecule expression, and neutrophil transmigration. Journal of Immunoogy 1996; 156 (10): 3961-3969.

Pizzirani C., Ferrari, D., Chiozzi P., Adinolfi E., Sandona D., Savaglio E. and Di Virgilio F. Stimulation of P2 receptors causes release of IL-1β-loaded microvesicles from human dendritic cells. Blood 2007; 109: 3856-3864.

Pollock A.S., Turck J. and Lovett D.H. The prodomain of interleukin 1α interacts with elements of the RNA processing apparatus and induces apoptosis in malignant cells. FASEB Journal 2003; 17: 203-213.

Pope W.H, Haase-Pettingell C. and King J. Protein folding failure sets high-temperature limit on growth of phage P22 in Salmonella enteric serovar Typhimurium. Applied and Environmental Microbiology 2004; 70: 4840-4847.

Porath J., Carlsson J., Olsson I. and Belfrage G. Metal chelate affinity chromatography, a new approach to protein fractionation. Nature 1975; 258: 598-599.

Prévost K., Desnoyers G., Jacques J.F.F., Lavoie F. and Massé E. Small RNA-induced mRNA degradation achieved through both translation block and activated cleavage. Genes & development 2011; 25(4): 385-396.

Price S.R., Bailey J.L., Wang X., Jurkovitz., Ding X., Phillips L.S. and Mitch W.E. Muscle wasting in insulin openic rats results from activation of the ATP-dependent, ubiquitin-proteasome proteolytic pathway by a mechanism including gene transcription. Journal of Clinical Investigation 1996; 98: 1703-1708.

Prudovsky I., Mandinova A., Soldi R., Bagala C., Graziani I., Landriscina M., Tarantini F., Duarte M., Bellum S., Doherty H. and Maciag T. The non-classical export routes: FGF1 and IL-1 alpha point the way. Journal of Cell Science 2003; 116: 4871-4881.

Puig O., Rutz B., Luukkonen B. G., Kandels-Lewis S., Bragado-Nilsson E. and Seraphin B. New constructs and strategies for efficient PCR-based gene manipulations in yeast 1998; Yeast 14: 1139-1146.

Rahmani M., Davis E.M., Bauer C., Dent P. and Grant S. Apoptosis induced by the kinase inhibitor BAY 43-9006 in human leukemia cells involves down-regulation of Mcl-1 through inhibition of translation. Journal of Biological Chemistry 2005; 280: 35217-35227.

Read M.A., Neish A.S., Luscinskas F.W., Palombella V.J., Maniatis T. and Collins T. The proteasome pathway is required for cytokine-induced endothelial-leukocyte adhesion molecule expression. Immunity 1995; 2: 493-506.

Rechsteiner M. Ubiquitin-mediated pathways for intracellular proteolysis. Annual Review of Cell Biology 1987; 3: 1-30.

Restifo N.P., Esquivel F., Kawakami Y., Yewdell J.W., Mule J.J., Rosenberg S.A. and Bennink J.R. Identification of human cancers deficient in antigen processing. Journal of Experimental Medicine 1993; 177: 265-272.

Rhoades K., Golub S.H. and Economou J.S. The regulation of the human tumor necrosis factor a promoter region in macrophage, T cell, and B cell lines. Journal of Biological Chemistry 1992; 267: 22102-22107.

Richards N., Schaner P., Diaz A., Stucke J., Shelden E., Wadhwa A. and Gumuci D.L. Interaction between pyrin and the apoptotic speck protein (ASC) modulates ASC-induced. Journal of Biological Chemistry 2001; 9: 9-17.

Rock K.L. and Goldberg A.L. Degradation of cell proteins and the generation of MHC class I-presented peptides. Annul Reveiw Immunology 1999; 17: 739-779.

Rock K.L., Gramm C., Rothstein L., Clark K., Stein R., Dick L., Hwang D. and Goldberg A.L. Inhibitors of the proteasome block the degradation of most cell proteins and the generation of peptides presented on MHC class I molecules. Cell 1994; 78: 761-771.

Rockwell P., Yuan H., Magnusson R. and Figueiredo-Pereira M.E. Proteasome inhibition in neuronal cells induces a pro-inflammatory response manifested by upregulation of cyclooxygenase-2, its accumulation as ubiquitin conjugates, and production of the prostaglandin PGE(2). Archives of Biochemistry and Biophysics 2000; 374: 325-333.

Rogers J., Cooper N.R., Webster S., Schultz J., McGeer P.l., Styren S.D., Civin W.H., Brachova L., Bradt B. and Ward P. Complement activation by β-amyloid in Alzheimer's disease. Proceedings of National Academy of Science USA 1992; 89: 10016-10020.

Rogers S., Wells R. and Rechsteiner M. Amino acid sequences common to rapidly degraded proteins: the PEST hypothesis. Science 1986; 234: 364-368.

Rohman M. and Harrison-Lavoie K. Separation of copurifying GroEL from glutathione-S-transferase fusion proteins. Protein Expression Purification 2000; 20 (1): 45-47.

Ross C.A. and Poirier M.A. Opinion: What is the role of protein aggregation in neurodegeneration? National Review Molecular Cell Biology 2005; 6: 891-898.

Rothwell N. and Luheshi G.N. Interleukin 1 in the brain: biology, pathology and therapeutic target. Trends in Neuroscience 2000; 23: 618-625.

Royston C., Rothwell N.J. and Roberts G.W. Alzheimer's disease: Pathology to potential treatment? TiPS 1992; 13: 131-135.

Rubartelli A., Cozzolino F., Talio M. and Sitia R. A novel secretory pathway for interleukin-1β, a protein lacking a signal sequence. EMBO Journal 1990; 9: 1503-1510.

Rubartelli A. and Sitia R. Secretion of mammalian proteins that lack a signal sequence. In: unusual secretory pathways. Landes 1997; 87-104.

Rubin D.M., Glickman M.H., Larsen C.N., Dhruvakumar S. and Finley D. Active site mutants in the six regulatory particle ATPases reveal multiple roles for ATP in the proteasome. EMBO Journal 1998; 17: 4909-4919.

Saijo Y., Tanaka M., Miki M., Usui K., Suzuki T., Maemondo M., Hong X., Tazawa R., Kikuchi T., Matsushima K. and Nukiwa T. Pro-inflammatory cytokine IL-1β promotes tumor growth of Lewis lung carcinoma by induction of angiogenic factors: *in vivo* analysis of tumor-stromal interaction. Journal of Immunology 2002; 169: 469-475.

Sakai N., Sawada M.T. and Sawada H. Non-traditional roles of ubiquitin-proteasome system in fertilization and gametogenesis. International Journal Biochemistry and Cell Biology 2004; 36: 776-784.

Salven P., Hattori K., Heissig B. and Rafii S. Interleukin-1α promotes angiogenesis *in vivo* via VEGFR-2 pathway by inducing inflammatory cell VEGF synthesis and secretion. FASEB Journal 2002; 16: 1471-1473.

Salvesen G. and Nagase H. Inhibition of proteolytic enzymes. Proteolytic Enzymes 1989; 83-104.

Sambrook J., Fritsch E.F., and Maniatis T. Molecular cloning a laboratory manual. Cold Spring Harbor, N.Y: Cold Spring Harbor Laboratory Press 1989.

Scharnagl C., Reif M. and Friedrich J. Stability of proteins: Temperature, pressure and the role of the solvent. Biochemistry and Biophysics 2005; 1749:187-213.

Schellman J.A. Temperature, stability, and the hydrophobic interaction. Biophysics Journal 1997; 73: 2960-2964.

Schmitz J., Owyang A., Oldham E., Song Y., Murphy E., McClanahan T.K., Zurawski G., Moshrefi M., Qin J., Li X., Gorman D.M., Bazan J.F., and Kastelein R.A. IL-33, an

interleukin-1-like cytokine that signals via the IL-1 receptor-related protein ST2 and induces T helper type 2-associated cytokines. Immunity 2005; 23: 479-490.

Schneider B.L., Seufert W., Steiner B., Yang Q.H. and Futcher A.B. Use of polymerase chain reaction epitope tagging for protein tagging in *Saccharomyces cerevisiae*. Yeast 1995; 11: 1265-1274.

Seliger B., Hohne A., Knuth A., Bernhard H., Meyer T., Tampe R., Momburg F. and Huber C. Analysis of the major histocompatibility complex class I antigen presentation machinery in normal and malignant renal cells: evidence for deficiencies associated with transformation and progression. Cancer Research 1996; 56: 1756-1760.

Shi Y., Chan D.W., Jung S.Y., Malovannaya A., Wang Y., and Qin J. A dataset of human endogenous ubiquitination sites. Molecular Cell Proteomics 2010.

Shi Y., Evans J.E. and Rock K.L. Molecular identification of a danger signal that alerts the immune system to dying cells. Nature 2003; 425: 516-521.

Shibata T., Imaizumi T., Tamo W., Matsumiya T., Kumagai M., CUI X., Yoshida H., Takaya S., Fukuda I. and Satoh K. Proteasome inhibitor MG132 enhances the expression of interleukin-6 in human umbilical vein endothelial cells: Involvement of MAP/ERK. Immunology and Cell Biology 2002; 80: 226-230.

Shinohara K., Tomioka M., Nakano H., Tone S., Ito H. and Kawashima S. Apoptosis induction resulting from proteasome inhibition. Biochemistry Journal 1996; 317: 385-388.

Simi A., Tsakiri N., Wang P. and Rothwell N.J. Interleukin-1 and inflammatory neurodegeneration. Biochemical Society Transactions 2007; 35: 1122-1126.

Sims J.A., Gayle M.A., Slack J.L., Alderson M.R., Bird T.A., Giri J.G., Colotta F., Re F., Mantovani A. and Shanebeck K. Interleukin 1 signaling occurs exclusively via the type I receptor. Proceedings National Academy of Science 1993; 90: 6155-6159.

Sims J.E., March C.J., Cosman D., Widmer M.B., MacDonald H.R., McMahan C.J., Grubin C.E., Wignall J.M., Jackson J.L., Call S.M., Friend D., Alpert A.R., Gillis S., Urdal D.L. and Dower S.K. cDNA expression cloning of the IL-1 receptor, a member of the immunoglobulin super-family. Science 1988; 241: 585-589.

Sleath P.R., Hendrickson R.C., Kronheim S.R., March C.J. and Black R.A. Substrate specificity of the protease that processes human interleukin-1β convertase activity. Proceedings National Academy of Science USA 1990; 86: 5227-5234.

Smith D.E., Renshaw B.R., Ketchem R.R., Kubin M., Garka K.E. and Sims J.E. Four new members expand the interleukin-1 superfamily. Journal of Biological Chemistry 2000; 275:1169-1175.

Smith D.M., Kafri G., Cheng Y., Ng D., Walz T. and Goldberg A.L. ATP binding to PAN or the 26S ATPases causes association with the 20S proteasomes, gate opening, and translocation of unfolded proteins. Molecular Cell 2005; 20:687-698.

Smith-Thomas L.C., Kent C., Mayer R.J. and Scotting P.J. Protein ubiquitination and neuronal differentiation in chick embryos. Brain Research 1994; 81: 171-177.

Sone T., Saeki Y., Toh-e A. and Yokosawa H. Sem1p is a novel subunit of the 26S proteasome from *Saccharomyces cerevisiae*. Journal of Biological Chemistry 2004; 279: 28807-28816.

Spataro V., Norbury C. and Harris A.L. The ubiquitin-proteasome pathway in cancer. British Journal of Cancer 1998; 77: 448-455.

Srisailam S., Wang H.M., Kumar T.K., Rajalingam D., Sivaraja V., Sheu H.S., Chang Y.C. and Yu C. Amyloid-like fibril formation in an all beta-barrel protein involves the formation of partially structured intermediate(s). Journal of Biological Chemistry 2002; 277: 19027-19036.

Stanley L.C. and Griffin W.S.T. Localization of IL-1α and IL-1β in diseases with gliosis, dementia, and immune suppression. Neuroscience Abstract 1990; 16: 1345.

Stevenson F.T., Torrano F., Locksley R.M. and Lovett D.H. Interleukin 1: the patterns of translation and intracellular distribution support alternative secretory mechanisms. Journal of Cell Physiology 1992; 152: 223-231.

Stevenson F.T., Turck J., Locksley R.M and Lovett DH. The N-terminal pro-piece of interleukin-1α is a transforming nuclear oncoprotein. Proceedings National Academy of Science USA 1997; 94: 508-513.

Strandberg L. and Enfors S.O. Factors influencing inclusion body formation in the production of a fused protein in *Escherichia coli*. Applied Environmental Microbiology 1991; 57: 1669-1674.

Strehl B., Seifert U., Krüger E., Heink S., Kuckelkorn U. and Kloetzel P.M. Interferon-γ the functional plasticity of the ubiquitin-proteasome system, and MHC class I antigen processing. Immunology Review 2005; 207: 19-30.

Sun Y. Targeting E3 ubiquitin ligases for cancer therapy. Cancer Biology and Therapy 2003; 2: 623-629.

Sunwoo J.B., Chen Z., Dong G., Yeh N., Bancroft C., Sausville E., Adams J., Elliott P. and VanWases C. Novel proteasome inhibitor PS-341 inhibits activation of nuclear factor-kappa B, cell survival, tumor growth, and angiogenesis in squamous cell carcinoma. Clinical Cancer Research 2001; 7: 1419-1428.

Swaan P., Knoell D., Hesper F. and Wewers D. Sequential processing of human pro-IL-1β by caspase-1 and subsequent folding determined by a combined *In Vitro* and In Silico approach. Pharmaceutical Research 2001; 18(8): 1083-1090.

Taillandier D. and Attaix D. Ubiquitin-proteasome-dependent muscle proteolysis responds slowly to insulin release and refeeding in starved rats. Journal of Physiology 2003; 546: 765-776.

Tanaka K., Kumatori A., Ii K. and Ichihara A. Direct evidence for nuclear and cytoplasmic colocalization of proteasomes (multiprotease complexes) in liver. Journal of Cell Physiology 1989; 139: 34-41.

Taylor C. and Jobin C. Ubiquitin protein modification and signal transduction: Implications for inflammatory bowel diseases. Inflammatory Bowel Disease 2005; 11: 1097-1107.

Temparis S., Asensi M., Taillandier D., Aurousseau E., Larbaud D., Obled A., Bechet D., Ferrara M., Estrela J.M. and Attaix D. Increased ATP-ubiquitin-dependent proteolysis in skeletal muscles of tumor-bearing rats. Cancer Research 1994; 54: 5568-5573.

Thain A., Gaston K., Jenkins O. and Clarke A.R. A method for the separation of GST fusion proteins from co-purifying GroEL. Trends in Genetics 1996; 12 (6): 209-210.

Thanos D. and Maniatis T. NF-κB: a lesson in family values. Cell 1995; 80: 529-532.

Thompson J.D., Gibson T.J., Frédéric, P.F. and Higgins D.G. The Clustal X windows interface: flexible strategies for multiple sequence alignment aided by quality analysis tools. Nucleic Acids Research 1997; 25(24): 4876-4882.

Thornberry A., Bull G., Calaycay R., Chapman T., Howard A., Kostura J., Miller K., Molineaux M., Weidner R. and Aunins J. A novel heterodimeric cysteine protease is required for interleukin-1 beta processing in monocytes. Nature 1992; 356: 768-774.

Thrower J.S., Hoffman L., Rechsteiner M. and Pickart C.M. Recognition of the polyqbiquitin proteolytic signal. The EMBO journal 2000; 1: 94-102.

Townsend A. and Trowsdale J. The transporters associated with antigen presentation. Cell Biology 1993; 4: 53-61.

Tsubuki S., Saito Y., Tomioka M., Ito H. and Kawashima S. Differential inhibition of calpain and proteasome activities by peptidyl aldehydes of di-leucine and tri-leucine. Journal of Biochemistry 1996; 119: 572-576.

Tsukamoto O., Minamino T., Okada K., Shintani Y., Takashima S., Kato H., Liao Y., Okazaki H., Asai M. and Hirata A. Depression of proteasomes activities during the progression of cardiac dysfunction in pressure-overloaded heart of mice. Biochemistry and Biophysics Research Communications 2006; 340: 1125-1133.

Unno M., Mizushima T., Morimoto Y., Tomisugi Y., Tanaka K., Yasuoka N. and Tsukihara T. The structure of the mammalian 20S proteasome at 2.75 Å resolution. Structure 2002; 10: 609-618.

Uzzau S., Figueroa-Bossi N., Rubino S., and Bossi L. Epitope tagging of chromosomal genes in Salmonella. Proceedings of the National Academy of Sciences 2001; 98 (26): 15264-15269.

Varshavsky A. The ubiquitin system. Trends in Biochemical Science 1997; 22: 383-387.

Vera A., Gonza´lez-Montalba´n N., Arı´s A. and Villaverde A. The conformational quality of insoluble recombinant proteins is enhanced at low growth temperatures. Biotechnology Bioengineering 2007; 96: 1101-1106.

Verma R., Aravind L., Oania R., McDonald W.H., Yates J.R., Koonin E.V. and Deshaies R.J. Role of Rpn11 Metalloprotease in Deubiquitination and Degradation by the 26S Proteasome. Science 2002; 298: 611-615.

Verma R., Chen S., Feldman R., Schieltz D., Yates J., Dohmen J. and Deshaies R.J. Proteasomal proteomics: Identification of nucleotide-sensitive proteasome-interacting proteins by mass spectrometric analysis of affinity-purified proteasomes. Molecular Biology of Cell 2000; 11: 3425-3439.

Viljoen M. Joint Meeting of the 19th Congress of the International Society of Haematology and the 17th Congress of the International Society of Blood Transfusion, Budapest, August 1982.

Vogelstein B., Lane D. and Levine A.J. Surfing the p53 network. Nature 2000; 408: 307-310.

Voges D., Zwickl P. and Baumeister W. The proteasome: a macromolecular assembly designed for controlled proteolysis. Annual Review Biochemistry 1999; 68: 1015-1068.

Walz J., Erdmann A., Kania M., Typke D., Koster A.J. and Baumeister W. 26S proteasome structure revealed by three-dimensional electron microscopy. Journal of Structural Biology 1998; 121: 19-29.

Warner S.J.C., Auger K.R. and Libby P. Recombinant human interleukin 1 induces interleukin 1 production by adult human vascular endothelial cells. Journal of Immnunology 1987(b); 139: 1911-1917.

Watanabe N. and Kobayashi Y. Selective release of a processed form of interleukin 1". Cytokine 1994; 6: 597-601.

Watkins L.R., Hansen M.K., Nguyen K.T., Lee J.E. and Maier S.F. Dynamic regulation of the pro-inflammatory cytokine, interleukin 1β: molecular biology for non-molecular

biologists. Life Sciences 1999; 65: 449-481.

Weber C., Erl W., Pietsch A. and Weber P.C. Aspirin inhibits nuclear factor-kappa B mobilization and monocyte adhesion in stimulated human endothelial cells. Circulation 1995; 91: 1914-1917.

Weinreich D.M., Elaraj D.M. and Puhlmann M. Effect of interleukin 1 receptor antagonist gene transduction on human melanoma xenografts in nude mice. Cancer Research 2003; 63: 5957-5961.

Werman A., Werman-Venkert R., White R., Lee J., Werman B., Voronov Y., Dinarello C.A. and Apte R.N. The precursor form of IL-1α is an intracrine pro-inflammatory activator of transcription. Journal of Immunology 2004; 101(8): 2434-2439.

Wewers M.D., Winnard A.V. and Dare H.A. Endotoxin- stimulated monocytes release multiple forms of IL-1 beta, including a proIL-1 beta form whose detection is affected by export. Journal of Immunology. 1999; 162: 4858-4863.

Wilkinson C.R., Seeger M., Hartmann-Petersen R., Stone M., Wallace M., Semple C. and Gordon C. Proteins containing the UBA domain are able to bind to multi-ubiquitin chains. Nature Cell Biology 2001; 3: 939-943.

Wilkinson K.D., Urban M.K. and Arthur L.S. Ubiquitin is the ATP-dependent Proteolysis Factor I of Rabbit Reticulocytes. The journal of biological chemistry 1980; 256 (16): 7529-7532.

Willerson J.T. and Ridker P.M. Inflammation as a cardiovascular risk factor. Circulation 2004; 109 (suppl II): 2-10.

Wilson K.P., Black J.A., Thomson J.A., Kim E.E., Griffith J.P., Navia M.A., Murcko M.A., Chambers S.P., Aldape R.A. and Raybuck S.A. Structure and mechanism of interleukin-1 beta converting enzyme. Nature 1994; 370: 270-275.

Wu C., Ying H., Bose S., Miller R., Medina L., Santora L. and Ghayur T. Molecular construction and optimization of anti-human IL-1α/β dual variable domain immunoglobulin (DVD-Ig™) molecules. mAbs 2009; 1(4): 339-347.

Wu C., Ying H., Grinnell C., Bryant S., Miller R. and Clabbers A. Simultaneous targeting of multiple disease mediators by a dual-variable-domain immunoglobulin. National Biotechnology; 2007; 25: 1290-1297.

Wu H.M., Wen H. and Lin W. Proteasome Inhibitors Stimulate Interleukin-8 expression via Ras and apoptosis Signal-Regulating Kinase-dependent Extracellular Signal-Related Kinase and c-Jun N-Terminal Kinase Activation. American Journal of Respiratory Cell and Molecular Biology 2002; 27: 234-243.

Xiong H., Wang D., Chen L., Choo Y.S., Ma H., Tang C., Xia K., Jiang W., Ronai Z., Zhuang X. and Zhang Z. Pakrin, PINK1, and DJ-1 form a ubiquitin E3 ligase complex promoting unfolded protein degradation. Journal of Clinical Investigation 2009; 119: 650-660.

Xu G., Paige J.S. and Jaffrey S.R. Global analysis of lysine ubiquitination by ubiquitin remnant immunoaffinity profiling. National Biotechnology 2010; 28: 868-873.

Yamamoto Y. and Gaynor R.B. Therapeutic potential of inhibition of the NF-κB pathway in the treatment of inflammation and cancer. Journal of Clinical Investigation 2001; 107: 135-142.

Yao T. and Cohen R.E. A cryptic protease couples de-ubiquitination and degradation by the proteasome Nature 2002; 419: 403-407.

Yin H., Morioka H., Towle C.A., Vidal M., Watanabe T. and Weissbach L. Cytokine 2001; 15: 122-137.

Young P., Deveraux Q., Beal R.E., Pickart C.M. and Rechsteiner M. Characterization of two polyubiquitin binding sites in the 26S protease subunit 5a. Journal of Biological Chemistry 1998; 273: 5461-5467.

Yu A. and Malek T.R. The proteasome regulates receptor-mediated endocytosis of interleukin-2. The Journal of Biological Chemistry 2001; 276(1): 381-385.

Yuan S., Duan H., Liu C., Liu X., Liu T., Tao H. and Zhang Z. The role of thioredoxin and disulfide isomerase in the expression of the snake venom thrombin-like enzyme calobin in *Escherichia coli* BL21(DE3). Protein Expression Purification 2004; 38: 51-60.

Zetterberg M., Petersen A., Sjostrand J. and Karlsson J. Proteasome activity in human lens nuclei and correlation with age, gender and severity of cataract. Current Eye Research 2003; 27: 45-53.

Zhang F., Hu M., Tian G., Zhang P., Finley D., Jeffrey P.D. and Shi Y. Structural insights into the regulatory particle of the proteasome from Methanocaldococcus jannaschii. Molecular cell Biology 2009; 34: 473-484.

Zhou H., Cao F., Wang Z., Yu Z.X., Nguyen H.P., Evans J., Li S.H. and Li X.J. Huntingtin forms toxic NH2-terminal fragment complexes that are promoted by the age-dependent decrease in proteasome activity. Journal of Cell Biology 2003; 163: 109-118.